Gdański Uniwersytet Medyczny
Wydział Lekarski

Karol P. Steckiewicz

„Wpływ modyfikacji mikrocząstek i nanocząstek na ich aktywność cytotoksyczną i właściwości przeciwbakteryjne w badaniach in vitro”

Rozprawa doktorska

Praca została wykonana w Katedrze i Zakładzie Chemii Medycznej
Gdańskiego Uniwersytetu Medycznego

Promotor: prof. dr hab. Iwona Inkielewicz - Stępniak
Kierownik Katedry i Zakładu Patofizjologii Farmaceutycznej
Gdańskiego Uniwersytetu Medycznego

Gdańsk 2020

SPIS TREŚCI

Pracę dedykuję pamięci mojej babci Reginy.

Pragnę serdecznie podziękować wszystkim, bez których niniejsza praca nie mogłaby powstać.

Mojej promotor Pani prof. Iwonie Inkielewicz - Stępniak za okazane zaufanie i poświęcony czas.

Pani dr Ewelinie Barcińskiej za pomoc w stawianiu pierwszych naukowych kroków i okazane wsparcie.

Współautorom prac wchodzących w skład mojej rozprawy doktorskiej za owocną współpracę.

Koleżankom i kolegom z Katedry i Zakładu Chemii Medycznej oraz panu prof. Michałowi Woźniakowi za towarzyszenie mi w mojej drodze naukowej.

Moim najbliższym, rodzicom i rodzeństwu za wszystko, a w szczególności za to, że nigdy we mnie nie wątpili.

Mojej rodzinie i przyjaciołom za okazane wsparcie, wyrozumiałość i cierpliwość.

WYKAZ PRAC WCHODZĄCYCH W SKŁAD ROZPRAWY DOKTORSKIEJ / LIST OF MANUSCRIPTS INCLUDED IN THE DOCTORAL DISSERTATION

Steckiewicz KP, Inkielewicz-Stępniak I.
Modified nanoparticles as potential agents in bone diseases: cancer and implant-related complications
Nanomaterials. 2020; 10:658
IF_{2019}: 4,324 | MNiSW: 70 pkt

Steckiewicz KP, Barcińska E, Malankowska A, Zauszkiewicz-Pawlak A, Nowaczyk G, Zaleska-Medynska A, Inkielewicz-Stępniak I.
Impact of gold nanoparticles shape on their cytotoxicity against human osteoblast and osteosarcoma in *in vitro* model: evaluation of the safety of use and anti-cancer potential
J Mater Sci Mater Med. 2019; 30(2):22
IF_{2019}: 2,489 | MNiSW: 70 pkt

Steckiewicz KP*, Barcińska E*, Sobczak K, Tomczyk E, Wójcik M, Inkielewicz-Stępniak I.
Assessment of anti-tumor potential and safety of application of glutathione stabilized gold nanoparticles conjugated with chemotherapeutics
Int J Med Sci. 2020;17(6)
IF_{2019}: 2,523 | MNiSW: 100 pkt
*Wskazani autorzy mają jednakowy wkład w przygotowanie publikacji.
* These authors contributed equally to this work.

Steckiewicz KP, Zwara J, Jaśkiewicz M, Kowalski S, Kamysz W, Zaleska-Medynska A, Inkielewicz-Stępniak I.
Shape-depended biological properties of Ag_3PO_4 microparticles: evaluation of antimicrobial properties and cytotoxicity in *in vitro* model - safety assessment of potential clinical usage
Oxid Med Cell Longev. 2019; 2019:6740325.
IF_{2019}: 5,076 | MNiSW: 100 pkt

Łączna wartość wskaźnika odziaływania (IF): **14.412**
Łączna wartość 5-cio letniego wskaźnika (IF): **15.713**
Łączna punktacja MNiSW: **340 pkt**

Badania będące podstawą ubiegania się o nadanie stopnia doktora były częściowo finansowane w ramach Grantu „Wspieramy rozwój" Cedrob SA (kierownik: Karol Steckiewicz)

STRESZCZENIE W JĘZYKU POLSKIM

I. WYKAZ STOSOWANYCH SKRÓTÓW

143B	linia komórkowa kostniakomięsaka
AgNPs	nanocząstki srebra
ATCC	*(ang. American Type Cell Culture),* Amerykańska Kolekcja Hodowli Komórkowych
AuNPs	nanocząstki złota
AuNPs-GSH	nanocząstki złota stabilizowane glutationem
AuNPs-GSH-CTA	nanocząstki złota stabilizowane glutationem i sprzężone z cytarabiną
AuNPs-GSH-DOX	nanocząstki złota stabilizowane glutationem i sprzężone z doksorubicyną
AuNPs-GSH-GEM	nanocząstki złota stabilizowane glutationem i sprzężone z gemcytabiną
b-SOMPs	*(ang. branched silver orthophosphate microparticles),* mikrocząstki fosforanu (V) srebra w kształcie rozgałęzionym
Bax	białko proapoptotyczne
Bcl-2	białko antyapoptotyczne
BrdU	5-bromo-2-deoksyurydyna
c-SOMPs	*(ang. cubic silver orthophosphate microparticles),* mikrocząstki fosforanu (V) srebra w kształcie sześciennym
C2C12	linia komórkowa mysich mioblastów
CTA	cytarabina
DCF-DA	dioctan 2,7'-dichlorodihydrofluoresceiny
DNA	kwas deoksyrybonukleinowy
DOX	doksorubicyna
ECDCC	*(ang. European Collection of Authenticated Cell Culture),* Europejska Kolekcja Hodowli Komórkowych
GEM	gemcytabina
GPX4	peroksydaza glutationowa 4
GSH	glutation
HA-NPs	nanocząstki hydroksyapatytu
HDF	linia komórkowa fibroblastów skóry

hTERT-HPNE	linia komórkowa nietransformowanych nowotworowo komórek przewodu trzustkowego
IC_{50}	stężenie inhibitora hamujące w 50%
IUPAC	*(ang. International Union of Pure and Applied Chemistry),* Międzynarodowa Unia Chemii Czystej i Stosowanej
MBEC	*(ang. minimal biofilm eradication concentration),* minimalne stężenie eradykujące biofilm
MC3T3-E1	linia komórkowa mysich preosteoblastów
MG-63	linia komórkowa kostniakomięsaka
MIC	*(ang. minimal inhibitory concentration),* minimalne stężenie hamujące
MMP1	metaloproteinaza 1
MMP3	metaloproteinaza 3
MPs	mikrocząstki
MRSA	*(ang. methicyllin-resistant Staphylococcus aureus),* gronkowiec złocisty (*Staphylococcus aureus*) oporny na metycylinę
MTT	bromek 3-(4,5-dimetyltiazol-2-ilo)-2,5-difenyloterazoliowy
NF-κB	*(ang. nuclear factor kappa-light-chain-enhancer of activated B cells),* jądrowy czynnik transkrypcyjny κB
NPs	nanocząstki
NR	*(ang. neutral red)* czerwień obojętna
p16-ARC	*(ang. actin-related protein 2/3 complex subunit 5),* białko kompleksu związanego z aktyną
PANC1	linia komórkowa nowotworu trzustki
PEG	*(ang. poli (ethylene glycol)),* poli (tlenek etylenu)
PI	jodek propidyny
rd-SOMPs	*(ang. rhombic dodecahedral silver orthophosphate microparticles),* mikrocząstki fosforanu (V) srebra w kształcie dwunastościennym
ROS	*(ang. reactive oxygen species),* reaktywne formy tlenu
s-SOMPs	*(ang. spherical silver orthophosphate microparticles)* mikrocząstki fosforanu (V) srebra w kształcie sferycznym
Saos-2	linia komórkowa kostniakomięsaka

SOD1	cytoplazmatyczna dysmutaza ponadtlenkowa, cynkowo - miedziowa
SOD2	mitochondrialna dysmutaza ponadtlenkowa, manganowa
SOD3	zewnątrzkomórkowa dysmutaza ponadtlenkowa, cynkowo - miedziowa
SOMPs	*(ang. silver orthophosphate microparticles),* mikrocząstki fosforanu (V) srebra
t-SOMPs	*(ang. tetrapod silver orthophosphate microparticles)* mikrocząstki fosforanu (V) srebra w kształcie tertrapodalnym
TEM	transmisyjny mikroskop elektronowy
th-SOMPs	*(ang. tetrahedral silver orthophosphate microparticles)* mikrocząstki fosforanu (V) srebra w kształcie czworościennym

II. WPROWADZENIE

Nowoczesne biomateriały takie jak mikrocząstki (MPs) i nanocząstki (NPs) dzięki swoim unikalnym właściwościom mogą być wykorzystywane w profilaktyce i leczeniu chorób człowieka. Badania na temat MPs i NPs są nową, prężnie rozwijającą się dziedziną nauki, na co wskazuje rosnąca liczba doniesień literaturowych. Do końca 2019 roku w bazie PubMed indeksowano ponad 230 000 artykułów o tej tematyce, z wyraźnym wzrostem ich liczby w ostatnim dziesięcioleciu. Obserwuje się również znaczny wzrost liczby produktów z dodatkiem NPs, co przekłada się również na wzrost wartości tej gałęzi gospodarki [1,2]. Należy pokreślić, że właściwości NPs są zdecydowanie lepiej poznane niż właściwości MPs. Jednakże, podział na mikrocząstki i nanocząstki ma charakter umowny, a w terminologii naukowej nie ma jasnych kryteriów rozdziału między nimi. Celem ujednolicenia nazewnictwa stosowałem wytyczne Międzynarodowej Unii Chemii Czystej i Stosowanej (IUPAC), zgodnie z którymi mikrocząstkami nazywamy struktury, których rozmiar mieści się w zakresie od 10^{-7} m do 10^{-4} m, a nanocząstkami takie, których rozmiar mieści w zakresie od 10^{-9} m do 10^{-7} m [3]. Natomiast według Komisji Europejskiej (zalecenie 2011/696/UE), nanomateriały to takie produkty, w których 50% rozkładu liczbowego wielkości cząstek ma jeden lub więcej wymiarów w zakresie 1 nm. - 100 nm. [4]. Jednakże, od powyższej definicji są pewne wyjątki takie jak fulereny, płytki grafenowe oraz jednościenne nanorurki węglowe, o co najmniej jednym wymiarze poniżej 1 nm. [4]. Zatem MPs i NPs są większe od cząsteczek organicznych (takich jak DNA czy białka), ale mniejsze od wirusów, bakterii czy komórek eukariotycznych. Niewielkie rozmiary w sposób znaczący wpływają na zmianę ich właściwości fizyko-chemicznych, w odniesieniu do odpowiedników w skali makro. Mikrocząstki i nanocząstki wykazują szereg korzystnych właściwości, m.in.: wysoki stosunek pola powierzchni do objętości, zdolność penetrowania przez błony komórkowe i bariery biologiczne oraz wysoką reaktywność [5]. Należy również wspomnieć o wielokierunkowych możliwościach funkcjonalizacji MPs i NPs, co znacznie zwiększa możliwości zastosowania ich w aspekcie biomedycznym [5]. MPs i NPs znajdują zastosowanie w biologii, chemii, medycynie, ochronie środowiska, genetyce, biotechnologii czy przemyśle [5–8] (Rycina 1.).

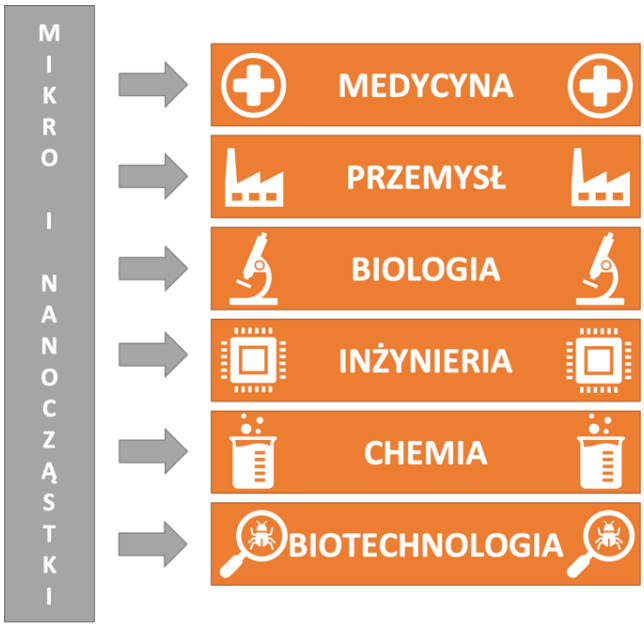

Rycina 1. *Zastosowanie praktyczne mikrocząstek i nanocząstek* [9]

W badaniach wchodzących w skład mojej pracy doktorskiej wykorzystałem mikrocząstki i nanocząstki metali szlachetnych i ich związków. Nanocząstki srebra (AgNPs) wykazują silne właściwości przeciwdrobnoustrojowe, przeciwnowotworowe, antyagregacyjne i fibrynolityczne [10–12]. Warto podkreślić, że AgNPs charakteryzuje aktywność przeciwbakteryjna również przeciwko biofilmowi i szczepom wielolekoopornym [6, 13]. Korzystne cechy warunkują wielokierunkowe zastosowanie nanocząstek, czego dowodem jest fakt, że AgNPs stanowią 30% NPs produkowanych w celach komercyjnych [14]. Nanocząstki złota (AuNPs) również charakteryzują się właściwościami przeciwnowotworowymi, ponadto są wykorzystywane w immunoterapii, diagnostyce obrazowej oraz jako biosensory [15–19]. AuNPs dodatkowo znalazły zastosowanie w diagnostyce chorób, np. gruźlicy [20]. AuNPs i AgNPs są również wykorzystywane jako platformy dostarczania leków [21, 22]. Mikrocząstki, np. fosforanu (V) srebra, tlenku miedzi (II) czy tlenku srebra również wykazują właściwości przeciwdrobnoustrojowe i przeciwnowotworowe [23–26]. Zarówno MPs, jak i NPs posiadają szereg korzystnych właściwości biologicznych co przekłada się na możliwość ich biomedycznego wykorzystania (rycina 2).

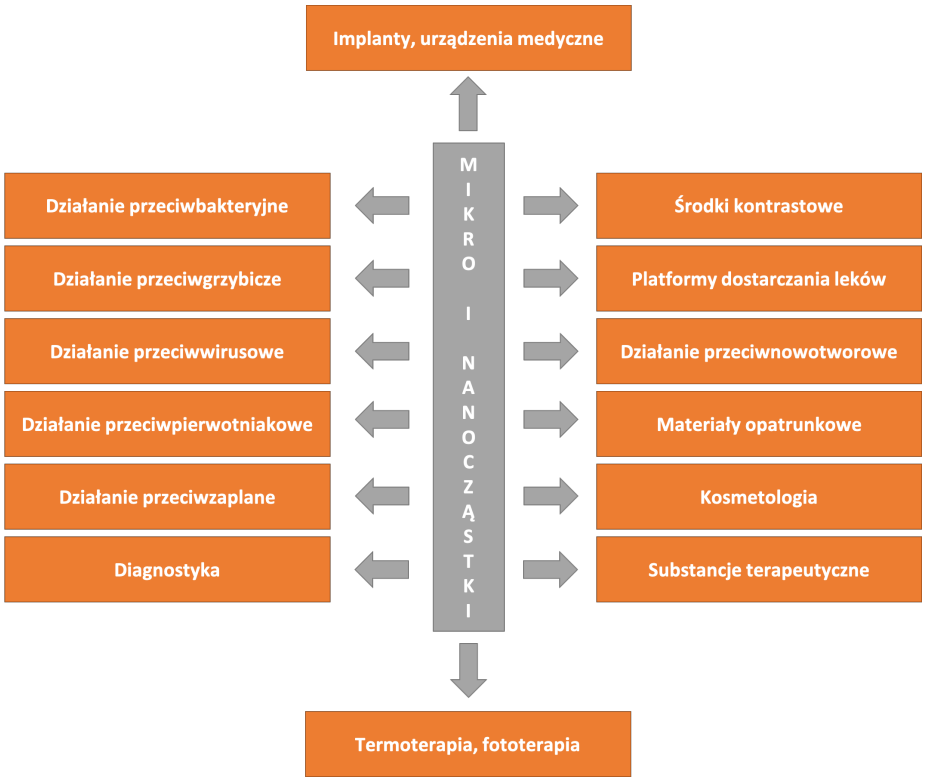

Rycina 2. *Potencjalne zastosowanie mikrocząstek i nanocząstek w naukach biomedycznych*

Niestety, nie do końca poznane działanie toksyczne i trudne do przewidzenia zagrożenia dla zdrowia człowieka ogranicza zastosowanie kliniczne MPs i NPs. Dotychczasowe badania dowodzą, że zarówno AgNPs, jak i AuNPs mogą być cytotoksyczne względem ludzkich osteoblastów, komórek fibroblastów dziąseł, progenitorowych komórek neuronalnych czy makrofagów [27–31]. Indukowanie stresu oksydacyjnego jest jednym z głównych mechanizmów cytotoksyczności NPs metali, jednakże działanie prozapalne czy powodowanie zaburzeń w wewnątrzkomórkowej puli wapnia jest również opisywane [28, 29, 32]. W efekcie ekspozycja na działanie NPs może prowadzić do śmierci komórki na drodze apoptozy, nekroptozy, nekrozy lub autofagii [33–39]. Mechanizmy cytotoksyczności MPs nie są dobrze poznane. Wykazano, że mikrocząstki hydroksyapatytu są cytotoksyczne względem ludzkich makrofagów, a mikrocząstki krzemionki względem komórek nowotworu piersi [40, 41]. Jednym z opisanych mechanizmów cytotoksyczności mikrocząstek jest indukcja stresu oksydacyjnego i wpływ na regulację cyklu komórkowego [42, 43]. Podsumowanie wybranych mechanizmów cytotoksyczności MPs i NPs na poziomie molekularnym i komórkowym przedstawiłem na rycinie 3.

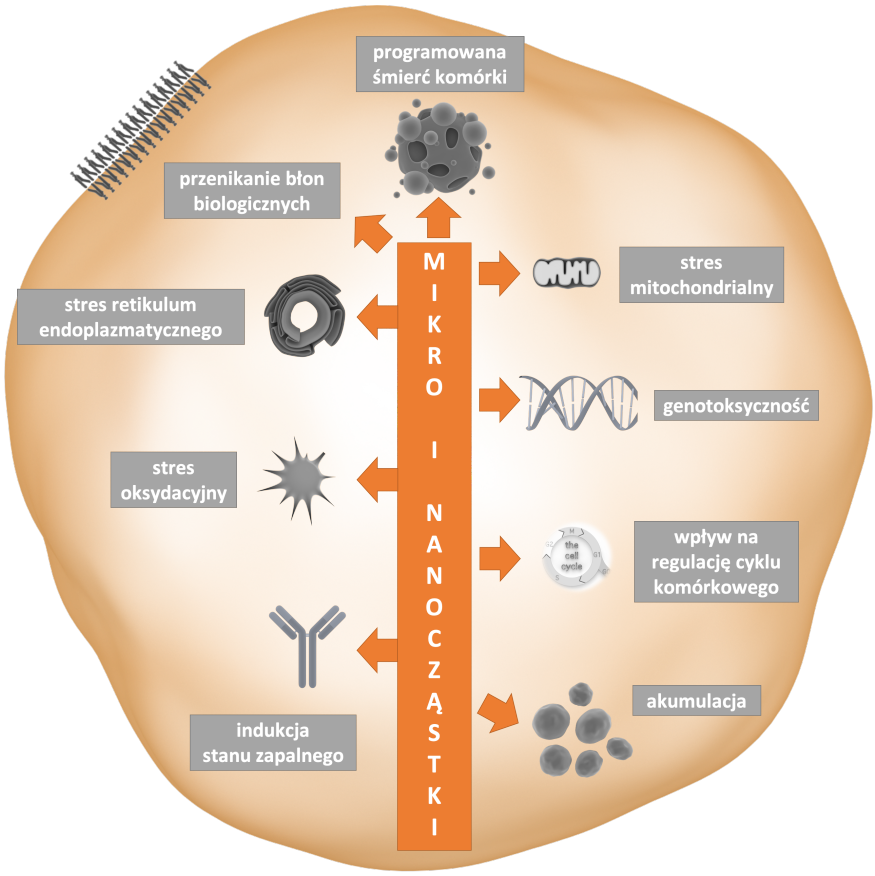

Rycina 3. *Wybrane mechanizmy cytotoksyczności mikrocząstek i nanocząstek na poziomie komórkowym i molekularnym*

Zarówno korzystne właściwości jak i toksyczność MPs i NPs zależą od wielu czynników. Funkcjonalizacja MPs i NPs może wpłynąć na poprawę ich profilu bezpieczeństwa jednocześnie nie upośledzając ich korzystnych właściwości. Szereg czynników moduluje właściwości MPs i NPs, a do najlepiej poznanych należą ich: rodzaj, wielkość, kształt, czas inkubacji, stężenie, pH środowiska oraz właściwości powierzchni. Ponadto właściwości biologiczne MPs i NPs zależą od rodzaju narażonych na ich działanie komórek. Podsumowanie czynników wpływających na właściwości MPs i NPs przedstawiłem na rycinie 4. Wielu autorów wskazuje, że im mniejsze MPs i NPs tym większa jest ich cytotoksyczność [30, 42, 44]. Jednakże, pojawiają się prace wykazujące wyższą cytotoksyczność MPs i NPs o większych rozmiarach [45]. Podobnie, wraz ze wzrostem stężenia i czasu inkubacji, obserwowany jest wzrost cytotoksyczności [46–48]. Również kształt wpływa na cytotoksyczność NPs i MPs, aczkolwiek ze względu na możliwość przyłączenia substancji biologicznie czynnych do powierzchni MPs i NPs o kształcie sferycznym, są one obecnie coraz częściej wykorzystywane [49]. Do powierzchni biomateriałów kowalencyjnie lub niekowalencyjnie można przyłączyć

między innymi fluorofory, leki, przeciwciała, kwasy nukleinowe, białka, wodorowęglany czy substancje organiczne takie jak poli(tlenek etylenu), (PEG) lub zredukowany glutation (GSH) [50, 51]. Funkcjonalizacja MPs i NPs za pomocą GSHa lub PEGu znacznie zwiększa ich biokompatybilność. Ponadto, PEG poprawia rozpuszczalność w wodzie i zapobiega opłaszczaniu przez białka, co wydłuża czas półtrwania w krwioobiegu [30]. Natomiast GSH ma silne właściwości antyoksydacyjne, co zmniejsza cytotoksyczność wynikającą z indukcji stresu oksydacyjnego przez MPs i NPs [30, 52]. Sugeruje się, że przyłączenie chemioterapeutyków do nanocząstek pozwala na stworzenie biomateriałów o lepszych właściwościach przeciwnowotworowych niż same leki (lepsza zdolność penetrowania guza nowotworowego, przełamywanie mechanizmów lekooporności) [53–55]. Podobnie połączenie nanocząstek z antybiotykami pozwala na osiągniecie synergistycznego efektu przeciwdrobnoustrojowego [56, 57].

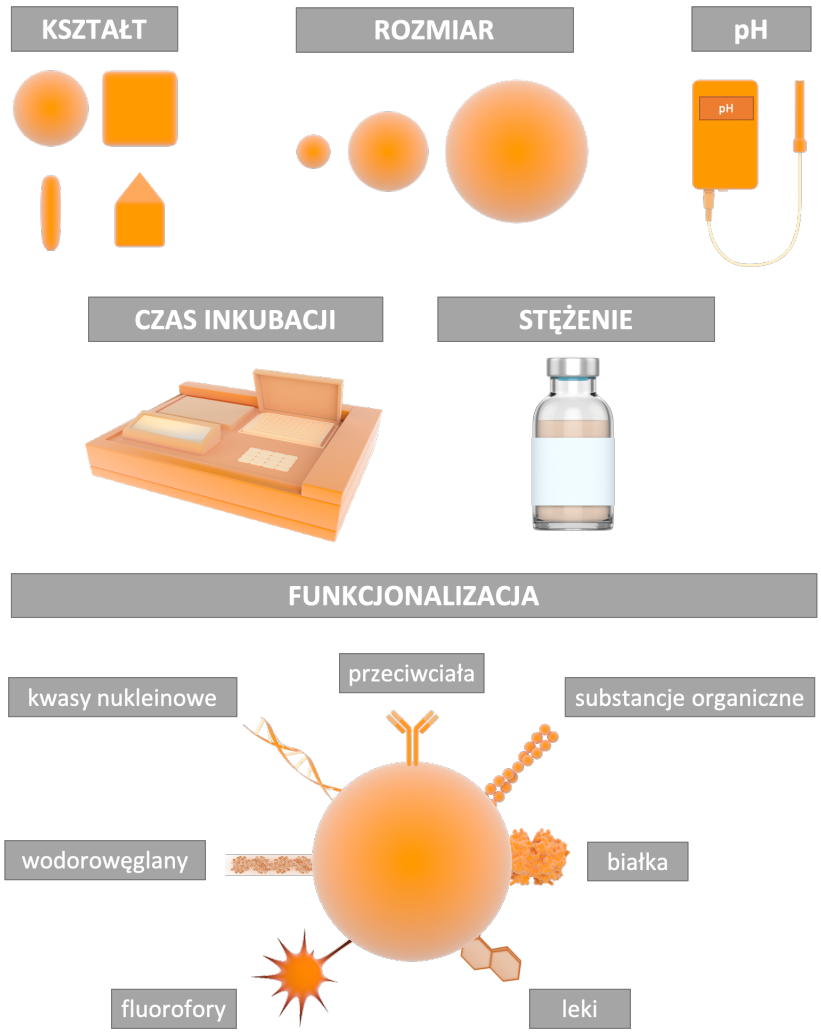

Rycina 4. *Podsumowanie wybranych czynników wpływających na właściwości biologiczne mikrocząstek i nanocząstek*

Mimo niezaprzeczalnego rozwoju medycyny jaki dokonał się w ostatnich dekadach, wciąż nie znaleziono efektywnego sposobu leczenia wielu chorób. Dzięki swoim unikalnym właściwościom, MPs i NPs mogą znaleźć zastosowanie kliniczne. Ponadto, zastosowanie farmaceutyków w skali mikro i nano pozwala na zmniejszenie dawek leku, co przekłada się na obniżenie kosztów terapii jak i jej skutków ubocznych [58, 59]. Choroby nowotworowe i zakażenia, które związane są z postępem cywilizacyjnym i wydłużaniem się średniej długości życia człowieka, są ogromnym wyzwaniem współczesnej medycyny. W ramach badań wchodzących w skład mojej rozprawy doktorskiej, podjąłem próbę odpowiedzi na pytanie jak funkcjonalizacja mikrocząstek i nanocząstek wpływa na ich właściwości przeciwbakteryjne i cytotoksyczne względem komórek nowotworowych. W Polsce i innych krajach rozwiniętych nowotwory stanowią drugą, po chorobach układu sercowo-naczyniowego, przyczynę zgonów [60]. Badania prowadziłem z użyciem modeli komórkowych trzech nowotworów: raka piersi, raka trzustki oraz kostniakomięsaka. Choroby te są ważnymi problem zarówno z epidemiologicznego, jak i ekonomicznego punktu widzenia. Nowotwór piersi jest najczęstszą chorobą nowotworową kobiet [60]. Nowotwór trzustki charakteryzuje się niskim odsetkiem 5-cio letnich przeżycia (ok 6%), a jego leczenie jest kosztowne (>65 tys. USD/pacjenta) [61, 62]. Natomiast kostniakomięsak to trzeci najczęstszy nowotwór populacji pediatrycznej, jednakże może on wystąpić w każdym wieku [63]. Leczenie chemiczne tych nowotworów rzadko pozwala na całkowite wyleczenie, zaś leczenie chirurgiczne jest okaleczające. Ponadto każda z tych metod obarczona jest powikłaniami, które znacząco obniżają jakość życia pacjenta.

Infekcje stanowią częsty problem medyczny, szacuje się że 3-5% pacjentów poddanych operacjom ortopedycznym i nawet 40% pacjentów z wszczepionymi sztucznymi materiałami do układu krążenia boryka się z zakażeniami związanymi z implantami, a tylko w USA roczne koszty leczenia powikłań związanych z implantacjami szacuje się na 3,3 miliarda USD [64, 65].

Dotychczasowe dane literaturowe nie pozwalają w sposób jednoznaczny określić wpływu modyfikacji mikrocząstek i nanocząstek na ich właściwości biologiczne. W związku z tym, konieczne są szczegółowe badania na temat wpływu właściwości fizykochemicznych MPs i NPs na ich aktywność względem komórek prokariotycznych i eukariotycznych (zarówno nowotworowych, jak i nietransformowanych nowotworowo).

III. CELE PRACY

Cel główny:

Ocena wpływu modyfikacji (kształtu, rozmiaru, funkcjonalizacji) nanocząstek i mikrocząstek na ich właściwości biologiczne: cytotoksyczność, właściwości przeciwdrobnoustrojowe oraz potencjalną aktywność przeciwnowotworową w badaniach *in vitro*.

Cele szczegółowe:

1) Ocena wpływu kształtu nanocząstek złota na ich selektywną aktywność cytotoksyczną względem komórek nowotworowych w porównaniu z komórkami nietransformowanymi nowotworowo.
2) Ocena potencjalnych właściwości przeciwnowotworowych sferycznych nanocząstek złota sprzężonych z glutationem i funkcjonalizowanych chemioterapeutykami (doksorubicyną, gemcytabiną, cytarabiną).
3) Ocena wpływu kształtu mikrocząstek fosforanu (V) srebra na ich właściwości przeciwdrobnoustrojowe i cytotoksyczność.
4) Ocena cytotoksycznych efektów oddziaływania nanocząstek i mikrocząstek z nietransformowanymi nowotworowo i nowotworowymi komórkami kości.

IV. MATERIAŁY I METODY

Mikrocząstki i nanocząstki

Nanocząstki złota w kształcie gwiazd, prętów i sfer zostały zsyntezowane przez zespół chemików z Uniwersytetu Gdańskiego pod kierunkiem prof. dr hab. Adriany Zaleskiej-Medynskiej.

Mikrocząstki fosforanu (V) srebra w kształcie: tetrapodalnym, sferycznym, czworościennym, sześciennym, rozgałęzionym oraz dwunastościennym zostały zsyntezowane przez zespół chemików z Uniwersytetu Gdańskiego pod kierunkiem prof. dr hab. Adriany Zaleskiej-Medynskiej.

Nanocząstki złota stabilizowane glutationem i sprzężone z chemioterapeutykami (doksorubicyną, gemcytabiną lub cytarabiną) zostały zsyntezowane przez zespół chemików z Uniwersytetu Warszawskiego pod kierunkiem dr. Michała Wójcika.

Hodowle komórkowe

W badaniach wykorzystano linie komórkowe: ludzkich płodowych osteoblastów (hFOB1.19), mysich preosteoblastów (MC3T3-E1), trzy linie komórkowe kostniakomięsaka (143B, MG63, Saos-2), fibroblastów skóry (HDF), mysich mioblastów (C2C12), ludzkiego raka epitelioidalnego komórek trzustkowych (PANC-1), komórek przewodu trzustkowego (hTERT-HPNE), gruczolakoraka piersi (MCF7) oraz komórek nabłonkowych gruczołu piersiowego (MCF10A). Linie komórkowe hFOB1.19, MC3T3-E1, 143B, MG63, Saos-2, HDF, PANC-1, hTERT-HPNE, MCF7, oraz MCF10A pochodziły z American Type Culture Collection (ATCC), a linia C2C12 z European Collection of Authenticated Cell Cultures (ECACC). Hodowla komórkowa była prowadzona w standardowych warunkach [66–68].

Ocena cytotoksycznego działania mikrocząstek i nanocząstek

Do oceny cytotoksycznego wpływu mikrocząstek i nanocząstek na linie komórkowe wykorzystano testy kolorymetryczne oparte na: (1) pomiarze aktywności metabolicznej komórek (MTT), (2) ilościowym pomiarze syntezy DNA w komórce (BrdU) oraz (3) ocenie zdolności gromadzenia czerwieni obojętnej w lizosomach komórki i integralności błon komórkowych (NR) [69–71].

Ocena internalizacji mikrocząstek i nanocząstek oraz indukowania zmian na poziomie ultrastruktury komórki

Zdolność przenikania przez błonę komórkową, lokalizację na poziomie komórkowym oraz indukowanie zmian na poziomie ultrastrukturalnym przez mikrocząstki i nanocząstki określono za pomocą Transmisyjnej Mikroskopii Elektronowej (TEM). Morfologia komórek była również oceniana za pomocą mikroskopii kontrastowo-fazowej.

Ocena poziomu wewnątrzkomórkowych reaktywnych form tlenu

Poziom wewnątrzkomórkowych reaktywnych form tlenu (ROS) oceniono przy użyciu cytometrii przepływowej z dwuoctananem 2,7 – dichlorofluoresceiny (DCF-DA) i analizowano przy użyciu programu CellQuest Pro.

Analiza cyklu komórkowego

Wpływ mikrocząstek fosforanu (V) srebra na regulację cyklu komórkowego oceniono za pomocą cytometrii przepływowej z barwieniem jodkiem propidyny (PI) i analizowano przy użyciu programu CellQuest Pro.

Oznaczenie całkowitego poziomu białka

Oznaczenie całkowitej zwartości białka w próbkach zostało wykonane metodą Bradforda [72].

Oznaczenie poziomu wybranych białek

Metodą Western-blot określono poziomy białek markerów: apoptozy (Bax, Bcl-2) i stanu zapalnego (MMP1, MMP3, NF-κB), systemu antyoksydacyjnego komórki (SOD1, SOD2, SOD3, GPX4) oraz białek związanych z tworzeniem cytoszkieletu (p16-ARC).

Analiza statystyczna

Analiza statystyczna została przeprowadzona przy użyciu jednoczynnikowej analizy wariancji (one-way ANOVA) i testu post-hoc Tukey'a. Wartość IC_{50} wyznaczono za pomocą analizy nieliniowej regresji log(inhibitor) vs znormalizowana odpowiedź. Analizę statystyczną przeprowadzono w programie GraphPad Prism (przedział ufności = 95%, α=0,05).

V. OMÓWIENIE PUBLIKACJI WCHODZĄCYCH W SKŁAD ROZPRAWY DOKTORSKIEJ

W skład mojej pracy doktorskiej wchodzą cztery prace (trzy oryginalne i jedna poglądowa) opublikowane w międzynarodowych czasopismach indeksowanych na Liście Filadelfijskiej. Artykuły skupiają się na tematyce wpływu modyfikacji na właściwości cytotoksyczne i przeciwbakteryjne nanocząstek i mikrocząstek, ze szczególnym uwzględnieniem komórek kości.

Publikacja 1.

Steckiewicz KP, Inkielewicz-Stępniak I.: *Modified nanoparticles as potential agents in bone diseases: cancer and implant-related complications*; Nanomaterials. 2020; 10:658

Problemy chorób kośćca dotyczą znacznego odsetka populacji, a wraz ze wzrastającą średnia długością życia, liczba osób dotkniętych tymi schorzeniami będzie rosnąć. W pracy dokonaliśmy przeglądu literatury na temat potencjalnej roli nanocząstek w profilaktyce i leczeniu wybranych problemów współczesnej ortopedii: nowotworów oraz powikłań związanych z alloplastykami stawów. Szczególny nacisk położyliśmy na wpływ modyfikacji nanobiomateriałów na ich korzystne właściwości i cytotoksyczność. Uwzględniliśmy również wpływ NPs na nietransformowane nowotworowo komórki kości, w celu określenia ich bezpieczeństwa w zastosowaniu klinicznym.

Publikację rozpoczęliśmy od krótkiego wprowadzenia do tematyki, którą zajmuje się nanotechnologia, zdefiniowaliśmy czym są nanocząstki, a także porównaliśmy ich rozmiar do innych obiektów. Następnie przybliżyliśmy historię nanotechnologii oraz jej współczesne zastosowania.

W głównej części pracy omówiliśmy tematykę nowotworów kości i potencjalną rolę NPs w ich leczeniu. Nanocząstki mogą być bezpośrednio cytotoksyczne względem linii komórkowych kostniakomięsaka, wykazano również ich skuteczność w leczeniu tej choroby w warunkach *in vivo.* Zarówno nieorganiczne jak i organiczne NPs wykazują aktywność przeciwnowotworową, która zależy od rodzaju NPs, ich kształtu, stężenia, a także pH środowiska. NPs mogą wykazywać również aktywność cytotoksyczną względem innych nowotworów kości jakimi są chrzęstniakomięsak, włókniakomięsak,

czy mięsak Ewinga. Warto podkreślić, że nowotworowe linie komórkowe są zazwyczaj bardziej wrażliwe na NPs niż linie nietransformowane nowotworowo. Poza bezpośrednią cytotoksycznością względem komórek nowotworowych, nanocząstki mogą być wykorzystane jako nośniki leków, co jest szczególnie istotne, gdy właściwości fizykochemiczne chemioterapeutyków (np. rozpuszczalność w wodzie) utrudniają ich wykorzystanie praktyczne. Zdolność NPs do akumulacji w mikrośrodowisku guza pozwala zmniejszyć toksyczność i zwiększyć efektywność leczenia. Nanocząstki mogą być sprzęgane z „klasycznymi" chemioterapeutykami (doksorubicyna, etopozyd, cytarabina, gemcytabina i inne), substancjami obecnie nieużywanymi w leczeniu (kurkumina) jak i z kwasami nukleinowymi. Ponadto magnetyczne nanocząstki, dzięki swoim unikatowym właściwościom, mogą być wykorzystane w termoterapii kostniakomięsaka. Warto podkreślić, że skuteczność NPs została wykazana zarówno w badaniach *in vitro* jak i *in vivo.*

W drugiej części publikacji podjęliśmy tematykę problemów, jakie stwarza wprowadzenie implantu do układu szkieletowego, czyli zakażeń i niskiej biokompatybilności. Omówiliśmy fizjologiczne podstawy, które powodują pojawienie się tych problemów, a następnie opisaliśmy jakie nanocząstki mogłyby im potencjalnie zapobiegać. Szereg nanocząstek zwiększa biokompatybilność implantów. Należą do nich między innymi nanocząstki srebra (AgNPs), tytanu, tlenku cynku czy hydroksyapatytu (HA-NPs). NPs mogą być również wykorzystane w medycynie regeneracyjnej do różnicowania komórek kości z komórek macierzystych. Właściwości te posiadają między innymi HA-NPs, AgNPs czy AuNPs. Ponadto NPs mogą wykazywać właściwości przeciwbakteryjne, przeciwgrzybicze, przeciwwirusowe orazprzeciwpasożytnicze. Najlepiej przebadane są pod tym względem AgNPs, ale takie właściwości posiadają między innymi AuNPs, NPs miedzi, NPs tlenków metali, NPs organiczne. Właściwości przeciwdrobnoustrojowe NPs zależą od ich rodzaju, rozmiaru, kształtu oraz funkcjonalizacji.

Publikację zakończyliśmy podsumowaniem danych na temat bezpieczeństwa klinicznego zastosowania nanocząstek. Omówiliśmy ich cytotoksyczność względem nietransformowanych nowotworowo linii komórkowych kości, a także zestawiliśmy te informacje z toksycznością obecnie używanych leków. Opisaliśmy również zdobycze nanotechnologii, które są obecnie dopuszczone do stosowania w medycynie.

Podsumowując, praca stanowi wstęp do dalszych rozważań na temat wpływu modyfikacji biomateriałów na ich właściwości biologiczne, ze szczególnym

uwzględnieniem komórek kości. Wykazaliśmy, że NPs wykazują wiele korzystnych właściwości, które mogą być wykorzystane w chorobach kości. Ponadto opisaliśmy szereg czynników modyfikujących właściwości farmakologiczne i toksykologiczne NPs (rodzaj NPs, kształt NPs, stężenie, czas inkubacji, pH środowiska, funkcjonalizacja, rodzaj substancji stabilizujących i inne). Zgodnie z naszą najlepszą wiedzą, jest to pierwsza publikacja, która w tak szczegółowy sposób omawia niniejszą tematykę.

Publikacja 2.

Steckiewicz KP, Barcińska E, Malankowska A, Zauszkiewicz-Pawlak A, Nowaczyk G, Zaleska-Medynska A, Inkielewicz-Stępniak I.: *Impact of gold nanoparticles shape on their cytotoxicity against human osteoblast and osteosarcoma in in vitro model: evaluation of the safety of use and anti-cancer potential*; J Mater Sci Mater Med. 2019;30(2):22

Mimo dynamicznego rozwoju medycyny, leczenie onkologiczne jest wciąż obarczone poważnymi powikłaniami i dużym odsetkiem niepowodzeń terapeutycznych. Dlatego zdecydowaliśmy się zająć problematyką wpływu modyfikacji NPs na ich potencjalne właściwości przeciwnowotworowe.

W pracy postanowiliśmy ocenić wpływ kształtu nanocząstek złota na ich aktywność cytotoksyczną względem komórek kostniakomięsaka. Zbadaliśmy również wpływ AuNPs w różnych kształtach na nietransformowane nowotworowo linie komórkowe kości.

W publikacji scharakteryzowano i wykorzystano trzy kształty nanocząstek złota: gwiazdy (170 - 260 nm.), pręty (długość ok. 45 nm., szerokość 16 nm.) oraz sfery (średnica 6 - 22 nm.). Badania biologiczne przeprowadziliśmy na liniach komórkowych kostniakomięsaka (143B i MG63) oraz nietransformowanej nowotworowo linii komórkowej ludzkich płodowych osteoblastów (hFOB1.19). Zdecydowaliśmy się na wykorzystanie w eksperymentach dwóch nowotworowych linii komórkowych, ze względu na różnice w ich charakterystyce molekularnej. Linia komórkowa 143B szybciej dokonuje podziałów komórkowych oraz ma większą zdolność do migracji niż linia komórkowa MG63. Ponadto, komórki linii 143B mają większą zdolność do generowania przerzutów odległych. Podsumowując, charakterystyka komórek linii 143B wskazuje, że fenotypowo są one bardziej agresywne.

Po 24 - godzinnej inkubacji komórek z AuNPs, przy użyciu testów MTT i NR, wykazaliśmy zależną od kształtu, stężenia i rodzaju linii komórkowej cytotoksyczność AuNPs. AuNPs w kształcie gwiazd były najbardziej cytotoksyczne, a sferyczne wywierały najmniejszy efekt na żywotność komórek. Ponadto linie komórkowe wykazały różną wrażliwość na badane AuNPs. Linia komórkowa hFOB1.19 była najbardziej oporna na działanie cytotoksyczne AuNPs, a linia komórkowa 143B najmniej. Dowiedliśmy, że obie linie nowotworowe były bardziej wrażliwe na nanocząstki w porównaniu z linią nietransformowaną nowotworowo. Warto podkreślić, że komórki „bardziej agresywnej" linii 143B były również bardziej wrażliwe na NPs. Ponadto metodą Western-blot wykazaliśmy, że AuNPs w kształcie gwiazd i prętów powodują zwiększoną produkcję proapoptotycznego białka Bax i spadek poziomu antyapoptotycznego białka Bcl-2 w komórkach. Analiza zdjęć TEM wykazała, że AuNPs gwiazdy (w stężeniu 10 μg/mL) ulegają internalizacji i lokalizują się w cytoplazmie i jądrze komórkowym, a także powodują zwiększoną wakuolizację komórki. Ponadto nanocząstki te w wyższych stężeniach (50 μg/mL) powodują degradację komórki i przerwanie ciągłości błony komórkowej. Natomiast AuNPs pręty (w stężeniu 10 μg/mL) ulegają internalizacji i lokalizują się w endosomach, a w wysokich stężeniach (50 μg/mL) powodują degradację komórki.

Podsumowując, wykazaliśmy, że efekty biologiczne AuNPs zależą od ich kształtu. Efekt działania nanocząstek zależy również od stężenia i rodzaju linii komórkowych przy wyraźnej różnicy między liniami nowotworowymi i nietransformowanymi nowotworowo. AuNPs obniżają żywotność komórek i mogą powodować ich apoptozę. AuNPs, w kształcie gwiazd mają największą aktywność przeciwnowotworową, a sferyczne AuNPs wykazują najlepszy profil bezpieczeństwa w badaniach *in vitro.* Jako pierwszy zespół na świecie określiliśmy wpływ nanocząstek złota w różnych kształtach na ludzkie płodowe osteoblasty i komórki kostniakomięsaka.

Publikacja 3.

Steckiewicz KP, Barcińska E, Sobczak K, Tomczyk E, Wójcik M, Inkielewicz-Stępniak I.: *Assessment of anti-tumor potential and safety of application of glutathione stabilized gold nanoparticles conjugated with chemotherapeutics;* Int J Med Sci. 2020;17(6)

Na podstawie badań wstępnych oraz wniosków płynących z omówionej wyżej publikacji [68] na temat roli kształtów AuNPs na ich aktywność przeciwnowotworową *in vitro* i profil bezpieczeństwa, do dalszych badań wybraliśmy sferyczne nanocząstki złota. Podjęliśmy próbę oceny możliwości wykorzystania AuNPs jako nośników leków. Połącznie leku z nanocząstką miało na celu poprawę skuteczność terapii, łagodzenie działań niepożądanych i tym samym obniżenie kosztów leczenia. Dodatkowo zdecydowaliśmy się ustabilizować nanocząstki za pomocą GSH, co miało zapewnić stabilniejsze połącznie nanocząstka - lek jak i wpłynąć na poprawę profilu bezpieczeństwa, poprzez zmniejszenie cytotoksyczności względem komórek nietransformowanych nowotworowo.

W pracy oceniliśmy potencjał sferycznych AuNPs stabilizowanych GSH jako platform dostarczania chemioterapeutyków. Określiliśmy wpływ badanych nanocząstek na nowotworowe i nietransformowane nowotworowo linie komórkowe.

W publikacji scharakteryzowano cztery rodzaje sferycznych AuNPs. Sferyczne AuNPs stabilizowane GSH (AuNPs-GSH), sferyczne AuNPs stabilizowane GSH i sprzężone odpowiednio z doksorubicyną (AuNPs-GSH-DOX) cytarabiną (AuNPs-GSH-CTA) oraz z gemcytabiną (AuNPs-GSH-GEM). Byliśmy pierwszym zespołem, na świecie który zsyntetyzował i zbadał właściwości biologiczne AuNPs-GSH-CTA. Badania biologiczne prowadziliśmy na modelach komórkowych: kostniakomięsaka (143B), nowotworu trzustki (PANC1) i nowotworu piersi (MCF7) oraz na liniach komórkowych będących nietransformowanymi nowotworowo odpowiednikami tych tkanek (hFOB1.19, hTERT-HPNE, MCF10A). Porównaliśmy również skuteczność uzyskanych koniugatów nanocząstek i chemioterapeutyków do samych leków. Zdecydowaliśmy się użyć aż sześciu linii komórkowych o różnej charakterystyce molekularnej, co dostarczyło nam informacji na temat wpływu NPs na różne rodzaje komórek i zwiększyło wiarygodność uzyskanych wyników.

Po 24-godzinnej inkubacji koniugatów NPs i leków wykazaliśmy, że ich właściwości biologiczne zależą od: rodzaju chemioterapeutyku, stężenia, oraz typu linii komórkowej. NPs sprzężone z lekami były bardziej cytotoksyczne od AuNPs-GSH, a nowotworowe linie komórkowe były bardziej wrażliwe na działanie NPs w porównaniu z liniami nietransformowanymi nowotworowo. Wykazaliśmy, że w wybranych warunkach NPs mogą być selektywnie cytotoksyczne jedynie wobec komórek nowotworowych, a także być skuteczniejsze od samych chemioterapeutyków.

Uzyskane wyniki sugerują, że połącznie NPs - lek może zmniejszyć toksyczność leczenia, koszty i jednocześnie poprawić skuteczność terapii.

Podsumowując wykazaliśmy, że AuNPs mogą być wykorzystane jako skuteczne nośniki leków przeciwnowotworowych. Ich właściwości zależą od modyfikacji: stabilizacji za pomocą GSH, obecność i rodzaju przyłączanego chemioterapeutyku.

Publikacja 4.

Steckiewicz KP, Zwara J, Jaśkiewicz M, Kowalski S, Kamysz W, Zaleska-Medynska A, Inkielewicz-Stępniak I.: *Shape-depended biological properties of Ag3PO4 microparticles evaluation of antimicrobial properties and cytotoxicity in in vitro model - safety assessment of potential clinical usage;* Oxid Med Cell Longev. 2019; 2019:6740325.

Na podstawie naszych wcześniejszych doświadczeń, podjęliśmy próbę odpowiedzi na pytanie, czy MPs wykorzystane do opracowania nowoczesnych biomateriałów mogą pomóc w rozwiązaniu jednego z ważniejszych problemów nowoczesnej ortopedii – powikłań infekcyjnych związanych z alloplastykami stawów. Ponownie postawiliśmy pytanie, jak modyfikacja MPs (kształt) wpłynie na ich właściwości biologiczne. W badaniach wykorzystaliśmy MPs fosforanu (V) srebra; ich budowa miała zwiększyć biokompatybilność (dzięki obecności fosforu, który jest ważnym elementem budulcowym kości) oraz zapewnić właściwości przeciwdrobnoustrojowe (dzięki obecności srebra, o udowodnionym działaniu przeciwbakteryjnym). Zdecydowaliśmy się zaprojektować MPs, gdyż dzięki swoim nieco większym rozmiarom powinny być mniej cytotoksyczne. Większy rozmiar miał również ograniczyć ich przenikanie do krwiobiegu i powodowanie odległej narządowej toksyczności przy wprowadzaniu do organizmu żywego.

W pracy oceniliśmy wpływ kształtu MPs fosforanu (V) srebra na ich właściwości przeciwdrobnoustrojowe oraz cytotoksyczność względem komórek ssaków, ze szczególnym uwzględnieniem komórek kości. Zaproponowaliśmy również mechanizmy cytotoksyczności MPs fosforanu (V) srebra.

W publikacji opisano metodykę syntezy i scharakteryzowano pod względem fizykochemicznym sześć kształtów MPs fosforanu (V) srebra (SOMPs): sferyczne (s-SOMPs), sześcienne (c-SOMPs), czworościennie (th-SOMPs); dwunastościenne (rd-SOMPs), rozgałęzione (b-SOMPs) oraz tetrapodalne (t-SOPMs).

Badania mikrobiologiczne wykonano na szczepach *Staphylococcus aureus, Staphylococcus aureus (MRSA), Candida albicans* oraz *Aspergillus niger.* Do oceny cytotoksyczność SOMPs wykorzystano linie komórkowe kości (hFOB1.19, MC3T3-E1, Saos-2), mięśni (C2C12) oraz skóry (HDF).

Wykazaliśmy, że właściwości przeciwdrobnoustrojowe SOMPs zależą od ich kształtu oraz rodzaju patogenu. Szczepy grzybicze były bardziej wrażliwe na SOMPs niż bakteryjne. c-SOMPs oraz s-SOMPs wykazywały największą aktywność przeciwdrobnoustrojową. Co ważne, SOMPs były skuteczne zarówno względem planktonicznych form drobnoustrojów jaki i względem biofilmu, jednakże wartości MIC był mniejsze od MBEC.

Cytotoksyczność SOMPs (mierzona testami MTT i BrdU) zależała od ich stężenia, kształtu i rodzaju badanej linii komórkowej. c-SOMPs były najbardziej, a t-SOMPs - najmniej cytotoksyczne. Linia komórkowa hFOB1.19 była najbardziej, a linia C2C12 - najmniej oporna na działanie SOMPs. Warto podkreślić, że SOMPs wykazują aktywność przeciwdrobnoustrojową w stężeniach nietoksycznych dla komórek ssaków. Na podstawie wstępnych wyników badań do dalszych eksperymentów wytypowaliśmy c-SOMPs, s-SOMPs, oraz b-SOMPs. Wykazaliśmy, że SOMPs mogą indukować wewnątrzkomórkową produkcję ROS, a także wpływać na poziom białek systemu antyoksydacyjnego (SOD1, SOD2, SOD3, GPX4), związanych ze stanem zapalnym (MMP1, MMP3, NF-κB) oraz związanych z cytoszkieletem (p16-ARC). Jedynie c-SOMPs miały wpływ na regulację cyklu komórkowego zmniejszając liczbę komórek w fazie G0/G1. Pomimo wpływu na poziom białka związanego z cytoszkieletem, analiza zdjęć TEM nie wykazała zmian w ultrastrukturze komórki. SOMPs nie ulegały również internalizacji.

Podsumowując, właściwości przeciwdrobnoustrojowe i cytotoksyczność SOMPs zależą od ich kształtu. Wykazaliśmy, że cytotoksyczność SOMPs wynika z indukcji stresu oksydacyjnego i stanu zapalnego. Nasze badania dowodzą, że s-SOMPs mają najkorzystniejsze właściwości przeciwdrobnoustrojowe i najlepszy profil bezpieczeństwa w warunkach *in vitro*. Byliśmy pierwszym zespołem na świecie, który zbadał wpływ SOMPs na komórki ssaków.

VI. PODSUMOWANIE

Dzięki ogromnemu postępowi jaki dokonał się w nauce, zdobycze nanotechnologii mogą znaleźć zastosowanie w wielu dziedzinach medycyny między innymi w onkologii i ortopedii. Mikrocząstki i nanocząstki, z uwagi na korzystne spektrum aktywności biologicznej, są wykorzystywane w profilaktyce, diagnostyce i terapii chorób człowieka. Niestety, jak każde inne substancje terapeutyczne i biomateriały, mogą wykazywać działania niepożądane. Pomimo unikalnych właściwości, ze względu na potwierdzoną cytotoksyczność w eksperymentach *in vitro* i *in vivo*, zastosowanie kliniczne mikrocząstek i nanocząstek pozostaje nadal ograniczone.

Badania przeprowadzone w ramach mojej pracy doktorskiej wykazały, że właściwości farmakologiczne oraz cytotoksyczność mikrocząstek i nanocząstek w warunkach *in vitro* zależą od wielu czynników: rodzaju, kształtu, stężenia, rozmiaru oraz funkcjonalizacji. Dowiedliśmy, że aktywność biologiczna jest nierozerwalnie związana z ich właściwościami fizykochemicznymi. Dlatego tak ważne jest dokładne określenie mechanizmów cytotoksyczności MPs i NPs, a także zdefiniowanie czynników determinujących te właściwości. W naszych badaniach skupiliśmy się na ocenie wpływu modyfikacji MPs i NPs na działanie przeciwdrobnoustrojowe i cytotoksyczne, ze szczególnym uwzględnieniem problematyki schorzeń ortopedycznych, co w sposób istotny uzupełniło istniejącą lukę w aktualnej wiedzy. W artykule przeglądowym, uwzględniając najnowsze osiągnięcia naukowe, szczegółowo omówiliśmy znaczenie nanocząstek w rozwiązywaniu problemów współczesnej ortopedii. Natomiast w badaniach eksperymentalnych jako pierwsi na świecie określiliśmy wpływ kształtu nanocząstek złota na ich cytotoksyczność względem linii komórkowych kostniakomięsaka, oceniliśmy potencjał nanocząstek złota stabilizowanych glutationem jako nośnika cytarabiny oraz zbadaliśmy interakcję mikrocząstek fosforanu (V) srebra z liniami komórkowymi w badaniach *in vitro.* Wykazaliśmy, że dzięki unikalnym cechom mikrocząstki i nanocząstki mogą być potencjalnymi substancjami terapeutycznymi lub też służyć do opracowania biomateriałów. Uzyskane przez nas wyniki oraz zebrane dane literaturowe mogą okazać się pomocne w zaprojektowaniu mikrocząstek i nanocząstek zmodyfikowanych w taki sposób, aby zmaksymalizować ich korzystne działania biologiczne i jednocześnie poprawić profil bezpieczeństwa. Mamy nadzieje,

że zdobyta przez nas wiedza umożliwi praktyczne zastosowanie mikrocząstek i nanocząstek metali w leczeniu schorzeń ortopedycznych i onkologicznych człowieka.

Wykorzystanie mikrocząstek i nanocząstek w medycynie może przyczynić się do rozwiązania kluczowych problemów, z którymi boryka się ta dziedzina wiedzy. Odpowiednia modyfikacja mikrocząstek i nanocząstek może wpłynąć na poprawę ich profilu bezpieczeństwa i maksymalizację korzystnych właściwości biologicznych (farmakologicznych). Dużą nadzieje wiąże się z wykorzystaniem mikrocząstek i nanocząstek w chorobach kości: nowotworach i powikłaniach związanych z alloplastykami stawów. Dlatego, przyszłe badania powinny skupić się przede wszystkim na ich modyfikacji, w celu optymalnego wykorzystania w medycynie.

SUMMARY IN ENGLISH

I. LIST OF ABBREVIATIONS

143B	osteosarcoma cell line
AgNPs	silver nanoparticles
ATCC	American Type Cell Culture
AuNPs	gold nanoparticles
AuNPs-GSH	gold nanoparticles stabilized with glutathione
AuNPs-GSH-CTA	gold nanoparticles stabilized with glutathione and conjugated with cytarabine
AuNPs-GSH-DOX	gold nanoparticles stabilized with glutathione and conjugated with doxorubicin
AuNPs-GSH-GEM	gold nanoparticles stabilized with glutathione and conjugated with gemcitabine
b-SOMPs	branched silver orthophosphate microparticles
Bax	proapoptotic protein
Bcl-2	antiapoptotic protein
BrdU	5-bromo-2-deoxyuridine
c-SOMPs	cubic silver orthophosphate microparticles
C2C12	murine myoblast cell line
CTA	cytarabine
DCF-DA	2',7'- dichlorodihydrofluorescein diacetate
DNA	deoxyribonucleic acid
DOX	doxorubicin
ECDCC	European Collection of Authenticated Cell Culture
GEM	gemcitabine
GPX4	glutathione peroxidase 4
GSH	glutathione
HA-NPs	hydroxyapatite nanoparticles
HDF	dermal fibroblast cell line
hTERT-HPNE	human immortalized pancreas ductal cell line
IC_{50}	half maximal inhibitory concentration
IUPAC	International Union of Pure and Applied Chemistry
MBEC	minimal biofilm eradication concentration

MC3T3-E1	mouse preosteoblast cell line
MG-63	osteosarcoma cell line
MIC	minimal inhibitory concentration
MMP1	metalloproteinase 1
MMP3	metalloproteinase 3
MPs	microparticles
MRSA	methicillin-resistant Staphylococcus aureus
MTT	3-(4,5-dimethylthiazol-2-yl)-2,5-diphenyltetrazolium bromide
NF-κB	nuclear factor kappa-light-chain-enhancer of activated B cells
NPs	nanoparticles
NR	neutral red
p16-ARC	actin-related protein 2/3 complex subunit 5
PANC1	pancreatic ductal adenocarcinoma cell line
PEG	poli (ethylene glycol)
PI	propionium iodine
rd-SOMPs	rhombic dodecahedral silver orthophosphate microparticles
ROS	reactive oxygen species
s-SOMPs	spherical silver orthophosphate microparticles
Saos-2	osteosarcoma cell line
SOD1	cytoplasmatic superoxide dismutase [Cu-Zn]
SOD2	mitochondrial superoxide dismutase [Mn]
SOD3	extracellular superoxide dismutase [Cu-Zn]
SOMPs	silver orthophosphate microparticles
t-SOMPs	tetrapod silver orthophosphate microparticles
TEM	transmission electron microscope
th-SOMPs	tetrahedral silver orthophosphate microparticles

II. INTRODUCTION

Modern biomaterials such as microparticles (MPs) and nanoparticles (NPs), due to their unique properties, can be used in the prevention and treatment of human diseases. Research on MPs and NPs is a novel but dynamically developing field of science, as indicated by the growing number of scientific reports. By the end of 2019, over 230,000 field-related articles have been indexed in by PubMed, with a significant increase in their number in the last decade. There is also a significant rise in the number of products with the addition of nanoparticles, which also increases the value of this branch of the industry [1,2]. It should be emphasized that the properties of NPs are much better known than the properties of MPs. However, the differentiation between microparticles and nanoparticles is arbitrary and there is no consensus in scientific terminology. In order to standardize the nomenclature, I used the guidelines of the International Union of Pure and Applied Chemistry (IUPAC), according to which microparticles are structures which size is in the range 10^{-7} - 10^{-4} m, and that of nanoparticles is in the range of 10^{-9} - 10^{-7} m [3]. However, according to the European Commission (Recommendation 2011/696/EU), nanomaterials are those products in which 50% of the numerical particle size distribution has one or more dimensions in the range 1 nm - 100 nm [4]. Nonetheless, there are some exceptions to the above definition such as fullerenes, graphene plates and single-walled carbon nanotubes with at least one dimension below 1 nm [4]. Thus, MPs and NPs are larger than organic molecules (such as DNA and proteins) but smaller than viruses, bacteria, and eukaryotic cells. The small size significantly changes their physicochemical properties in relation to their equivalents in the macro scale. Microparticles and nanoparticles possess favorable properties such as: high surface to volume ratio, ability to penetrate cell membranes and biological barriers, as well as high reactivity [5]. The multidirectional possibilities of NPs' and MPs' functionalization possibilities are also worth mentioning as they significantly amplify their potential for biomedical applications [5]. MPs and NPs are used in biology, chemistry, medicine, environmental protection, genetics, biotechnology and industry [5-8] (Figure 1.).

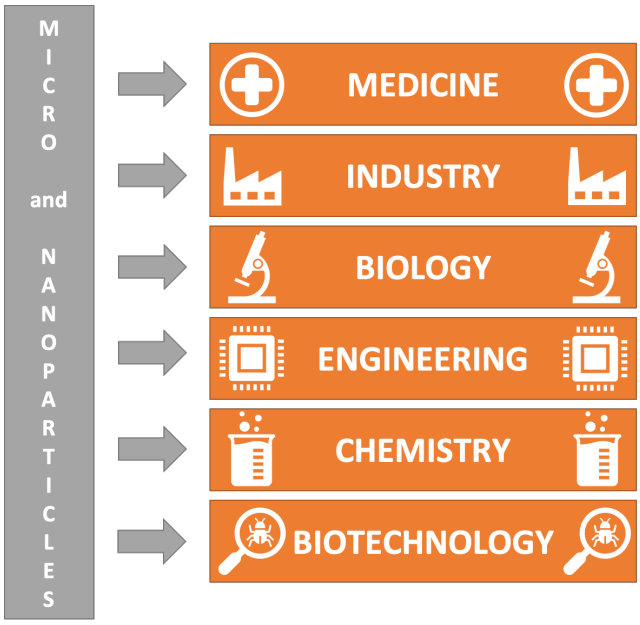

Figure 1. *Practical application of microparticles and nanoparticles [9]*

In the research included in my doctoral dissertation, I used microparticles and nanoparticles of noble metals and their compounds. Silver nanoparticles (AgNPs) exhibit strong antimicrobial, anticancer, anti-aggregating and fibrinolytic properties [9–11]. It is worth emphasizing that AgNPs also show antibacterial activity against biofilm and multi-drug resistant bacterial strains [6,13]. These beneficial features allow for a multidirectional application of nanoparticles, thus AgNPs constitute 30% of NPs produced for commercial purposes [14]. Gold nanoparticles (AuNPs) also have anti-cancer properties and are used in immunotherapy, imaging diagnostics and as biosensors [15–19]. Additionally, AuNPs are used in the diagnosis of diseases, such as tuberculosis [20]. Moreover, AuNPs and AgNPs are widely used as drug delivery platforms [21,22]. Microparticles such as silver phosphate, copper (II) oxide or silver oxide, also exhibit antimicrobial and anticancer properties [23–26]. Both MPs and NPs show a number of favorable biological properties which translates into the possibility of their biomedical use (Figure 2).

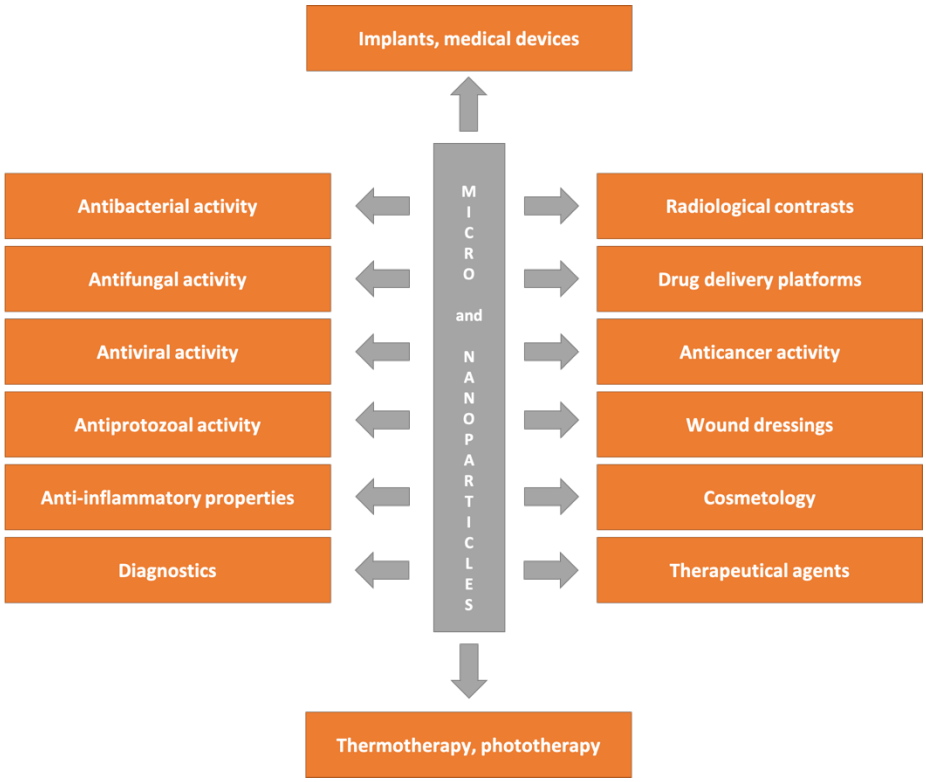

Figure 2. *Potential application of microparticles and nanoparticles in biomedical sciences*

Unfortunately, the clinical application of MPs and NPs is limited due to their not fully explored toxicity and resulting unpredictable risks to human health. Previous studies have shown that both AgNPs and AuNPs can be cytotoxic to human osteoblasts, gingival fibroblast cells, neuronal progenitor cells and macrophages [27–31]. Induction of oxidative stress is one of the main mechanisms of the cytotoxicity of metal NPs, however, pro-inflammatory effects or disturbances in the intracellular calcium levels have also been described [28, 29, 32]. Exposure to NPs may therefore lead to cell death through apoptosis, necroptosis, necrosis or autophagy [33–39]. The mechanisms of the cytotoxicity of MPs are not well understood. Hydroxyapatite microparticles have been shown to be cytotoxic to human macrophages, while silica microparticles to affect breast cancer cells [40,41]. One of the described mechanisms of microparticle cytotoxicity is the induction of oxidative stress and the effect on the regulation of the cell cycle [42,43]. A summary of selected mechanisms of MPs and NPs cytotoxicity at the molecular and cellular level is presented in figure 3.

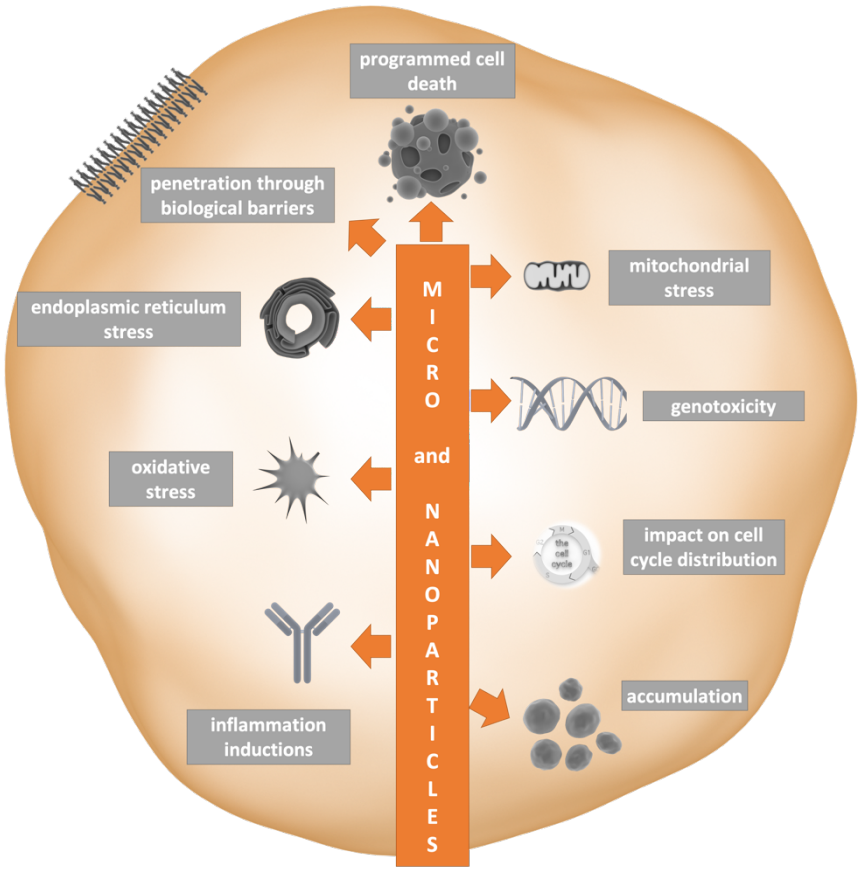

Figure 3. *Selected cytotoxicity mechanisms of microparticles and nanoparticles at the cellular and molecular level*

The beneficial properties and toxicity of MPs and NPs depend on multiple factors. Functionalization of MPs and NPs aims at improving their safety profile without compromising their properties. A number of variables modulate the properties of MPs and NPs: type, size, shape, incubation time, concentration, pH of the environment or surface properties. In addition, the biological properties of MPs and NPs depend on the type of cells exposed to them. A summary of the factors influencing the properties of MPs and NPs is presented in figure 4. Many authors indicate that the smaller MPs and NPs are, the greater their cytotoxicity is [30,42,44]. However, there are studies reporting higher cytotoxicity of MPs and NPs of larger sizes [45]. Similarly, with increasing concentration and incubation time, an increase in cytotoxicity is observed [46–48]. The shape also influences the cytotoxicity of NPs and MPs. Nowadays, the use of MPs and NPs of spherical shape is becoming more prevalent, because it allows for biologically active substances to be attached to their surface [49]. Fluorophores, drugs, antibodies, nucleic acids, proteins, bicarbonates or organic substances such as polyethylene oxide (PEG) or reduced glutathione (GSH) can be attached to the surface

of biomaterials either covalently or non-covalently [50,51]. Functionalization of MPs and NPs with GSH or PEG significantly increases their biocompatibility. In addition, PEG improves water solubility and prevents protein coating, increasing their bloodstream half-life [30]. GSH has strong antioxidant properties, which reduces the oxidative stress related cytotoxicity of MPs and NPs. [30,52]. It has been suggested that the functionalization of NPs with chemotherapeutic agents will allow the creation of biomaterials with better anti-cancer properties than the drugs themselves (in terms of their ability to penetrate tumors and to overcome drug resistance mechanisms) [53–55]. Similarly, the nanoparticles functionalization with antibiotics allows for a synergistic antimicrobial effect [56,57].

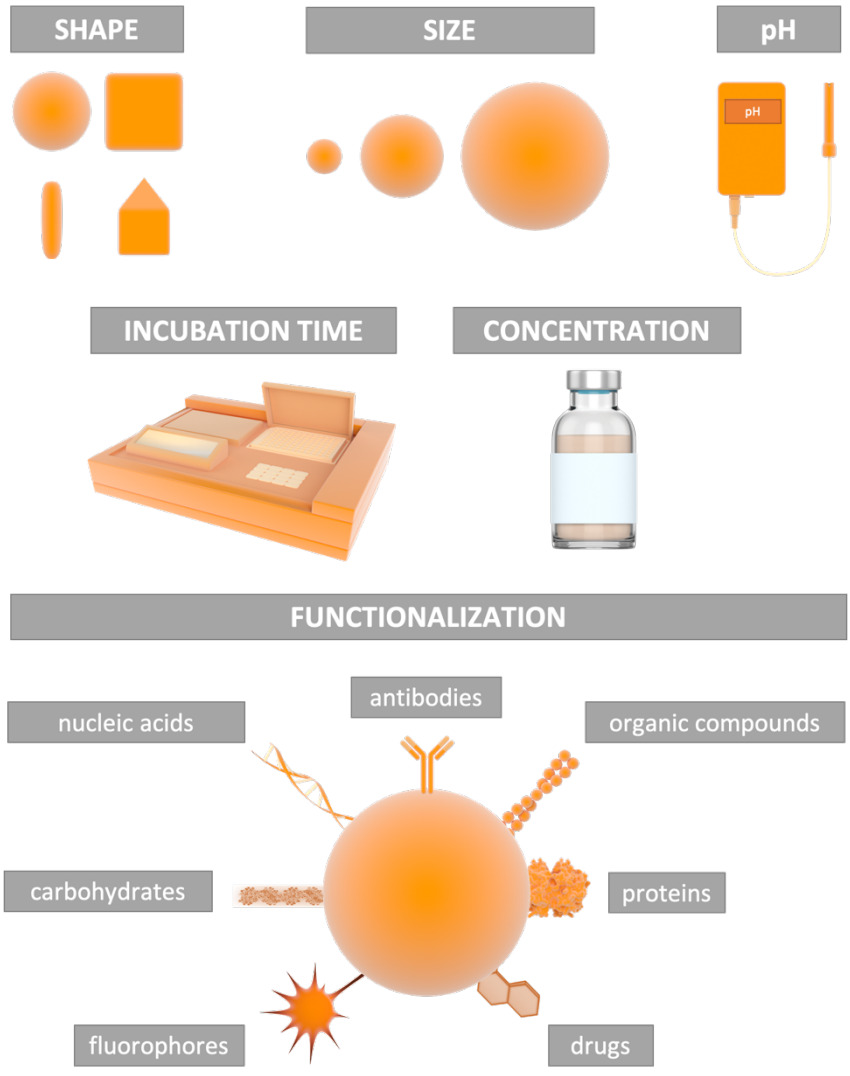

Figure 4. *Summary of selected factors influencing biological properties of microparticles and nanoparticles*

Despite the recent advances in medicine, there is still no effective way to treat many diseases. Thanks to their unique properties, MPs and NPs have the potential for clinical application. Moreover, the use of pharmaceuticals in the micro and nano scale allows the reduction of drugs doses, which reduces the cost and toxicity of the treatment [58, 59]. Due to the development of civilization and the increased life expectancy, cancers and drug-resistant infections are a serious challenge in modern medicine. As part of the research included in my doctoral dissertation, I explored the issue of the functionalization of microparticles, and nanoparticles impact on their antibacterial and cytotoxic properties towards cancer cells. In Poland and other developed countries, cancer is the second cause of death, after cardiovascular diseases. [60] In my research I used cellular models of three cancers: breast cancer, pancreatic cancer, and osteosarcoma. These diseases are important from both an epidemiological and economic point of view. Breast cancer is the most common female neoplasm [60]. Pancreatic cancer has a low 5-year survival rate (about 6%), and its treatment is expensive (> $ 65,000 / patient) [61,62]. Osteosarcoma is the third most common pediatric cancer; nonetheless, it can occur at any age [63]. Chemotherapy rarely allows for a radical treatment of those cancers, and the surgical options are often mutilating. Moreover, each of these methods has complications that significantly reduce the patient's quality of life. Infections are a common medical problem; it is estimated that 3 to 5% of patients after an orthopedic surgery and up to 40% of patients with artificial materials implanted into the circulatory system suffer from implant-related infections. Only in the USA, the annual cost of treating complications related to implantation is estimated at $ 3.3 billion [64,65].

The data from scientific research in this field is still insufficient to clearly determine the influence of modification of microparticles and nanoparticles on their biological properties. Therefore, detailed studies on the influence of the physicochemical properties of MPs and NPs on their activity against prokaryotic and eukaryotic cells (both cancerous and non-cancerous) are necessary.

III. AIM OF THE STUDY

Main aim:

Assessment of the influence of modification (shape, size, functionalization) of nanoparticles and microparticles on their biological properties: cytotoxicity, antimicrobial properties, potential antitumor activity in *in vitro* model.

Specific aims:

1) Assessment of the influence of the shape of gold nanoparticles on their selective cytotoxic activity towards neoplastic cells in comparison to non-transformed cells.
2) Evaluation of the potential anticancer properties of spherical gold nanoparticles stabilized with glutathione and functionalized with chemotherapeutics (doxorubicin, gemcitabine, cytarabine).
3) Assessment of the influence of the shape of silver phosphate (V) microparticles on their antimicrobial properties and cytotoxicity.
4) Evaluation of the cytotoxic effects of interaction of nanoparticles and microparticles with non-transformed and cancer bone cells.

IV. MATERIALS AND METHODS

Microparticles and nanoparticles

Gold nanoparticles in the shape of stars, rods and spheres were synthesized by a team of chemists from the University of Gdańsk under the supervision of prof. dr hab. Adriana Zaleska-Medynska.

Silver phosphate (V) microparticles in the following shapes: tetrapodal, spherical, tetrahedral, cubic, branched and dodecahedron were synthesized by a team of chemists from the University of Gdańsk under the supervision of prof. dr hab. Adriana Zaleska-Medynska.

Gold nanoparticles stabilized with glutathione and conjugated with chemotherapeutic agents (doxorubicin, gemcitabine and cytarabine) were synthesized by a team of chemists from the University of Warsaw under the supervision of dr Michał Wójcik.

Cell culture

The following cell lines were used in the studies: human fetal osteoblasts (hFOB1.19), mouse preosteoblasts (MC3T3-E1), three osteosarcoma cell lines (143B, MG63, Saos-2), skin fibroblasts (HDF), murine myoblasts (C2C12), human pancreatic ductal adenocarcinoma (PANC-1), pancreatic duct cells (hTERT-HPNE), breast adenocarcinoma (MCF7), and breast epithelial cells (MCF10A). hFOB1.19, MC3T3-E1, 143B, MG63, Saos-2, HDF, PANC-1, hTERT-HPNE, MCF7, and MCF10A cell lines were purchased form American Type Culture Collection (ATCC), whereas C2C12 cell line originated form the European Collection of Authenticated Cell Cultures (ECACC). Cell culture was performed under standard conditions [66–68].

Assessment of the cytotoxic effect of microparticles and nanoparticles

To assess the cytotoxic effect of microparticles and nanoparticles on cell lines, colorimetric tests were used, based on: (1) measurement of the metabolic activity of cells (MTT), (2) quantitative measurement of DNA synthesis in the cell (BrdU) and (3) assessment of the ability to accumulate neutral red in lysosomes and cell membrane integrity (NR) [69–71].

Assessment of the internalization of microparticles and nanoparticles and induction of changes in the cell ultrastructure

The ability to penetrate the cell membrane, localization in the cells and induction of changes in the cellular ultrastructure by microparticles and nanoparticles were determined by Transmission Electron Microscopy (TEM). Cell morphology was also assessed by phase-contrast microscopy.

Assessment of intracellular reactive oxygen species levels

Intracellular reactive oxygen species (ROS) levels were assessed with 2,7-dichlorofluorescein diacetate (DCF-DA) staining and measured by flow cytometry. Data were analyzed using the CellQuest Pro software.

Cell cycle analysis

The effect of silver phosphate microparticles on the regulation of the cell cycle was assessed with propidium iodide (PI) staining by flow cytometry and analyzed using the CellQuest Pro software.

Total protein level determination

Bradford method was used to determine total protein level in the samples [72].

Determination of selected proteins levels

The Western-blot method was used to determine the levels of selected proteins; markers of apoptosis (Bax, Bcl-2) and inflammation (MMP1, MMP3, NF-κB), proteins of the antioxidant system of the cell (SOD1, SOD2, SOD3, GPX4), and proteins associated with the formation of the cytoskeleton (p16- ARC).

Statistical analysis

Statistical analysis was performed using one-way ANOVA and Tukey's post-hoc test. The IC_{50} value was determined by log(inhibitor) vs normalized response nonlinear regression analysis. Statistical analysis was performed in GraphPad Prism (confidence interval = 95%, $\alpha = 0.05$).

V. DESCRIPTION OF THE PUBLICATIONS INCLUDED IN THE DOCTORAL THESIS

My doctoral thesis consists of four papers (three original and one review) published in international journals indexed on the ISI Master List. The articles focus on the impact of modification on the cytotoxic and antibacterial properties of nanoparticles and microparticles, with particular emphasis on bone cells.

Publication 1

Steckiewicz KP, Inkielewicz-Stępniak I.: *Modified nanoparticles as potential agents in bone diseases: cancer and implant-related complications*; Nanomaterials. 2020; 10:658

Skeletal system problems affect a significant percentage of the population, and with increasing life expectancy, the number of people affected by these diseases will only increase. In this work, we reviewed the literature on the potential role of nanoparticles in the prevention and treatment of selected problems of modern orthopedics: cancer and arthroplasty related complications. We put particular emphasis on the influence of nanobiomaterials modification on their beneficial properties and cytotoxicity. We also considered the impact of NPs on non-transformed bone cells to determine their safety for potential clinical use.

The publication started with an introduction to the subject of nanotechnology, we defined what nanoparticles are, and we compared their size to other objects. Then we presented the history of nanotechnology and its modern applications.

In the main part of the work, we discussed bone cancers and the potential role of NPs in their treatment. Nanoparticles may be directly cytotoxic to osteosarcoma cell lines and have been shown to be effective in disease treatment in *in vivo* model. Both inorganic and organic NPs exert antitumor activity, which depends on the type of NPs, their shape, concentration, and the pH of the environment. NPs can also show cytotoxic activity against other bone cancers such as chondrosarcoma, fibrosarcoma or Ewing's sarcoma. It is worth noting that tumor cell lines are usually more sensitive to NPs than non-transformed lines. Apart from the direct cytotoxicity to neoplastic cells, nanoparticles can be used as drug carriers, which is particularly important when the physicochemical properties of chemotherapeutic agents

(e.g. water solubility) make their application in clinical practice difficult. The ability of NPs to accumulate in the tumor microenvironment reduces toxicity and increases the effectiveness of treatment. Nanoparticles can be conjugated with "classic" chemotherapeutic agents (doxorubicin, etoposide, cytarabine, gemcitabine, and others), substances currently not used in treatment (curcumin) and with nucleic acids. Moreover, magnetic nanoparticles, owing to their unique properties, can be used in the thermotherapy of osteosarcoma. It is worth noting that the effectiveness of NPs has been demonstrated both *in vitro* and *in vivo*.

In the second part of the publication, we examined issues related to bone implants, i.e. infections and low biocompatibility. We discussed the physiological basis of these problems, and then described how nanoparticles could potentially prevent them. A number of nanoparticles increase the biocompatibility of implants. These include silver nanoparticles (AgNPs), titanium, zinc oxide and hydroxyapatite (HA-NPs). NPs can also be used in regenerative medicine to differentiate bone cells from stem cells. These properties are exhibited by i.a. HA-NPs, AgNPs and AuNPs. Moreover, NPs can present antibacterial, antifungal, antiviral and antiparasitic properties. Properties of AgNPs are most widely documented, but AuNPs, copper NPs, metal oxide NPs, organic NPs, and others also have such properties. The antimicrobial properties of NPs depend on their type, size, shape, and functionalization.

We concluded the publication with a summary of the safety of potential clinical application of nanoparticles. We discussed their cytotoxicity to non-transformed bone cell lines, and we compared this information with the toxicity of currently used drugs. We have also provided information on which nanoproducts are currently approved for use in a clinical setting.

To sum up, the paper is an introduction to further studies on the influence of modification of biomaterials on their biological properties, with particular emphasis on bone cells. We have shown that NPs have a number of beneficial properties that can be used in bone diseases. Moreover, we described numerous factors modifying the pharmacological and toxicological properties of NPs (type of NPs, shape of NPs, concentration, incubation time, environment pH, functionalization, type of stabilizing agent, and others). To the best of our knowledge, this is the first publication that discusses this subject in such a detailed way.

Publication 2

Steckiewicz KP, Barcińska E, Malankowska A, Zauszkiewicz-Pawlak A, Nowaczyk G, Zaleska-Medynska A, Inkielewicz-Stępniak I.: *Impact of gold nanoparticles shape on their cytotoxicity against human osteoblast and osteosarcoma in in vitro model: evaluation of the safety of use and anti-cancer potential*; J Mater Sci Mater Med. 2019;30(2):22

Despite the recent advances in the medicine, oncological treatment is still connected with serious complications and a high percentage of therapeutic failures. Therefore, we decided to address the issue of the influence of NPs modification on their potential anti-cancer properties.

In this work, we decided to assess the influence of the shape of gold nanoparticles on their cytotoxicity towards osteosarcoma cells. We also investigated the effect of AuNPs in various shapes on non-transformed bone cell lines.

Three shapes of gold nanoparticles: stars (170 - 260 nm), rods (length approx. 45 nm, width 16 nm) and spheres (diameter 6 - 22 nm) were synthesized and characterized. In biological studies, we used two osteosarcoma cell lines (143B and MG63) and a non-transformed cell line - human fetal osteoblast cell line (hFOB1.19). We decided to use two cancer cell lines due to the differences in their molecular characteristics. The 143B cell line divides more quickly and migrates faster than the MG63 cell line. Moreover, cells of the 143B cell line have a greater ability to cause distant metastases. In all, the characteristics of the 143B cell line indicate that the cell are phenotypically more aggressive.

We demonstrated the shape-, concentration- and type-dependent cytotoxicity of AuNPs after incubation cells with AuNPs for 24 hours, using MTT and NR assays. AuNPs stars were the most cytotoxic and the spherical ones had the smallest effect on cell viability. Moreover, cell lines show different sensitivity to the tested AuNPs. The hFOB1.19 cell line was the most resistant to the cytotoxic effect of AuNPs, and the 143B cell line was the least resistant one. We found that both tumor cell lines were more sensitive to nanoparticles than the non-transformed cells. It is worth noting that the cells of the "more aggressive" cell line 143B were also more sensitive to NPs. Moreover, we showed via the Western-blot method that the star and rod-shaped AuNPs cause increased production of the pro-apoptotic protein Bax and a decrease in the level of the anti-apoptotic protein Bcl-2 in the cells. The analysis of TEM images showed

that the AuNPs stars (concentration of 10 µg/mL) were internalized and localized in both the cytoplasm and cell nucleus, they also caused increased cell vacuolization. Moreover, higher concentrations (50 µg/mL) of these nanoparticles caused cell degradation and disruption of the cell membrane. On the other hand, AuNPs rods (concentration of 10 µg/mL) were internalized and localized in endosomes, and high concentrations (50 µg/mL) caused cell degradation.

To conclude, we reported that the biological effects of gold nanoparticles are shape dependent. The effect of nanoparticles also depends on their concentration and which type of cell lines is exposed to them, with a clear difference between neoplastic and non-transformed cell lines. AuNPs reduced the viability of cells and could cause their apoptosis. The AuNPs stars had the highest anti-tumor activity, and the AuNPs spheres had the best safety profile in *in vitro* studies. We were the first to describe the effects of gold nanoparticles in various shapes on human fetal osteoblasts and osteosarcoma cells.

Publication 3

Steckiewicz KP, Barcińska E, Sobczak K, Tomczyk E, Wójcik M, Inkielewicz-Stępniak I.: *Assessment of anti-tumor potential and safety of application of glutathione stabilized gold nanoparticles conjugated with chemotherapeutics;* Int J Med Sci. 2020;17(6)

Based on the preliminary research and above-mentioned publication [67] on the role of AuNPs shapes on their *in vitro* anti-tumor activity and safety profile, we chose spherical gold nanoparticles for further research. We have made an attempt to evaluate the possibility of using AuNPs as drug carriers. Conjugating NPs with a drug was supposed to increase the effectiveness of the therapy while reducing its adverse effects and costs. In addition, we decided to stabilize nanoparticles with GSH, to ensure a more stable nanoparticle-drug connection and improve their safety profile by reducing cytotoxicity in non-cancerous cells.

In the study, we assessed the potential of GSH-stabilized spherical AuNPs as delivery platforms for chemotherapeutic agents. We assessed the influence of tested nanoparticles on neoplastic and non-transformed cell lines.

Four types of spherical AuNPs were characterized in the publication. AuNPs stabilized with GSH (AuNPs-GSH), AuNPs stabilized with GSH and conjugated with doxorubicin (AuNPs-GSH-DOX), cytarabine (AuNPs-GSH-CTA) and gemcitabine

(AuNPs-GSH-GEM) respectively. We were the first to synthesize and study the biological properties of AuNPs-GSH-CTA. We conducted biological studies on cellular models of osteosarcoma (143B cell line), pancreatic cancer (PANC1 cell line) and breast cancer (MCF7 cell line), as well as on non-transformed cells (hFOB1.19, hTERT-HPNE, MCF10A cell lines). We also compared the effectiveness of the obtained conjugates of nanoparticles and chemotherapeutic agents to that of doxorubicin, cytarabine, and gemcitabine alone. We decided to use as many as six cell lines with different molecular characteristics, which provided us with information on the influence of NPs on different types of cells and increased the reliability of the obtained results.

The results after 24 hours of incubation of NPs conjugates with cells showed that biological properties of NPs depend on the type of chemotherapeutic agent, concentration, and the type of cell line. NPs conjugated with drugs were more cytotoxic than AuNPs-GSH, and tumor cell lines were more sensitive to the NPs than non-transformed cell lines. We showed that, in selected conditions, NPs may be selectively cytotoxic to cancer cells, and be more effective than chemotherapeutic agents alone. This suggests that conjugating NPs with drugs can reduce the toxicity of the treatment and its cost while improving its effectiveness.

To conclude, we showed that AuNPs can be used as effective carriers of anti-cancer drugs. NPs properties depend on the modification: GSH stabilization, the presence and the type of chemotherapeutic agent.

Publication 4

Steckiewicz KP, Zwara J, Jaśkiewicz M, Kowalski S, Kamysz W, Zaleska-Medynska A, Inkielewicz-Stępniak I.: *Shape-depended biological properties of Ag_3PO_4 microparticles: evaluation of antimicrobial properties and cytotoxicity in in vitro model - safety assessment of potential clinical usage;* Oxid Med Cell Longev. 2019; 2019:6740325.

Based on our previous research, we attempted to answer the question of whether MPs used to develop modern biomaterials can help solve one of the most important problems of modern orthopedics – infections as a surgery-related complication after arthroplasty. Again, we tried to determine whether the modification of MPs regarding their shape would affect their biological properties. In the research, we used silver

orthophosphate MPs in order to maximize their biocompatibility (the presence of phosphorus, which is an important compound of bones) and provide antimicrobial properties (the presence of silver). We decided to use the shape of MPs as a variable because larger particles should be less cytotoxic, and more limited in their ability to penetrate into the bloodstream and therefore express distant toxicity when introduced into a living organism.

In the study, we assessed the influence of the shape of silver orthophosphate MPs on their antimicrobial properties and cytotoxicity against mammalian cells, with particular emphasis on bone cells. We also suggested the mechanisms of cytotoxicity of silver orthophosphate microparticles.

The publication describes the methodology of synthesis and physicochemical characteristics of six shapes of silver orthophosphate MPs (SOMPs): spherical (s-SOMPs), cubic (c-SOMPs), tetrahedral (th-SOMPs); dodecahedrons (rd-SOMPs), branched (b-SOMPs), and tetrapodal (t-SOPMs). Microbiological analyses were performed on *Staphylococcus aureus, Staphylococcus aureus* (MRSA)*, Candida albicans* and *Aspergillus niger strains*. Bone (hFOB1.19, MC3T3-E1, Saos-2), muscle (C2C12) and skin (HDF) cell lines were used to assess the cytotoxicity of SOMPs.

We showed that the antimicrobial properties of SOMPs depend on their shape and the type of pathogen. The fungal strains were more sensitive to SOMPs than the bacterial ones. c-SOMPs and s-SOMPs showed the highest antimicrobial activity. Importantly, SOMPs were effective against both planktonic forms of microbes and biofilm, however, the MIC values were lower than MBEC.

Cytotoxicity of SOMPs (measured by MTT and BrdU tests) depended on their concentration, shape, and type of the tested cell line. c-SOMPs were the most cytotoxic and t-SOMPs the least. The hFOB1.19 cell line was the most and C2C12 cell line was the least resistant to the SOMPs. It is worth emphasizing that SOMPs exhibit antimicrobial activity at concentrations that are non-toxic to mammalian cells. Based on the preliminary results, we selected c-SOMPs, s-SOMPs, and b-SOMPs for further experiments. We showed that SOMPs can increase intracellular ROS production as well as affect the levels of antioxidant system proteins (SOD1, SOD2, SOD3, GPX4), inflammation related (MMP1, MMP3, NF-κB) and cytoskeleton (p16-ARC) proteins. The regulation of the cell cycle was only influenced by c-SOMPs, which reduced the number of cells in the G0/G1 phase. Despite the effect on cytoskeleton-

related proteins, the analysis of TEM images showed no changes in cell ultrastructure; SOMPs were not internalized either.

To sum up, the antimicrobial properties and cytotoxicity of SOMPs depend on their functionalization (shape). We showed that the cytotoxicity of SOMPs was related to the induction of oxidative stress and inflammation. Our research showed that s-SOMPs had the best antimicrobial properties and the best safety profile in *in vitro* conditions. We were the first team in the world to investigate the effects of SOMPs on mammalian cells.

VI. CONCLUSION

Thanks to the enormous progress that has been made in science, the achievements of nanotechnology can be applied in many fields of medicine, including oncology and orthopedics. Microparticles and nanoparticles, thanks to their spectrum of beneficial biological activity, are used in the prevention, diagnostics and therapy of human diseases. Unfortunately, like any other therapeutic agents and biomaterials, microparticles and nanoparticles exhibit adverse effects. Despite their unique advantageous properties, their cytotoxicity confirmed by *in vitro* and *in vivo* tests severely limits the clinical application of microparticles and nanoparticles.

Research included in my PhD dissertation has shown that the properties of microparticles and nanoparticles depend on many factors: their type, shape, concentration, size, and functionalization. Therefore, we proved that the biological activity of microparticles and nanoparticles is inextricably linked with their physicochemical properties Thus, it is important to precisely define the mechanisms of cytotoxicity of examined microparticles and nanoparticles and to define the factors modifying their properties. In our research, we focused on the assessment of the influence of their modification on the antimicrobial and cytotoxic properties, with particular emphasis on orthopedic diseases, which significantly reduced the existing gap in the current knowledge. In the review article, taking into account the latest scientific achievements, we discussed in detail the potential role of nanoparticles in solving problems of modern orthopedics. In experimental research we were the first to: determine the influence of the shape of gold nanoparticles on their cytotoxicity against osteosarcoma cell lines, investigate the potential of glutathione stabilized gold nanoparticles as a carriers of cytarabine and examined interaction of silver phosphate (V) microparticles with cell lines *in vitro*. We showed that thanks to their unique properties, the microparticles and nanoparticles can potentially be therapeutic substances. The results and knowledge we gained will enable us to create microparticles and nanoparticles modified to maximize their beneficial biological effects while improving their safety profile. We hope that this knowledge will facilitate the practical application of metal microparticles and nanoparticles and their compounds in the future treatment of orthopedic and oncological diseases.

The use of microparticles and nanoparticles in medicine can contribute to solving the key problems faced by this field of knowledge. Appropriate modification of microparticles and nanoparticles may improve their safety profile and maximize their beneficial biological (pharmacological) properties. There are high hopes for the use of microparticles and nanoparticles in bone diseases: cancer and alloplastic joint complications. Therefore, future research should primarily focus on finding their optimal modifications for medical application.

WYKAZ CYTOWANEGO PIŚMIENNICTWA

/

BIBLIOGRAPHY

[1] Vance, M.E., Kuiken, T., Vejerano, E.P., McGinnis, S.P., et al., Nanotechnology in the real world: Redeveloping the nanomaterial consumer products inventory. *Beilstein J. Nanotechnol.* 2015, *6*, 1769–1780.

[2] Charitidis, C.A., Georgiou, P., Koklioti, M.A., Trompeta, A.F., et al., Manufacturing nanomaterials: From research to industry. *Manuf. Rev.* 2014, *1*, 11.

[3] Vert, M., Doi, Y., Hellwich, K.H., Hess, M., et al., Terminology for biorelated polymers and applications (IUPAC recommendations 2012). *Pure Appl. Chem.* 2012, *84*, 377–410.

[4] Commission Recommendation of 18 October 2011 on the definition of nanomaterial Text with EEA relevance OJ L 275, 20.10.2011, p. 38–40 (BG, ES, CS, DA, DE, ET, EL, EN, FR, IT, LV, LT, HU, MT, NL, PL, PT, RO, SK, SL, FI, SV. *Eur. Comm.* 2011.

[5] Rai, M., Ingle, A.P., Birla, S., Yadav, A., et al., Strategic role of selected noble metal nanoparticles in medicine. *Crit. Rev. Microbiol.* 2015, *00*, 1–24.

[6] Dos Santos, C.A., Seckler, M.M., Ingle, A.P., Gupta, I., et al., Silver nanoparticles: Therapeutical uses, toxicity, and safety issues. *J. Pharm. Sci.* 2014, *103*, 1931–1944.

[7] Selvaraj, M., Pandurangan, P., Ramasami, N., Rajendran, S.B., et al., Highly potential antifungal activity of quantum-sized silver nanoparticles against Candida albicans. *Appl. Biochem. Biotechnol.* 2014, *173*, 55–66.

[8] Niska, K., Zielinska, E., Radomski, M.W., Inkielewicz-Stepniak, I., Metal nanoparticles in dermatology and cosmetology: Interactions with human skin cells. *Chem. Biol. Interact.* 2018, *295*, 38–51.

[9] Steckiewicz, K.P., Inkielewicz-Stepniak, I., Modified Nanoparticles as Potential Agents in Bone Diseases: Cancer and Implant-Related Complications. *Nanomaterials* 2020, *10*, 658.

[10] Niska, K., Knap, N., Kędzia, A., Jaskiewicz, M., et al., Capping Agent-Dependent Toxicity and Antimicrobial Activity of Silver Nanoparticles: An In Vitro Study. Concerns about Potential Application in Dental Practice. *Int. J. Med. Sci.* 2016, *13*, 772–782.

[11] Hajtuch, J., Hante, N., Tomczyk, E., Wojcik, M., et al., Effects of functionalized silver nanoparticles on aggregation of human blood platelets. *Int. J. Nanomedicine* 2019, *14*, 7399–7417.

[12] Sharma, H., Mishra, P.K., Talegaonkar, S., Vaidya, B., Metal nanoparticles: A theranostic nanotool against cancer. *Drug Discov. Today* 2015, *20*, 1143–1151.

[13] Wu, D., Fan, W., Kishen, A., Gutmann, J.L., et al., Evaluation of the antibacterial efficacy of silver nanoparticles against Enterococcus faecalis biofilm. *J. Endod.* 2014, *40*, 285–290.

[14] Skalska, J., Strużyńska, J., Toxic effects of silver nanoparticles in mammals - does a risk of neurotoxicity exist? *Folia Neuropathol.* 2015, *53*, 281–300.

[15] Lee, U., Yoo, C.-J., Kim, Y.-J., Yoo, Y.-M., Cytotoxicity of gold nanoparticles in human neural precursor cells and rat cerebral cortex. *J. Biosci. Bioeng.* 2016, *121*, 341–344.

[16] Tripathi, R.M., Shrivastav, A., Shrivastav, B.R., Biogenic gold nanoparticles: As a potential candidate for brain tumor directed drug delivery. *Artif. Cells, Nanomedicine, Biotechnol.* 2014, 1–7.

[17] Kafshdooz, L., Kafshdooz, T., Razban, Z., Akbarzadeh, A., The application of gold nanoparticles as a promising therapeutic approach in breast and ovarian cancer. *Artif. Cells, Nanomedicine, Biotechnol.* 2015, 1–6.

[18] Ahn, S., Lee, I.H., Kang, S., Kim, D., et al., Gold nanoparticles displaying tumor-associated self-antigens as a potential vaccine for cancer immunotherapy. *Adv. Healthc. Mater.* 2014, *3*, 1194–1199.

[19] Banu, H., Sethi, D.K., Edgar, A., Sheriff, A., et al., Doxorubicin loaded polymeric gold nanoparticles targeted to human folate receptor upon laser photothermal therapy potentiates chemotherapy in breast cancer cell lines. *J. Photochem. Photobiol. B Biol.* 2015, *149*, 116–128.

[20] Hussain, M.M., Samir, T.M., Azzazy, H.M.E., Unmodified gold nanoparticles for direct and rapid detection of Mycobacterium tuberculosis complex. *Clin. Biochem.* 2013, *46*, 633–637.

[21] Ravindra, S., Mulaba-Bafubiandi, A.F., Rajinikanth, V., Varaprasad, K., et al., Development and Characterization of Curcumin Loaded Silver Nanoparticle Hydrogels for Antibacterial and Drug Delivery Applications. *J. Inorg. Organomet. Polym. Mater.* 2012, *22*, 1254–1262.

[22] Khan, A.K., Rashid, R., Murtaza, G., Zahra, A., Gold nanoparticles: Synthesis and applications in drug delivery. *Trop. J. Pharm. Res.* 2014, *13*, 1169–1177.

[23] Chudobova, D., Cihalova, K., Dostalova, S., Ruttkay-Nedecky, B., et al., Comparison of the effects of silver phosphate and selenium nanoparticles on Staphylococcus aureus growth reveals potential for selenium particles to prevent infection. *FEMS Microbiol. Lett.* 2014, *351*, 195–201.

[24] Liu, J.K., Luo, C.X., Wang, J.D., Yang, X.H., et al., Controlled synthesis of silver phosphate crystals with high photocatalytic activity and bacteriostatic activity. *CrystEngComm* 2012, *14*, 8714–8721.

[25] Yeo, B.E., Seo, Y., Park, H., Huh, Y.D., Facet effect of Ag3PO4 crystals on antibacterial activities. *Bull. Korean Chem. Soc.* 2015, *36*, 1904–1907.

[26] Nair, S., Sasidharan, A., Divya Rani, V. V., Menon, D., et al., Role of size scale of ZnO nanoparticles and microparticles on toxicity toward bacteria and osteoblast cancer cells, in: *Journal of Materials Science: Materials in Medicine*, J Mater Sci Mater Med, 2009.

[27] Zielinska, E., Tukaj, C., Radomski, M.W., Inkielewicz-Stepniak, I., Molecular Mechanism of Silver Nanoparticles-Induced Human Osteoblast Cell Death: Protective Effect of Inducible Nitric Oxide Synthase Inhibitor. *PLoS One* 2016, *11*, e0164137.

[28] Inkielewicz-Stepniak, I., Santos-Martinez, M.J., Medina, C., Radomski, M.W., Pharmacological and toxicological effects of co-exposure of human gingival fibroblasts to silver nanoparticles and sodium fluoride. *Int. J. Nanomedicine* 2014, *9*, 1677–1687.

[29] Carlson, C., Hussein, S.M., Schrand, A.M., Braydich-Stolle, L.K., et al., Unique cellular interaction of silver nanoparticles: Size-dependent generation of reactive oxygen species. *J. Phys. Chem. B* 2008, *112*, 13608–13619.

[30] Pan, Y., Neuss, S., Leifert, A., Fischler, M., et al., Size-dependent cytotoxicity of gold nanoparticles. *Small* 2007, *3*, 1941–1949.

[31] Soenen, S.J., Manshian, B., Montenegro, J.M., Amin, F., et al., Cytotoxic effects of gold nanoparticles: A multiparametric study. *ACS Nano* 2012, *6*, 5767–5783.

[32] Asharani, P. V, Hande, M.P., Valiyaveettil, S., Anti-proliferative activity of silver nanoparticles. *BMC Cell Biol.* 2009, *10*, 65.

[33] Lee, Y.H., Cheng, F.Y., Chiu, H.W., Tsai, J.C., et al., Cytotoxicity, oxidative stress, apoptosis and the autophagic effects of silver nanoparticles in mouse embryonic fibroblasts. *Biomaterials* 2014, *35*, 4706–4715.

[34] Cifti, H., Turk, M., Tamer, U., Karahan, S., et al., Silver nanoparticles: Cytotoxic, apoptotic, and necrotic effects on MCF-7 cells. *Turkish J. Biol.* 2013, *37*, 573–581.

[35] Sathishkumar, M., Pavagadhi, S., Mahadevan, A., Balasubramanian, R., Biosynthesis of gold nanoparticles and related cytotoxicity evaluation using A549 cells. *Ecotoxicol. Environ. Saf.* 2015, *114*, 232–40.

[36] Lee, J.S., Murphy, W.L., Functionalizing calcium phosphate biomaterials with antibacterial silver particles. *Adv. Mater.* 2013, *25*, 1173–1179.

[37] Selim, M.E., Hendi, A.A., Gold nanoparticles induce apoptosis in MCF-7 human breast cancer cells. *Asian Pacific J. Cancer Prev.* 2012, *13*, 1617–1620.

[38] Pan, Y., Leifert, A., Ruau, D., Neuss, S., et al., Gold nanoparticles of diameter 1.4 nm trigger necrosis by oxidative stress and mitochondrial damage. *Small* 2009, *5*, 2067–2076.

[39] Li, J.J., Hartono, D., Ong, C.N., Bay, B.H., et al., Autophagy and oxidative stress associated with gold nanoparticles. *Biomaterials* 2010, *31*, 5996–6003.

[40] Motskin, M., Wright, D.M., Muller, K., Kyle, N., et al., Hydroxyapatite nano and microparticles: Correlation of particle properties with cytotoxicity and biostability. *Biomaterials* 2009, *30*, 3307–3317.

[41] He, Q., Zhang, Z., Gao, Y., Shi, J., et al., Intracellular localization and cytotoxicity of spherical mesoporous silica nano-and microparticles. *Small* 2009, *5*, 2722–2729.

[42] Santos, H.A., Riikonen, J., Salonen, J., Mäkilä, E., et al., In vitro cytotoxicity of porous silicon microparticles: Effect of the particle concentration, surface chemistry and size. *Acta Biomater.* 2010, *6*, 2721–2731.

[43] Chinde, S., Poornachandra, Y., Panyala, A., Kumari, S.I., et al., Comparative study of cyto- and genotoxic potential with mechanistic insights of tungsten oxide nano- and microparticles in lung carcinoma cells. *J. Appl. Toxicol.* 2018, *38*, 896–913.

[44] Gliga, A.R., Skoglund, S., Odnevall Wallinder, I., Fadeel, B., et al., Size-dependent cytotoxicity of silver nanoparticles in human lung cells: The role of cellular uptake, agglomeration and Ag release. *Part. Fibre Toxicol.* 2014, *11*, 1–17.

[45] Vetten, M.A., Tlotleng, N., Tanner Rascher, D., Skepu, A., et al., Label-free in vitro toxicity and uptake assessment of citrate stabilised gold nanoparticles in three cell lines. *Part. Fibre Toxicol.* 2013, *10*, 1–15.

[46] Prabhu, B.M., Ali, S.F., Murdock, R.C., Hussain, S.M., et al., Copper nanoparticles exert size and concentration dependent toxicity on somatosensory neurons of rat. *Nanotoxicology* 2010, *4*, 150–160.

[47] Paknejadi, M., Bayat, M., Salimi, M., Razavilar, V., Concentration-and time-dependent cytotoxicity of silver nanoparticles on normal human skin fibroblast cell line. *Iran. Red Crescent Med. J.* 2018, *20*.

[48] Vujačić, A., Vodnik, V., Joksić, G., Petrović, S., et al., Particle size and concentration dependent cytotoxicity of citrate capped gold nanoparticles. *Dig. J. Nanomater. Biostructures* 2011, *6*, 1367–1376.

[49] Truong, N.P., Whittaker, M.R., Mak, C.W., Davis, T.P., The importance of nanoparticle shape in cancer drug delivery. *Expert Opin. Drug Deliv.* 2015, *12*, 129–142.

[50] Cobley, C.M., Chen, J., Chul Cho, E., Wang, L. V., et al., Gold nanostructures: A class of multifunctional materials for biomedical applications. *Chem. Soc. Rev.* 2011, *40*, 44–56.

[51] Conde, J., Dias, J.T., Grazú, V., Moros, M., et al., Revisiting 30 years of biofunctionalization and surface chemistry of inorganic nanoparticles for nanomedicine. *Front. Chem.* 2014, *2*.

[52] Dreaden, E.C., Alkilany, A.M., Huang, X., Murphy, C.J., et al., The golden age: Gold nanoparticles for biomedicine. *Chem. Soc. Rev.* 2012, *41*, 2740–2779.

[53] Susa, M., Iyer, A.K., Ryu, K., Hornicek, F.J., et al., Doxorubicin loaded polymeric nanoparticulate delivery system to overcome drug resistance in osteosarcoma. *BMC Cancer* 2009, *9*, 399.

[54] Wang, B., Yu, X.C., Xu, S.F., Xu, M., Paclitaxel and etoposide co-loaded polymeric nanoparticles for the effective combination therapy against human osteosarcoma. *J. Nanobiotechnology* 2015, *13*, 22.

[55] Manivasagan, P., Bharathiraja, S., Bui, N.Q., Jang, B., et al., Doxorubicin-loaded fucoidan capped gold nanoparticles for drug delivery and photoacoustic imaging. *Int. J. Biol. Macromol.* 2016, *91*, 578–588.

[56] Zhang, L., Pornpattananangkul, D., Hu, C.-M., Huang, C.-M., Development of Nanoparticles for Antimicrobial Drug Delivery. *Curr. Med. Chem.* 2010, *17*, 585–594.

[57] Hallaj-Nezhadi, S., Hassan, M., Nanoliposome-based antibacterial drug delivery. *Drug Deliv.* 2015, *22*, 581–589.

[58] Giljohann, D.A., Seferos, D.S., Daniel, W.L., Massich, M.D., et al., Gold nanoparticles for biology and medicine. *Angew. Chemie - Int. Ed.* 2010, *49*, 3280–3294.

[59] Doane, T.L., Burda, C., The unique role of nanoparticles in nanomedicine: Imaging, drug delivery and therapy. *Chem. Soc. Rev.* 2012, *41*, 2885–2911.

[60] Siegel, R.L., Miller, K.D., Jemal, A., Cancer statistics, 2019. *CA. Cancer J. Clin.* 2019, *69*, 7–34.

[61] Du, W., Touchette, D., Vaitkevicius, V., Peters, W., et al., Cost Analysis of Pancreatic Carcinoma Treatment. *Cnacer* 2000, *89*, 1917–1924.

[62] Rahib, L., Smith, B.D., Aizenberg, R., Rosenzweig, A.B., et al., Projecting cancer incidence and deaths to 2030: The unexpected burden of thyroid, liver, and pancreas cancers in the united states. *Cancer Res.* 2014, *74*, 2913–2921.

[63] Luetke, A., Meyers, P.A., Lewis, I., Juergens, H., Osteosarcoma treatment - Where do we stand? A state of the art review. *Cancer Treat. Rev.* 2014, *40*, 523–532.

[64] Van de Belt, H., Neut, D., Schenk, W., Van Horn, J.R., et al., Infection of orthopedic implants and the use of antibiotic-loaded bone cements. *Acta Orthop. Scand.* 2001, *72*, 557–571.

[65] Darouiche, R.O., Treatment of infections associated with surgical implants. *N. Engl. J. Med.* 2004, *350*, 1422–1429.

[66] Steckiewicz, K.P., Zwara, J., Jaskiewicz, M., Kowalski, S., et al., Shape-Depended Biological Properties of Ag 3 PO 4 Microparticles : Evaluation of Antimicrobial Properties and Cytotoxicity in In Vitro Model — Safety Assessment of Potential Clinical Usage. *Oxid. Med. Cell Longev* 2019, *2019*, 1–19.

[67] Steckiewicz, K.P., Barcińska, E., Sobczak, K., Tomczyk, E., et al., Assessment of anti-tumor potential and safety of application of glutathione stabilized gold nanoparticles conjugated with chemotherapeutic. *Int. J. Med. Sci.* 2020, *17*, 824–833.

[68] Steckiewicz, K.P., Barcinska, E., Malankowska, A., Zauszkiewicz-Pawlak, A., et al., Impact of gold nanoparticles shape on their cytotoxicity against human osteoblast and osteosarcoma in in vitro model . Evaluation of the safety of use and anti-cancer potential. *J. Mater. Sci. Mater. Med.* 2019, *30*, 1–15.

[69] Muir, D., Varon, S., Manthorpe, M., An enzyme-linked immunosorbent assay for bromodeoxyuridine incorporation using fixed microcultures. *Anal. Biochem.* 1990, *185*, 377–382.

[70] Mosmann, T., Rapid colorimetric assay for cellular growth and survival: Application to proliferation and cytotoxicity assays. *J. Immunol. Methods* 1983, *65*, 55–63.

[71] Borenfreund, E., Puerner, J.A., A simple quantitative procedure using monolayer cultures for cytotoxicity assays (HTD/NR-90). *J. Tissue Cult. Methods* 1985, *9*, 7–9.

[72] Bradford, M.M., A rapid and sensitive method for the quantitation of microgram quantities of protein utilizing the principle of protein-dye binding. *Anal. Biochem.* 1976, *72*, 248–254.

PUBLIKACJE WCHODZĄCE W SKŁAD ROZPRAWY DOKTORSKIEJ

/

MANUSCRIPTS INCLUDED IN THE DOCTORAL DISSERTATION

nanomaterials

MDPI

Review

Modified Nanoparticles as Potential Agents in Bone Diseases: Cancer and Implant-Related Complications

Karol P. Steckiewicz and Iwona Inkielewicz-Stepniak *

Chair and Department of Medical Chemistry, Faculty of Medicine, Medical University of Gdansk, ul. Dębinki 1, 80-211 Gdansk, Poland; karol.steckiewicz@gumed.edu.pl

* Correspondence: iinkiel@gumed.edu.pl

Received: 9 March 2020; Accepted: 30 March 2020; Published: 1 April 2020

Abstract: Materials sized 1–100 nm are the nanotechnology's field of interest. Because of the unique properties such as the ability to penetrate biological barriers and a high surface to volume ratio, nanoparticles (NPs) are a powerful tool to be used in medicine and industry. This review discusses the role of nanotechnology in bone-related issues: osteosarcoma (bone cancer), the biocompatibility of the implants and implant-related infections. In cancer therapy, NPs can be used as (I) cytotoxic agents, (II) drug delivery platforms and (III) in thermotherapy. In implant-related issues, NPs can be used as (I) antimicrobial agents and (II) adjuvants to increase the biocompatibility of implant surface. Properties of NPs depend on (I) the type of NPs, (II) their size, (III) shape, (IV) concentration, (V) incubation time, (VI) functionalization and (VII) capping agent type.

Keywords: nanotechnology; nanoparticles; osteosarcoma; antimicrobial properties; nanotoxicology; biocompatibility; bone diseases; implant-related infections

1. Introduction

Miniaturisation affects every aspect of human life; medicine and science are no exceptions. Nanotechnology is interested in particles within the 1–100 nm size range [1]. For a better understanding of the size range in Figure 1 we compare nano size to other objects. Although it was Richard Zsigmondy who used the term 'nanometre' as early as in 1925, Richard Feynman is the indisputable father of nanotechnology [1]. In 1959 he gave a lecture entitled 'There's Plenty Room at the Bottom' and suggested that manipulation on the atomic level would soon be possible. However, the term 'nanotechnology' was unknown until the seventies. Norio Taniguchi is thought to be the first to use it [1]. Almost a century after its beginning, nanotechnology is a rapidly developing branch of science. In 2015, nontechnology industry employed 7 million people and was worth $1 billion [2,3]. Nanoscale, because of quantum effects, causes nanoparticles (NPs) to have different properties than macromolecules. NPs have a large surface to volume ratio, and the ability to penetrate cellular membranes and structural barriers, which greatly expand its potential applications [4]. NPs are used in biology, genetic engineering, medicine, biotechnology and industry (Figure 2) [4–6]. Moreover, the ability to modify NPs (size, shape, surface functionalisation, capping agent) increases their potential [4].

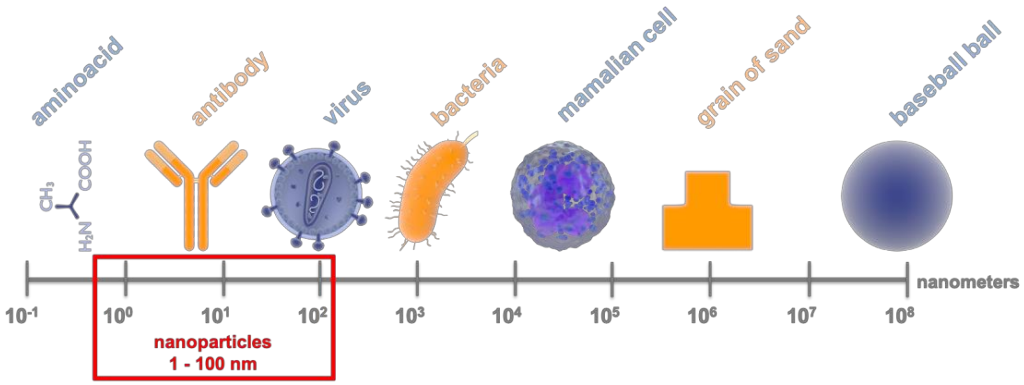

Figure 1. Comparison of nanoparticle size to other objects; presented on a logarithmic scale.

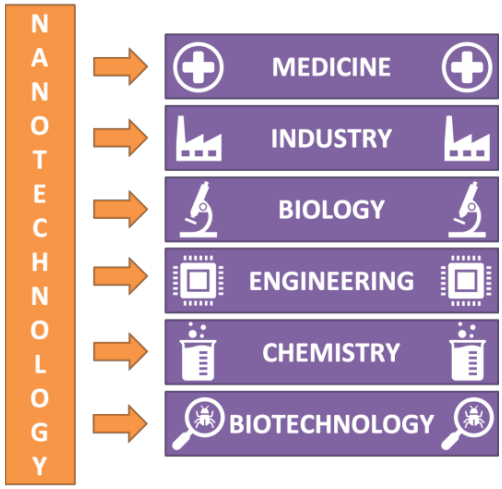

Figure 2. Applications of nanotechnology.

In this review, we discuss the role of nanotechnology in the novel treatment of bone diseases. The human body has over 206 bones, which serve a variety of functions: locomotion, protection of internal organs, ion homeostasis and blood cells production [7–9]. Unfortunately, every bone can suffer from diseases and be the cause of health-related issues. Implantation-related issues and bone neoplasm have been taken in concerns.

2. Cancer

Cancer is one of the leading causes of death in developed countries. Just in 2018 more than 18 million new cancer cases were diagnosed worldwide. Furthermore, cancer was the cause of death for more than 9.5 million people [10]. Between 1987 and 2005 cancer treatment costs have doubled and reached almost $50 billion in the United States alone [11]. Although primary bone cancers are relatively rare (7% of new neoplasm cases in adolescents), bone metastases happen often and by causing excruciating pain severely decrease the patients' quality of life in end-stage disease [12,13].

2.1. Osteosarcoma

Although osteosarcoma (OS) is a primary mesenchymal bone neoplasm characteristic for the paediatric population, it can occur at any age [14]. Unfortunately, in the elderly the survival rate is roughly 2–8 times lower than in adolescents [15]. Even though OS is objectively rare (3.5–4 cases/million population/year), it is the third most common cancer in children [15]. OS is typically located in expeditiously growing long bones (femur, tibia, humerus) [15]. Less typical locations such as skull,

chest or pelvis are unfavourable prognostic factors [15]. As OS quickly gives distant metastases, the disease is often already advanced at diagnosis. Lungs are the most common location of OS metastases [14]. Apart from therapeutic radiation (as treatment of previous cancer), no other risk factors of OS are known and neither are prevention methods [15]. Interestingly, OS occurs more frequently in some genetic diseases (Li-Fraumeni Syndrome, Retinoblastoma, Werner Syndrome, Bloom Syndrome, etc.,) [15]. OS treatment consists of chemo and/or radiotherapy followed by surgery. In chemotherapy methotrexate (MTX), doxorubicin (DOX), cisplatin (CDDP) and ifosfamide (IFO) are used [14]. Unfortunately up to 40–50% of OS tumours are chemo-resistant [16]. Several mechanisms are known to cause multidrug resistance (MDR) in cancer cells, i.e., enhanced detoxification, efflux pumps, decreased drug uptake and up-regulation of DNA repair mechanism [17]. Therefore, the outcome of the treatment is often poor with a 5-year survival rate of 55% (5.7–86.8% as it is localisation-dependent) [15]. Tumour recurrence due to incomplete resection and lung metastases are noted as the leading reasons for treatment failure [18]. It is worth emphasising that the current treatment protocols severely impair patients' quality of life. Therefore, novel approaches to OS are searched.

2.2. Nanoparticles Cytotoxicity to Osteosarcoma Cells

In literature, several papers suggest the anticancer activity of NPs. Rahim et al. have shown that 24.3 nm gold nanoparticles (AuNPs) capped with advance glycation products can decrease cell viability and trigger apoptosis in Saos-2 (osteosarcoma) cells [19]. Interestingly, other studies suggested that the anticancer activity of AuNPs is shape dependent. 143b and MG63 osteosarcoma cells were sensitive to AuNPs rods and stars but not to AuNPs spheres [20]. AuNPs are not the only NPs with anticancer activity. AgNPs can decrease the viability of the MG63 (osteosarcoma) cells [21]. The question is whether the observed effect is nano-size-related or due to the presence of silver. It was shown that 15–34 nm AgNPs are more cytotoxic than $AgNO_3$ to the A-431 (osteosarcoma) cells [22]. Likewise, Kovacs et al. have shown that 5 nm and 35 nm citrate-AgNPs influenced the viability of two osteosarcoma cell lines U2OS and Saos-2 [23]. They have shown that cytotoxicity is size-dependent: the smaller the AgNPs were, the stronger their cytotoxic abilities. Moreover, AgNPs also inhibited cell proliferation and were more effective than cisplatin in the same concentration. AgNPs act by triggering mitochondrial stress and eventually, apoptosis [23]. Another metal with anticancer activity in nano-form is copper. Copper nanoparticles (CuNPs) embedded in alginial hydrogel in a concentration of >0.5% wt. decreased viability of the Saos-2 cells [24]. Unfortunately, there is no literature data on the mechanism of CuNPs cytotoxicity in osteosarcoma cells. We were unable to find any data about the impact of iron or aluminium nanoparticles on osteosarcoma cells either.

Additionally, metal oxide nanoparticles can have anticancer activity. It has been shown that 3.8 nm titanium oxide nanoparticles (TiO_2NPs) in the concentration of >0.5 μg/mL were cytotoxic against the U2OS cells in a time- and concentration-dependent manner. TiO_2NPs induced excessive ROS production and depletion of glutathione (GSH), triggering oxidative stress [25]. In another study, cytotoxicity of TiO_2NPs was also confirmed. Di Virgil et al. examined the anticancer activity of 15 nm TiO_2NPs and 50 nm aluminium oxide nanoparticles (Al_2O_3NPs) [26]. Both NPs types were cytotoxic against the UMR-106 cells in the concentration of >50 μg/mL (MTT assay) [26]. Among others, pH is one of the factors influencing cancer cells response to NPs. It was reported that 3–4 nm dextran-coated cerium oxide nanoparticles (CeO_2NPs) were more effective against osteosarcoma cells in acid pH (pH = 6) than other pH levels (pH = 7, pH = 9). Interestingly, in the same condition, cytotoxicity of CeO_2NPs to non-cancerous bone cells was minimal. The study suggested increased ROS production as a mechanism of CeO_2NPs cytotoxicity [27]. This observation was confirmed in another study which proved that zinc oxide nanoparticles (ZnONPs) could be harmful to MG63 as they triggered ROS production [28].

Not only metal nanoparticles can be used against osteosarcoma. Kimura et al. showed that fucoidan nanoparticles (100 nm) in the concentration of 1–8 mg/mL decreased the viability of the 143B cells by triggering apoptosis [29]. In the study, fucoidan NPs had higher anticancer activity

than macro-size fucoidan in CH3 mice in vivo osteosarcoma model. Interestingly, as in the in vitro model, fucoidan NPs triggered apoptosis in osteosarcoma in vivo as well. Moreover, fucoidan NPs did not affect the bodyweight of the animals, therefore they should not have severe side effects [29]. Also, hydroxyapatite nanoparticles (HA-NPs) were shown to have beneficial properties. HA-NPs are especially interesting because of the similarity of their composition and crystal structure to the microarchitecture of a bone [30]. Interestingly, it was shown that HA-NPs can induce apoptosis in the MG63 cells and promote the viability of healthy osteoblasts [30]. Beside selective cytotoxicity only to cancer cells, HA-NPs also caused ultrastructure changes. Swollen mitochondria, ribosome detachment from rough endoplasmic reticulum, and changes in nuclear morphology were observed [30].

For better understanding of NPs biological activity, it is essential to know whether NPs are being internalised or not. It has been shown that different nanoparticles can be uptaken and accumulated by osteosarcoma cells. Azarami et al. have proven that the uptake of 112–303 nm gelatine nanoparticles by the 143B cells is size-dependent. The larger the nanoparticles were, the less efficiently they were internalised [31]. Similarly, it was shown that 100 nm PGLA NPs can be internalised by the MG63 cells. PLGA NPs were internalised by endocytosis and accumulated in the cytoplasmic region [32].

To sum up, different nanoparticles (metal, metal oxide, HA) can have anticancer activity, typically mediated by increased ROS production. Modification of NPs such as size, shape, type of NPs and/or capping agent can affect their anticancer activity of NPs. The summary of NPs anti-osteosarcoma activity is presented in Table 1.

Table 1. Summary of nanoparticles (NPs) effects in in vitro model of osteosarcoma.

Nanoparticles Type	Osteosarcoma Cell Line	Effect	Additional Comment	Reference
Gold NPs 24.3 nm capped with advance glycation products	Saos-2	Cytotoxicity		[19]
Gold NPs rods Gold NPs stars Gold NPs spheres	143B MG63	Cytotoxicity Apoptosis induction	Cytotoxicity was shape-dependent	[20]
Citrate silver NPs 5 nm and 35 nm	U2OS Saos-2	Cytotoxicity Proliferation inhibition Mitochondrial stress and apoptosis induction	Cytotoxicity was size-dependent NPs were more effective than cisplatin	[23]
Copper NPs 10 nm	Saos-2	Cytotoxicity		[24]
Titanium oxide NPs 3.8 nm	U2OS	Cytotoxicity Increased ROS production Depletion of GSH		[25]
Titanium oxide NPs 15 nm	UMR-106	Cytotoxicity NPs were present in phagocytic vesicle within the cells		[26]
Aluminium oxide NPs 50 nm	UMR-106	Cytotoxicity NPs were present in phagocytic vesicle within the cells		[26]
Dextran coated cerium oxide NPs 3–4 nm	MG63	Cytotoxicity Increased ROS production	Cytotoxicity was pH-dependent Cells were more susceptible to NPs in an acidic environment	[27]

Table 1. *Cont.*

Nanoparticles Type	Osteosarcoma Cell Line	Effect	Additional Comment	Reference
Zinc oxide NPs 22 nm	MG63	Cytotoxicity Increased ROS production Apoptosis induction		[28]
Cerium oxide NPs 26 nm	MG63	Cytotoxicity Increased ROS production Apoptosis induction		[28]
Fucoidan NPs 100 nm	C3H	Cytotoxicity Apoptosis induction	Fucoidan in NPs were more effective than fucoidan itself	[29]
Hydroxyapatite NPs 40 nm	MG63	Selective cytotoxicity only to cancer cells Ultrastructure changes	HA-NPs were cytotoxic to osteosarcoma cells and stimulated the growth of healthy osteoblast	[30]

2.3. Nanoparticles Cytotoxicity to Other Bone Cancer Types

Chondrosarcoma, Ewing's sarcoma and fibrosarcoma are other types of cancers, however they are far less common than OS. Unfortunately, data about NPs cytotoxicity against them is limited. Sha et al. examined the effect of 3.8 nm TiO_2NPs on the SW1353 chondrosarcoma cells [25]. They observed time- and concentration-dependent cytotoxicity of TiO_2NPs. Interestingly, the chondrosarcoma cells in the study were more susceptible to NPs than the osteosarcoma cells (U2OS). Authors suggested the induction of oxidative stress as TiO_2NPs cytotoxicity mechanism [25]. NPs were also used as a strategy to treat Ewing's sarcoma. Elhamess et al. used genetically modified NIH/3T3 cells as Ewing sarcoma model in which they have shown that oligonucleotides-chitosan nanospheres may be an efficient gene delivery platform [33]. A summary of NP's effect on fibrosarcoma in vitro model is presented in Table 2.

Table 2. Summary of NPs effects in in vitro model of fibrosarcoma.

Nanoparticles Type	Fibrosarcoma Cell Line	Effect	Additional Comment	Reference
Gold NPs 127 nm	HT-1080	Anti-metastatic effect	NPs did not affect cells viability AuNPs interfered actin-polymerisation pathway AuNPs inhabited cells migration	[34]
Silver NPs 6 nm	WEHI164	Cytotoxicity	IC_{50} of AgNPs was 2.6 μg/mL	[35]
Iron (II, III) oxide NPs 10 nm	HT-1080	Cytotoxicity	NPs had magnetic properties NPs may be used as drug delivery platform	[36]

Table 2. *Cont.*

Nanoparticles Type	Fibrosarcoma Cell Line	Effect	Additional Comment	Reference
Iron (II, III) oxide NPs 10 nm, 100 nm	HT-1080	Cytotoxicity Genotoxicity	NPs were coated with: -OH, -NH_2, -TEOS, -AMPTS or TEOS/AMPTS functional groups Cytotoxicity and genotoxicity were function group – dependent AMPTS coated NPs were the most cytotoxic Positively charged NPs were more genotoxic than negatively charged	[37]
Cerium oxide NPs 25 nm	HT-1080	Non-cytotoxic		[38]
Cerium oxide NPs 30 nm	WEHI164	Cytotoxicity	Cancer cells were more susceptible to NPs than non-transformed ones NPs triggered oxidative stress NPs caused apoptosis	[39]
Chromium oxide NPs	L929	Cytotoxicity	NPs triggered oxidative stress NPs caused apoptosis	[40]

2.4. Nanoparticles as Drug Delivery Platforms

NPs as drug delivery platforms have a lot of advantages: improved efficiency, reduced toxicity, smaller cost of therapy, potential effectiveness in MDR cancers [31]. It has been shown that NPs can accumulate in the cancer microenvironment because of the improper structure and function of endothelial cells in the tumour vasculature (wider junctions, fenestration, incomplete basal membrane) which makes it easier to penetrate [41]. This observation was called enhanced permeability and retention effect, and it is probably the basis of NPs anticancer effect [42]. The summary of all NPs as drug delivery platforms is presented in Table 3.

Dhule et al. have shown that liposomal NPs can be used as curcumin drug delivery platforms [43]. Curcumin is not yet being used in clinical practice, however, its anticancer effect is well established and cancer cells are more susceptible to curcumin than non-transformed ones [43]. Moreover, liposomal NPs with curcumin trigger apoptotic death of KHOS (osteosarcoma) cells, whereas curcumin alone induces autophagy [43]. It proves that wisely used drug delivery platforms can change compound properties to more favourable ones. Also, Shu-Fen et al. have shown the effectiveness of curcumin. Their 250 nm curcumin-loaded PGLA NPs significantly decreased the viability of U2OS cells [16]. In that study, curcumin in NPs induced apoptotic osteosarcoma cell death by triggering mitochondria-dependent apoptosis [16]. Curcumin was not the only drug to be conjugated with NPs. Ni et al. designed 150 nm spherical, salinomycin-loaded PEG nanoparticles with aptamer to target osteosarcoma stem cells [18]. Salinomycin is an old chemotherapeutic drug with high anticancer stem cells activity [18]. Unfortunately, its potential is greatly reduced by its water insolubility [18]. Salinomycin loaded PEG NPs were effective against Saos-2, U2OS and MG63 cells and even more effective against cancer stem cells (CD133 positive) [18]. Moreover, in Saos-2 population, cancer stem cells were greatly

reduced by adding an aptamer to salinomycin PEG-NPs treatment [18]. Those findings were also confirmed in in vivo model. In Balb/c mice with an osteosarcoma tumour (from Saos-2 cells) treated with NPs had their tumour weight, number of mammospheres formed and amount of cancer stem cells reduced compared to control [18]. NPs loaded with two different cytostatic were also studied. Wang et al. created complex NPs. They encapsulated paclitaxel (PTX) and etoposide (ETP) in 100 nm PEG-ylated PLGA nanoparticles (PTX-ETP/PLGANPs). Plain NPs (without PTX or ETP) were not cytotoxic, which proves the safety of application [32]. The nanoparticles were more effective against MG63 and Saos-2 cancer cells than PTX or ETP in combination, which demonstrated that nano form significantly changes the properties of NPs. In a more detailed analysis it was demonstrated that PTX-ETP/PLGANPs are more effective in inducing MG63 cell apoptosis than drugs without carrier [32]. Some scientists went further and combined chemotherapy with gene therapy to overcome drug resistance. Sun et al. prepared 200 nm dextran-g-PEI NPs (DEX-PEI NPs) to be an adriamycin (ADM) and plasmid transporter. They have shown that DEX-PEI-ADM NPs were more cytotoxic against the MG63 and Saos-2 osteosarcoma than ADM or DEX-PEI NPs [41]. Next, they examined properties of DEX-PEI-ADM NPs as a plasmid carrier. They tried to express a green fluorescent protein (GFP) in the MG63 and Saos-2 cells. GFP was chosen, as it is easy to determine whether the transfection was effective or not. DEX-ADM-PEI NPs with GFP pcDNA turned out to be an effective transfection reagent [41]. However, NPs were less effective than Lipofectamine 2000, a typically used transfection reagent (transfection effectiveness for NPs were 18.6% and 15.3% for MG63 and Saos-2 cells respectively, whereas for Lipofectamine 2000 it was 26.6% and 21.8%). Also, Susa et al. established DEX-containing NPs. They created 112.4 nm stearylamine-dextran nanoparticles loaded with DOX (STE-DEX-DOXNPs) [17]. They examined STE-DEX-DOXNPs on the U2OS, KHOS and MDR osteosarcoma cell lines. Interestingly, after treatment with NPs DOX were more accumulated in the drug-resistant cancer cell lines than in the regular KHOS or U2OS cells. Moreover DOX in a free form accumulated in osteosarcoma cells cytoplasm, whereas STE-DEX-DOXNPs were trafficked to the nucleus of the cells [17]. Also, STE-DEX-DOXNPs have an antiproliferative effect and caused apoptosis of OS cells. This effect was more prominent than in cells treated only with DOX.

Table 3. Summary of NPs properties as drug delivery treatment.

Nanoparticle Type	Cell Line	Drug	Comment	Reference
PGLA NPs	U2OS	Curcumin	NPs triggered mitochondria-dependent apoptosis	[16]
Streamline-dextran NPs	KHOS U2OS Drug-resistant osteosarcoma cells	Doxorubicin	The drug was more accumulated in drug-resistant cell lines Antiproliferative effect and apoptosis induction DOX in NPs were more effective than free drug	[17]
PEG NPs with stem-cell aptamer	Saos-2 U2OS MG63	Sialomycin	NPs were more effective against cancer cell line than non-cancerous cell	[18]
PEGylated PLGA NPs	MG63 Saos-2	Paclitaxel Etoposide	NPs were more effective than PTX and ETP in combination Apoptosis induction G2/M arrest	[32]

Table 3. *Cont.*

Nanoparticle Type	Cell Line	Drug	Comment	Reference
Dextran-g-PEI NPs	MG63 Saos-2	Adriamycin Plasmid DNA	Anticancer activity NPs were almost as good as typically used transfection reagent	[41]
Glutathione coated gold NPs	143B	Doxorubicin Gemcitabine Cytarabine	Cancer cell lines were more susceptible to NPs than non-transformed ones NPs conjugated with chemotherapeutic may be more effective than chemotherapeutic alone	[44]
Liposomal NPs	KHOS	Curcumin	Liposomal NPs with curcumin triggers apoptotic death whereas curcumin alone induces autophagy	[43]

2.5. Magnetic Nanoparticles

Hyperthermia defined as the treatment of cancer with heat is a well-established practice. It is proven that cancer cells are more susceptible to heat and in the temperature > 43 °C they undergo necrosis [45]. The main problem of this approach is the impossibility to provide heat only to the tumour and avoid healthy tissues. The use of magnetic nanoparticles that can be directed to the tumour and then heated could enable overcoming that issue [46]. The most clinically promising method of NPs heating is capacitive heating using a radiofrequency electric field [47]. Makridis et al. have suggested 26 nm Mn-Fe_2O_4 NPs in cancer treatment. They have proven that Mn-Fe_2O_4 NPs were internalised by Saos-2 cells in energy-dependent endocytosis, also the cancer cells were more susceptible to heating than the non-transformed ones. The magnetic field used to heat nanoparticles was not harmful to the cells [46]. Hyperthermic treatment's effectiveness was also proven in vivo. Matsuoka et al. created magnetic cationic liposomes (MCL) based on supramagnetic iron oxide nanoparticles [48]. They injected MCL directly into an osteosarcoma tumour in a female Syrian hamster. Next, tumour was heated to above 42 °C. They observed >15 days regression in all tested animals (75% animals had complete regression). Moreover, tumour mass in treated animals was 0.1% (1/1000) of tumour mass in control subjects [48]. A similar observation was made by Shido et al. [47]. They also used MCL and heated the tumour to above 43 °C. They used C2/He mice model. They were able to achieve suppression of tumour growth in all treated animals, with complete regression in 43% of treated animals, whereas in control animals tumour volume was increasing over time [47]. The group which underwent treatment also presented less metastases in comparison to control animals (mean number of lung metastasis 56.8 versus 17.6) [47]. Interestingly, However, magnetic NPs are used not only in hyperthermic treatment. Xeu-Song et al. created poly-lactic acid arsenic trioxide nanoparticles (ATONPs) [49]. Arsenic trioxide is a compound used in the treatment of acute promyelocytic leukaemia. In the study, they created 60–70 nm magnetic ATONPs and examined their anticancer abilities. They have shown that with the usage of a magnetic field, ATONPs can be directed to a specific place. They observed 40% higher concentrations of ATONPs in the kidneys of a New Zealand white rabbit if magnetic field was used [49]. Moreover, the ATONPs were effective against osteosarcoma in in vivo model (BALB/c nude mice). Also, Kubo et al. used magnetic liposomes in drug delivery. They created 146 nm magnetic liposomes incorporated with adriamycin (MLA) [50]. In vivo assessment (Syrian hamster) have shown that only MLA under magnetic force were able to suppress tumour growth [50].

To summarise, magnetic NPs in OS treatment can be used two-fold: as hyperthermic agents or delivery platforms. In both approaches, NPs are effective both in vitro and in vivo.

3. Nanoparticles in Orthopaedic Implants

Because medical advancement societies are aging, it brings forward new health issues such as osteoarthritis for which conservative treatment is often not sufficient and joint replacement surgery is needed. Unfortunately, epidemiological data are terrifying. Ten percent of >15 years old Canadians suffer from osteoarthritis. Almost half of the population at the age of 65 or older has osteoarthritis of at least one joint [51]. Pain and movement impairment are the most prominent symptoms, severely decreasing patient's quality of life. It is the obligation of the scientific community to address main issues regarding joint replacement surgery: implant-related infections and poor biocompatibility. NPs may both increase biocompatibility of the implants and be the prophylaxis of the implant-related infections [52,53]. This knowledge can be also used in other orthopaedic implantable devices such as artificial ligaments or tendons, bone nails or screws.

3.1. Implant-Related Infections

In total, half of all nosocomial infections are related to implantable devices [54]. Although not very common among orthopaedic patients (2–5%), this complication is costly ($1.86 billion annually only in the United States) [54,55], especially if we consider that 500,000 people have a hip or knee replacement in the United States alone [56]. Infections related to orthopaedic devices are often a cause of their failure, leading to another surgery [54]. They can also be a facilitator for other serious complications and even death, as they increase the risk of cardiac arrest, pulmonary embolism, myocardial infection and acute renal failure [57]. Age, obesity and comorbidities are the main risk factors of serious complications [57]. Moreover, the diagnosis of implant-related infection is complicated and the symptoms may occur many months after surgery [56]. Treatment typically consists of broad-spectrum systemic antibiotic treatment and removal of the infected implant [54]. Typically infection is caused by aerobic Gram-positive bacteria such as *Staphylococcus aureus* (34%), *Streptococcus epidermidis* (32%) and other coagulases negative streptococci (13%) [54]. However, Gram-negative pathogens (*Pseudomonas* spp., *Enterococcus* spp., *Escherichia* spp.) and fungi (*Candida* spp., *Aspergillus* spp.) also may cause the infection [54,56,58]. Planktonic bacteria are far less dangerous than the ones forming a biofilm. A biofilm is defined as a complex structure made of bacterial cells and extracellular matrix, which allows cells to exchange virulence factors via plasmids [59]. Importantly pathogens in the biofilm are more resistant to treatment than planktonic form, typically 100–1000 times [60]. Moreover, neither antibiotics nor immune cells can penetrate a biofilm easily, which makes the treatment challenging. It can occur on any surface that bacterial cells can adhere to, orthopaedic devices included [59].

3.2. Biocompatibility

Bone is a metabolically active tissue with a great remodelling potential [7]. Therefore, it is important that the implant or any other device is incorporated into the surrounding tissue. Titanium is one of the most popular implant materials, so naturally, the modification of titanium surface to increase its biocompatibility is the most popular choice. Ren et al. proposed titanium-AgNPs-titanium nanostructure [61]. Such nanostructures have good antimicrobial properties; moreover, the MC3T3-E1 cells (mouse preosteoblast) attached and proliferated on the nanostructure easily. Preosteoblast had proper morphology and appropriate amount of alkaline phosphatase (ALP) activity which is a marker of osteogenesis [61]. Unfortunately, high concentration of nanostructure and prolonging incubation impacted the cellular proliferation and morphology [61]. A strategy to enhance antimicrobial properties of the implants was also used by Xiang et al. They used poly(lactic-*co*-glycolic acid)/ZnO nanorods/Ag nanoparticles hybrid coating on Ti implants (PLGA-ZnO-AgNPs) [62]. Their coating had antimicrobial activity against both Gram-positive and Gram-negative bacteria (*Staphylococcus aureus*, *Escherichia coli*). A biocompatibility assessment showed that PLGA-ZnO-AgNPs were less cytotoxic than ZnO

or ZnO-Ti against MC3T3-E1 cells [62]. They also used ALP as a marker of osteogenesis and an increased level of that enzyme in cells on the PLGA-ZnO-AgNPs surface was noted [62]. As further confirmation they observed the proper formation of cytoskeleton within the MC3T3-E1 cells [62]. Also, Neupane et al. modified titanium nanotubes with AuNPs (TiO_2-AuNPs). They compared TiO_2-AuNPs to polished Ti (Ti_p) and TiO_2 nanotubes (TiO_2NPs). In comparison to other materials, the MC3T3-E1 cells on the surface of TiO_2-AuNPs had more visible nuclei and more filopodia, and therefore higher osteoblast activity [53]. It was further confirmed by MTT assay that the MC3T3-E1 cells were more viable when treated with TiO_2-AuNPs than Ti_p or TiO_2NPs [53]. In another paper, titanite nanotubes were modified with AgNPs [63]. The created material was expected to have antibacterial properties against *Escherichia coli* [63]. In comparison to the titanium control the proposed coating did not affect MC3T3-E1 proliferation, moreover, it promoted cells adhesion and migration [63]. Hydroxyapatite (HA) may promote the proliferation of healthy bone cells [30], and thus several attempts were made to functionalise the implants with HA. Fomin et al. functionalised titanium surface with hydroxyapatite nanoparticles (HA-NPs). They have found that this modification improved fibroblast fixation to the surface [64]. Salaie et al. modified medical titanium alloy with AgNPs and HA-NPs [65]. Unfortunately, their coating was slightly toxic (cell viability was decreased by around 30%), however, in a morphological analysis cells showed no signs of distress and filopodia formed well [65]. Those findings have proven that the modifications of implants surface with NPs may increase their biocompatibility and act as an antimicrobial agent. They had shown so much promise that some of the modifications were even patented [66].

3.3. Nanoparticles in Bone Regenerative Strategies

Because of their unique properties, some NPs may promote osteogenesis. Wei et al. reported that AgNPs promoted osteogenesis by inducing autophagy [67]. AgNPs assessed in human mesenchymal stem cells model in a non-toxic concentration were internalised, promoted osteogenesis (increased mineralisation and alkaline phosphatases activity) and matrix protein synthesis [67]. 53-nm AuNPs modified with advanced-platelet-rich-plasma were non-cytotoxic and promoted osteogenesis (by increasing alkaline phosphates activity and calcium content) [68]. Patel et al. have created hydroxyapatite NPs (HA-NPs) and examined their effect on bone marrow-delivered mesenchymal stem cells (BMSCs) [69]. They have proven that HA-NPs were non-toxic to BMSCs and promoted osteogenesis (increased level of calcium and gene expression of osteoblast markers) [69]. NPs made of hydroxyapatite and gold (HA-Au-NPs) had particularly beneficial properties. Liang et al. have shown that HA-Au-NPs were internalised by endocytic pathway and promoted osteogenesis, [70]. Increased alkaline phosphatase activity and expression of osteogenic genes were reported. Authors suggested that the observed effect was Wnt/ß-catenin pathway-dependent [70]. In another study HA-NPs were enriched in Li^+ ions [71]. The created biomaterial promoted osteogenesis and mitochondrial dynamic and inhibited apoptosis in adipose tissue-derived mesenchymal stem cells model [71]. Also, calcium polyphosphate NPs (polyP-NPs) can stimulate osteogenesis. Hatt et al. have proven that polyP-NPs can be a source of phosphate for matrix mineralisation and increased osteogenesis marker levels [72]. Graphene oxide may be an interesting biomaterial too. Several studies have shown that it has the abilities to promote osteogenesis and it can also be effective against *Staphylococcus aureus* [73,74]. Pro-osteogenic properties of NPs have also been proven in in vivo model. Wang et al. have reported that aptamer-functionalised NPs (AP-NPs) may increase the osteogenesis markers level (osteopontin, osteocalcin, alkaline phosphatase) and improve the femur bone regeneration [75]. Moreover, AP-NPs were non-toxic in in vitro BMSCs model. Also, sinopic acid-loaded chitosan NPs (SA-CH-NPs) promoted osteogenesis in vivo (observed as better regeneration of cervical bone) [76]. Those results corresponded with in vitro assessment, where NPs were non-toxic and promoted osteoblast formations from BMSCs through activation of the TGF-ß1/BMP/Smads/Runx2 pathway [76]. Study designed by Kuang et al. is especially interesting because they created an injectable material containing nanocomposite hydrogel and CaPNPs [77]. The injectable material was potentially convenient to use and its effectiveness in promoting osteogenesis was proven both in vitro and in vivo [77].

To summarise, both organic and inorganic NPs can promote osteogenesis and be non-toxic to mammalian cells. These abilities may be used in regenerative medicine.

3.4. Antimicrobial Properties of Nanoparticles

AgNPs are the ones with the best-described antimicrobial activity. Baker et al. have shown that 75 nm AgNPs can be effective against *Escherichia coli* [52]. However, the antibacterial properties of silver are size-dependent. The study has proven that the smaller AgNPs (7 nm) were more effective than the bigger ones (29 nm, 89 nm). That observation was made by a comparison of minimal inhibitory concentration (MIC) of two bacterial strains *E. coli* and *Staphylococcus aureus* [78]. Another paper showed that AgNPs are more effective against Gram-negative bacteria than against Gram-positive ones [79]. Moreover, AgNPs can also act against drug-resistant bacteria (ampicillin-resistant *Escherichia coli* and multi-drug resistant *Salmonella typhi*) [79]. In other studies, AgNPs inhibited the growth of *Bacillus subtilis, Klebsiella mobilis, Vibrio cholera, Pseudomonas aeruginosa, Shigella flexneri, Mycobacterium smegmatis* and *Mycobacterium tuberculosis* [5,80,81]. It was only the size that influenced the antimicrobial properties of AgNPs. Niska et al. examined the role of the capping agent on antimicrobial properties of AgNPs [82]. They examined uncapped AgNPs, AgNPs capped with lipolic acid (LA), tannic acid (TA) or PEG. UC-AgNPs and LA-AgNPs had the strongest antimicrobial activity, whereas TA-AgNPs the smallest. Their AgNPs had also an antibiofilm activity. In their study, Gram-positive strains were more susceptible to AgNPs which is contrary to the findings of Shrivastava et al. [79,82]. Several mechanisms of AgNPs antimicrobial properties are suggested (Figure 3); the inhibition of transduction of signalling pathways, lytic effect on the cellular membrane, increased ROS production, inhibition of enzymes, inactivation of nucleic acids are worth mentioning [79,83–85]. AgNPs can also have an antifungal activity [84]. It was reported that 25-nm AgNPs inhibited the growth of four strains of *Candida* spp., AgNPs were used in concentrations non-cytotoxic for mammalian cells [86]. Moreover, stabilisation with surfactants or polymers improved the antifungal activity of AgNPs [86]. This observation was in accordance with other studies, and also found that 3-nm AgNPs are effective against *Trichophyton mentagrophytes* [87]. AgNPs were more effective than commonly used medication: amphotericin b and fluconazole [87]. AgNPs possibly have antiviral and antiprotozoal activity as well, however viruses and protozoa almost never cause bone infections [88,89].

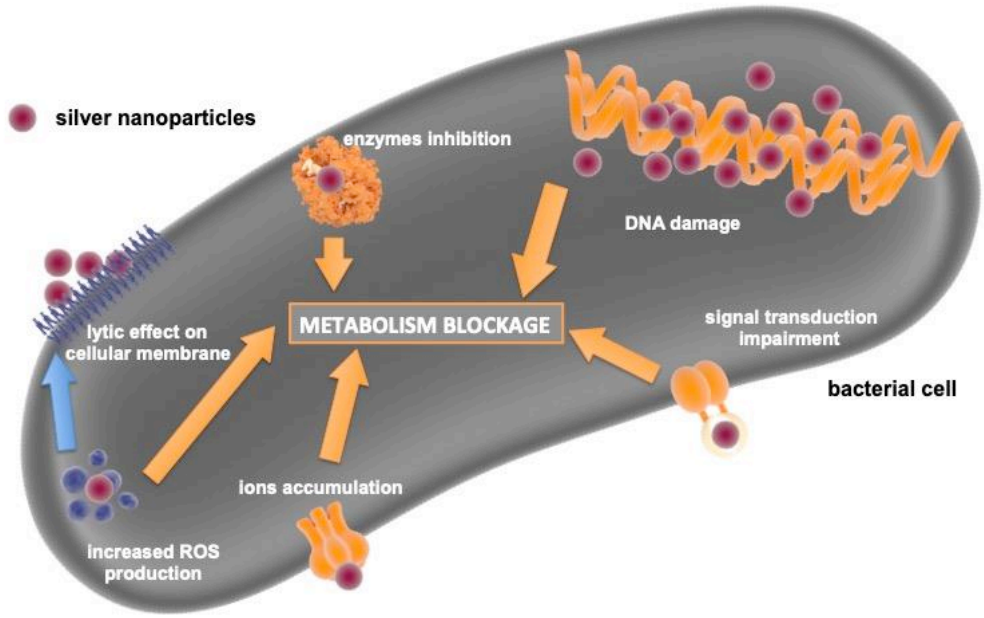

Figure 3. Schematic summary of AgNPs antibacterial activity mechanism.

Also, AuNPs can be an interesting antimicrobial agent. Cui et al. reported the antibacterial activity of AuNPs against *E. coli* [90]. AuNPs inhibited the growth of both planktonic form and biofilm [90]. AuNPs impacted the expression of 359 genes, decreased ATP concentration within the bacterial cells and triggered ROS production [90]. Also, Gram-positive bacteria may be susceptible to AuNPs. The same paper has shown that 11–22 nm AuNPs can be an antifungal agent against *Candida* spp. and *Aspergillus* spp. [91]. Transmission electron microscopy (TEM) has shown that AuNPs attached themselves to bacterial cells and caused improper respiration and permeability [91]. Other papers also supported that AuNPs can be an antibacterial agent [92]. Unfortunately, some studies did not prove the antibacterial properties of AuNPs [93,94]. NPs types such as copper, zinc oxide, titanium oxide and others can also have antimicrobial properties [95–99]. A more detailed description of those NPs antimicrobial properties is presented in Table 4. NPs may be potentially used as antimicrobial agents for bacteria and fungi in planktonic form or biofilm. Their properties depend on: type of NPs, size, shape and capping agent type [78,82,86,98,99].

Table 4. Summary of antimicrobial activity of nanoparticles.

Nanoparticles Type	Microorganism	Comment	Reference
Silver NPs 75 nm	*Escherichia coli*	NPs had antibacterial activity.	[52]
Silver NPs 7 nm, 29 nm and 89 nm	*Escherichia coli* *Staphylococcus aureus*	MIC values were size-dependent. Bigger nanoparticles were less effective than smaller ones	[78]
Silver NPs 10–15 nm	*Escherichia coli* *Staphylococcus aureus* *Ampicillin resistant* *Escherichia coli* *Multi drug resistant* *Salmonella typhi*	Gram-negative bacteria are more susceptible to NPs NPs were effective against drug-resistant bacteria NPs inhibited signal transduction	[79]
Silver NPs Starch stabilised 20–40 nm *	*Staphylococcus aureus* *Pseudomonas aeruginosa* *Shigella flexneri* *Salmonella typhi* *Mycobacterium smegmatis*	NPs had antibacterial activity.	[80]
Lipolic acid- silver NPs 9.5 nm PEG- silver NPs 9.8 nm Tannic acid – silver NPs 10 nm Silver NPs 11.2 nm	17 different gram-negative strains 9 different gram-positive strains	Antimicrobial activity was capping agent dependent Gram-positive bacteria were more susceptible to NPs NPs had antibiofilm activity	[82]
Silver NPs 13,5 nm	*Escherichia coli* *Staphylococcus aureus* Yeast	NPs had antibacterial and antifungal activity	[84]
Silver NPs 25 nm	*Candida albicans* *Candida parapsilosis* *Candida tropicalis*	NPs stabilised with surfactants or polymers had higher antifungal activity The antifungal effect was present in non-cytotoxic concentrations	[86]
Silver NPs 3 nm	*Candida albicans* *Candida tropicalis* *Candida parapsilosis* *Candida krusei* *Candida glabrata* *Trichophyton mentagrophytes*	NPs were more effective than amphotericin B and fluconazole	[87]

Table 4. *Cont.*

Nanoparticles Type	Microorganism	Comment	Reference
Gold NPs (No size info)	*Escherichia coli*	NPs impacted expression of 359 genes NPs inhibited ATP synthesis and dissipated membrane potential NPs increased ROS production	[90]
Gold NPs 11–22 nm	*Listeria monocytogenes* *Bacillus cereus* *Staphylococcus aureus* *Escherichia coli* *Pseudomonas aeruginosa* *Salmonella typhimurium* *Candida albicans* *Aspergillus niger* *Aspergillus flavus*	NPs were effective against Gram-positive and Gram-negative bacteria NPs were more effective than ciprofloxacin against bacteria	[91]
Gold NPs 18.32 nm	*Staphylococcus aureus* *Pseudomonas aeruginosa*	NPs had antibacterial activity.	[92]
Copper NPs 62.5 nm	*Escherichia coli*	NPs caused dissipation of cell membrane, generation of ROS, lipid peroxidation, protein and DNA degradation in bacterial cells	[95]
Copper NPs (No size info)	*Micrococcus luteus* *Staphylococcus aureus* *Klebsiella pneumoniae* *Pseudomonas aerugionsa* *Aspergillus flavus* *Aspergillus niger* *Candida albicans*	NPs had antibacterial and antifungal activity	[96]
Zinc oxide NPs 200 nm	*Escherichia coli* *Listeria monocytogenes*	NPs had antibacterial activity.	[97]
Zinc oxide NPs 10 nm, 100 nm, 1 μm	*Candida albicans*	NPs antifungal activity was size-dependent NPs antifungal action is ROS mediated	[98]
Copper oxide NPs Titanium oxide NPs Zinc oxide NPs Aluminium oxide NPs Silicon oxide NPs Iron oxide NPs Cerium oxide NPs 25–50 nm	*Escherichia coli*	NPs antibacterial properties were material dependent (CuONPs > TiO_2NPS > ZnONPs > Al_2O_3NPs > SiO_2NPs > Fe_2O_3NPs > CeO_2NPs) NPs antimicrobial activity was correlated with increased ROS production	[99]
Copper NPs 12 nm	*Escherichia coli*	NPs had antibacterial activity.	[100]

* No detailed size information.

4. Safety Concerns

NPs have beneficial properties discussed in the previous sections of this article. But as any potential treatment, they will have side effects if used in clinical practice. Unfortunately, data on cytotoxicity of NPs against healthy bone cells is insufficient; only a few papers examined this aspect. Albers et al. have reported that 50 nm AgNPs can decrease the viability and proliferation rate of primary osteoblast and primary osteoclast [101]. Another study has shown that 15-nm AgNPs can trigger hFOB1.19 (human foetal osteoblast) apoptosis and necrosis via increased production of nitric oxide [102]. Also, AuNPs can influence the bone cell viability. AuNPs in the shape of rods and stars decreased the viability of hFBO1.19 cells, whereas the spherical-shaped ones did not [20]. Also, TiO_2NPs may be harmful to the

bone cells. TiO_2NPs (10–15 nm) were internalised by hFOB1.19 cells and decreased their viability in a concentration-dependent manner by triggering oxidative stress [103]. We are unable to find any other data about in vitro cytotoxicity of NPs to healthy bone cells. Unfortunately, there was only one animal study regarding that matter. In in vivo (Wistar rats) assay, neither 20 nm AgNPs nor 21 nm TiO_2NPs were toxic to red and white cells in the bone marrow [104]. Unfortunately, reticulocytes and leucocytes in the bone marrow responded negatively to AgNPs and TiO_2NPs [104].

Although the available data are scarce, it is clear that NPs can be harmful. However, we should keep in mind that it is true for any other drug as well. Many commonly used antimicrobial agents (polymyxin B, amphotericin B, colistin M, cefazolin, ciprofloxacin, tetracycline, rifampicin, clindamycin, azithromycin, chloramphenicol, linezolid) can affect cell viability and/or proliferation [105–107]. Moreover, commonly used chemotherapeutics have numerous side effects; for example gemcitabine causes myelosuppression, hearing loss and liver failure, cytarabine damages the brain, heart and gastrointestinal tract and is also myelotoxic, and doxorubicin destroys bone marrow and causes nausea [108–110].

5. Clinical Usage

More than 51 products with nanotechnology developments are FDA approved [111]. Several products with hydroxyapatite or calcium phosphate in nanocrystal form were approved as bone substitutes (Vitoss®, Ostim®, OsSarura®, NanoOss®, EquivaBone®) [111]. Regarding matters discussed in this review the usage of carbon NPs and supramagnetic iron oxide NPs in lymph node biopsy [112,113] or medical imaging [111] is especially interesting. In all mentioned studies there were no information concerning side effects after application of NPs.

6. Conclusions

Despite the recent advancements in orthopaedics bone cancers and implant-related infections are still unsolved problems. However, in the future, NPs may be applied as therapeutic agents. Because of their unique properties, both organic and inorganic NPs could potentially be used. In cancer therapy, NPs can be (I) directly cytotoxic to cancer cells, (II) drug delivery platforms or (III) hyperthermic agents. Moreover, NPs can be more effective than the drugs currently used in the clinic. As an adjuvant to the implant, NPs can (I) increase their biocompatibility by promoting osteogenesis and (II) be antimicrobial agents. Unfortunately, NPs can be also harmful to healthy cells. Several factors influence the biological properties of NPs (I) type of NPs, (II) concentration, (III) size, (IV) shape, (V) pH of environment, (VI) capping agents, (VII) functionalisation.

In future research, there is a need for a better understanding of the mechanisms of NPs biological properties, especially the antimicrobial ones. While focusing on the positive aspect of NPs in bioscience, we should also peruse nanotoxicological studies—the better we understand the NPs harmful effect the better we can avoid the side effects. Detailed knowledge about interaction between NPs and living cells in terms of cytotoxicity, anticancer and antimicrobial properties will allow designing nanoparticles-based drugs and biomaterials with highly favourable pharmacological/toxicological profile. Indisputably, NPs are a powerful tool, however there is still a lot to be done before we acknowledge that they can be used without any unknown risks.

Author Contributions: Conceptualization, K.P.S. and I.I.-S.; methodology, K.P.S. and I.I.-S.; investigation, K.P.S.; resources, K.P.S. and I.I.-S.; data curation, K.P.S.; writing—original draft preparation, K.P.S.; writing—review and editing, K.P.S. and I.I.-S.; visualization, K.P.S.; supervision, I.I.-S.; project administration, K.P.S. and I.I.-S.; All authors have read and agreed to the published version of the manuscript.

Funding: K.P.S and I.I.-S acknowledges funding from Medical University of Gdansk (ST-02-0046/07/259).

Acknowledgments: The authors would like to thank Magdalena Bazgier MD for contribution to language proofread. Some elements of figures were downloaded from 'www.somersault1824.com' with creators' permission for usage in this article. The authors are grateful for that kindness.

Conflicts of Interest: The authors declare no conflict of interest.

References

1. Hulla, J.E.; Sahu, S.C.; Hayes, A.W. Nanotechnology: History and future. *Hum. Exp. Toxicol.* **2015**, *34*, 1318–1321. [CrossRef]
2. Fernández, M.D.; Alonso-Blázquez, M.N.; García-Gómez, C.; Babin, M. Evaluation of zinc oxide nanoparticle toxicity in sludge products applied to agricultural soil using multispecies soil systems. *Sci. Total Environ.* **2014**, *497–498*, 688–696. [CrossRef]
3. Kim, J.S.; Adamcakova-Dodd, A.; O'Shaughnessy, P.T.; Grassian, V.H.; Thorne, P.S.; Roco, M.; Karlsson, H.; Cronholm, P.; Gustafsson, J.; Möller, L.; et al. Effects of copper nanoparticle exposure on host defense in a murine pulmonary infection model. *Part. Fibre Toxicol.* **2011**, *8*, 29. [CrossRef]
4. Rai, M.; Ingle, A.P.; Birla, S.; Yadav, A.; Santos, C.A. Dos Strategic role of selected noble metal nanoparticles in medicine. *Crit. Rev. Microbiol.* **2016**, *42*, 696–719.
5. Dos Santos, C.A.; Seckler, M.M.; Ingle, A.P.; Gupta, I.; Galdiero, S.; Galdiero, M.; Gade, A.; Rai, M. Silver nanoparticles: Therapeutical uses, toxicity, and safety issues. *J. Pharm. Sci.* **2014**, *103*, 1931–1944. [CrossRef] [PubMed]
6. Selvaraj, M.; Pandurangan, P.; Ramasami, N.; Rajendran, S.B.; Sangilimuthu, S.N.; Perumal, P. Highly potential antifungal activity of quantum-sized silver nanoparticles against Candida albicans. *Appl. Biochem. Biotechnol.* **2014**, *173*, 55–66. [CrossRef] [PubMed]
7. Stevens, M.M. Biomaterials for bone tissue engineering. *Mater. Today* **2008**, *11*, 18–25. [CrossRef]
8. Moll, N.M.; Ransohoff, R.M. CXCL12 and CXCR4 in bone marrow physiology. *Expert Rev. Hematol.* **2010**, *3*, 315–322. [CrossRef] [PubMed]
9. Bosman, A.J.; Hol, M.K.S.; Snik, A.F.M.; Mylanus, E.A.M.; Cremers, C.W.R.J. Bone-anchored hearing aids in unilateral inner ear deafness. *Proc. Acta Oto Laryngol.* **2003**, *123*, 258–260. [CrossRef]
10. Bray, F.; Ferlay, J.; Soerjomataram, I.; Siegel, R.L.; Torre, L.A.; Jemal, A. Global cancer statistics 2018: GLOBOCAN estimates of incidence and mortality worldwide for 36 cancers in 185 countries. *CA Cancer J. Clin.* **2018**, *68*, 394–424. [CrossRef]
11. Tangka, F.K.; Trogdon, J.G.; Richardson, L.C.; Howard, D.; Sabatino, S.A.; Finkelstein, E.A. Cancer treatment cost in the United States: Has the burden shifted over time? *Cancer* **2010**, *116*, 3477–3484. [CrossRef] [PubMed]
12. Ward, E.; DeSantis, C.; Robbins, A.; Kohler, B.; Jemal, A. Childhood and adolescent cancer statistics. *CA Cancer J. Clin.* **2014**, *64*, 83–103. [CrossRef] [PubMed]
13. Chow, E.; Harris, K.; Fan, G.; Tsao, M.; Sze, W.M. Palliative radiotherapy trials for bone metastases: A systematic review. *J. Clin. Oncol.* **2007**, *25*, 1423–1436. [CrossRef] [PubMed]
14. Luetke, A.; Meyers, P.A.; Lewis, I.; Juergens, H. Osteosarcoma treatment—Where do we stand? A state of the art review. *Cancer Treat. Rev.* **2014**, *40*, 523–532. [CrossRef] [PubMed]
15. Savage, S.A.; Mirabello, L. Using epidemiology and genomics to understand osteosarcoma etiology. *Sarcoma* **2011**, *2011*, 14–16. [CrossRef]
16. Peng, S.F.; Lee, C.Y.; Hour, M.J.; Tsai, S.C.; Kuo, D.H.; Chen, F.A.; Shieh, P.C.; Yang, J.S. Curcumin-loaded nanoparticles enhance apoptotic cell death of U2OS human osteosarcoma cells through the Akt-Bad signaling pathway. *Int. J. Oncol.* **2014**, *44*, 238–246. [CrossRef]
17. Susa, M.; Iyer, A.K.; Ryu, K.; Hornicek, F.J.; Mankin, H.; Amiji, M.M.; Duan, Z. Doxorubicin loaded polymeric nanoparticulate delivery system to overcome drug resistance in osteosarcoma. *BMC Cancer* **2009**, *9*, 399. [CrossRef]
18. Ni, M.Z.; Xiong, M.; Zhang, X.C.; Cai, G.P.; Chen, H.W.; Zeng, Q.M.; Yu, Z.C. Poly(lactic-co-glycolic acid) nanoparticles conjugated with CD133 aptamers for targeted salinomycin delivery to CD133+ osteosarcoma cancer stem cells. *Int. J. Nanomed.* **2015**, *10*, 2537–2554.
19. Rahim, M.; Iram, S.; Khan, M.S.; Khan, M.S.; Shukla, A.R.; Srivastava, A.K.; Ahmad, S. Glycation-assisted synthesized gold nanoparticles inhibit growth of bone cancer cells. *Colloids Surf. B Biointerfaces* **2014**, *117*, 473–479. [CrossRef]
20. Steckiewicz, K.P.; Barcinska, E.; Malankowska, A.; Zauszkiewicz-Pawlak, A.; Nowaczyk, G.; Zaleska-Medynska, A.; Inkielewicz-Stepniak, I. Impact of gold nanoparticles shape on their cytotoxicity against human osteoblast and osteosarcoma in in vitro model. Evaluation of the safety of use and anti-cancer potential. *J. Mater. Sci. Mater. Med.* **2019**, *30*, 1–15. [CrossRef]

21. Nayak, D.; Ashe, S.; Rauta, P.R.; Kumari, M.; Nayak, B. Bark extract mediated green synthesis of silver nanoparticles: Evaluation of antimicrobial activity and antiproliferative response against osteosarcoma. *Mater. Sci. Eng. C* **2016**, *58*, 44–52. [CrossRef] [PubMed]
22. Mohanta, Y.K.; Panda, S.K.; Jayabalan, R.; Sharma, N.; Bastia, A.K.; Mohanta, T.K. Antimicrobial, Antioxidant and Cytotoxic Activity of Silver Nanoparticles Synthesized by Leaf Extract of *Erythrina suberosa* (Roxb.). *Front. Mol. Biosci.* **2017**, *4*, 14. [CrossRef] [PubMed]
23. Kovács, D.; Igaz, N.; Keskeny, C.; Bélteky, P.; Tóth, T.; Gáspár, R.; Madarász, D.; Rázga, Z.; Kónya, Z.; Boros, I.M.; et al. Silver nanoparticles defeat p53-positive and p53-negative osteosarcoma cells by triggering mitochondrial stress and apoptosis. *Sci. Rep.* **2016**, *6*, 27902. [CrossRef] [PubMed]
24. Palza, H.; Galarce, N.; Bejarano, J.; Beltran, M.; Caviedes, P. Effect of copper nanoparticles on the cell viability of polymer composites. *Int. J. Polym. Mater. Polym. Biomater.* **2017**, *66*, 462–468. [CrossRef]
25. Sha, B.; Gao, W.; Han, Y.; Wang, S.Q.; Wu, J.; Xu, F.; Lu, T.J. Potential Application of Titanium Dioxide Nanoparticles in the Prevention of Osteosarcoma and Chondrosarcoma Recurrence. *J. Nanosci. Nanotechnol.* **2013**, *13*, 1208–1211. [CrossRef] [PubMed]
26. Di Virgilio, A.L.; Reigosa, M.; Lorenzo De Mele, M.F. Response of UMR 106 cells exposed to titanium oxide and aluminum oxide nanoparticles. *J. Biomed. Mater. Res. Part A* **2010**, *92*, 80–86. [CrossRef]
27. Alpaslan, E.; Yazici, H.; Golshan, N.H.; Ziemer, K.S.; Webster, T.J. PH-Dependent Activity of Dextran-Coated Cerium Oxide Nanoparticles on Prohibiting Osteosarcoma Cell Proliferation. *ACS Biomater. Sci. Eng.* **2015**, *1*, 1096–1103. [CrossRef]
28. Sisubalan, N.; Ramkumar, V.S.; Pugazhendhi, A.; Karthikeyan, C.; Indira, K.; Gopinath, K.; Hameed, A.S.H.; Basha, M.H.G. ROS-mediated cytotoxic activity of ZnO and CeO2 nanoparticles synthesized using the *Rubia cordifolia* L. leaf extract on MG-63 human osteosarcoma cell lines. *Environ. Sci. Pollut. Res.* **2018**, *25*, 10482–10492. [CrossRef]
29. Kimura, R.; Rokkaku, T.; Takeda, S.; Senba, M.; Mori, N. Cytotoxic effects of fucoidan nanoparticles against osteosarcoma. *Mar. Drugs* **2013**, *11*, 4267–4278. [CrossRef]
30. Qing, F.; Wang, Z.; Hong, Y.; Liu, M.; Guo, B.; Luo, H.; Zhang, X. Selective effects of hydroxyapatite nanoparticles on osteosarcoma cells and osteoblasts. *J. Mater. Sci. Mater. Med.* **2012**, *23*, 2245–2251. [CrossRef]
31. Azarami, S.; Huang, Y.; Chen, H.; McQuarrie, S.; Abrams, D.; Roa, W.; Ginlay, W.; Miller, G.; Lobenberg, R. Optimization of a two-step desolvation method for preparing gelatin nanoparticles and cell uptake studies in 143B osteosarcoma cancer cells. *J. Pharm. Pharm. Sci.* **2006**, *9*, 124–132.
32. Wang, B.; Yu, X.C.; Xu, S.F.; Xu, M. Paclitaxel and etoposide co-loaded polymeric nanoparticles for the effective combination therapy against human osteosarcoma. *J. Nanobiotechnol.* **2015**, *13*, 22. [CrossRef] [PubMed]
33. Elhamess, H.; Bertrand, J.R.; MacCario, J.; Maksimenko, A.; Malvy, C. Antitumor vectorized oligonucleotides in a model of ewing sarcoma: Unexpected role of nanoparticles. *Oligonucleotides* **2009**, *19*, 255–264. [CrossRef] [PubMed]
34. Karuppaiya, P.; Satheeshkumar, E.; Chao, W.T.; Kao, L.Y.; Chen, E.C.F.; Tsay, H.S. Anti-metastatic activity of biologically synthesized gold nanoparticles on human fibrosarcoma cell line HT-1080. *Colloids Surf. B Biointerfaces* **2013**, *110*, 163–170. [CrossRef]
35. Safaepour, M.; Shahverdi, A.R.; Shahverdi, H.R.; Khorramizadeh, M.R.; Gohari, A.R. Green Synthesis of Small Silver Nanoparticles Using Geraniol and Its Cytotoxicity against Fibrosarcoma-Wehi. *Avicenna J. Med. Biotechnol.* **2009**, *1*, 111–115.
36. Khorramizadeh, M.R.; Esmail-Nazari, Z.; Zarei-Ghaane, Z.; Shakibaie, M.; Mollazadeh-Moghaddam, K.; Iranshahi, M.; Shahverdi, A.R. Umbelliprenin-coated Fe3O4 magnetite nanoparticles: Antiproliferation evaluation on human Fibrosarcoma cell line (HT-1080). *Mater. Sci. Eng. C* **2010**, *30*, 1038–1042. [CrossRef]
37. Yang, W.J.; Lee, J.H.; Hong, S.C.; Lee, J.; Lee, J.; Han, D.W. Difference between toxicities of iron oxide magnetic nanoparticles with various surface-functional groups against human normal fibroblasts and fibrosarcoma cells. *Materials* **2013**, *6*, 4689–4706. [CrossRef]
38. Akhtar, M.J.; Ahamed, M.; Alhadlaq, H.A.; Khan, M.A.M.; Alrokayan, S.A. Glutathione replenishing potential of CeO_2 nanoparticles in human breast and fibrosarcoma cells. *J. Colloid Interface Sci.* **2015**, *453*, 21–27. [CrossRef]

39. Nourmohammadi, E.; Khoshdel-sarkarizi, H.; Nedaeinia, R.; Sadeghnia, H.R.; Hasanzadeh, L.; Darroudi, M.; Kazemi oskuee, R. Evaluation of anticancer effects of cerium oxide nanoparticles on mouse fibrosarcoma cell line. *J. Cell. Physiol.* **2019**, *234*, 4987–4996. [CrossRef]
40. Alarifi, S.; Ali, D.; Alkahtani, S. Mechanistic investigation of toxicity of chromium oxide nanoparticles in murine fibrosarcoma cells. *Int. J. Nanomed.* **2016**, *11*, 1253–1259.
41. Sun, K.; Wang, J.; Zhang, J.; Hua, M.; Liu, C.; Chen, T. Dextran-g-PEI nanoparticles as a carrier for co-delivery of adriamycin and plasmid into osteosarcoma cells. *Int. J. Biol. Macromol.* **2011**, *49*, 173–180. [CrossRef] [PubMed]
42. Palakurthi, S.; Yellepeddi, V.K.; Vangara, K.K. Recent trends in cancer drug resistance reversal strategies using nanoparticles. *Expert Opin. Drug Deliv.* **2012**, *9*, 287–301. [CrossRef] [PubMed]
43. Dhule, S.S.; Penfornis, P.; Frazier, T.; Walker, R.; Feldman, J.; Tan, G.; He, J.; Alb, A.; John, V.; Pochampally, R. Curcumin-loaded γ-cyclodextrin liposomal nanoparticles as delivery vehicles for osteosarcoma. *Nanomed. Nanotechnol. Biol. Med.* **2012**, *8*, 440–451. [CrossRef]
44. Steckiewicz, K.P.; Barcińska, E.; Sobczak, K.; Tomczyk, E.; Wójcik, M.; Inkielewicz-Stepniak, I. Assessment of anti-tumor potential and safety of application of glutathione stabilized gold nanoparticles conjugated with chemotherapeutic. *Int. J. Med. Sci.* **2020**, *17*, 824–833. [CrossRef]
45. Kobayashi, T. Cancer hyperthermia using magnetic nanoparticles. *Biotechnol. J.* **2011**, *6*, 1342–1347. [CrossRef] [PubMed]
46. Makridis, A.; Topouridou, K.; Tziomaki, M.; Sakellari, D.; Simeonidis, K.; Angelakeris, M.; Yavropoulou, M.P.; Yovos, J.G.; Kalogirou, O. In vitro application of Mn-ferrite nanoparticles as novel magnetic hyperthermia agents. *J. Mater. Chem. B* **2014**, *2*, 8390–8398. [CrossRef]
47. Shido, Y.; Nishida, Y.; Suzuki, Y.; Kobayashi, T.; Ishiguro, N. Targeted hyperthermia using magnetite cationic liposomes and an alternating magnetic field in a mouse osteosarcoma model. *J. Bone Jt. Surg. Ser. B* **2010**, *92*, 580–585. [CrossRef]
48. Matsuoka, F.; Shinkai, M.; Honda, H.; Kubo, T.; Sugita, T.; Kobayashi, T. Hyperthermia using magnetite cationic liposomes for hamster osteosarcoma. *Biomagn. Res. Technol.* **2004**, *2*, 3. [CrossRef]
49. Li, X.S.; Li, W.Q.; Wang, W.B. Using targeted magnetic arsenic trioxide nanoparticles for osteosarcoma treatment. *Cancer Biother. Radiopharm.* **2007**, *22*, 772–778. [CrossRef]
50. Kubo, T.; Sugita, T.; Shimose, S.; Nitta, Y.; Ikuta, Y.; Murakami, T. Targeted systemic chemotherapy using magnetic liposomes with incorporated adriamycin for osteosarcoma in hamsters. *Int. J. Oncol.* **2001**, *18*, 121–125. [CrossRef]
51. MacDonald, K.V.; Sanmartin, C.; Langlois, K.; Marshall, D.A. Symptom onset, diagnosis and management of osteoarthritis. *Health Rep.* **2014**, *25*, 10–17.
52. Baker, C.; Pradhan, A.; Pakstis, L.; Pochan, D.J.; Shah, S.I. Synthesis and antibacterial properties of silver nanoparticles. *J. Nanosci. Nanotechnol.* **2005**, *5*, 244–249. [CrossRef] [PubMed]
53. Neupane, M.P.; Park, I.S.; Bae, T.S.; Yi, H.K.; Uo, M.; Watari, F.; Lee, M.H. Titania nanotubes supported gelatin stabilized gold nanoparticles for medical implants. *J. Mater. Chem.* **2011**, *21*, 12078–12082. [CrossRef]
54. Darouiche, R.O. Treatment of infections associated with surgical implants. *N. Engl. J. Med.* **2004**, *350*, 1422–1429. [CrossRef] [PubMed]
55. Steckiewicz, K.P.; Zwara, J.; Jaskiewicz, M.; Kowalski, S.; Kamysz, W.; Zaleska-medynska, A.; Inkielewicz-stepniak, I. Shape-Depended Biological Properties of Ag 3 PO 4 Microparticles: Evaluation of Antimicrobial Properties and Cytotoxicity in In Vitro Model—Safety Assessment of Potential Clinical Usage. *Oxidative Med. Cell. Longev.* **2019**, *2019*. [CrossRef] [PubMed]
56. Campoccia, D.; Montanaro, L.; Arciola, C.R. The significance of infection related to orthopedic devices and issues of antibiotic resistance. *Biomaterials* **2006**, *27*, 2331–2339. [CrossRef]
57. Parvizi, J.; Mui, A.; Purtill, J.; Sharkey, P.; Hozack, W.; Rothman, R. Total Joint Arthroplasty: When Do Fatal or Near-Fatal Complications Occur? *J. Bone Jt. Surg. Am.* **2007**, *89*, 27–32.
58. Trampuz, A.; Widmer, A.F. Infections associated with orthopedic implants. *Curr. Opin. Infect. Dis.* **2006**, *19*, 349–356. [CrossRef]
59. Markowska, K.; Grudniak, A.M.; Wolska, K.I. Silver nanoparticles as an alternative strategy against bacterial biofilms. *Acta Biochim. Pol.* **2013**, *60*, 523–530. [CrossRef]

60. Saginur, R.; StDenis, M.; Ferris, W.; Aaron, S.D.; Chan, F.; Lee, C.; Ramotar, K. Multiple combination bactericidal testing of staphylococcal biofilms from implant-associated infections. *Antimicrob. Agents Chemother.* **2006**, *50*, 55–61. [CrossRef]
61. Ren, N.; Li, R.; Chen, L.; Wang, G.; Liu, D.; Wang, Y.; Zheng, L.; Tang, W.; Yu, X.; Jiang, H.; et al. In situ construction of a titanate-silver nanoparticle-titanate sandwich nanostructure on a metallic titanium surface for bacteriostatic and biocompatible implants. *J. Mater. Chem.* **2012**, *22*, 19151–19160. [CrossRef]
62. Xiang, Y.; Li, J.; Liu, X.; Cui, Z.; Yang, X.; Yeung, K.W.K.; Pan, H.; Wu, S. Construction of poly(lactic-co-glycolic acid)/ZnO nanorods/Ag nanoparticles hybrid coating on Ti implants for enhanced antibacterial activity and biocompatibility. *Mater. Sci. Eng. C* **2017**, *79*, 629–637. [CrossRef] [PubMed]
63. Wang, Z.; Sun, Y.; Wang, D.; Liu, H.; Boughton, R.I. In situ fabrication of silver nanoparticlefilled hydrogen titanate nanotube layer on metallic titanium surface for bacteriostatic and biocompatible implantation. *Int. J. Nanomed.* **2013**, *8*, 2903–2916.
64. Fomin, A.A.; Rodionov, I.V.; Steinhauer, A.B.; Fomina, M.A.; Zakharevich, A.M.; Skaptsov, A.A.; Petrova, N.V. Structure of composite biocompatible titania coatings modified with hydroxyapatite nanoparticles. *Proc. Adv. Mater. Res.* **2013**, *787*, 376–381. [CrossRef]
65. Salaie, R.N.; Besinis, A.; Le, H.; Tredwin, C.; Handy, R.D. The biocompatibility of silver and nanohydroxyapatite coatings on titanium dental implants with human primary osteoblast cells. *Mater. Sci. Eng. C* **2020**, *107*, 110210. [CrossRef]
66. Liping, T. Nanocoating for Improving Biocompatibility of Medical Implants. U.S. Patent 10/896376, 21 April 2005.
67. He, W.; Zheng, Y.; Feng, Q.; Elkhooly, T.A.; Liu, X.; Yang, X.; Wang, Y.; Xie, Y. Silver nanoparticles stimulate osteogenesis of human mesenchymal stem cells through activation of autophagy. *Nanomedicine* **2020**, *15*, 337–353. [CrossRef]
68. Ghaznavi, D.; Babaloo, A.; Shirmohammadi, A.; Zamani, A.R.N.; Azizi, M.; Rahbarghazi, R.; Ghaznavi, A. Advanced platelet-rich fibrin plus gold nanoparticles enhanced the osteogenic capacity of human mesenchymal stem cells. *BMC Res. Notes* **2019**, *12*, 721. [CrossRef]
69. Patel, D.K.; Jin, B.; Dutta, S.D.; Lim, K.T. Osteogenic potential of human mesenchymal stem cells on eggshells-derived hydroxyapatite nanoparticles for tissue engineering. *J. Biomed. Mater. Res. Part B Appl. Biomater.* **2019**. [CrossRef]
70. Liang, H.; Xu, X.; Feng, X.; Ma, L.; Deng, X.; Wu, S.; Liu, X.; Yang, C. Gold nanoparticles-loaded hydroxyapatite composites guide osteogenic differentiation of human mesenchymal stem cells through Wnt/β-catenin signaling pathway. *Int. J. Nanomed.* **2019**, *14*, 6151–6163. [CrossRef]
71. Alicka, M.; Sobierajska, P.; Kornicka, K.; Wiglusz, R.J.; Marycz, K. Lithium ions (Li +) and nanohydroxyapatite (nHAp) doped with Li + enhance expression of late osteogenic markers in adipose-derived stem cells. Potential theranostic application of nHAp doped with Li + and co-doped with europium (III) and samarium (III) i. *Mater. Sci. Eng. C* **2019**, *99*, 1257–1273. [CrossRef]
72. Phelipe Hatt, L.; Thompson, K.; Müller, W.E.G.G.; Stoddart, M.J.; Armiento, A.R.; Hatt, L.P.; Thompson, K.; Müller, W.E.G.G.; Stoddart, M.J.; Armiento, A.R. Calcium polyphosphate nanoparticles act as an effective inorganic phosphate source during osteogenic differentiation of human mesenchymal stem cells. *Int. J. Mol. Sci.* **2019**, *20*, 5801. [CrossRef] [PubMed]
73. Palmieri, V.; Barba, M.; Di Pietro, L.; Gentilini, S.; Braidotti, M.C.; Ciancico, C.; Bugli, F.; Ciasca, G.; Larciprete, R.; Lattanzi, W.; et al. Reduction and shaping of graphene-oxide by laser-printing for controlled bone tissue regeneration and bacterial killing. *2D Mater.* **2018**, *5*, 015027. [CrossRef]
74. Palmieri, V.; Barba, M.; Di Pietro, L.; Conti, C.; De Spirito, M.; Lattanzi, W.; Papi, M. Graphene Oxide Induced Osteogenesis Quantification by In-Situ 2D-Fluorescence Spectroscopy. *Int. J. Mol. Sci.* **2018**, *19*, 3336. [CrossRef] [PubMed]
75. Wang, M.; Wu, H.; Li, Q.; Yang, Y.; Che, F.; Wang, G.; Zhang, L. Novel aptamer-functionalized nanoparticles enhances bone defect repair by improving stem cell recruitment. *Int. J. Nanomed.* **2019**, *14*, 8707–8724. [CrossRef]
76. Balagangadharan, K.; Trivedi, R.; Vairamani, M.; Selvamurugan, N. Sinapic acid-loaded chitosan nanoparticles in polycaprolactone electrospun fibers for bone regeneration in vitro and in vivo. *Carbohydr. Polym.* **2019**, *216*, 1–16. [CrossRef]

77. Kuang, L.; Ma, X.; Ma, Y.; Yao, Y.; Tariq, M.; Yuan, Y.; Liu, C. Self-Assembled Injectable Nanocomposite Hydrogels Coordinated by in Situ Generated CaP Nanoparticles for Bone Regeneration. *ACS Appl. Mater. Interfaces* **2019**, *11*, 17234–17246. [CrossRef]
78. Martínez-Castañón, G.A.; Niño-Martínez, N.; Martínez-Gutierrez, F.; Martínez-Mendoza, J.R.; Ruiz, F. Synthesis and antibacterial activity of silver nanoparticles with different sizes. *J. Nanopart. Res.* **2008**, *10*, 1343–1348. [CrossRef]
79. Shrivastava, S.; Bera, T.; Roy, A.; Singh, G.; Ramachandrarao, P.; Dash, D. Characterization of enhanced antibacterial effects of novel silver nanoparticles. *Nanotechnology* **2007**, *18*, 225103–225112. [CrossRef]
80. Mohanty, S.; Mishra, S.; Jena, P.; Jacob, B.; Sarkar, B.; Sonawane, A. An investigation on the antibacterial, cytotoxic, and antibiofilm efficacy of starch-stabilized silver nanoparticles. *Nanomed. Nanotechnol. Biol. Med.* **2012**, *8*, 916–924. [CrossRef]
81. Franci, G.; Falanga, A.; Galdiero, S.; Palomba, L.; Rai, M.; Morelli, G.; Galdiero, M. Silver nanoparticles as potential antibacterial agents. *Molecules* **2015**, *20*, 8856–8874. [CrossRef]
82. Niska, K.; Knap, N.; Kędzia, A.; Jaskiewicz, M.; Kamysz, W.; Inkielewicz-Stepniak, I. Capping Agent-Dependent Toxicity and Antimicrobial Activity of Silver Nanoparticles: An In Vitro Study. Concerns about Potential Application in Dental Practice. *Int. J. Med. Sci.* **2016**, *13*, 772–782. [CrossRef] [PubMed]
83. Morones, J.R.; Elechiguerra, J.L.; Camacho, A.; Holt, K.; Kouri, J.B.; Ram, J.T.; Yacaman, M.J.; Ramírez, J.T.; Yacaman, M.J. The bactericidal effect of silver nanoparticles. *Nanotechnology* **2005**, *16*, 2346–2353. [CrossRef]
84. Kim, J.H.J.S.; Kuk, E.; Yu, K.N.; Kim, J.H.J.S.; Park, S.J.; Lee, H.J.; Kim, S.H.; Park, Y.H.Y.K.; Park, Y.H.Y.K.; Hwang, C.Y.; et al. Antimicrobial effects of silver nanoparticles. *Nanomed. Nanotechnol. Biol. Med.* **2007**, *3*, 95–101. [CrossRef] [PubMed]
85. Pereira, L.; Dias, N.; Carvalho, J.; Fernandes, S.; Santos, C.; Lima, N. Synthesis, characterization and antifungal activity of chemically and fungal-produced silver nanoparticles against *Trichophyton rubrum*. *J. Appl. Microbiol.* **2014**, *117*, 1601–1613. [CrossRef]
86. Panáček, A.; Kolář, M.; Večeřová, R.; Prucek, R.; Soukupová, J.; Kryštof, V.; Hamal, P.; Zbořil, R.; Kvítek, L. Antifungal activity of silver nanoparticles against *Candida* spp. *Biomaterials* **2009**, *30*, 6333–6340. [CrossRef] [PubMed]
87. Kim, K.J.; Sung, W.S.; Moon, S.K.; Choi, J.S.; Kim, J.G.; Lee, D.G. Antifungal effect of silver nanoparticles on dermatophytes. *J. Microbiol. Biotechnol.* **2008**, *18*, 1482–1484. [PubMed]
88. Galdiero, S.; Falanga, A.; Vitiello, M.; Cantisani, M.; Marra, V.; Galdiero, M. Silver nanoparticles as potential antiviral agents. *Molecules* **2011**, *16*, 8894–8918. [CrossRef] [PubMed]
89. Saleh, M.; Abdel-Baki, A.A.; Dkhil, M.A.; El-Matbouli, M.; Al-Quraishy, S. Antiprotozoal effects of metal nanoparticles against *Ichthyophthirius multifiliis*. *Parasitology* **2017**, *114*, 1802–1810. [CrossRef]
90. Cui, Y.; Zhao, Y.; Tian, Y.; Zhang, W.; Lü, X.; Jiang, X. The molecular mechanism of action of bactericidal gold nanoparticles on *Escherichia coli*. *Biomaterials* **2012**, *33*, 2327–2333. [CrossRef]
91. Zawrah, M.F.; El-Moez, S.A.; Center, D. Antimicrobial Activities of Gold Nanoparticles against Major Foodborne Pathogens. *Life Sci. J.* **2011**, *8*, 37–44.
92. Bindhu, M.R.; Umadevi, M. Antibacterial activities of green synthesized gold nanoparticles. *Mater. Lett.* **2014**, *120*, 122–125. [CrossRef]
93. Hernández-Sierra, J.F.; Ruiz, F.; Cruz Pena, D.C.; Martínez-Gutiérrez, F.; Martínez, A.E.; de Jesús Pozos Guillén, A.; Tapia-Pérez, H.; Martínez Castañón, G. The antimicrobial sensitivity of Streptococcus mutans to nanoparticles of silver, zinc oxide, and gold. *Nanomed. Nanotechnol. Biol. Med.* **2008**, *4*, 237–240. [CrossRef] [PubMed]
94. Shankar, S.; Jaiswal, L.; Aparna, R.S.L.; Prasad, R.G.S.V. Synthesis, characterization, in vitro biocompatibility, and antimicrobial activity of gold, silver and gold silver alloy nanoparticles prepared from Lansium domesticum fruit peel extract. *Mater. Lett.* **2014**, *137*, 75–78. [CrossRef]
95. Chatterjee, A.K.; Chakraborty, R.; Basu, T. Mechanism of antibacterial activity of copper nanoparticles. *Nanotechnology* **2014**, *25*. [CrossRef]
96. Ramyadevi, J.; Jeyasubramanian, K.; Marikani, A.; Rajakumar, G.; Rahuman, A.A. Synthesis and antimicrobial activity of copper nanoparticles. *Mater. Lett.* **2012**, *71*, 114–116. [CrossRef]
97. Kairyte, K.; Kadys, A.; Luksiene, Z. Antibacterial and antifungal activity of photoactivated ZnO nanoparticles in suspension. *J. Photochem. Photobiol. B Biol.* **2013**, *128*, 78–84. [CrossRef]

98. Lipovsky, A.; Nitzan, Y.; Gedanken, A.; Lubart, R. Antifungal activity of ZnO nanoparticles-the role of ROS mediated cell injury. *Nanotechnology* **2011**, *22*, 105101. [CrossRef]
99. Li, Y.; Zhang, W.; Niu, J.; Chen, Y. Mechanism of photogenerated reactive oxygen species and correlation with the antibacterial properties of engineered metal-oxide nanoparticles. *ACS Nano* **2012**, *6*, 5164–5173. [CrossRef]
100. Raffi, M.; Mehrwan, S.; Bhatti, T.M.; Akhter, J.I.; Hameed, A.; Yawar, W.; Ul Hasan, M.M. Investigations into the antibacterial behavior of copper nanoparticles against Escherichia coli. *Ann. Microbiol.* **2010**, *60*, 75–80. [CrossRef]
101. Albers, C.E.; Hofstetter, W.; Siebenrock, K.A.; Landmann, R.; Klenke, F.M. In vitro cytotoxicity of silver nanoparticles on osteoblasts and osteoclasts at antibacterial concentrations. *Nanotoxicology* **2013**, *7*, 30–36. [CrossRef]
102. Zielinska, E.; Tukaj, C.; Radomski, M.W.; Inkielewicz-Stepniak, I. Molecular Mechanism of Silver Nanoparticles-Induced Human Osteoblast Cell Death: Protective Effect of Inducible Nitric Oxide Synthase Inhibitor. *PLoS ONE* **2016**, *11*, e0164137. [CrossRef] [PubMed]
103. Niska, K.; Pyszka, K.; Tukaj, C.; Wozniak, M.; Radomski, M.W.; Inkielewicz-Stepniak, I. Titanium dioxide nanoparticles enhance production of superoxide anion and alter the antioxidant system in human osteoblast cells. *Int. J. Nanomed.* **2015**, *10*, 1095–1107.
104. Dobrzyńska, M.M.; Gajowik, A.; Radzikowska, J.; Lankoff, A.; Dušinská, M.; Kruszewski, M. Genotoxicity of silver and titanium dioxide nanoparticles in bone marrow cells of rats in vivo. *Toxicology* **2014**, *315*, 86–91. [CrossRef]
105. Duewelhenke, N.; Krut, O.; Eysel, P. Influence on mitochondria and cytotoxicity of different antibiotics administered in high concentrations on primary human osteoblasts and cell lines. *Antimicrob. Agents Chemother.* **2007**, *51*, 54–63. [CrossRef]
106. Wang, H.-Z.; Chang, C.-H.; Lin, C.-P.; Tsai, M.-C. Using MTT Viability Assay to Test the Cytotoxicity of Antibiotics and Steroid to Cultured Porcine Corneal Endothelial Cells. *J. Ocul. Pharmacol. Ther.* **2009**, *12*, 35–43. [CrossRef]
107. Duwe, A.K.; Rupar, C.A.; Horsman, G.B.; Vas, S.I. In vitro cytotoxicity and antibiotic activity of polymyxin B nonapeptide. *Antimicrob. Agents Chemother.* **1986**, *30*, 340–341. [CrossRef]
108. Kubicka, S.; Rudolph, K.L.; Tietze, M.K.; Lorenz, M.; Manns, M. Phase II study of systemic gemcitabine chemotherapy for advanced unresectable hepatobiliary carcinomas. *Hepatogastroenterology* **2001**, *48*, 783–789.
109. Speth, P.A.J.; van Hoesel, Q.G.C.M.; Haanen, C. Clinical Pharmacokinetics of Doxorubicin. *Clin. Pharmacokinet.* **1988**, *15*, 15–31. [CrossRef]
110. Juel-Jensen, B.E. Severe generalized primary herpes treated with cytarabine. *Br. Med. J.* **1970**, *2*, 154–155. [CrossRef]
111. Bobo, D.; Robinson, K.J.; Islam, J.; Thurecht, K.J.; Corrie, S.R. Nanoparticle-Based Medicines: A Review of FDA-Approved Materials and Clinical Trials to Date. *Pharm. Res.* **2016**, *33*, 2373–2387. [CrossRef]
112. Taruno, K.; Kurita, T.; Kuwahata, A.; Yanagihara, K.; Enokido, K.; Katayose, Y.; Nakamura, S.; Takei, H.; Sekino, M.; Kusakabe, M. Multicenter clinical trial on sentinel lymph node biopsy using superparamagnetic iron oxide nanoparticles and a novel handheld magnetic probe. *J. Surg. Oncol.* **2019**, *120*, 1391–1396. [CrossRef] [PubMed]
113. Xu, X.F.; Gu, J. The application of carbon nanoparticles in the lymph node biopsy of cN0 papillary thyroid carcinoma: A randomized controlled clinical trial. *Asian J. Surg.* **2017**, *40*, 345–349. [CrossRef] [PubMed]

Journal of Materials Science: Materials in Medicine (2019) 30:22
https://doi.org/10.1007/s10856-019-6221-2

BIOCOMPATIBILITY STUDIES

Original Research

Impact of gold nanoparticles shape on their cytotoxicity against human osteoblast and osteosarcoma in in vitro model. Evaluation of the safety of use and anti-cancer potential

Karol P. Steckiewicz[1] · Ewelina Barcinska[1] · Anna Malankowska[2] · Agata Zauszkiewicz–Pawlak[3] · Grzegorz Nowaczyk[4] · Adriana Zaleska-Medynska[2] · Iwona Inkielewicz-Stepniak[1]

Received: 24 September 2018 / Accepted: 10 January 2019 / Published online: 12 February 2019

Abstract

Due to development of nanotechnology and gold nanoparticles (AuNPs) increasing use in different areas of medicine, especially in oncology, better understanding of their potential cytotoxicity is necessary to protect patients safety. Shape and size of AuNPs is an important modulator of their cytotoxicity. Therefore, we investigated the cytotoxicity of AuNPs rods (≈39 nm length, 18 nm width), AuNPs stars (≈ 215 nm) and AuNPs spheres (≈ 6.3 nm) against human fetal osteoblast (hFOB 1.19), osteosarcoma (143B, MG63) and pancreatic duct cell (hTERT-HPNE) lines by MTT and neutral-red uptake assay. Moreover, influence of AuNPs on level of proapoptotic protein (Bax) and anti-apoptotic protein (Bcl-2) was measured by western blot. Cellular uptake of nanoparticles and ultrastructure changes were examined by transmission electron microscopy (TEM). In the present study we have proven that AuNPs stars are the most cytotoxic against human cells. We observed that cancer cells are more susceptible to AuNPs cytotoxic effect. Furthermore, AuNPs rods and AuNPs stars caused increased expression of Bax and decreased expression of Bcl-2 protein in osteosarcoma cells. We found that AuNPs penetrated through the cell membrane and caused ultrastructural changes. Our results clearly demonstrated that the cytotoxicity of AuNPs was shape-dependent. AuNPs stars with the highest anti-cancer potential were also the most cytotoxic type of tested NPs, whereas AuNPs spheres which appears to be the safest one had small anti-cancer potential.

Supplementary information The online version of this article (https://doi.org/10.1007/s10856-019-6221-2) contains supplementary material, which is available to authorized users.

✉ Iwona Inkielewicz-Stepniak
iinkiel@gumed.edu.pl

[1] Department of Medical Chemistry, Medical University of Gdansk, Debinki 1, 80-211 Gdansk, Poland

[2] Department of Environmental Technology, Faculty of Chemistry, University of Gdansk, Wita Stwosza 63, 80-308 Gdansk, Poland

[3] Department of Histology, Medical University of Gdansk, Debinki 1, 80-211 Gdansk, Poland

[4] NanoBioMedical Center, Adam Mickiewicz University, 61-614 Poznan, Poland

Graphical Abstract

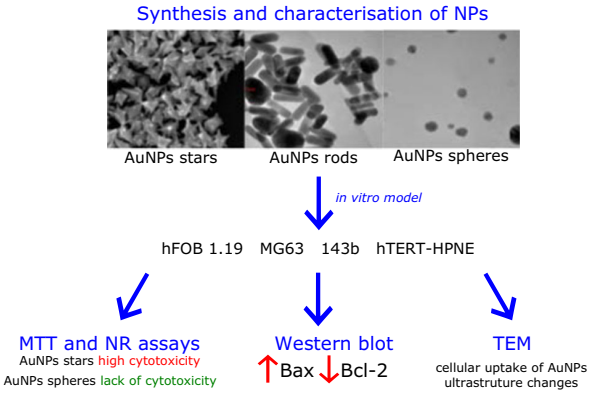

1 Introduction

In 21st century nanotechnology is rapidly developing and its achievements may be used in biology and medicine. Nobel metals nanoparticles seem to be particularly interesting in biomedical application. Gold nanoparticles (AuNPs) due to small size, high surface area to volume ratio and good biocompatibility have great potential for a wide range of applications in medicine [1]. Furthermore, there are many different shapes of AuNPs, they can have one, two or even three dimension which also expand variety of potential usages [2]. It is also important that AuNPs can penetrate through biological barriers and cellular membranes. [3]. The unique properties causes that AuNPs are widely applied in diagnostic and therapy, from medical imaging [4] to bacteria and viruses detection [5, 6]. They are also component of thermal ablation [7] and cancer immunotherapy [8]. Moreover, AuNPs may be part of drug delivery systems [9]. Unfortunately, it has been shown that AuNPs can accumulate in vacuoles and induce cell death [4, 10]. In addition, AuNPs may cause increased synthesis of proapoptotoic proteins [3].

There are not enough studies which compare different shapes of AuNPs on the same cell lines using identical methodology and because of variety of potential bioapplication of AuNPs, we decided to assess the impact of shape and size of AuNPs on human cells in in vitro model. Cytotoxicity of different concentration of AuNPs rods, AuNPs stars and AuNPs spheres were tested on four cell lines: hFOB 1.19, 143B, MG63 and hTERT-HPNE. According to our knowledge it is the first study, which compares impact of shape of AuNPs on their cytotoxicity against human osteoblast, osteosarcoma and pancreatic duct cells. The main purpose of this research was to assess the cytotoxic activity against cancer cells as well as the safety of use.

2 Materials and methods

2.1 Chemical reagents

Cetyltrimethylammonium bromide (99%, CTAB), sodium borohydrate (>98%), L-ascorbic acid (99%, AA), silver nitrate (99%), tannic acid were purchased from Sigma Aldrich. Gold (III) chloride trihydrate was purchased from Alfa Aesar.

2.2 Synthesis of AuNPs

The AuNPs spheres, rods and stars were prepared and characterized as described in our previous articles [11, 12], with some modification indicated below.

2.2.1 Au nanospheres

AuNPs spheres were obtained by mixing solution of tannic acid (3 ml, 6×10^{-3} M) and hot solution of $HAuCl_4$ (50 ml, 1.3×10^{-4} M) for 1 min.

2.2.2 Au nanostars

Firstly, an aqueous solution of gold precursor (0.2 mL, 0.01 M) was added to the 0.1 M CTAB. After that 0.01 M $AgNO_3$ solution and 0.1 M AA solution were added. In the next step, 20 µL of AuNPs stars solution was added. The obtained solution was kept for 20 h at 28–30 °C. The color of the solution became blue indicating the formation of AuNPs stars. The products were isolated and washing with water.

2.2.3 Au nanorods

Firstly, seed solution was obtained by stirring 0.2 M CTAB solution with 0.5 mM gold precursor and 0.6 ml of 0.01 M $NaBH_4$. The solution was kept at 30 °C for 4 h.

Then, AuNPs rods were prepared by mixing 5 mL CTAB, 40 mM $AgNO_3$ solution, 5 mL $HAuCl_4$ solution followed by the addition of 70 µL AA. The final step was the addition of 12 µL of the seed solution to the growth solution at 30 °C. The AuNPs rods were isolated and washed with water.

2.3 Characterization of synthesized AuNPs

UV–Vis absorption spectra were obtained using a spectrophotometer Thermo Scientific Evolution 220 (Waltham, MA, USA) in the range of 200–1400 nm. The morphology and distribution size of obtained particles were observed using SEM Jeol 7001TTLS microscope operated at 12 kV and HR-TEM (ARM 200 F) operating at 200 kV. For HR-TEM sample preparation, a drop of a aqueous gold dispersion was deposited on cooper grid covered with a formal-carbon membrane. For SEM analysis aqueous solution of AuNPs was deposited on cleaned silicon wafer substrates.

2.4 Cell culture

Cell lines were obtained from the American Type Culture Collection (ATCC). Human fetal osteoblast cell line (hFOB 1.19, ATCC CRL-11372), was cultured in 1:1 mixture of Ham's F12 Medium and Dulbecco's Modified Eagle's Medium (PanBiotech, Germany), by supplemented 2.5 mM L-glutamine, 10% fetal bovine serum (FBS) and 1% of penicillin/streptomycin (P/S). Human bone osteosarcoma cell line (143B, ATCC CRL 8303) was cultured in Minimum Essential Medium (Eagle) in Earle's BSS (PanBiotech, Germany) with 0.015 mg/mL 5-bromo-2′-deoxyuridine, 2.5 mM L-glutamine, with an addition of 10% FBS and 1% of P/S. Human osteosarcoma cell line (MG-63, ATCC CRL-1427) was cultured in Eagle's Minimum Essential Medium (PanBiotech, Germany) supplemented by 10% FBS and 1% of P/S. hTERT-HPNE cell line (pancreatic duct cells) (ATCC CRL-4023) was cultured in medium which consist of 75% Dulbecco's Modified Eagle's Medium without glucose (Sigma Aldrich), 25% of M3 Base (Sigma Aldrich, USA), 5% of FBS, 1% of antibiotics, 5.5 mM D-glucose, 2 mM of L-glutamine, 1.5 g/L sodium bicarbonate and 10 ng/mL human recombinant EGF. All cells were cultured under standard conditions. All cell cultures were cultured at 37 °C in a humidified atmosphere of 5% CO_2. Cells were maintained in 75 cm^2 tissue culture flask. The medium was replaced every 48 h. When confluent cells were detached with trypsin-EDTA solution and subcultured into a newer flask. Subcultivation ratio was 1:4 for hFOB 1.19, 143B, and MG-63 cells and 1:8 for hTERT-HPNE cells.

2.5 Treatments

hFOB 1.19, MG-63, 143B and hTERT-HPNE cells were treated using AuNPs in the three different shapes rods, stars, and roods for 24 h. Concentrations used in experiments were determined by preliminary studies (in range of 0.3–5 µg/mL). Each time, just before, experiment AuNPs were diluted in FBS-free media and shaken well to ensure equal dispersion of AuNPs in solution. AuNPs solutions were shaken before use to avoid agglomeration of nanoparticles. Control samples were treated with AuNPs-free, FBS-free culture media. The medium was not change during the incubation process.

2.6 MTT viability assay

MTT assay was used to determine cell viability. Cells were seeded in 96 plates at a density of 1×10^4 cell per well. After 24 h cells were treated as described in *Treatments* section. For rods, stars and spheres concentration 0.3, 0.6, 1.2, 2.5 and 5 µg/mL were examined. After 24 h incubation the media was supplemented of water-soluble tetrazolium salt [3-(4,5-dimethylthiazol-2-yl)-2,5-diphenyltetrazolium bromide (final concentration 0,45 mg/mL). Next, microplates were incubated at 37 °C in 5% CO_2 for 2 h. After incubation media was replaced and formazan crystals were diluted in 100 µL of dimethyl sulfoxide (DMSO). After 15 min, cell viability was assessed by measuring absorbance at 540 nm (reference 630 nm) using microplate reader. Viability was determined as a percentage of control (viability of control cells was set as 100%). Absorbance values were corrected with blank NPs.

2.7 Neutral red uptake viability assay

The assay is based on the ability of viable, uninjured cells to accumulate neutral red dye solution in lysosomes. Cells were seeded in 96 plates at a density of 1×10^4 cell/well. After 24 h cells were treated as described in treatments section. For rods, stars and spheres concentration 0.3, 0.6, 1.2, 2.5 and 5 µg/mL were examined. Next, to each wall, the neutral red dye was added to final concentration of 100 µg/mL. Then, microplates were incubated at 37 °C in 5% CO_2 for 2 h and medium was removed, cells washed with phosphate buffered saline (PBS) (NaCl 0.138 M, KCl 0.0027 M, pH = 7.4, without Ca^{2+} and Mg^{2+}) and fixated with neutral red fixative solution (0.5% formaldehyde, 0.1% $CaCl_2$). Subsequently, the dye was dissolved in neutral red solubilization solution (50% ethanol, 1% acetic acid) and gentle shaking for 10 min. Cell viability was assessed by measuring of absorbance at 540 nm (reference 630 nm) using microplate reader. Viability was determined as a percentage of control

(viability of control cells was set as 100%). Absorbance values were corrected with blank NPs.

2.8 Western blotting

Western blotting was used to examining the influence of AuNPs on pro and anti-apoptotic proteins levels. Briefly, MG-63 and 143B cells were treated with nanoparticles in FBS-free media as described in *Treatments* section. For AuNPs rods concentrations of NPs were 1 and 2 µg/mL, for AuNPs stars concentrations were 0.1, 0.3, 0.6, 1 µg/mL. Cells were seeded in 10 cm^2 Petri dish. When confluence was about 80–90% cells were treated with AuNPs for 24 h and Western blotting analysis was performed according to protocol previously established by our team [13]. Before electrophoresis protein level was measured by Bradford method [14]. Rabbit polyclonal anti-Bcl-2 and anti-Bax IgG antibodies and anti-rabbit secondary antibodies were used (Santa Cruz, USA). Dilution of antibodies according to manufacturer protocol was 1:250 for Bax; 1:100 for Bcl-2 and 1:20000 for anti-rabbit secondary antibodies. β-actin was used as loading control. Immunoactive proteins level were examined by chemiluminescence (ECL) Western-blotting kit.. Proteins levels were quantified using densitometry software (ImageQuant Software, GE Healthcare, UK).

2.9 TEM analysis

Cellular uptake of nanoparticles and ultrastructure changes were examined by transmission electron microscopy (TEM). Briefly, hTERT-HPNE cells were cultured in 10 cm^2 Petri-dish. When 80–90% confluent cells were treated with AuNPs rods and stars in concentration 10 and 50 µg/mL as described in *Treatment* section. After 24 h of incubation cells were fixated with 2.5% glutaraldehyde in 0.1 mM sodium-cocodylate buffer. Then cells were detached and centrifuged. Cells plates was postfixaited in 2% osmium tetroxide. Next dehydration in graded solution of ethanol was applied. Cell were infiltrated with propylen dioxide, eopn mixture and pure eopn. Then cell were settled to polymerise. Prior to TEM examination at 100 kV (JEM 1200EX II, Jeol, Japan), ultra-thin section (Reichert OmU3 ultramicrotome, Austria), were contrasted by uranyl acetate and lead citrate.

2.10 Statistical analysis

All statistical analysis was performed with GraphPad Prism 5 software (GraphPad Software, Inc, USA). All data on graphs are presented as the mean ± standard error of 3-4 independent experiments. Statistical analysis was determined by one-way analysis of variance (ANOVA) and Tukey's posthoc test. The IC_{50} was calculated by analyzing of non-linear regression log(inhibitor) vs normalized response.

3 Results and discussion

3.1 Morphology of AuNPs

The morphology of prepared samples was studied by SEM and TEM microscopy. The average gold size was calculated from average size of 100 AuNPs using ImageJ Analysis Software. As clearly shown (Fig. 1a–c), the *AuNPs* stars have well-developed with the tip-to-tip diameter in range 170–260 nm with various numbers of tips. The major fraction of AuNPs stars appears with an average size of ~ 200 nm. SEM analysis also showed that all of AuNPs stars particles have a branched structure. The fractions in diameter about 170 nm and 260 nm represented a small part in the test sample. The AuNPs rods with narrow size distribution of ~ 45 nm in length and ~16 nm diameter are shown in Fig. 1d–f. The major fraction of AuNPs rods appears with an average length size ~ 45 nm. Moreover, observation at high magnification shows that the surface of the AuNPs rods is smooth. The TEM results also confirmed that small fraction of the formed particles have a spherical shape. Nikoobakht *et al*. showed that formation of a large fraction of spherical particles can be overcome by use of a (CTAB)-capped seed instead of a citrate-capped one [15]. After reduction of gold precursor by tannic acid, the gold AuNPs spheres with diameters in the range from 6 to approximately 22 nm were formed (Fig. 1g–i). AuNPs spheres were rather uniform in shape. The major fraction of AuNPs spheres appears with an average size equaled to 14 nm.

3.2 UV-Vis properties of gold nanoparticles

The UV-Vis properties of prepared gold nanoparticles were characterized by UV–Vis spectroscopy in range 200–1400 nm (Fig. 2). The AuNPs exhibit a distinct optical feature commonly referred to as localized surface plasmon resonance (LSPR). The position and intensity of the LSPR band depends on the size and surface morphology of gold particles (a–b). For AuNPs spheres, the plasmon peak shifts to higher wavelengths with increasing particle size, from the visible to the IR light [16]. The absorption band at 530 nm was observed for AuNPs spheres and this peak position comes from small particles, which is also confirmed by TEM results. According to the literature, the one plasmon band around 527 nm is corresponding to the spherical gold with size about 20 nm [17]. For AuNPs stars a plasmon band ranging from 500 to 1400 nm was observed.

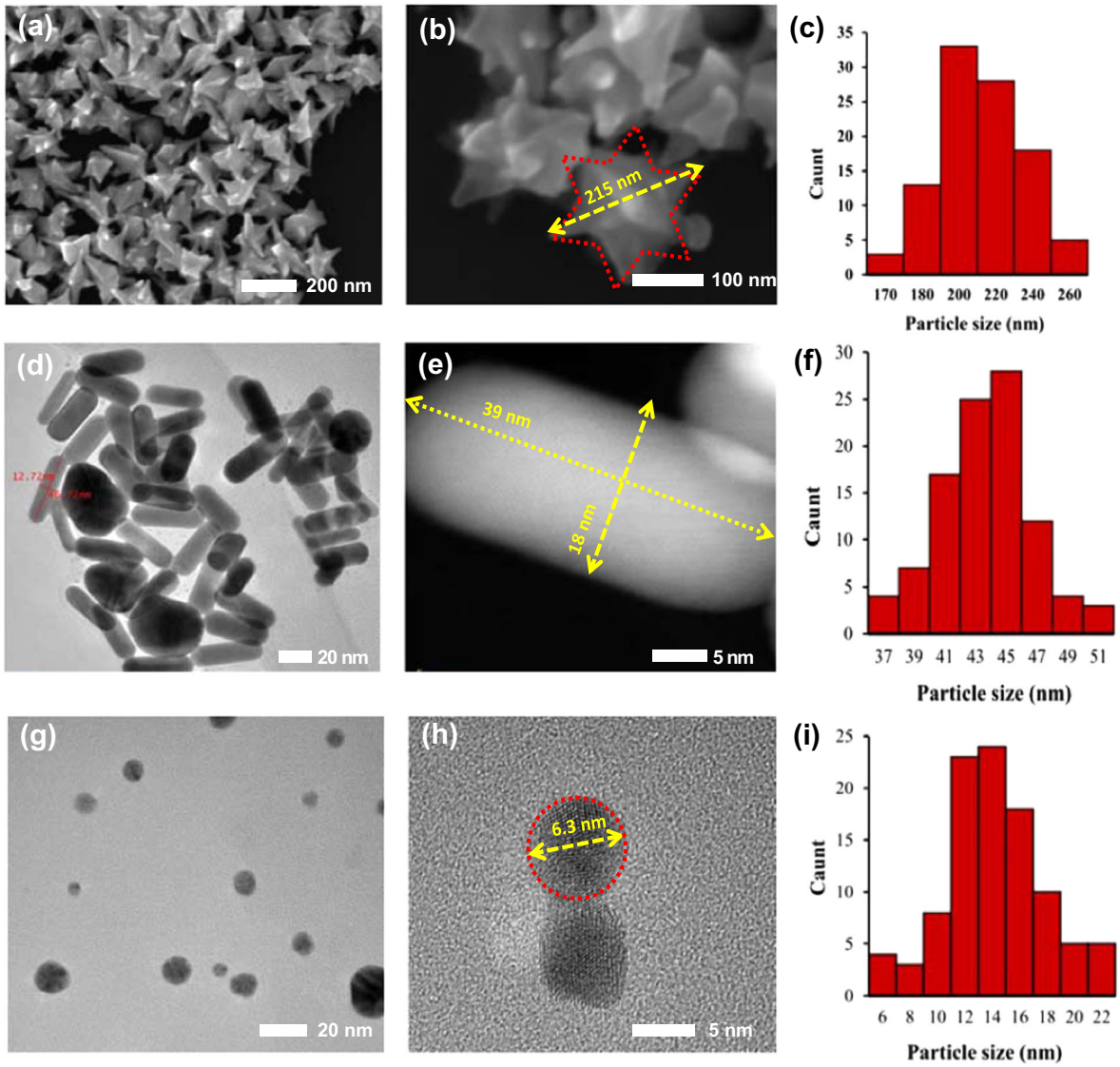

Fig. 1 Morphology (TEM/SEM images) and average size distribution of **a–c** AuNPs stars, **d–f** AuNPs rods, **g–i** AuNPs spheres

According to the literature, the absorption peak in the IR region depends on the number of tips of gold nanoparticles [18]. It is know that the shape of the branches and their each other interaction of AuNPs stars determine the absorption ranges [16]. For AuNPs rods, typically two plasmon resonances are observed. The transverse and longitudinal LSPR extinction peaks located around 520 and 680 nm respectively, was observed for AuNPs rods prepared using seed-mediated synthesis. Appearance of transverse and longitudinal plasmon resonances is evident of the formation of AuNPs rods. Further, the presence of two characteristic peaks suggests that the sample was homogenous.

3.3 Determination of cell viability

Analysis of MTT assay and NR assay results have shown that shape and concentration of nanoparticles has an impact on their cytotoxicity (Fig. 3)

The highest impact on cells survival had AuNPs stars and decreased cells viability in a concentration-dependent manner. MTT assay has shown that AuNPs stars significantly decreased the viability of hFOB 1.19 in concentration range 1.2–5 µg/mL, MG-63 in concentration 1.2–5 µg/mL, and 143B in concentration range 0.3–5 µg/mL, whereas NR assay did not prove the cytotoxic effect of

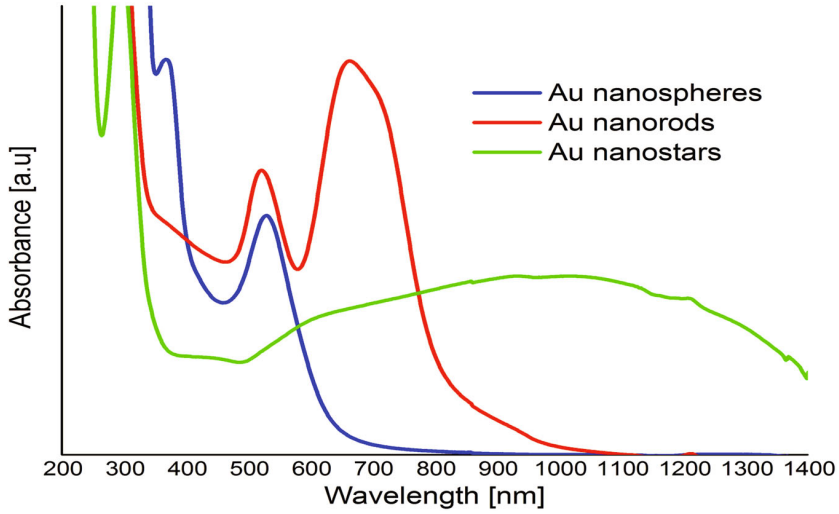

Fig. 2 UV-Vis spectra of AuNPs spheres, AuNPs rods and AuNPs stars

AuNPs stars in the lowest concentration (0.3 µg/mL). The most susceptible to cytotoxic effect of AuNPs stars were 143B cells. For the high concentration of AuNPs stars (2.5 and 5 µg/mL) hFOB 1.19 cells were the most resistant one. After exposure to the low concentrations of AuNPs stars (0.3 and 0.6 µg/mL) hFOB 1.19 and MG-63 cells had similar viability.

In MTT assay AuNPs rods significantly decreased the viability of hFOB 1.19, MG-63 and 143B cells. However, other assay (NR assay) has proven that hFOB 1.19 are resistant to cytotoxic effect of AuNP rods in concentration between 0.3–2.5 µg/mL, MG-63 in concentration range 0.3–0.6 µg/mL and 143B cells were resistant to AuNPs rods in concentration range of 0.3–1.2 µg/mL.

AuNPs spheres exerted the smallest cytotoxic effect compared to other analysed nanoparticles. AuNPs spheres did not decrease the viability of hFOB1.19 and MG-63 cells, examined by MTT assay. AuNPs spheres, in concentration 5 µg/mL, decreased the viability of 143B cells but the effect was lower in comparison to other shapes. In NR assay AuNPs spheres did not have any statistically significant effect on the viability of hFOB1.19, MG63 and 143B cells in the analysed range of concentration. Non-linear regression analysis: log(inhibitor) vs. normalized response has been performed to calculate log IC_{50} values (online resource 1). IC_{50} values for AuNPs stars are presented in Table 1. In order to show higher cytotoxicity of AuNPs stars against cancer cell lines compered to non-cancer cells.

3.4 Protein level of Bax and Bcl-2

We determined the impact of AuNPs rods and AuNPs stars on apoptosis-related protein. Level of proapoptotic protein (Bax) and anti-apoptotic protein (Bcl-2) in MG-63 and 143B cells was demonstrated (Fig. 4). Due to lack cytotoxicity showed in NR assay and small cytotoxic effect (only in concentration 5 µg/mL) against 143B cells only showed by MTT assay, we did not determine the influence of AuNPs spheres on the level of protein, which are crucial regulators of cell death. AuNPs rods significantly increased the protein level of Bax in both cell lines, however, decreased the level of Bcl-2 was observed only in MG-63 cells. AuNPs stars significantly increased level of Bax and decreased level of Bcl-2 in all tested cell lines. For MG-63 cells AuNPs stars increased level of Bax protein in concentration between 0.1–1 µg/mL and decreased level of Bcl-2 protein in concentration of 1 µg/mL. AuNPs rods in concentration between 1–2 µg/mL increased level of Bax protein and in concentration of 2 µg/mL decreased level of Bcl-2 protein in MG-63 cells. AuNPs stars in concentration of 1 µg/mL increased level of Bax protein and decreased level of Bcl-2 protein on 143B cells. In 143B cells AuNPs rods in concentration of 2 µg/mL increased level of Bax protein, however AuNPs rods in tested range of concentration did not, statistically significant, influence level of Bcl-2 protein in 143B cells.

3.5 TEM analysis

TEM analysis have shown that AuNPs rods and AuNPs stars can be internalized by hTERT-HPNE cells and caused ultrastructure changes. AuNPs stars in concentration of 10 µg/mL were internalized in the cytoplasm (Fig. 5c as well as in the nucleus of the cell (Fig. 5a). Additionally, we observed intensive vacuolization of the cytoplasm, and numerous autophagic vacuoles (Fig. 5a, b). In hTERT-

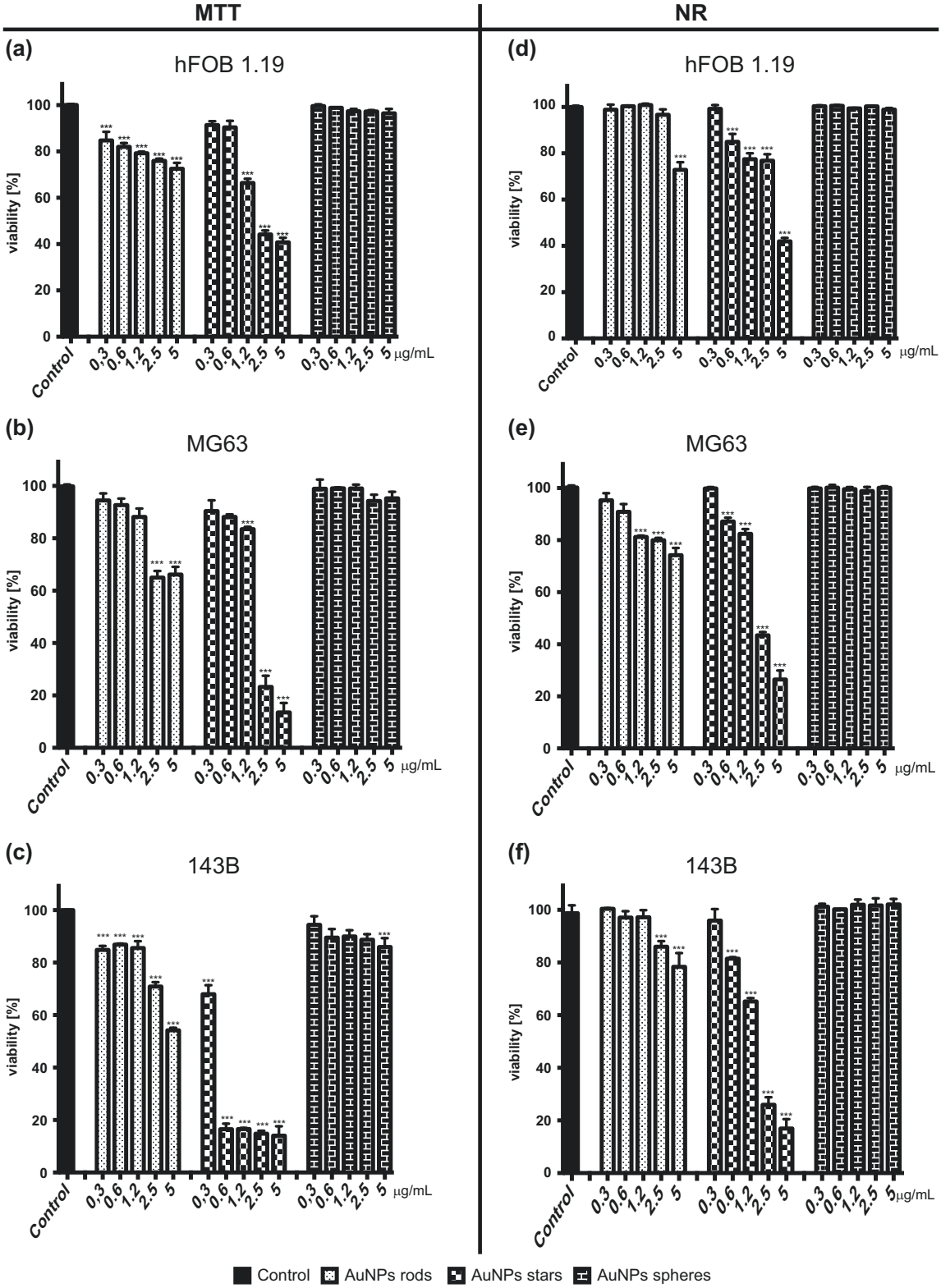

Fig. 3 Different shapes of AuNPs decreased cell viability in a concentration-dependent manner. Viability, measured by MTT test, of **a** hFOB1.19 cells, **b** MG-63, **c** 143B cells exposed to different shapes of AuNPs after 24 h. Viability, measured by NR test, of **d** hFOB1.19 cells, **e** MG-63, **f** 143B cells exposed to different shapes of AuNPs after 24 h. Data are presented as mean ± SD. $*p < 0.05$, $**p < 0.01$, ***, $p < 0.001$

HPNE cells after treatment with high (50 µg/mL) concentrations of AuNPs stars, we have observed major impairment of the cells such as cell membrane rupture, cytoplasm vacuolization and general degeneration. AuNPs stars were present within cell debris (Fig. 6a–d). AuNPs rods in concentration of 10 µg/mL were found outside the cell along the cell membrane as well as internalized inside a small dense vesicles (endosomes) (Fig. 7a–f). Morphology of the cells treated with rods of AuNPs revealed normal/unchanged rough endoplasmic reticulum and numerous autophagosomes. After treatment with higher concentrations of AuNPs rods (50 µg/mL) cells underwent major

Table 1 I_{C50} for AuNPs stars

	HFOB1.19	MG-63	143B
MTT ASSAY	1.241 µg/mL	1.760 µg/mL	0.4266 µg/mL
NR ASSAY	3.961 µg/mL	1.841 µg/mL	1.396 µg/mL

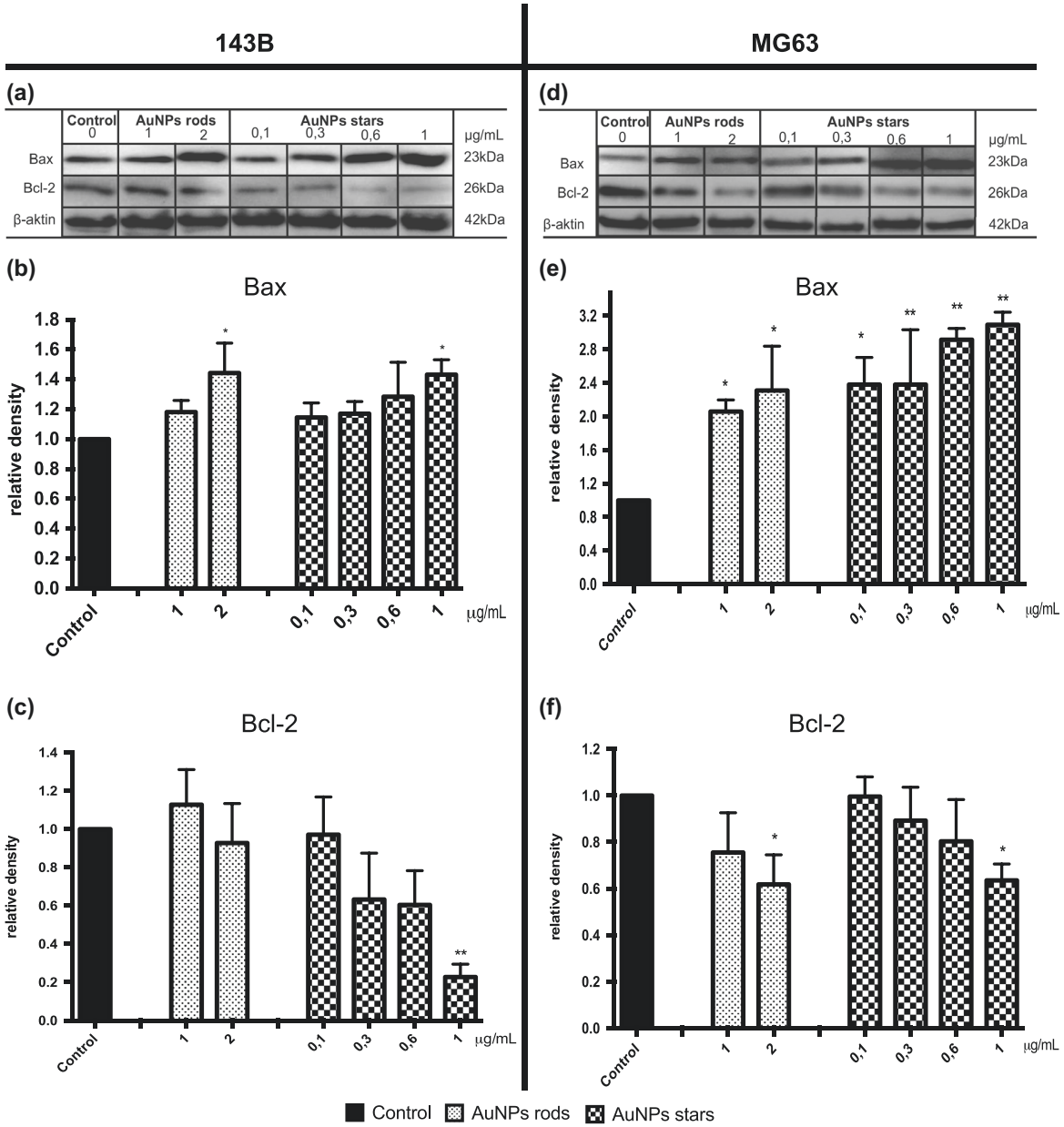

Fig. 4 Western-blot analysis of apoptosis-related protein level in 143B and MG-63 cells after 24 h of incubation with AgNPs. Representative Western blot analysis of Bax and Bcl-2 in **a**) 143Bcells and **d** MG-63. Quantitive analysis of **b**, **e** Bax and **c**, **f** Bcl-2 proteins in 143B and MG-63 cells, respectively. Data are presented as mean ± SD. $*p < 0.05$, $**p < 0.01$

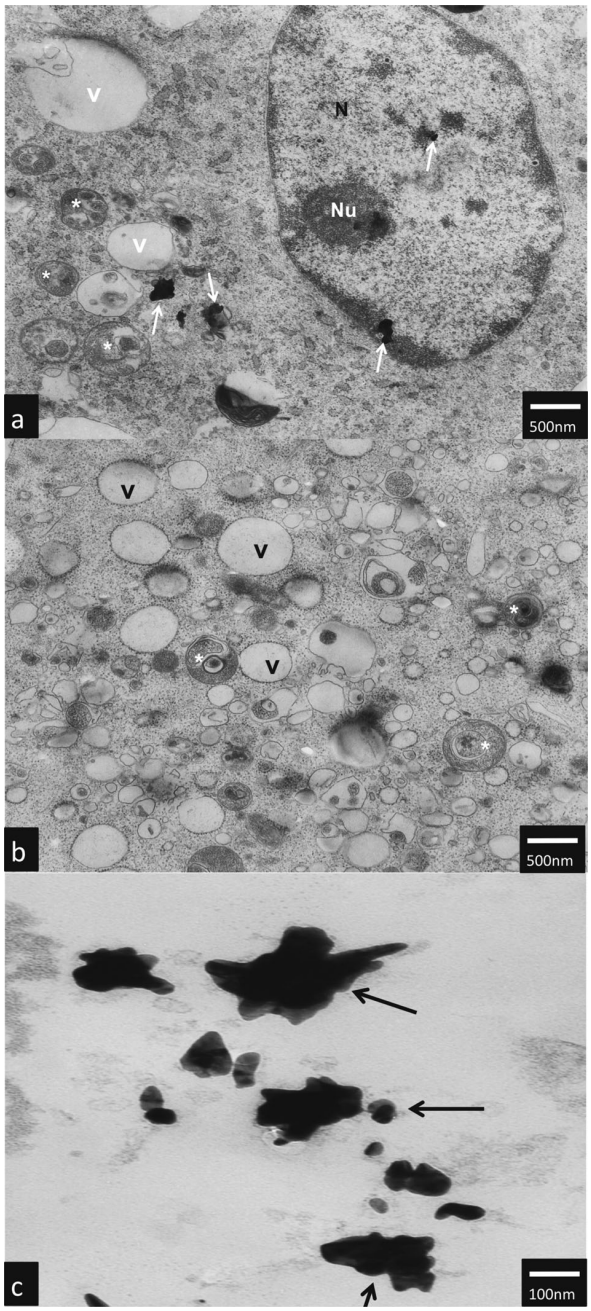

Fig. 5 Ultrastructure changes in hTERT-HPNE cells after 24 h incubation with 10 µg/mL AuNPs stars. AuNPs stars are indicated by arrows, N nulceus, NU nucleous, V vaculoes, *-authophagic vacuoles. The scale bar is present on the left side of each picture

degeneration. AuNPs rods have been observed along the cell membranes or cell debris (Fig. 8a–c). Some internalized of AuNPs rods have been found near the nuclear membrane (Fig. 8a). Despite the fact that the majority of cells have been seriously damaged, some cells remained normal. However, internalized AuNPs rods have been found in the cell perikaryon (Fig. 8d). The cell showed prominent rough endoplasmic reticulum as well as autophagic vacuole.

4 Discussion

The aim of our research was to determine the dependence of shape and concentration on the cytotoxicity of AuNPs against human fetal osteoblast and osteosarcoma cells. We also were focused on determining the type of programmed cell death induced by AuNPs We found that, AuNPs exerted their cytotoxic effect in a shape- and concentration-dependent manner. AuNPs stars were the most cytotoxic, whereas AuNPs spheres were the less cytotoxic ones. NR assay has shown that hFOB1.19 cells were the most resistant and 143B cells were the most susceptible to all examined AuNPs. In general, the NR assay has shown the higher viability of the cells than MTT test in the same condition. Our study has proven that both cytotoxicity of AuNPs and anti-cancer potential is shape-dependent. Thus, it should be taken in concern when designing NPs for biomedical usage, in order to increase safety of NPs application.

Osteosarcoma is highly metastatic mesenchymal cells carcinoma [19]. It is the third most common cancer in youth, so osteosarcoma is substantial epidemiological problem [19]. Typical treatment of this neoplasm consists of surgery, chemotherapy and radiotherapy, so therapy is crippling and the outcome is poor [19]. There is strong requirement for improved treatment, it has been demonstarted that nanoparticles may be interesting alternative for the ‘classical’ treatment [20]. Rahim et al., demonstrated that 24.3 nm spherical AuNPs capped with glication products (Schiff’s base, Heyns products, fructosylamine etc.) inhibit growth of SaoS-2 (human osteosarcoma cell line) [21]. Similarly, Cebrain et al. have shown that 6 nm poly (ethylenimine) coated AuNPs decreased viability of SaoS-2 cells [22]. However, there was no study compering cytotoxicity of different shapes of AuNPs against osteosarcoma cells. In our study, we decided to use four cell lines hFOB1.19, hTERT-HPNE, MG-63 and 143B, because it has been proven that response to AuNPs exposure is very cell line dependent. [23]. We have chosen two osteosarcoma cell lines (MG-63 and 143B) because of their different characteristics. 143B cells proliferate and migrate more intensively than MG-63 cells, also 143B cells have higher tumorigenicity and colony forming ability [24, 25]. Taken together,143B cell line is more aggressive one. We used non-transformed and cancer cell lines, as studies suggest that cancer cells are more vulnerable to xenobiotics, due to faster and bigger uptake caused by hyper metabolism [26]. Non-transformed cells (hFOB1.19 and hTERT-HPNE) were used to assess the safety of potential in vivo

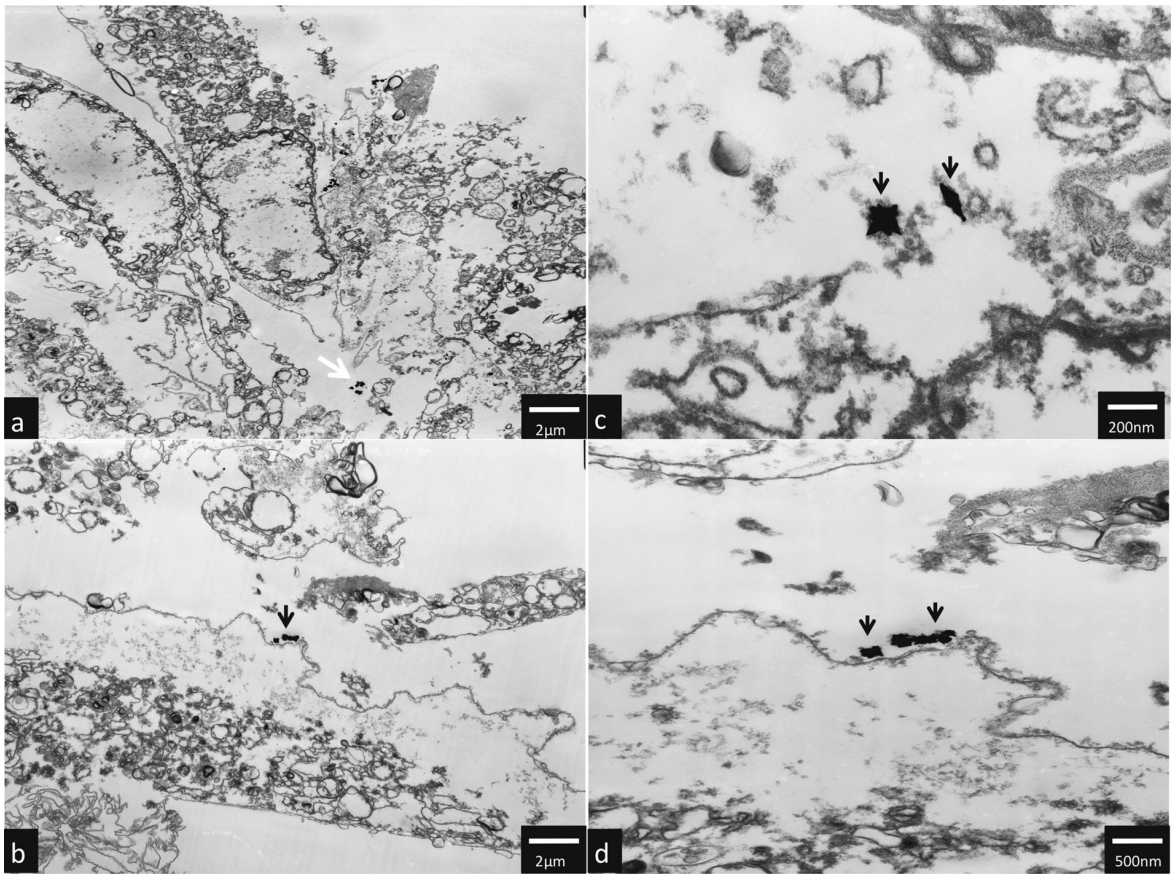

Fig. 6 Ultrastructure changes in hTERT-HPNE cells after 24 h incubation with 50 μg/mL AuNPs stars. AuNPs stars are indicated by arrows. The scale bar is present on the left side of each picture

application of AuNPs of different shapes. In other studies hTERT-HPNE cells were used as a comparison for selective cytotoxicity of tested compound against cancer cells. For example, Ramalho et al. compared the cytotoxicity of functionalized nanoparticles (PLGA-AuNPs) with potential anti-cancer activity against A549 cells (human lung carcinoma) and hTERT-HPNE [27]. Wada et al., also compered cytotoxicity of tested compunds on different cell lines CHO-K1 (chinese hamster ovary), HeLa (cervix cancer cells) and SH-SY5Y (neuroblast cells) [28].

4.1 Cytotoxicity of AuNPs

In order to provide the most reliable results, we decided to use two test: MTT and NR. NR assay is based on the ability of viable cells to uptake and accumulate dye in lysosomes and measured cellular membrane integrity [29]. MTT assay measured the activity of cellular NAD(P)H dependent oxidoreductase [29]. Decreased cell viability measured by MTT may indicate the cells underwent apoptosis [29, 30]. Because of different characteristic of both assays, they do not give equal results [31]. MTT test, as well as NR assay, are commonly used to assess the cytotoxicity of nanoparticles [32–34].

Recently, several groups have focused their attention on the cytotoxic activity of AuNPs [35, 36]. Size, shape, concentration, incubation time, synthesis method, surface functionalization, type of cells are thought to have an impact of cytotoxicity of AuNPs [37]. It has been proven that AuNPs can reduce the viability of human hepatocellular carcinoma [38] and human breast adenocarcinoma [39]. On the other hand, Gannon et al. have found that AuNPs in concentration between 1 and 67 μM/L are not cytotoxic to Hep3B (hepatocellular carcinoma) and Panc-1 (pancreatic epithelioid carcinoma) cells [40]. Patra et al., demonstrated that 33 nm AuNPs were toxic to human carcinoma lung cell line (A549 cells), and did not decrease viability of human hepatocellular carcinoma cells (Hepg-2) cells [41]. In other study it has been shown that 10 and 50 nm citrate coated AuNPs were not toxic to embryonic fibroblast [42].

Size of nanoparticles is important if considering their cytotoxicity. Generally, it seems that the larger the size of

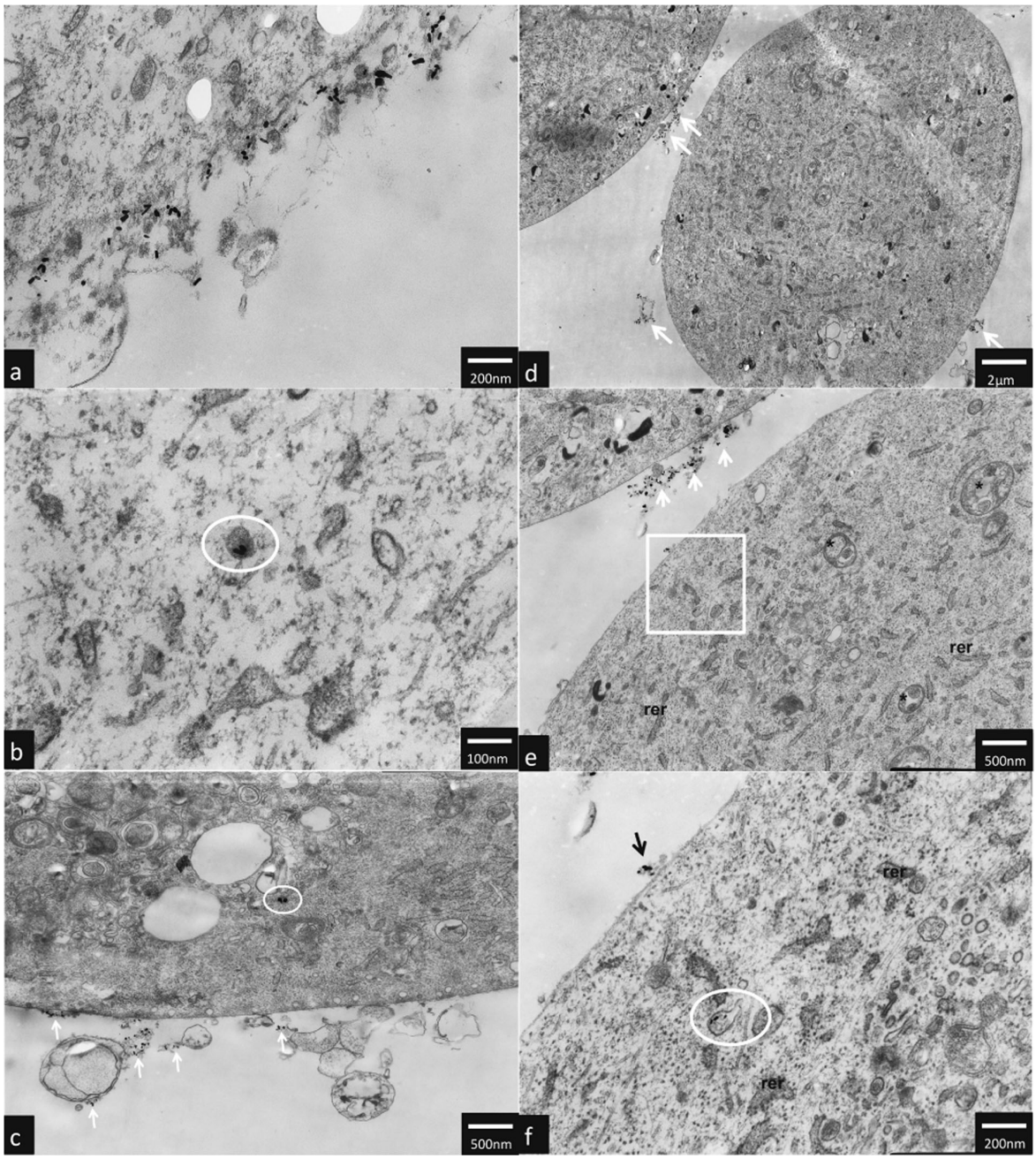

Fig. 7 Ultrastructure changes in hTERT-HPNE cells after 24 h incubation with 10 μg/mL AuNPs rods. AuNPs rods are indicated by arrows. Endosomes are circled, RER rough endoplasmatic reticulum, * authophagosomes. The scale bar is present on the left side of each picture

nanoparticles is the less cytotoxic they exerted [43]. Indeed, Coradeghini et al. have proven that 5 nm AuNPs were more cytotoxic in comparison to 15 nm AuNPs on Balb/3T3 (mouse fibroblast) cells. [44]. Similarly, Senut et al. have proven that 1.5 nm AuNPs are more cytotoxic to hESC (human embryonic stem cells) cells than 4 and 15 nm AuNPs [45]. However, Vetten et al., demonstrated that 20 nm AuNPs were more cytotoxic than 14 nm on BEAS-2B cells [46].

Although extensive knowledge about AuNPs cytotoxicity there is only few publication which has taken in concern shape of NPs as an important modulator of cytotoxicity. Our results suggest that AuNPs exerted their cytotoxicity mainly by influencing mitochondria

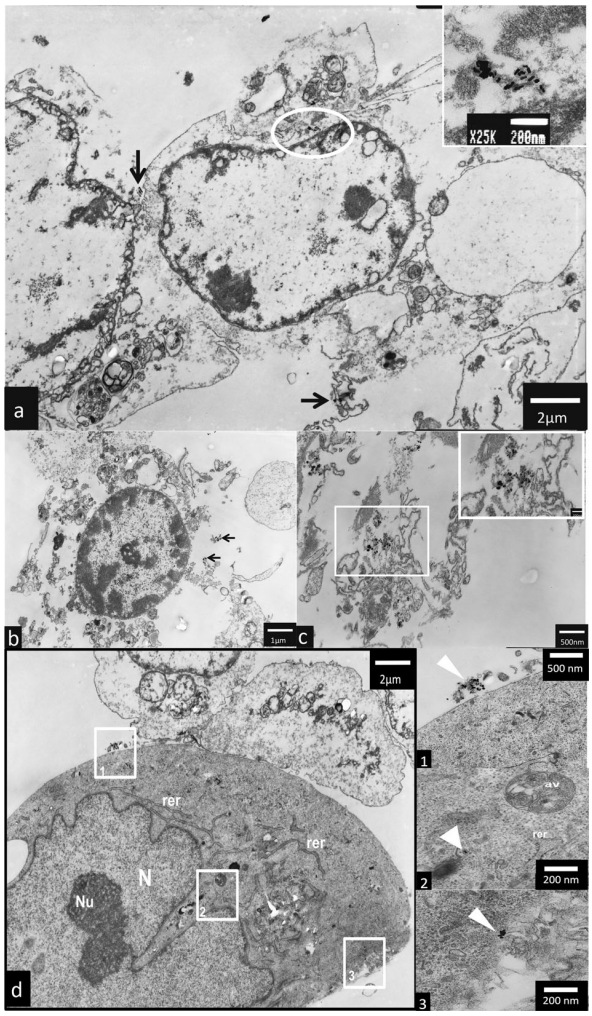

Fig. 8 Ultrastructure changes in hTERT-HPNE cells after 24 h incubation with 50 µg/mL AuNPs rods. AuNPs rods are indicated by arrows. AuNPs rods were founded near the nuclear membrane (boxed), RER rough endoplasmatic reticulum, AV authophagic vacuoles. The scale bar is present on the left side or at the bottom of each picture

functioning (MTT assay). However, the decreased viability of cells in NR assay suggested that NPs affected integrity of cellular membranes. It has been found that AuNPs rods exerted cytotoxic effect against canine MDCK (canine kidney epithelial cells) and HEp-2 (human HeLa contaminant epithelial cells) cell lines in a concentration-dependent manner (viability of cells was measured by MTT assay) [47]. In in vitro study, Favi et. al examined the impact of AuNPs rods (length 534 ± 38 nm, width 65 ± 8 nm) on the viability of human dermal fibroblast. They observed that viability of the cells measured by MTS assay was decreased by 10–15% by AuNPs rods at concentration of 400 µg/mL [48]. In our study, AuNPs rods in concentration of 5 µg/mL decreased MG-63 cells viability (measured by MTT assay) by approximately 34% and 143B cells by 46%. There are significant differences between our results and results presented by Favi et al. Firstly, they examined AuNPs rods in bigger size, and it has been proven that the bigger nanoparticles are the smaller effect on cells viability they have [43]. Furthermore, MTT and MTS test give similar but not equal results [49]. Other studies have proven that AuNPs rods decreased the viability of A549 cells (human lung adenocarcinoma cells) in a concentration-dependent manner. Further, it has been observed, consistent with our results, that AuNPs rods (length 40 nm) are more cytotoxic than AuNPs spheres [47]. In several studies, it has demonstrated that AuNPs spheres did not have cytotoxic activity [43, 50].

4.2 AuNPs-induced programmed cell death

Choudhury et al., observed decreased level of Bcl-2 (anti-apoptotic protein) and increased level of Bax (proapoptotic protein) in A549 cells after incubation with 40 nm AuNPs [51]. Selim et al., have reported that AuNPs may increase mRNA level of proapoptotic protein Bax, and decreased the level of a protein Bcl-2 in MCF-7 cells (human mammary adenocarcinoma) [39]. Similar results were presented for Hepg-2 cells incubated with 14.5 nm spherical AuNPs [52]. AuNPs rods are thought to induce apoptosis [30, 47]. Furthermore, Chueh et al., have proven that AuNPs rods (length 10–40 nm) induce apoptosis and autophagy in NIH3T3 cells (mouse fibroblast) [23]. Ding et al., have observed that spherical AuNPs (5, 13 nm) caused autophagy in HK2 cells (human renal proximal tubular cells) [53]. Tang et al., have ascertained that AuNPs rods (width 23–26 nm, length 35–58 nm) may cause necrosis of A549 cells. Furthermore, necrotic cells ratio increases in presence of high concentration of AuNPs rods (in concentration > 10 µg/mL) [54]. Our results suggest that AuNPs rods and AuNPs stars may induced apoptosis in MG-63 and 143B cells, which is similar to observations made by several other authors [30, 47, 52].

4.3 Cellular uptake and ultrastructure changes

AuNPs may be internalized into cells and caused ultrastructural changes. Generally, molecules with positively charger surfaces have higher uptake ratio but lower intracellular stability in comparison to neutral or negatively charged molecules [55]. Furthermore, size of nanoparticles influence effectivity of their internalization [56]. There are two main mechanisms of AuNPs internalisation by membrane-bound vesicles [35] and endosomes [57]. Receptor-mediated endocytosis and fluid-phase endocytosis are the additional way of AuNPs internalisation [58]. Mironava et al., have demonstrated that way of AuNPs internalisation depends on diameter

of AuNPs [10]. 45 nm AuNPs penetrate into human dermal fibroblast by clathrin-mediated endocytosis, while for 13 nm AuNPs phagocytosis is main way of internalisation [59]. It has been proven that AuNPs rods may be internalised by endosomes and vesicular bodies into human dermal fibroblasts (AuNPs rods: width 11.2–12.8 nm length 58–62 nm), colon adenocarcinoma and other cells [60, 61]. Other studies have shown that AuNPs are internalised by phagocytosis in A549 (AuNPs rods: width 23–26 nm, length: 35–58 nm) and HBL-100 cells (AuNPs spheres 20–45 nm) [54, 58]. Furthermore, AuNPs can be found in the cytosol, lysosomes and perinuclear region either in form of aggregates or single NPs [53, 54, 58]. Exposition of A549 cells to AuNPs rods (width 23–26 nm, length 35–58 nm) caused an increased number of lysosomes and swallowing of mitochondria [54]. The nucleus of A549 cells was not affected by AuNPs rods [54]. The data about uptake and cytotoxicity of AuNPs are inconsistent. Connor et al., have proven that AuNPs spheres may be taken up by K562 (chronic myelogenous leukemia) cells, but they are not cytotoxic [62]. Gannon et al. proved that AuNPs can be internalized by Panc-1 cells, however, TEM analysis has shown that AuNPs do not harm cellular organelles [40].

To the our knowledge this is the first study to compare shape- and size-dependent cytotoxic against human fetal osteoblast and osteosarcoma cells including the type of cell death and ultrastructure alterations caused by AuNPs.

5 Conclusions

In the present study we demonstrated that cytotoxicity of AuNPs is depended on the shape. We found that AuNPs stars are the most cytotoxic ones. Furthermore, we observed that cancer cells are more susceptible to AuNPs. For AuNPs in all investigated shapes, IC_{50} values were the lowest for 143B cell line in comparison to hFOB 1.19 and MG-63 cell lines. We proved that AuNPs induced apoptosis in human osteosarcoma cells, both in 143B and MG-63. Moreover, AuNPs penetrated through the cell membrane and caused ultrastructural changes. Our study has proven that shape is important modulator of AuNPs cytotoxicity. Both anti-cancer potential and cytotoxicity of AuNPs is shape-dependent. It should be concerned in order to provide the highest efficiency with the highest safety of AuNPs application.

Acknowledgements The author AM acknowledges funding from Foundation for Polish Science (START. FNP). Authors KPS, EB, and IIS acknowledge funding from the Medical University of Gdansk (ST-02-0046/07/259).

Compliance with ethical standards

Conflict of interest The authors declare that they have no conflict of interest.

References

1. Rai M, Ingle AP, Birla S, Yadav A, Santos CA, Dos. Strategic role of selected noble metal nanoparticles in medicine. Crit Rev Microbiol. 2015;00:1–24. https://doi.org/10.3109/1040841X.2015.1018131
2. Elahi N, Kamali M, Baghersad MH. Recent biomedical applications of gold nanoparticles: a review. Talanta. 2018;184:537–56. https://doi.org/10.1016/j.talanta.2018.02.088
3. Banu H, Sethi DK, Edgar A, Sheriff A, Rayees N, Renuka N, et al. Doxorubicin loaded polymeric gold nanoparticles targeted to human folate receptor upon laser photothermal therapy potentiates chemotherapy in breast cancer cell lines. J Photochem Photobiol B Biol. 2015;149:116–28. https://doi.org/10.1016/j.jphotobiol.2015.05.008
4. Lee U, Yoo C-J, Kim Y-J, Yoo Y-M. Cytotoxicity of gold nanoparticles in human neural precursor cells and rat cerebral cortex. J Biosci Bioeng. 2016;121:341–4. https://doi.org/10.1016/j.jbiosc.2015.07.004
5. Draz MS, Shafiee H. Applications of gold nanoparticles in virus detection. Theranostics. 2018;8:1985–2017. https://doi.org/10.7150/thno.23856
6. Hussain MM, Samir TM, Azzazy HME. Unmodified gold nanoparticles for direct and rapid detection of Mycobacterium tuberculosis complex. Clin Biochem. 2013;46:633–7. https://doi.org/10.1016/j.clinbiochem.2012.12.020
7. Murphy CJ, Thompson LB, Alkilany AM, Sisco PN, Boulos SP, Sivapalan ST, et al. The many faces of gold nanorods. J Phys Chem Lett. 2010;1:2867–75. https://doi.org/10.1021/jz100992x
8. Ahn S, Lee IH, Kang S, Kim D, Choi M, Saw PE, et al. Gold nanoparticles displaying tumor-associated self-antigens as a potential vaccine for cancer immunotherapy. Adv Healthc Mater. 2014;3:1194–9. https://doi.org/10.1002/adhm.201300597
9. Wang F, Yu L, Monopoli MP, Sandin P, Mahon E, Salvati A, et al. The biomolecular corona is retained during nanoparticle uptake and protects the cells from the damage induced by cationic nanoparticles until degraded in the lysosomes. Nanomedicine. 2013;9:1159–68. https://doi.org/10.1016/j.nano.2013.04.010
10. Mironava T, Hadjiargyrou M, Simon M, Rafailovich MH. Gold nanoparticles cellular toxicity and recovery: adipose derived stromal cells. Nanotoxicology. 2014;8:189–201. https://doi.org/10.3109/17435390.2013.769128
11. Woźniak A, Malankowska A, Nowaczyk G, Grześkowiak BF, Tuśnio K, Słomski R, et al. Size and shape-dependent cytotoxicity profile of gold nanoparticles for biomedical applications. J Mater Sci Mater Med. 2017;28:1–11. https://doi.org/10.1007/s10856-017-5902-y
12. Gołabiewska A, Malankowska A, Jarek M, Lisowski W, Nowaczyk G, Jurga S, et al. The effect of gold shape and size on the properties and visible light-induced photoactivity of Au-TiO2. Appl Catal B Environ. 2016;196:27–40. https://doi.org/10.1016/j.apcatb.2016.05.013
13. Zielinska E, Tukaj C, Radomski MW, Inkielewicz-Stepniak I. Molecular mechanism of silver nanoparticles-induced human

osteoblast cell death: protective effect of inducible nitric oxide synthase inhibitor. PLoS One. 2016;11:e0164137 https://doi.org/10.1371/journal.pone.0164137
14. Bradford MM. A rapid and sensitive method for the quantitation of microgram quantities of protein utilizing the principle of protein-dye binding. Anal Biochem. 1976;72:248–54. https://doi.org/10.1016/0003-2697(76)90527-3
15. Nikoobakht B, El-Sayed M. Preparation and growth mechanism of gold nanorods (NRs) using seed—mediated growth method. Chem Mater. 2003;15:1957–62. https://doi.org/10.1021/Cm0207321
16. Kooij ES, Ahmed W, Hellenthal C, Zandvliet HJW, Poelsema B. From nanorods to nanostars: tuning the optical properties of gold nanoparticles. Colloids. Surf A Physicochem Eng Asp. 2012;413:231–8. https://doi.org/10.1016/j.colsurfa.2012.01.041
17. Zhong X, Chai YQ, Yuan R. A novel strategy for synthesis of hollow gold nanosphere and its application in electrogenerated chemiluminescence glucose biosensor. Talanta. 2014;128:9–14. https://doi.org/10.1016/j.talanta.2014.03.071
18. Navarro JRG, Liotta A, Faure A-C, Lerouge F, Chaput F, Micouin G, et al. Tuning dye-to-particle interactions toward luminescent gold nanostars. Langmuir. 2013;29:10915–21. https://doi.org/10.1021/la402222c
19. Luetke A, Meyers PA, Lewis I, Juergens H. Osteosarcoma treatment—where do we stand? A state of the art review. Cancer Treat Rev. 2014;40:523–32. https://doi.org/10.1016/j.ctrv.2013.11.006
20. Sha B, Gao W, Han Y, Wang S, Wu J, Xu F, et al. Potential application of titanium dioxide nanoparticles in the prevention of osteosarcoma and chondrosarcoma recurrence. J Nanosci Nanotechnol. 2013;13:1208–11. https://doi.org/10.1166/jnn.2013.6081
21. Rahim M, Iram S, Khan MS, Khan MS, Shukla AR, Srivastava AK, et al. Glycation-assisted synthesized gold nanoparticles inhibit growth of bone cancer cells. Colloids Surf B Biointerfaces. 2014;117:473–9. https://doi.org/10.1016/j.colsurfb.2013.12.008
22. Cebrian V, Martin-Saavedra F, Yague C, Arruebo M, Santamaria J, Vilaboa N. Size-dependent transfection efficiency of PEI-coated gold nanoparticles. Acta Biomater. 2011;7:3645–55. https://doi.org/10.1016/j.actbio.2011.06.018
23. Chueh PJ, Liang R-Y, Lee Y-H, Zeng Z-M, Chuang S-M. Differential cytotoxic effects of gold nanoparticles in different mammalian cell lines. J Hazard Mater. 2014;264:303–12. https://doi.org/10.1016/j.jhazmat.2013.11.031
24. Yuan J, Ossendorf C, Szatkowski JP, Bronk JT, Yaszemski M, Bolander ME, et al. Osteoblastic and osteolytic human osteosarcomas can be studied with a new xenograft mouse model producing spontaneous metastases. Cancer Invest. 2009;27:435–42. https://doi.org/10.1080/07357900802491477.Osteoblastic
25. Lauvrak SU, Munthe E, Kresse SH, Stratford EW, Namløs HM, Meza-Zepeda LA, et al. Functional characterisation of osteosarcoma cell lines and identification of mRNAs and miRNAs associated with aggressive cancer phenotypes. Br J Cancer. 2013;109:2228–36. https://doi.org/10.1038/bjc.2013.549
26. Sun DJ, Liu Y, Lu DC, Kim W, Lee JH, Maynard J, et al. Endothelin-3 growth factor levels decreased in cervical cancer compared with normal cervical epithelial cells. Hum Pathol. 2007;38:1047–56. https://doi.org/10.1016/j.humpath.2006.12.015
27. Ramalho MJ, Loureiro JA, Gomes B, Frasco MF, Coelho MAN, Carmo Pereira M. PLGA nanoparticles as a platform for vitamin D-based cancer therapy. Beilstein J Nanotechnol. 2015;6:1306–18. https://doi.org/10.3762/bjnano.6.135
28. Wada T, Hanyu T, Nozaki K, Kataoka K, Kawatani T, Asahi T, et al. Antioxidant activity of Ge-132, a synthetic organic germanium, on cultured mammalian cells. Biol Pharm Bull. 2018. https://doi.org/10.1248/bpb.b17-00949
29. Husøy T, Syversen T, Jenssen J. Comparisons of four in vitro cytotoxicity tests: the MTT assay, NR assay, uridine incorporation and protein measurements. Toxicol Vitr. 1993;7:149–54. https://doi.org/10.1016/0887-2333(93)90125-O
30. Tian F, Clift MJD, Casey A, del Pino P, Pelaz B, Conde J, et al. Investigating the role of shape on the biological impact of gold nanoparticles in vitro. Nanomed (Lond). 2015;10:2643–57. https://doi.org/10.2217/nnm.15.103
31. Borenfreund E, Babich H, Martin-Alguacil N. Comparisons of two in vitro cytotoxicity assays—the neutral red (NR) and tetrazolium MTT tests. Toxicol Vitr. 1988;2:1–6. https://doi.org/10.1016/0887-2333(88)90030-6
32. Ahamed M, Akhtar MJ, Alhadlaq HA, Khan MAM, Alrokayan SA. Comparative cytotoxic response of nickel ferrite nanoparticles in human liver HepG2 and breast MFC-7 cancer cells. Chemosphere. 2015;135:278–88. https://doi.org/10.1016/j.chemosphere.2015.03.079
33. Liu YK, Ye J, Han QL, Tao R, Liu F, Wang W. toxicity and bioactivity of cobalt nanoparticles on the monocytes. Orthop Surg. 2015;7:168–73. https://doi.org/10.1111/os.12180
34. Zielinska E, Zauszkiewicz-Pawlak A, Wojcik M, Inkielewicz-Stepniak I. Silver nanoparticles of different sizes induce a mixed type of programmed cell death in human pancreatic ductal adenocarcinoma. Oncotarget. 2017;9:4675–97.
35. Liu Z, Wu Y, Guo Z, Liu Y, Shen Y, Zhou P, et al. Effects of internalized gold nanoparticles with respect to cytotoxicity and invasion activity in lung cancer cells. PLoS One. 2014;9:1–11. https://doi.org/10.1371/journal.pone.0099175
36. Huang D, Zhou H, Liu H, Gao J. The cytotoxicity of gold nanoparticles is dispersity-dependent. Dalt Trans. 2015;44:17911–5. https://doi.org/10.1039/C5DT02118A
37. Khlebtsov N, Dykman L. Biodistribution and toxicity of engineered gold nanoparticles: a review of in vitro and in vivo studies. Chem Soc Rev. 2011;40:1647–71. https://doi.org/10.1039/C0CS00018C
38. Paino IMM, Marangoni VS, de Oliveira R de CS, Antunes LMG, Zucolotto V. Cyto and genotoxicity of gold nanoparticles in human hepatocellular carcinoma and peripheral blood mononuclear cells. Toxicol Lett. 2012;215:119–25. https://doi.org/10.1016/j.toxlet.2012.09.025
39. Selim ME, Hendi AA. Gold nanoparticles induce apoptosis in MCF-7 human breast cancer cells. Asian Pac J Cancer Prev. 2012;13:1617–20. https://doi.org/10.7314/APJCP.2012.13.4.1617
40. Gannon CJ, Patra CR, Bhattacharya R, Mukherjee P, Curley SA. Intracellular gold nanoparticles enhance non-invasive radiofrequency thermal destruction of human gastrointestinal cancer cells. J Nanobiotechnology. 2008;6:2 https://doi.org/10.1186/1477-3155-6-2
41. Patra HK, Banerjee S, Chaudhuri U, Lahiri P, Dasgupta AK. Cell selective response to gold nanoparticles. Nanomedicine. 2007;3:111–9. https://doi.org/10.1016/j.nano.2007.03.005
42. Qu Y, Lü X. Aqueous synthesis of gold nanoparticles and their cytotoxicity in human dermal fibroblasts-fetal. Biomed Mater. 2009;4:2–7. https://doi.org/10.1088/1748-6041/4/2/025007
43. Skalska J, Strużyńska J. Toxic effects of silver nanoparticles in mammals—does a risk of neurotoxicity exist? Folia Neuropathol. 2015;53:281–300. https://doi.org/10.5114/fn.2015.56543
44. Coradeghini R, Gioria S, García CP, Nativo P, Franchini F, Gilliland D, et al. Size-dependent toxicity and cell interaction mechanisms of gold nanoparticles on mouse fibroblasts. Toxicol Lett. 2013;217:205–16. https://doi.org/10.1016/j.toxlet.2012.11.022
45. Senut M-C, Zhang Y, Liu F, Sen A, Ruden DM, Mao G. Size-dependent toxicity of gold nanoparticles on human embryonic stem cells and their neural derivatives. Small. 2016;12:631–46. https://doi.org/10.1002/smll.201502346
46. Vetten MA, Tlotleng N, Tanner Rascher D, Skepu A, Keter FK, Boodhia K, et al. Label-free in vitro toxicity and uptake

assessment of citrate stabilised gold nanoparticles in three cell lines. Part Fibre Toxicol. 2013;10:1–15. https://doi.org/10.1186/1743-8977-10-50
47. Zhang Y, Xu D, Li W, Yu J, Chen Y. Effect of size, shape, and surface modification on cytotoxicity of gold nanoparticles to human HEp-2 andcanine MDCK Cells. J Nanomater. 2012. https://doi.org/10.1155/2012/375496
48. Favi PM, Valencia MM, Elliott PR, Restrepo A, Gao M, Huang H, et al. Shape and surface chemistry effects on the cytotoxicity and cellular uptake of metallic nanorods and nanospheres. J Biomed Mater Res A. 2015;103:3940–55. https://doi.org/10.1002/jbm.a.35518
49. Wang P, Henning SM, Heber D. Limitations of MTT and MTS-based assays for measurement of antiproliferative activity of green tea polyphenols. PLoS One. 2010. https://doi.org/10.1371/journal.pone.0010202
50. Freese C, Uboldi C, Gibson MI, Unger RE, Weksler BB, Romero IA, et al. Uptake and cytotoxicity of citrate-coated gold nanospheres: comparative studies on human endothelial and epithelial cells. Part Fibre Toxicol. 2012;9:23 https://doi.org/10.1186/1743-8977-9-23
51. Choudhury D, Xavier PL, Chaudhari K, John R, Dasgupta AK, Pradeep T, et al. Unprecedented inhibition of tubulin polymerization directed by gold nanoparticles inducing cell cycle arrest and apoptosis. Nanoscale. 2013;5:4476 https://doi.org/10.1039/c3nr33891f
52. Shanmugasundaram T, Radhakrishnan M, Gopikrishnan V, Kadirvelu K, Balagurunathan R. Biocompatible silver, gold and silver/gold alloy nanoparticles for enhanced cancer therapy: in vitro and in vivo perspectives. Nanoscale. 2017;9:16773–90. https://doi.org/10.1039/C7NR04979J
53. Ding FA, Li YP, Liu J, Liu L, Yu WM, Wang Z, et al. Over-endocytosis of gold nanoparticles increases autophagy and apoptosis in hypoxic human renal proximal tubular cells. Int J Nanomed. 2014;9:4317–30. https://doi.org/10.2147/ijn.s68685
54. Tang Y, Shen Y, Huang L, Lv G, Lei C, Fan X, et al. In vitro cytotoxicity of gold nanorods in A549 cells. Environ Toxicol Pharmacol. 2015;39:871–8. https://doi.org/10.1016/j.etap.2015.02.003
55. Landgraf L, Müller I, Ernst P, Schäfer M, Rosman C, Schick I, et al. Comparative evaluation of the impact on endothelial cells induced by different nanoparticle structures and functionalization. Beilstein J Nanotechnol. 2015;6:300–12. https://doi.org/10.3762/bjnano.6.28
56. Jiang W, Kim BYS, Rutka JT, Chan WCW. Nanoparticle-mediated cellular response is size-dependent. Nat Nanotechnol. 2008;3:145–50. https://doi.org/10.1038/nnano.2008.30
57. Liu Y, He M, Niu M, Zhao Y, Zhu Y, Li Z, et al. Delivery of vincristine sulfate-conjugated gold nanoparticles using liposomes: a light-responsive nanocarrier with enhanced antitumor efficiency. Int J Nanomed. 2015;10:3081–95. https://doi.org/10.2147/IJN.S79550
58. Amarnath K, Mathew NL, Nellore J, Siddarth CRV, Kumar J. Facile synthesis of biocompatible gold nanoparticles from Vites vinefera and its cellular internalization against HBL-100 cells. Cancer Nanotechnol. 2011;2:121–32. https://doi.org/10.1007/s12645-011-0022-8
59. Mironava T, Hadjiargyrou M, Simon M, Jurukovski V, Rafailovich MH. Gold nanoparticles cellular toxicity and recovery: effect of size, concentration and exposure time. Nanotoxicology. 2010;4:120–37. https://doi.org/10.3109/17435390903471463
60. Favi PM, Gao M, Johana Sepúlveda Arango L, Ospina SP, Morales M, Pavon JJ, et al. Shape and surface effects on the cytotoxicity of nanoparticles: gold nanospheres versus gold nanostars. J Biomed Mater Res - Part A. 2015;103:3449–62. https://doi.org/10.1002/jbm.a.35491
61. Afrooz ARMN, Sivalapalan ST, Murphy CJ, Hussain SM, Schlager JJ, Saleh NB. Spheres vs. rods: the shape of gold nanoparticles influences aggregation and deposition behavior. Chemosphere. 2013;91:93–8. https://doi.org/10.1016/j.chemosphere.2012.11.031
62. Connor EE, Mwamuka J, Gole A, Murphy CJ, Wyatt MD. Gold nanoparticles are taken up by human cells but do not cause acute cytotoxicity. Small. 2005;1:325–7. https://doi.org/10.1002/smll.200400093

IVYSPRING INTERNATIONAL PUBLISHER

International Journal of Medical Sciences

2020; 17(6): 824-833. doi: 10.7150/ijms.40827

Research Paper

Assessment of Anti-Tumor potential and safety of application of Glutathione stabilized Gold Nanoparticles conjugated with Chemotherapeutics

Karol P. Steckiewicz[1]*, Ewelina Barcinska[1]*, Katarzyna Sobczak[2], Ewelina Tomczyk[2], Michał Wojcik[2], Iwona Inkielewicz-Stepniak[1]✉

1. Chair and Department of Medical Chemistry, Medical University of Gdansk, Debinki street 1, 80-211 Gdansk, Poland.
2. Faculty of Chemistry, University of Warsaw, Pasteura 1, 02-093 Warsaw, Poland.

*These authors contributed equally to this work.

✉ Corresponding author: Prof. Iwona Inkielewicz-Stepniak Ph.D. E-mail: iinkiel@gumed.edu.pl. Telephone: +4858 359 1450.

Received: 2019.10.01; Accepted: 2020.01.08; Published: 2020.03.12

Abstract

Due to the high toxicity of currently used chemotherapeutics, novel methods of cancer treatment are needed. Gold nanoparticles (AuNPs) seem to be an interesting alternative due to penetration through biological membranes and systemic barriers. AuNPs as carriers of chemotherapeutics allow for reduced concentrations whilst maintaining the expected effect, and thus reducing the costs of therapy and adverse effects. We synthesized AuNPs stabilized with reduced glutathione (GSH) and conjugated with doxorubicin (DOX), gemcitabine (GEM) or cytarabine (CTA). This is the first study in which cytarabine-AuNPs were synthesized and characterized. Transmission electron microscopy (TEM), thermogravimetric analysis (TGA), nuclear magnetic resonance spectroscopy (NMR) and high-performance liquid chromatography (HPLC) were used to chemically characterize obtained nanoparticles. Antitumor activity and safety of application were assessed by MTT assay in *in vitro* model (human osteosarcoma cells -143B, human osteoblast- hFOB1.19, breast cancer cells - MCF7, breast epithelial cells - MCF10A, pancreatic cancer cells – PANC-1, and pancreatic cells - hTERT-HPNE cells). We have shown that cellular response varies according to the type and concentration of AuNPs. At some concentrations, we were able to show selective cytotoxicity of our AuNPs conjugates only to cancer cell lines. Synthesized nanoparticles were more cytotoxic to tumor cell lines than chemotherapeutics alone.

Key words: Gold nanoparticles; Cancer; Drug deliver platform; Gold nanoparticles conjugate; Chemotherapeutic

Introduction

Cancer is one of the leading causes of death and emerging epidemiological problem in clinical practice furthermore cancer treatment is expensive [1,2]. AuNPs, that have established a role in nanotechnology, may be a possible answer to that matter. It has been proven that AuNPs may be used in cancer diagnostic and therapy [3,4]. They can penetrate through cellular membranes, which is crucial for biomedical applications [5]. Furthermore, AuNPs as drug delivery platforms can accumulate in the cancer microenvironment, which protects healthy tissue [6]. Importantly, AuNPs can be efficient in drug-resistant neoplasm [7]. Another advantage of the usage of AuNPs is a variety of sizes and possible surface modifications, which greatly expands their clinical application [8–10]. AuNPs have also good safety-profile [11]. Furthermore, it has been shown that GSH stabilized AuNPs have good biocompatibility profile and low immunogenicity [12]. Moreover, GSH as a peptide present in each cell can increase the biocompatibility of possessed AuNPs, which will be beneficial for potential applications [13].

Pancreatic cancer, osteosarcoma, and breast cancer are types of cancer were different oncological approaches may be used. Pancreatic cancer is

associated with poor prognosis (6% of 5-years survival rate) [14]. There are several treatment options for this cancer: surgery, radiotherapy, chemotherapy or combination of those [14]. Among the others, gemcitabine (GEM) is used in chemotherapy for pancreatic cancer [14]. Unfortunately, GEM has severe side-effects, among the others: nausea, mielosuppression, liver damage or heart failure which may decrease patient quality of life [15]. Pancreatic cancer is thought to become the second most popular type of cancer in 2030 and the average cost of lifetime treatment per patient is as high as $65335 [16,17]. Another cancer considered with poor outcome is osteosarcoma, which is one of the most common cancers of the youth [18]. In general treatment options are similar to pancreatic cancer (surgery, chemotherapy, radiotherapy) [18]. Treatment of osteosarcoma in many cases requires amputation, which severely decreased the patient's quality of life. One of the agents used in osteosarcoma therapy is doxorubicin (DOX) [18]. Also, it has been proven that AuNPs may be cytotoxic to osteosarcoma cell lines [19]. For breast cancer apart from the "classical" treatment, we can use hormone-blocking therapy and monoclonal antibodies against described molecular targets. DOX and cytarabine (CTA) are effective drugs in breast cancer therapy [20,21]. Unfortunately, both drugs have serious aftereffects. For DOX it will be mielosuppression, cardiotoxicity hair loos and others [22]. Usage of CTA can lead to brain damage, mielosuppression, gastrointestinal tract disturbances and others [23]. Surgery with healthy tissue margin typically gives the best treatment outcome; however, it is limited only to small tumors. Thus, chemotherapy still is one of the main treatment strategies in oncology. However, due to multidrug resistance of cancer and poor penetration of active agents through the tumor, its effectiveness is limited. Thus, novel drug delivery platforms, such as AuNPs, may be an interesting solution to this problem.

In this research we assessed the anti-tumor potential of GSH stabilized AuNPs conjugated with chemotherapeutics (DOX, CTA, GEM). As chemotherapeutics have severe side effects and limited effectiveness we tried to overcome their disadvantages by using AuNPs as drug delivery platforms. Our modification allows using a smaller concentration (dose) of a drug, which will increase patients' comfort, also better penetration may upsurge the efficiency of treatment.

Effectiveness against pancreatic adenocarcinoma, breast cancer, and osteosarcoma cell lines was evaluated. We also assessed the safety of AuNPs application by *in vitro* cytotoxicity assay on non-transformed cell lines.

Materials and methods

Synthesis

Synthesis of AuNPs stabilized with GSH

93.5 µL (0.135 mmol) of 30% chloroauric acid solution ($HAuCl_4$) was diluted using 26 mL of distilled water. The reaction mixture was placed in a water/ice bath and then 162 mg (0.537 mmol) of reduced glutathione was added slowly in small portions. The solution turned from light yellow through brown into transparent with white suspension. After 1.5 hours a few drops of a saturated solution of sodium bicarbonate was added, which caused an increase of pH and consequently disappearance of the precipitate. Next, 50 mg (1.322 mmol) of $NaBH_4$ dissolved in 6.5 mL of water was added quickly with high-speed magnetic stirring. The solution turned brown and the reaction mixture was stirred an additional 2 hours. Then, 20 mL of methanol was added to precipitate nanoparticles. The precipitate was centrifuged (5000 rpm, 10 min) washed with methanol: water 1:1 mixture and dissolved in 1 mL of distilled water. The significant concentration of nanoparticles left in supernatant and was subjected to additional precipitation. The obtained supernatant was mixed with 55 mL of methanol and was centrifuged (10000 rpm, 15 min.) yielding brown sediments. The precipitate was washed with methanol: water 4:1 mixture and was dried. The additional precipitate was used in this study. Then nanoparticles were precipitated an additional two times. Resulted precipitates were left to dry in the air.

Synthesis of AuNPs stabilized with GSH and DOX

4 mg of AuNPs stabilized with GSH were dissolved in 0.4 mL of distilled water. Then, 2 mL of prepared DOX water solution (1 mg/mL) was added slowly. The reaction mixture was stirred 12 hours and then nanoparticles were purified using centrifugal filters (Amicon® Ultra 0.5 mL) in a centrifuge (10000 rpm, 5 min) and washed two times with PBS.

AuNPs stabilized with GSH and GEM

20 mg of AuNPs stabilized with GSH were dissolved in 2 mL of distilled water. Then, 1 mg (0.003 mmol) of GEM dissolved in 1 ml of water was added and the reaction was mixed for 12 hours. Next, nanoparticles were purified using centrifugal filters (Amicon® Ultra 0.5 mL) in a centrifuge (10000 rpm, 5 min).

AuNPs stabilized with GSH and CTA

20 mg of AuNPs stabilized with GSH were dissolved in 2 mL of distilled water. Then 1 mg (0.004

mmol) of CTA dissolved in 1 mL of water was introduced and the reaction was mixed for 12 hours. Next, nanoparticles were purified using centrifugal filters (Amicon® Ultra 0.5 mL) in a centrifuge (10000 rpm, 5 min).

Cell culture

143B (ATCC CRL-8303) were cultured in Minimum essential medium (Eagle) with 0.015 mg/mL 5-bromo-2'-deoxyuridine. Media was supplemented with 10% of heat-inactivated fetal bovine serum (FBS) and 1% of penicillin and streptomycin (P/S) hFOB 1.19 (ATCC CRL-11372) were cultured in 1:1 mixture of Ham's F12 Medium and Dulbecco's Modified Eagle's Medium (DMEM/F12) with 2,5 mM of L-glutamine. The media was supplemented with 10% of FBS and 1% of P/S. hTERT-HPNE (ATCC CRL-4023) were cultured in DMEM with 2 mM of L-glutamine and Medium M3 base in ratio 3:1. Media was supplemented with 5% of FBS, 10 ng/mL of EGF, 1g/L of D-glucose, 750 ng/mL of puromycin and 1% of P/S. MCF 10A (ATCC HTB-2 2) were cultured in DMEM/F12 media supplemented with 5% of horse serum, 20 ng/mL of EGF, 0,5 mg/mL of hydrocortisone, 100 ng/mL of cholera toxin, 10 g/mL of insulin and 1% of P/S. MCF 7 (ATCC CRL-10317) were cultured in DMEM (4mM L-glutamine and 4500 mg/L of glucose). The media was supplemented with 10% of FBS and 1% of P/S. PANC 1 (ATCC CRL-1496) were cultured in DMEM (4mM L-glutamine and 4500 mg/L of glucose). The media was supplemented with 10% of FBS and 1% of P/S. All cells were possessed from the American Type Culture Collection. Cells were kept in T-75 flask under the sterile condition at 37°C in a humidified atmosphere of 5% of CO_2 (medium renewal every 2 days). When confluent cells were detached with a trypsin-EDTA solution and subcultivated according to ATCC guidelines.

Treatments

Each time just before experiment new dilutions of synthesized AuNPs in FBS-free media were prepared. The stock solution was shaken well to ensure an equal dispersion of AuNPs. Cells were incubated with 1, 10, 25, 50 and 100 µg/mL of all synthesized nanoparticles (AuNPs-GSH, AuNPs-GSH-GEM, AuNPs-GSH-DOX, AuNPs-GSH-CTA). Prior to incubation solutions were shaken in order to prevent agglomeration of investigated AuNPs. Control cells were kept in FBS-free media without AuNPs addition. Cells were incubated in 37°C, 5% CO_2 for 24h.

MTT assay

Cell viability was measured by MTT assay with a previously established method [19,24]. Briefly, cells were seeded into a 96-well dish (density $1x10^4$ cells/well). After 24h cells were incubated with synthesized AuNPs and chemotherapeutics as described in the ''Treatments" section. After 24h solution water-soluble tetrazolium salt was added to a final concentration of 0.5 mg/mL. Next, the plate was incubated for 2h in standard condition. Formazan crystals were diluted in dimethyl sulfoxide. Cell viability was assessed by absorbance measurements. Absorbance values were adjusted with blank NPs. The viability of control cells was set to 100%.

Statistical analysis

All statistical analysis was performed with GraphPad Prism 5 software (GraphPad Software, Inc., USA). Statistical analysis was determined by a one-way analysis of variance (ANOVA) and Tukey's posthoc test.

Results

AuNPs characteristic

AuNPs stabilized with GSH (AuNPs-GSH)

To determine the size and monodispersity of obtained nanoparticles we conducted TEM measurements. Figure 1 shows the TEM image of AuNPs (Figure 1a) and histograms of the size distribution (Figure 1b). The obtained nanoparticles have an average diameter of about 2.1 +/- 0.3 nm.

The presence of GSH on the surface of nanoparticles has been confirmed by thermogravimetric analysis. The given thermogram (Figure 2) shows the weight loss of the sample during heating (red line). The first derivative of TGA curve (blue line) shows a single sharp peak in the temperature range 220-250°C. It corresponds to the rapid decomposition of nanoparticles as a result of the loss of GSH from the surface of nanoparticles. This analysis showed that GSH is ~24% of the mass of AuNPs.

The presence of GSH on the surface of the nanoparticles was also confirmed by ^{1}H NMR spectra (Figure 3a), for comparison spectra of GSH is shown in Figure 3b. In Figure 3a there are clearly visible four signals characteristic for GSH (strong signal 3.42 ppm arises from methanol). All signals are broadened which is characteristic for NMR spectra protons from molecules conjugated to the surface of nanoparticles (no sharp signals indicate that sample was purified properly and there is no unbounded GSH). Signals at 2.30 ppm, 2.69 ppm, and 3.89 ppm are assigned respectively to protons from carbons 3, 4 and 9. The broad signal at 3.89 ppm is probably a screening signal from proton from carbon 2, which should

appear at 3.84 ppm. Protons from carbons 6 and 7 are in β and α position to a thiol group, which is located in direct neighborhood to gold atoms, which cannot be analyzed by 1D spectra.

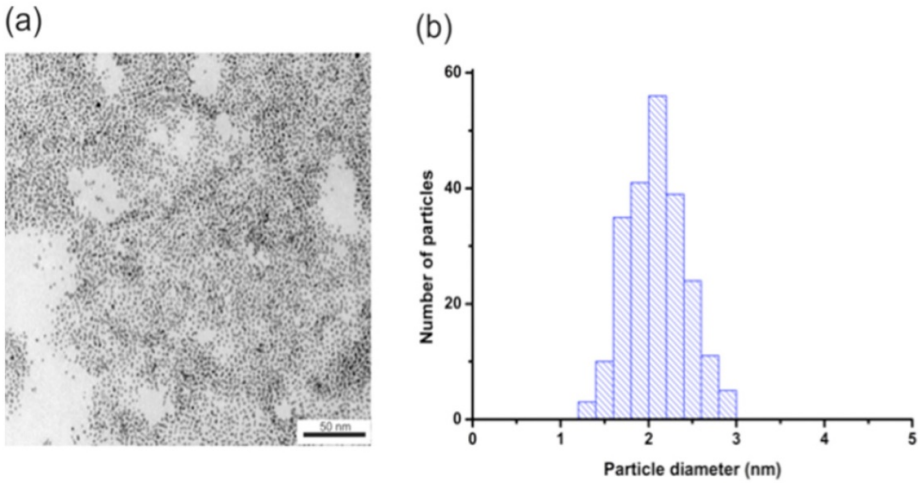

Figure 1. (a) AuNPs-GSH TEM image and (b) AuNPs-GSH histogram of size distribution. Scale bar corresponds to 50 nm.

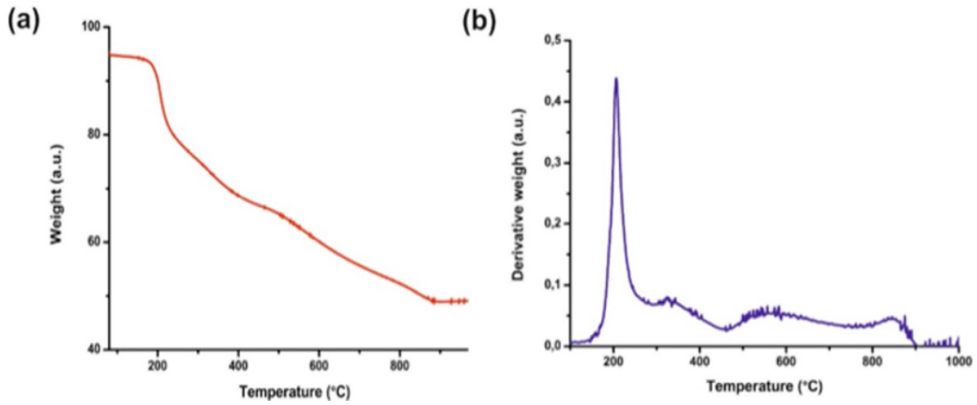

Figure 2. TGA analysis of AuNPs-GSH: (a) TGA curves of the studied sample and (b) the first derivative of its weight loss.

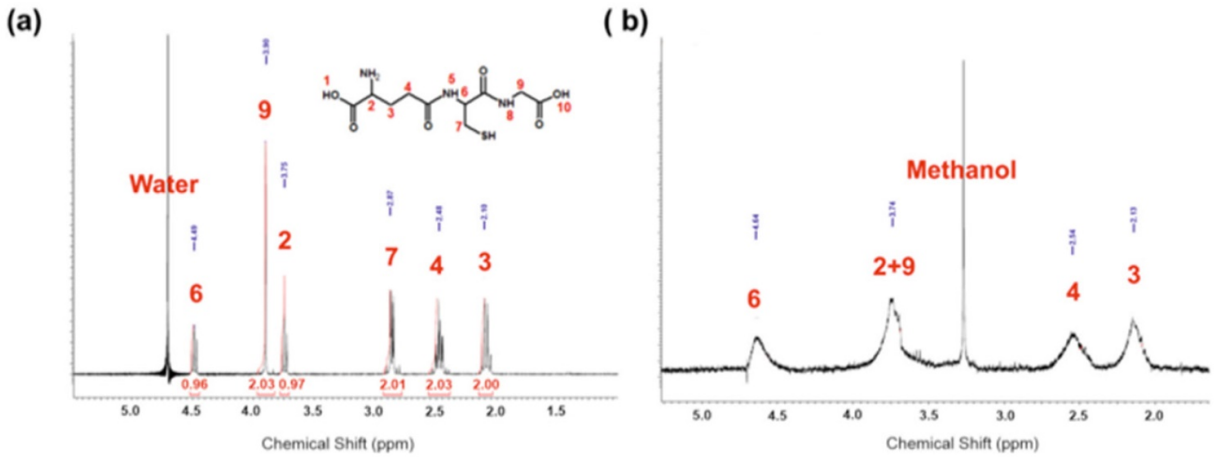

Figure 3. (a) 1H NMR of AuNPs-GSH (b) simulation of 1H NMR spectra of GSH.

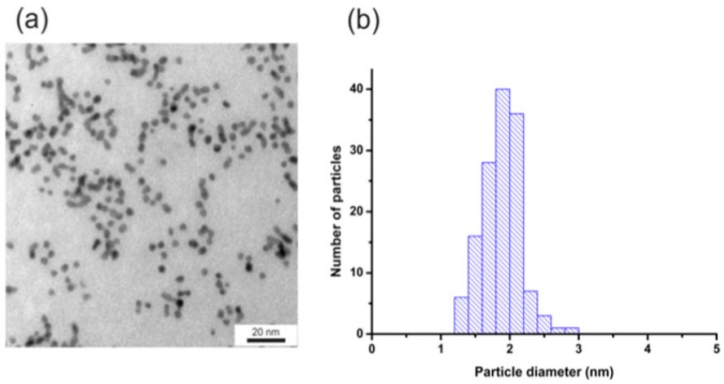

Figure 4. (a) TEM image and (b) histogram of NPs size distribution for AuNPs-GSH-DOX. Scale bar corresponds to 20 nm.

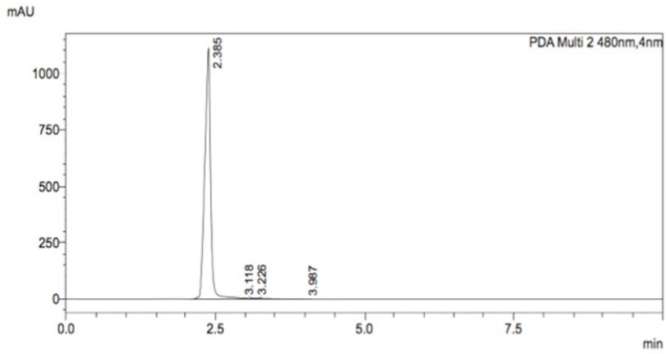

Figure 5. HPLC chromatogram of decomposed AuNPs-GSH-DOX solution.

AuNPs stabilized with GSH and DOX (AuNPs-GSH-DOX)

Figure 4 shows the TEM image (Figure 4a) and the histogram of the size distribution (Figure 4b) of nanoparticles. AuNPs-GSH-DOX have an average diameter of about 1.9+/- 0.3 nm after the surface modification. The lower diameter value of these nanoparticles is related to lower contrast characteristics for samples with higher organic fraction concentration.

Sample of these nanoparticles was treated with iodine in order to break bonds between nanoparticles and ligands. Ligands solution was separated from nanoparticles aggregates and HPLC measurement was performed. The mobile phase consisted of 10 mM KH_2PO4 and 0.1% (v/v) trifluoroacetic acid in water and acetonitrile as the organic phase. A gradient method was used in which the mobile phase started as 75% aqueous phase and 25% of the organic phase and changed in a linear manner to 60/40 within 7 minutes. Peaks were monitored using a UV-VIS detector. Figure 5 shows a strong signal (2.385 min), which is characteristic of DOX.

AuNPs stabilized with GSH and GEM (AuNPs-GSH-GEM)

Figure 6 shows the TEM image (Figure 6a) and the histogram of the size distribution (Figure 6b). The obtained nanoparticles have an average diameter of about 2.11+/- 0.33 nm.

AuNPs stabilized with GSH and CTA (AuNPs-GSH-CTA)

Figure 7 shows the TEM image (Figure 7a) and the histogram of the size distribution (Figure 7b). AuNPs-GSH-CTA have an average diameter of about 2.10+/- 0.35 nm. The lower diameter value of these nanoparticles is related to lower contrast characteristics for samples with higher organic faction concentration.

AuNPs decreased the viability of the cells in a concentration-dependent manner

AuNPs-GSH-DOX and AuNPs-GSH-GEM and all AuNPs-GSH-CTA decreased the viability of 143B cells. All tested AuNPs decreased the viability of hFOB 1.19 cells. The highest impact on 143B cells viability had AuNPs-GSH-CTA; this AuNPs in the concentration of 100 µg/mL demonstrated approximately 45% decreased viability of 143B cells.

In contrast, the highest impact on the viability of hFOB 1.19 cells had AuNPs-GSH-GEM (in the concentration of 100 μg/mL). Interestingly, in lower concentrations (1, 10 μg/mL) hFOB 1.19 were more susceptible to AuNPs than 143B cells (Figure 8).

All tested AuNPs decreased the viability of PNAC-1 and hTERT-HPNE cells in a concentration-dependent manner. Importantly, hTERT-HPNE cells were more resistant to AuNPs than PANC-1 cells. The highest impact on PANC-1 viability had AuNPs-GSH-GEM. AuNPs-GSH-CTA to around 30% and AuNPs-GSH-GEM decreased the viability of the cells to around 25%. Similarly for hTERT-HPNE AuNPs-GSH-CTA and AuNPs-GSH-GEM decreased the viability of the cells to around 45% (Figure 8).

All tested AuNPs decreased the viability of MCF7 cells and all tested AuNPs apart from AuNPs-GSH decreased viability of MCF10A cells. MCF10A were more resistant to AuNPs than MCF7 cells. The highest impact on MCF7 cells viability had AuNPs-GSH-GEM (decreased viability to around 25%). AuNPs-GSH-DOX and AuNPs-GSH-GEM in 100 μg/mL concentrations decreased viability of MCF10A cells to 50% (Figure 8).

We have proven that AuNPs-GSH-DOX in concentration 1 μg/mL, AuNPs-GSH-CTA in concentration 1 μg/mL and AuNPs-GSH-GEM in concentration 10 μg/mL are selectively cytotoxic to osteosarcoma cell line (143B) in comparison to non-transformed cells. AuNPs-GSH-GEM in concentration 1 μg/mL is selectively cytotoxic against pancreatic ductal adenocarcinoma cells (PANC-1). AuNPs-GSH-CTA in concentration 1 and 10 μg/mL is selectively cytotoxic to epithelial breast adenocarcinoma cells (MCF7).

Generally, cancer cell lines (143B, PANC1, MCF7) were more susceptible to our conjugates that non-transformed cell lines (hFOB1.19, hTERT-HPNE, MCF10A). In Figure 8 red boxes indicate selective cytotoxicity of AuNPs only to cancer cells (in comparison to non-transformed cells).

As a reference, we assessed the impact of chemotherapeutics on the viability of cancer cell lines (Figure 9). DOX in a concentration equal or higher 0.49 μg/mL decreased the viability of 143B and MCF7 cells and in a concentration equal or higher 0.99 μg/mL of PANC1 cells. CTA decreased the viability of 143B, PANC-1 and MCF7 cells in concentrations equal to or higher than 2.47 μg/mL. GEM significantly decreased the viability of 143B cells in a concentration equal or higher 0.49 μg/mL, PANC-1 2.47 μg/mL and MCF7 0.99 μg/mL.

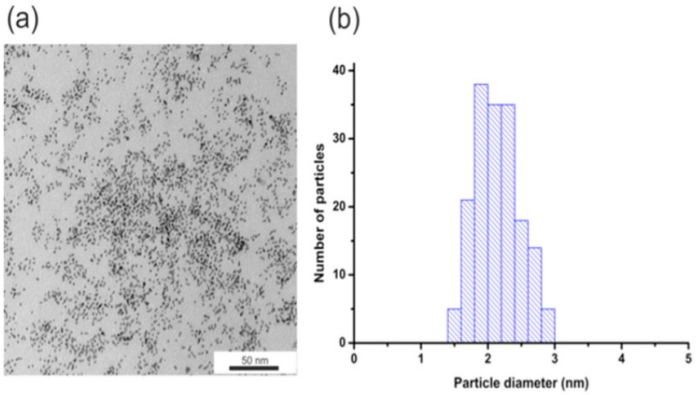

Figure 6. (a) TEM image and (b) histogram of NPs size distribution for AuNPs-GSH-GEM. Scale bar corresponds to 50 nm.

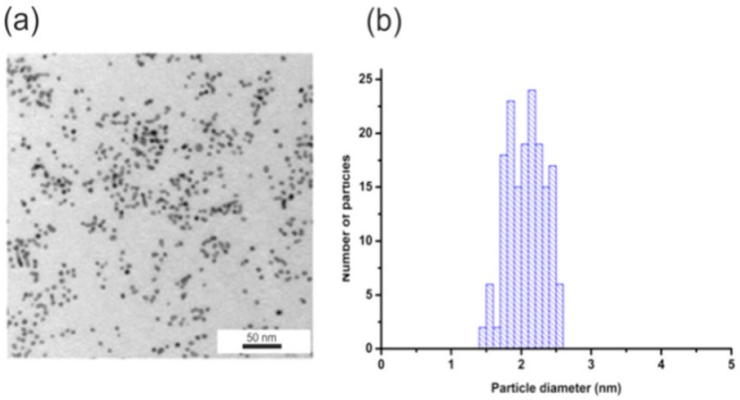

Figure 7. (a) TEM image and (b) histogram of NPs size distribution for AuNPs-GSH-CTA. Scale bar corresponds to 50 nm.

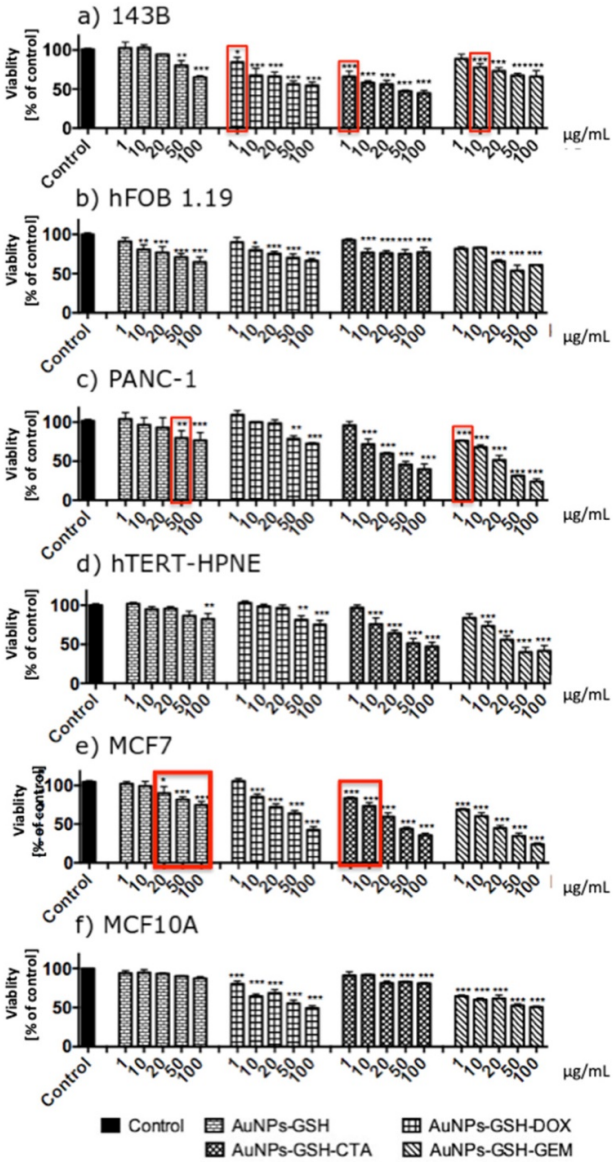

Figure 8. AuNPs-GSH conjugated with chemotherapeutics: DOX, GEM, CTA decreased viability of the cells in a concentration-dependent manner after 24 h of incubation. The viability measured by MTT assay of (a) 143B, (b) hFOB 1.19, (c) PNAC-1, (d) hTERT-HPNE, (e) MCF7 and (f) MCF10A cells exposed to AuNPs for 24h. Data are presented as mean ±SD. *p<0.05, **p<0.01, ***p<0.001. Red boxes indicate selective cytotoxicity of AuNPs only to cancer cells (in comparison to non-transformed cells).

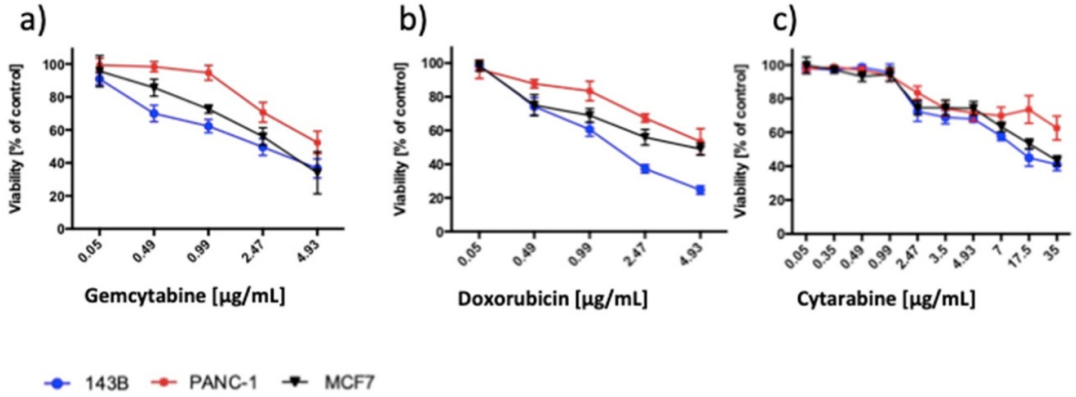

Figure 9. Chemotherapeutics decreased the viability of the cancer cells in a concentration-dependent manner. Viability measured by MTT assay of the 143B, PANC-1 and MCF7 cells exposed to (a) GEM, (b) DOX and (c) CTA for 24h. The viability of control was set to 100%. Data are presented as mean ± SD.

In the conditions listed below, our AuNPs-chemotherapeutic conjugates significantly decreased the viability of cancer cells, whereas corresponding chemotherapeutic concentrations did not. AuNPs-GSH-DOX (1 μg/mL), AuNPs-GSH-CTA (1, 10, 20, 50 μg/mL) on 143B cells; AuNPs-GSH-CTA (10, 20, 50 μg/mL), AuNPs-GSH-GEM (1, 10, 20 μg/mL) on PANC-1 cells; AuNPs-GSH-CTA (1, 10, 20, 50 μg/mL) and AuNPs-GSH-GEM (1, 10 μg/mL) on MCF7cells, respectively.

Importantly, tested AuNPs had anti-cancer potential. Nanoparticles coated only with GSH had the smallest impact on the viability of the cells. Furthermore, tumor cells line were more susceptible to tested AuNPs that non-transformed cell lines. As mentioned above AuNPs conjugated with chemotherapeutics exerted selective cytotoxicity.

Discussion

In 2018, more than 18 million people were diagnosed with cancer and 9.5 million people died of it [25]. Among cancers: breast cancer (>2 088 000 new cases, >626 000 deaths in 2018), pancreatic cancer (>458 000 new cases, 432 000 deaths in 2018) and osteosarcoma (morbidity rate of 4 cases/million people yearly), are emerging clinical problems [25,26]. Unfortunately, prognosis in those cancers is poor. Only 60% of patients with osteosarcoma and breast cancer survive at least 5 years from diagnosis, whereas almost no patients with pancreatic cancer survive 5 years (median survival 5.5 months) [26–28]. Moreover, the treatment of cancer: chemotherapy, radiotherapy, hormonotherapy, and surgery severely decrease patients' quality of life. Among the others: myelosuppression, hepatotoxicity, renal failure, heart failure, gastrointestinal tract damage, nausea and hair loss are the most important side effect of chemotherapy [15,22,23]. Therefore, novel approaches with better effectiveness and less severe side effects are needed.

The main aim of the study was to evaluate the anti-tumor and safety of AuNPs stabilized with GSH and conjugated with chemotherapeutics under *in vitro* condition. We decided to use AuNPs as it had been proven that they have a good safety profile and established a role as a drug delivery platform [29,30]. Furthermore, our nanoparticles are coated with GSH in order to increase biocompatibility [13]. Indeed, we have shown that AuNPs-GSH had small effects on the viability of mammalian cells. Importantly, typically AuNPs conjugated with chemotherapeutics have a higher impact on the viability of cancer cell lines than non-transformed ones. Furthermore, in some concentrations of AuNPs-chemotherapeutics, we were able to show selective cytotoxicity. Differences in effects exerted by AuNPs-chemotherapeutic and chemotherapeutic alone may be due to a different way of internalization. The drug can be internalized by passive diffusion whereas when conjugated with AuNPs internalization mechanism is endocytosis or other active transport mechanisms [31]. More importantly AuNPs-chemotherapeutic conjugate, in some cases, were more effective than chemotherapeutic alone. We compared the cytotoxicity of chemotherapeutics on cell lines used in this study (143B, PANC-1, MCF7) with literature data, and generally, we had similar results [31,32,41,42,33-40]. For DOX, Kamba et al., reported that IC_{50} was around 0.5μg/mL (MG63, osteosarcoma cells), Yui et al, showed that IC_{50} was approximately equal 2 μg/mL (PANC1 cells).

Data on cytotoxicity of AuNPs-GSH or AuNPs conjugated with chemotherapeutics are limited. However, several studies have proven the safety of AuNPs. Leite et al, have demonstrated that 4.5 nm PEG-AuNPs in concentration up to 5×10^{13} particles/mL did not influence the viability of mouse myoblastoma (C2C12 cells) measured by MTT assay [43]. Similarly, IC_{50} of HeLa cells treated with 1.4 nm GSH-coated AuNPs was 3130 μM. In our study, which was similar to already published data, AuNPs-GSH had the lowest cytotoxicity potential, which have proven that functionalization of AuNPs with GSH ensures good safety-profile of synthesized AuNPs. Size of AuNPs is one of the main factors impacting AuNPs cytotoxicity [44]. Pan et al have examined the cytotoxicity of spherical AuNPs against human cell lines (fibroblast, melanoma, epithelial cells, and macrophages). They have chosen AuNPs in size range between 0.8 and 15 nm [44]. 1.4 nm AuNPs were the most cytotoxic whereas 15 nm AuNPs were 60-100 times less toxic [44].

Manivasagan et al. assessed potential anti-cancer AuNPs-fucoidan-DOX on human breast adenocarcinoma cells (MDA-MB-231). Similarly to our results they have shown that AuNPs coated with DOX had a higher impact on cancer cells viability than AuNPs-fucoidan or DOX alone [45]. Correspondingly, Venkatourwar et al., assessed the impact of porphyrin-coated AuNPs conjugated with DOX as a potential drug delivery platform. They also showed that conjugated DOX and AuNPs are more cytotoxic against human glioma cells (LN-299) than any of the compounds alone [46].

According to best of our knowledge, it is the first study to examine the impact of CTA conjugated metal nanoparticles on mammalian cells in which we indicated that AuNPs stabilized with GSH and conjugated with CTA can be more effective in

inducing cell death that CTA alone on osteosarcoma, pancreatic cancer cells breast cancer cells.

We have found that AuNPs may be an interesting drug delivery platform. AuNPs-chemotherapeutic conjugates may be more effective than the drug alone and can have a selective effect only on cancer cells. AuNPs-chemotherapeutic conjugates allow using lesser concentration (dose) of the drug, which decreases the severity of side effects and reduces the treatment cost.

Conclusions

In the presented study, we demonstrated the anti-cancer potential of AuNPs stabilized with GSH and conjugated with chemotherapeutics. We have shown that our nanoparticles can be selectively cytotoxic to cancer cell lines (in comparison to non-transformed ones). Furthermore, in some cases, synthesized AuNPs conjugates were more effective than the drug alone. Modern methods of chemical synthesis of nanoparticles conjugated with chemotherapeutics may increase the effectiveness of anti-cancer therapy. At the same time, it allows for a significant reduction of treatment costs and relieves of side effects.

Abbreviations

GEM: gemcitabine; DOX: doxorubicin; CTA: cytarabine; NPs: nanoparticles; AuNPs: gold nanoparticles; GSH: glutathione; $HAuCl_4$: chloroauric acid; TEM: transmission electron microscopy; TGA: thermogravimetric analysis; NMR: nuclear magnetic resonance spectroscopy; HPLC: high-performance liquid chromatography.

Acknowledgments

MCF7 and MCF10A cells were a kind gift from prof. Anna Herman-Antosiewicz from the University of Gdansk.

Funding

This work was supported by the Grant from the Medical University of Gdansk, Poland (ST-02-705 0046/07/259). The funders had no role in study design, data collection, and analysis, decision to publish, or preparation of the article.

Authors' contributions

All authors contributed to the study conception and design. KPS, EB, KS and ET performed material preparation, data collection and analysis. IIS and MW provided supervision. The first draft of the manuscript was written by KPS and all authors commented on previous versions of the manuscript. All authors read and approved the final manuscript.

Competing Interests

The authors have declared that no competing interest exists.

References

1. Dalrymple KL, Martinez J, Rosenstein L, Kneeland ET, Zimmerman M. Psychiatric disorder-weight associations and the moderating effect of sex in an outpatient psychiatric sample. Ann. Clin. Psychiatry. 2015;27:108–117.
2. Tangka FK, Trogdon JG, Richardson LC, Howard D, Sabatino SA, Finkelstein EA. Cancer treatment cost in the United States: Has the burden shifted over time? Cancer. 2010;116:3477–3484.
3. Lee U, Yoo C-J, Kim Y-J, Yoo Y-M. Cytotoxicity of gold nanoparticles in human neural precursor cells and rat cerebral cortex. J. Biosci. Bioeng. 2016;121:341–344.
4. Ahn JM, Eom HJ, Yang X, Meyer JN, Choi J. Comparative toxicity of silver nanoparticles on oxidative stress and DNA damage in the nematode, Caenorhabditis elegans. Chemosphere. 2014;108:343–352.
5. Gromnicova R, Kaya M, Romero IA, et al. Transport of gold nanoparticles by vascular endothelium from different human tissues. PLoS One. 2016;11:1–17.
6. Ho BN, Pfeffer CM, Singh ATK. Update on Nanotechnology-based Drug Delivery Systems in Cancer Treatment. Anticancer Res. 2017;37:5975–5981.
7. Gu YJ, Cheng J, Man CWY, Wong WT, Cheng SH. Gold-doxorubicin nanoconjugates for overcoming multidrug resistance. Nanomedicine Nanotechnology, Biol. Med. 2012;8:204–211.
8. Banu H, Sethi DK, Edgar A, et al. Doxorubicin loaded polymeric gold nanoparticles targeted to human folate receptor upon laser photothermal therapy potentiates chemotherapy in breast cancer cell lines. J. Photochem. Photobiol. B Biol. 2015;149:116–128.
9. Mahmoodi NO, Ghavidast A, Amirmahani N. A comparative study on the nanoparticles for improved drug delivery systems. Journal of Photochemistry and Photobiology B: Biology. 2016;162:681–693.
10. Brown SD, Nativo P, Smith JA, et al. Gold nanoparticles for the improved anticancer drug delivery of the active component of oxaliplatin. J. Am. Chem. Soc. 2010;132:4678–4684.
11. Zabielska-Koczywas K, Dolka I, Król M, et al. Doxorubicin conjugated to glutathione stabilized gold nanoparticles (Au-GSH-Dox) as an effective therapeutic agent for feline injection-site sarcomas - Chick embryo chorioallantoic membrane study. Molecules. 2017;22:253.
12. Simpson CA, Salleng KJ, Cliffel DE, Feldheim DL. In vivo toxicity, biodistribution, and clearance of glutathione-coated gold nanoparticles. Nanomedicine Nanotechnology, Biol. Med. 2013;9:257–263.
13. Liu Y, Ma W, Liu W, et al. Silver(i)-glutathione biocoordination polymer hydrogel: Effective antibacterial activity and improved cytocompatibility. J. Mater. Chem. 2011;21:19214–19218.
14. Kamisawa T, Wood LD, Itoi T, Takaori K. Pancreatic cancer. Lancet. 2016;388:73–85.
15. Kubicka S, Rudolph KL, Tietze MK, Lorenz M, Manns M. Phase II study of systemic gemcitabine chemotherapy for advanced unresectable hepatobiliary carcinomas. Hepatogastroenterology. 2001;48:783–789.
16. Du W, Touchette D, Vaitkevicius V, Peters W, Shields A. Cost Analysis of Pancreatic Carcinoma Treatment. Cnacer. 2000;89:1917–1924.
17. Rahib L, Smith BD, Aizenberg R, Rosenzweig AB, Fleshman JM, Matrisian LM. Projecting cancer incidence and deaths to 2030: The unexpected burden of thyroid, liver, and pancreas cancers in the united states. Cancer Research. 2014;74:2913–2921.
18. Luetke A, Meyers PA, Lewis I, Juergens H. Osteosarcoma treatment - Where do we stand? A state of the art review. Cancer Treat. Rev. 2014;40:523–532.
19. Steckiewicz KP, Barcinska E, Malankowska A, et al. Impact of gold nanoparticles shape on their cytotoxicity against human osteoblast and osteosarcoma in in vitro model . Evaluation of the safety of use and anti-cancer potential. J. Mater. Sci. Mater. Med. 2019;30:1–15.
20. Cohen O, Lam G, Choi M, Karp N, Ceradini D. Does the Timing of Chemotherapy Affect Post-Mastectomy Breast Reconstruction Complications? Clin. Breast Cancer. 2017;17:307–315.
21. Niwińska A, Rudnicka H, Murawska M. Breast cancer leptomeningeal metastasis: The results of combined treatment and the comparison of methotrexate and liposomal cytarabine as intra-cerebrospinal fluid chemotherapy. Clin. Breast Cancer. 2015;15:66–72.
22. Speth PAJ, van Hoesel QGCM, Haanen C. Clinical Pharmacokinetics of Doxorubicin. Clinical Pharmacokinetics. 1988;15:15–31.
23. Juel-Jensen BE. Severe generalized primary herpes treated with cytarabine. Br. Med. J. 1970;2:154–5.
24. Steckiewicz KP, Zwara J, Jaskiewicz M, et al. Shape-Depended Biological Properties of Ag 3 PO 4 Microparticles : Evaluation of Antimicrobial Properties and Cytotoxicity in In Vitro Model — Safety Assessment of Potential Clinical Usage. 2019.
25. Bray F, Ferlay J, Soerjomataram I, Siegel RL, Torre LA, Jemal A. Global cancer statistics 2018: GLOBOCAN estimates of incidence and mortality worldwide for 36 cancers in 185 countries. CA. Cancer J. Clin. 2018;68:394–424.
26. Savage SA, Mirabello L. Using epidemiology and genomics to understand osteosarcoma etiology. Sarcoma. 2011;2011:14–16.

27. Von Hoff DD, Ervin T, Arena FP, et al. Increased survival in pancreatic cancer with nab-paclitaxel plus gemcitabine. N. Engl. J. Med. 2013;369:1691–1703.
28. Gakwaya A, Kigula-Mugambe JB, Kavuma A, et al. Cancer of the breast: 5-Year survival in a tertiary hospital in Uganda. Br. J. Cancer. 2008;99:63–67.
29. Paciotti GF, Kingston DGI, Tamarkin L. Colloidal gold nanoparticles: A novel nanoparticle platform for developing multifunctional tumor-targeted drug delivery vectors. Drug Development Research. 2006;67:47–54.
30. Guglielmo C Di, Lapuente J De, Porredon C, Ramos-López D, Sendra J, Borrás M. In Vitro Safety Toxicology Data for Evaluation of Gold Nanoparticles–Chronic Cytotoxicity, Genotoxicity and Uptake. J. Nanosci. Nanotechnol. 2012;12:6185–6191.
31. Kamba SA, Ismail M, Hussein-Al-Ali SH, Ibrahim TAT, Zakaria ZAB. In vitro delivery and controlled release of doxorubicin for targeting osteosarcoma bone cancer. Molecules. 2013;18:10580–10598.
32. Yin F, Yang C, Wang Q, et al. A light-driven therapy of pancreatic adenocarcinoma using gold nanorods-based nanocarriers for co-delivery of doxorubicin and siRNA. Theranostics. 2015;5:818–833.
33. Varbanov HP, Kuttler F, Banfi D, Turcatti G, Dyson PJ. Repositioning approved drugs for the treatment of problematic cancers using a screening approach. PLoS One. 2017;12:1–16.
34. Jenie RI, Handayani S, Susidarti RA, Udin LZ, Meiyanto E. The cytotoxic and antimigratory activity of Brazilin-doxorubicin on MCF-7/HER2 cells. Adv. Pharm. Bull. 2018;8:507–516.
35. Zhang P, Yi W, Hou J, Yoo S, Jin W, Yang Q. Acarbon nanotube-gemcitabine-lentinan three-component composite for chemo-photothermal synergistic therapy of cancer. Int. J. Nanomedicine. 2018;13:3069–3080.
36. Xu Y, Huang Y, Zhang X, Lu W, Yu J, Liu S. Carrier-free Janus nano-prodrug based on camptothecin and gemcitabine: Reduction-triggered drug release and synergistic in vitro antiproliferative effect in multiple cancer cells. Int. J. Pharm. 2018;550:45–56.
37. Lev-Ari S, Vexler A, Starr A, et al. Curcumin augments gemcitabine cytotoxic effect on pancreatic adenocarcinoma cell lines. Cancer Invest. 2007;25:411–418.
38. Zheng C, Jiao X, Jiang Y, Sun S. ERK1/2 activity contributes to gemcitabine resistance in pancreatic cancer cells. J. Int. Med. Res. 2013;41:300–360.
39. Popescu RC, Andronescu E, Vasile B Ștefan, et al. Fabrication and cytotoxicity of gemcitabine-functionalized magnetite nanoparticles. Molecules. 2017;22.
40. Anantharaman NV, Udhumansha U, Rathnam G, Metha CLB. ISSN : 2320-2831 In-vitro diffusion studies and anticancer activity of cytarabine loaded nanocochleates against MCF-7 cell lines. 2018;7:285–294.
41. Wang Y, Wang S, Liu J, Lu Y, Li D. Licoricidin enhances gemcitabine-induced cytotoxicity in osteosarcoma cells by suppressing the Akt and NF-κB signal pathways. Chem. Biol. Interact. 2018;290:44–51.
42. Choupani J, Alivand MR, M. Derakhshan S, Zaeifizadeh M, S. Khaniani M. Oleuropein inhibits migration ability through suppression of epithelial-mesenchymal transition and synergistically enhances doxorubicin-mediated apoptosis in MCF-7 cells. J. Cell. Physiol. 2018;1–12. doi:10.1002/jcp.27586.
43. Leite PEC, Pereira MR, Santos CA do N, Campos APC, Esteves TM, Granjeiro JM. Gold nanoparticles do not induce myotube cytotoxicity but increase the susceptibility to cell death. Toxicol. Vitr. 2015;29:819–827.
44. Pan Y, Neuss S, Leifert A, et al. Size-dependent cytotoxicity of gold nanoparticles. Small. 2007;3:1941–1949.
45. Manivasagan P, Bharathiraja S, Bui NQ, et al. Doxorubicin-loaded fucoidan capped gold nanoparticles for drug delivery and photoacoustic imaging. Int. J. Biol. Macromol. 2016;91:578–588.
46. Venkatpurwar V, Shiras A, Pokharkar V. Porphyran capped gold nanoparticles as a novel carrier for delivery of anticancer drug: In vitro cytotoxicity study. Int. J. Pharm. 2011;409:314–320.

Hindawi
Oxidative Medicine and Cellular Longevity
Volume 2019, Article ID 6740325, 19 pages
https://doi.org/10.1155/2019/6740325

Research Article

Shape-Depended Biological Properties of Ag_3PO_4 Microparticles: Evaluation of Antimicrobial Properties and Cytotoxicity in *In Vitro* Model—Safety Assessment of Potential Clinical Usage

Karol P. Steckiewicz,[1,2] Julia Zwara,[3] Maciej Jaskiewicz,[4] Szymon Kowalski,[1] Wojciech Kamysz,[4] Adriana Zaleska-Medynska,[3] and Iwona Inkielewicz-Stepniak[1]

[1]*Department of Medical Chemistry, Medical University of Gdansk, Faculty of Medicine, Gdansk, Poland*
[2]*Department of Histology, Medical University of Gdansk, Faculty of Medicine, Gdansk, Poland*
[3]*Department of Environmental Technology, Faculty of Chemistry, University of Gdansk, Gdansk, Poland*
[4]*Department of Inorganic Chemistry, Faculty of Pharmacy, Medical University of Gdansk, Gdansk, Poland*

Correspondence should be addressed to Iwona Inkielewicz-Stepniak; iinkiel@gumed.edu.pl

Received 14 August 2019; Accepted 27 September 2019; Published 20 November 2019

Academic Editor: Pablo Muriel

Implant-related infections are an emerging clinical and economic problem. Therefore, we decided to assess potential clinical usefulness and safety of silver orthophosphate microparticles (SOMPs) regarding their shape. We synthesized and then assessed antimicrobial properties and potential cytotoxicity of six shapes of SOMPs (tetrapod, cubes, spheres, tetrahedrons, branched, and rhombic dodecahedron). We found that SOMPs had a high antimicrobial effect; they were more efficient against fungi than bacteria. SOMPs exerted an antimicrobial effect in concentrations not toxic to mammalian cells: human fetal osteoblast (hFOB1.19), osteosarcoma (Saos-2), mouse preosteoblasts (MC3T3-E1), skin fibroblast (HDF), and mouse myoblast (C2C12). At higher concentration SOMPs, induced shape- and concentration-dependent cytotoxicity (according to MTT and BrdU assays). Tetrapod SOMPs had the smallest effect, whereas cubical SOMPs, the highest on cell viability. hFOB1.19 were the most resistant cells and C2C12, the most susceptible ones. We have proven that the induction of oxidative stress and inflammation is involved in the cytotoxic mechanism of SOMPs. After treatment with microparticles, we observed changes in levels of reactive oxygen species, first-line defense antioxidants-superoxide dismutase (SOD1, SOD3), and glutathione peroxidase (GPX4), metalloproteinase (MMP1, MMP3), and NF-κB protein. Neither cell cycle distribution nor ultrastructure was altered as determined by flow cytometry and transmission electron microscopy, respectively. In conclusion, silver orthophosphate may be a safe and effective antimicrobial agent on the implant surface. Spherical-shaped SOMPs are the most promising for biomedical application.

1. Introduction

Nowadays, due to the development of medicine, life span and quality increased. Unfortunately, to achieve that goal, the patient sometimes needs to undergo surgery with implantation of a foreign body (e.g., valve or joint replacement and bone fracture treatment). These procedures are not complication-free and among many others, the infections may appear. Implant-related infections are a severe clinical and epidemiological problem, which can occur up to 3-5% of orthopedic patients and can affect even up to 40% of patients with cardiovascular implants (regardless of prophylaxis) [1, 2]. Among several etiological factors of those infections, *Staphylococcus aureus*, especially methicillin-resistant strains (MRSA) and fungi like *Candida albicans* and *Aspergillus niger* are the most common [2, 3]. As a matter of fact, in foreign bodies, there is no microcirculation, which is crucial for host defense and drug delivery [3]. Furthermore, medical devices (implants, bone nails, vascular grafts, artificial valves, etc.) can be easily colonized by pathogens and lead

to biofilm formation. Biofilm can be described as a complex structure consisting of high-concentration tightly attached bacterial cells and extracellular matrix; therefore, antibodies or drugs poorly penetrate it [4]. Furthermore, biofilm can produce substances which will deactivate antimicrobial agents, which makes treatment less likely to succeed [2, 4]. This should be noted that planktonic forms of bacteria can be 100-1000 times more susceptible to antimicrobial substances compared to those in biofilm form [5]. Implant-related infections are treated by either antibiotic therapy, surgery, or both. Unfortunately, this medical condition is fatal even in 30% of patients with prosthetic valve endocarditis [2, 5]. Moreover, only in the US treatment of all implant-related infection costs around 3.3 billion USD annually (1.86 billion USD, orthopedic implants-related infection alone) [2]. Thus, it is also a major economic issue. However, apart from emphasizing the importance of aseptic surgery techniques, any new solution to that matter has not been recently proposed [6].

Thus, novel approaches are being searched. Recently Zhang et al. reported that nanohydroxyapatite/polyurethane/silver composite may be successfully used to treat osteomyelitis in rabbits [7]. Also Jinag et al. suggested nanohydroxyapatite/polyurethane/silver phosphate composite as an antibacterial agent [8]. In another study, calcium phosphate/silver biomaterial has been proposed as antibacterial implant coating [9]. Similarly, calcium phosphate/silver phosphate particles may be used in dentistry as an antibacterial and remineralising factor [10].

Silver orthophosphate microparticles (SOMPs) may be an interesting solution to implant-related infections but their usefulness is yet to be examined. Antimicrobial properties of silver are well known, and the presence of phosphorus in the compound may increase biocompatibility [11–13]. Firstly discovered by Yi et al., SOMPs currently are studied as photocatalysts [14]. Their photocatalytic activity under visible light is used to remove pollution from the natural environment [15]. In this study, we aim to determine whether antimicrobial properties and cytotoxicity of silver phosphate microparticles are shape-dependent. It has been proven that chemical properties of SOMPs are shape-dependent. Their photocatalytic activity is reliant on surface morphology and properties [16]. Therefore, we hypothesize that the difference in surface properties of shapes of SOPMs will have an impact on their characteristics in *in vitro* systems. We synthesized six shapes of SOMPs (tetrapod, cubes, spheres, branches, tetrahedrons, and rhombic dodecahedrons) and examined them in *in vitro* model. Potential clinical usefulness and safety of application were taken into concern. According to our best knowledge, it is the first study in which either silver phosphate nanoparticles (SONPs) or SOMPs were studied in mammalian cell lines.

2. Materials and Methods

2.1. Materials and Instruments. The silver nitrate (98%, Sigma-Aldrich) was used as a precursor for the synthesis of Ag_3PO_4 powder. PVP (Mw = 300,000), sodium dihydrogen phosphate dihydrate ($NaH_2PO_4{\cdot}2H_2O$, 99%), sodium phosphate decahydrate ($Na_3PO_4{\cdot}10H_2O$, 99%), N,N-dimethylformamide (DMF), hexamethylenetetramine (HMT), and urea ($CO(NH_2)_2$) were purchased from Sigma-Aldrich. Phosphoric acid (H_3PO_4, 85%), ammonia ($NH_3{\cdot}H_2O$, 10%), and ethanol (CH_3CH_2OH, 96%) were purchased from POCH S.A., Poland. All chemicals were used without further purification. The morphology of Ag_3PO_4 semiconductors was measured by scanning electron microscope (SEM, JEOL JSM-7610F) working in high vacuum mode. DRS UV–Vis spectra of the synthesized samples were recorded in the scan range 300–700 nm using UV–Vis spectrophotometer (Evolution 220, Thermo Scientific) and $BaSO_4$ as the reference.

2.2. Synthesis of Different Shapes of SOMPs. The spherical SOMPs (s-SOMPs) were obtained by a chemical precipitation method [17]. In the first step, 7.9416 g of polyvinylpyrrolidone (PVP) was dissolved in 200 mL of deionized water. Then, 0.4246 g of $AgNO_3$ was dissolved in 100 mL of deionized water and added to the PVP solution. Aqueous Na_2HPO_4 solution (0.5678 g in 200 mL) was added dropwise and stirred until the solution turned yellow. The resulting yellow precipitate was separated by centrifugation, washed 3 times with deionized water and ethanol, and then dried in a vacuum oven at 60°C until the liquid completely evaporated. The cubic SOMPs (c-SOMPs) were obtained by the ion exchange method [15]. 0.5096 g $AgNO_3$ was dissolved in 90 mL of deionized water under stirring. A solution of aqueous ammonia was added to the solution thus prepared to obtain a brown solid completely dissolved in the solution. The next step was to add 0.1639 g of Na_3PO_4 dissolved in 30 mL of deionized water. After stirring for 5 minutes, the precipitate was collected, washed several times with deionized water, and dried in a desiccator. The tetrahedral SOMPs (th-SOMPs) were obtained by the soft chemical method [18]. First, 10 mL of N,N-dimethylformamide (DMF) with 10 mL of deionized water were mixed. 0.5096 g $AgNO_3$ was added to the above transparent solution and then 1 mL H_3PO_4 was added dropwise. The resulting mixture was sonicated for 2 h. Ag_3PO_4 microcrystals were collected, washed several times with distilled water and ethanol to remove DMF residues, and dried in a vacuum oven overnight at 80°C. Rhombic dodecahedral SOMPs (rd-SOPMs) were obtained by the hydrothermal method [19]. In the first step, 1.34 g of $AgNO_3$ was dissolved in 10 mL of deionized water. Then, 0.92 g (0.0006 mol) $NaH_2PO_4{\cdot}2H_2O$ was dissolved in 6 mL of deionized water and added dropwise to the $AgNO_3$ solution. The solution was allowed to stir for 5 minutes. After this time, an aqueous solution of ammonia was added until the pH was adjusted to 7. The resulting mixture was transferred into a Teflon-lined stainless steel autoclave and treated at 160°C for 6 h. After cooling to room temperature, the yellow precipitate was separated by centrifugation, washed three times with deionized water and methanol, and dried overnight at 60°C. Branched SOMPs (b-SOMPs) were obtained by a chemical precipitation method [20]. 0.318 g of $AgNO_3$ was dissolved in 40 mL of deionized water, and then 41 μL of 85 wt.% H_3PO_4 was added dropwise. In the next step,

0.197 g of hexamethylenetetramine was added to the solution and mixed for 5 minutes to change color to yellow. The resulting precipitate was collected, washed with deionized water3 times, and dried in a vacuum oven at 60°C. Tetrapod SOMPs (t-SOMPs) were obtained by the hydrothermal method [21]. In the first step, 3 mmol of 85 wt.% H_3PO_4 and 2.5 mmol $AgNO_3$ were dissolved in 80 mL of deionized water. 37.5 mmol of urea was added to the above solution and mixed for 5 minutes until complete dissolution. Immediately afterward, the resulting mixture was transferred into a Teflon-lined stainless steel autoclave and kept at 80°C for 24 h. The yellow powder was separated by centrifugation, washed 3 times with deionized water and ethanol, and then dried overnight at 60°C.

2.3. Reference Strains of Microorganisms. Reference strains of staphylococci, namely *Staphylococcus aureus* ATCC 25923 and MRSA ATCC 33591, before the tests were cultivated in Mueller–Hinton Broth (BioMaxima, Lublin, Poland) for 24 hours with shaking. For fungi, *Candida albicans* ATCC 10231 and *Aspergillus niger* ATCC 16404, the cultivation was held in the RPMI 1640 medium (Sigma-Aldrich, Steinheim, Germany) for 24 hours and 5 days, respectively.

2.4. Determination of Antimicrobial Activity. The minimal inhibitory concentrations (MICs) for bacteria and fungi were determined by the broth microdilution method according to the Clinical and Laboratory Standards Institute (CLSI) recommendation [22, 23]. For this purpose, the initial inoculums of bacteria (5×10^5 CFU/mL) in Mueller–Hinton Broth were exposed to the ranging concentrations of the test compounds (1–512 μg/mL) and incubated for 18 h at 37°C. For fungi, the initial inoculums of 2×10^3 CFU/mL in RPMI 1640 were exposed to the ranging concentrations of the test compounds (1–256 μg/mL) and incubated at 37°C for 24 h and 48 h, respectively. The experiments were conducted on 96-well microtiter plates, with the final volume of 100 μL. Cell densities were adjusted spectrophotometrically (Multiskan™ GO Microplate Spectrophotometer, Thermo Scientific) at the wavelengths of 600 nm for bacteria and 530 nm for fungi. The MIC was taken as the lowest drug concentration at which a noticeable growth of microorganisms was inhibited.

Minimum biofilm eradication concentrations (MBECs) were determined as previously described [11, 24, 25]. For this purpose, 96-well polystyrene flat-bottom plates and a resazurin (7-hydroxy-3H-phenoxazin-3-one 10-oxide) as a cell viability reagent were used. In this assay, a specific feature of resazurin is utilized, which upon the contact with living cells is metabolized and reduced from the basic blue form to pink resorufin. Briefly, the preprepared cultures of microorganisms were diluted to obtain the final density of 5×10^5 CFU/mL in Mueller–Hinton Broth for bacteria and 2×10^5 CFU/mL in RPMI-1640 for fungi per well (100 μL). After 24 h of incubation at 37°C, the wells of the plates were rinsed three times with phosphate buffer saline (PBS) to remove nonadherent cells. Subsequently, 100 μL of tested compounds in a concentration range (diluted in appropriate media) was added to each well. After 24 h of incubation at 37°C, 20 μL of the resazurin (4 mg/mL) was added. The MBEC was read after 1 h. MBECs were determined as the lowest concentration at which the reduction of resazurin was lower or equal (10% ± 0.5%) as compared to positive (100%) and negative (0%) controls. All experiments were performed in triplicate using Multiskan™ GO Microplate Spectrophotometer.

2.5. Cell Culture. hFOB 1.19 (human fetal osteoblast), MC3T3-E1 (mouse preosteoblast), SaoS-2 (human osteosarcoma), C2C12 (mouse myoblast), and HDF (human dermal fibroblasts) cells were used in the study. hFOB 1.19 (ATCC CRL-11372) were cultured in a 1 : 1 mixture of Ham's F12 Medium Dulbecco's Modified Eagle's Medium supplemented with 2.5 mM L-glutamine, 10% fetal bovine serum (FBS), and 1% of penicillin/streptomycin (P/S). MC3T3-E1 subclone 4 (ATCC CRL-2593) were cultured in the Alpha Minimum Essential Medium with ribonucleosides, deoxyribonucleosides, 2 mM L-glutamine, and 1 mM sodium pyruvate, 10% of FBS, and 1% of P/S, but without ascorbic acid. Saos-2 (ATCC HTB-85) were cultured in McCoy's 5a Medium Modified supplemented with 15% of FBS and 1% of P/S. C2C12 (ECACC no. 91031101) were cultured in high-glucose Dulbecco's Modified Eagle's Medium (DMEM) supplemented with 10% of FBS and 1% of P/S. HDF cells were cultured in high-glucose DMEM supplemented with 10% of FBS and 1% of P/S. All cells were cultured under sterile condition. Cells were kept at 37°C in a humidified atmosphere of 5% CO_2. Cells were maintained in 75 cm^2 tissue culture flask. The medium was replaced every 48 h. When confluent, cells were detached with a trypsin-EDTA solution and subcultured into a newer flask.

2.6. Treatments. hFOB1.19, MC3T3-E1, Saos-2, C2C12, and HDF cells were treated with different shapes of SOMPs for 24 h. Concentrations used in experiments were determined by preliminary studies. Each time, just before, experiment SOMPs were diluted in FBS-free media and shaken well to ensure equal dispersion of SOMPs in solution. Control samples were treated with SOMPs-free and FBS-free culture media. During the incubation process, the medium was not changed.

2.7. MTT Viability Assay. hFOB1.19, MC3T3-E1, Saos-2, C2C12, and HDF cells were used in the assay. Cells were seeded in 96-well plates. After 24 h of incubation, media were changed and cells were treated with microparticles in the concentration range of 0.01-10 μg/mL as described in Treatments. After 24 h, media were supplemented with water-soluble tetrazolium salt (final concentration 0.5 mg/mL) and incubated for 2 h. Next, media were removed and crystals were dissolved in DMSO. After 15 min, cell viability was assessed by measuring absorbance at 540 nm (reference 630 nm) using a microplate reader. Viability was determined as a percentage of control (viability of control cells was set as 100%). Absorbance values were corrected with blank microparticles.

2.8. BrdU Proliferation Assay. BrdU proliferation Elisa kit (Roche) was used to measure cell proliferation. hFOB1.19, MC3T3-E1, SaoS-2, C2C12, and HDF-1 cells were used in the assay. Cells were seeded in 96-well dish and treated with microparticles, in a concentration range 0.01-10 μg/mL as described in Treatments. Next, the antiproliferative activity of microparticles was measured by BrdU incorporation according to the manufacturer protocol. Data are shown as a percentage of control (proliferation rate of control cells was set as 100%). Absorbance values were corrected with blank microparticles.

For ROS detection, flow cytometry, and Western blotting, we decide to use two cell lines. hFOB1.19 and C2C12 cells had been chosen due to their different molecular characteristic and response to SOMPs in the preliminary study. Based on the antimicrobial assay and preliminary cytotoxicity studies for those assays, we decided to use three shapes (c-SOMPs, s-SOMPs, and b-SOPMs).

2.9. Detection of Reactive Oxygen Species. hFOB1.19 and C2C12 were seeded into 6-well plates; the next day, the medium was replaced and cells were treated with selected shapes as described in Treatments. Cells were treated with microparticles in 1, 3, and 5 μg/mL concentrations. After the incubation, media were discarded and replaced with a new solution supplemented with 10 μM 2,7-dichlorofluorescein diacetate (DCF-DA). After 30 min, fluorescence of oxidized DCF was measured by flow cytometry (excitation wavelength: 480 nm; an emission wavelength: 525 nm). Data were expressed as a percentage of untreated cells (which was set as 100%).

2.10. Cell Cycle Analysis. hFOB1.19 and C2C12 were seeded into 6-well plates and treated with SOMPs in 3 and 5 μg/mL concentrations for 24 h as described in Treatments. After incubation, cells were washed, harvested, and fixed (70% ethanol, 4°C). Next, cells were centrifuged and suspended in PBS with RNAse A (50 μg/mL) and propidium iodide (50 μg/mL). After 30 min, samples were analyzed by flow cytometry (BD FACSCalibur™, CellQuest Pro software). FSC/SSC and FL2-A/FL2-W plots were gated to avoid doublets and debris. The number of cells in each cell cycle phase was determined by software usage (sample size of at least 15,000 cells).

2.11. Western Blotting. Western blot analysis was performed to determine the impact of SOMPs on SOD1 (superoxide dismutase [Cu-Zn]), SOD2 (mitochondrial superoxide dismutase), SOD3 (extracellular superoxide dismutase [Cu-Zn]), GPX4 (glutathione peroxidase 4), NF-κB (nuclear factor kappa-light-chance-enhancer of activated B cells), MMP-1 (matrix metalloproteinase 1), MMP-3 (matrix metalloproteinase 3), and p16-ARC (human p16 actin-related complex) expressions. The method was previously established and described [26]. Briefly, hFOB1.19 and C2C12 cells were seeded into 100 mm Petri dishes. When the confluent medium was changed and cells were treated with c-SOMPs, s-SOMPs, or b-SOPMs in 3 and 5 μg/mL concentrations as described in Treatments. After 24 h, the medium was removed and cells were washed, detached, and lysed. Next, protein levels were measured by the Bradford method [27], samples prepared, and electrophoresis performed. After electrophoresis, proteins were transferred onto nitrocellulose membranes (Protran®, Schleicher and Schuell BioScience) and detected using antibodies. β-Actin was used as a loading control. The immunoactive proteins were detected using an enhanced chemiluminescence Western blotting detection kit (Amersham Biosciences, Piscataway, NJ, USA). Protein levels were quantified using densitometry software (Image-Lab, Bio-Rad).

2.12. Transmission Electron Microscopy. Transmission electron microscopy (TEM) was used to determine SOMP uptake and ultrastructure changes in the cells. C2C12 cells were used for TEM analysis. As previously described [26], cells were plated into 100 mm Petri dishes. After 24 h, cells were treated with c-SOMPs, s-SOMPs, or b-SOPMs in a concentration of 3 μg/mL as described in Treatments. Next, cells were fixed (2.5% glutaraldehyde in 0.1 mM sodium-cacodylate buffer), detached, and centered. The cell pellets were postfixed (2% osmium tetroxide) and dehydrated (graded series of ethanol). After infiltration (propylene dioxide: epon mixture, pure epon), pelleted cells were embedded to polymerize. Finally, the ultrathin sections (Reichert OmU3 Ultramicrotome, Austria) were contrasted (uranyl acetate, lead citrate) prior to examination in transmission electron microscope at 100 kV (JEM 1200EX II, Jeol, Japan).

2.13. Statistical Analysis. Data are shown as the mean ± standard error of 4 independent experiments. Statistical analysis was determined by one-way analysis of variance (ANOVA) and Tukey's post hoc test. The IC_{50} was calculated by analyzing a nonlinear regression log(inhibitor) vs. normalized response. Statistical analysis was made with GraphPad5 software.

3. Results

3.1. Morphology of Silver Phosphate Microparticles. The SEM images of the samples obtained are shown in Figure 1. s-SOMPs (Figure 1(a)) are characterized by an irregular shape with a particle diameter of approximately 500 nm. s-SOMPs also show a tendency to rapid nucleation and particle growth, which leads to their agglomeration. In this case, the geometrical shape and size of the particles are responsible for PVP, which is added at the stage of synthesis [17]. c-SOMPs are shown in Figure 1(b). The structure is characterized by a smooth surface ending with sharp edges with an average length of 1-1.5 μm. In this case, the addition of ammonia during the synthesis led to the formation of c-SOMPs [28]. The characteristic morphology of th-SOMPs are demonstrated in Figure 1(c). The SEM image shows the high efficiency of forming structures with sharp corners, edges, and smooth surfaces. Furthermore, a polyhedron with four triangular walls has side lengths from 4 to 0.5 μm. Dong et al. also synthesized Ag_3PO_4 particles; however, their length was from 0.5 to 1 μm, and the lateral edges and vertices were rounded [29]. Wan et al. received crystals with an average size of 740 nm

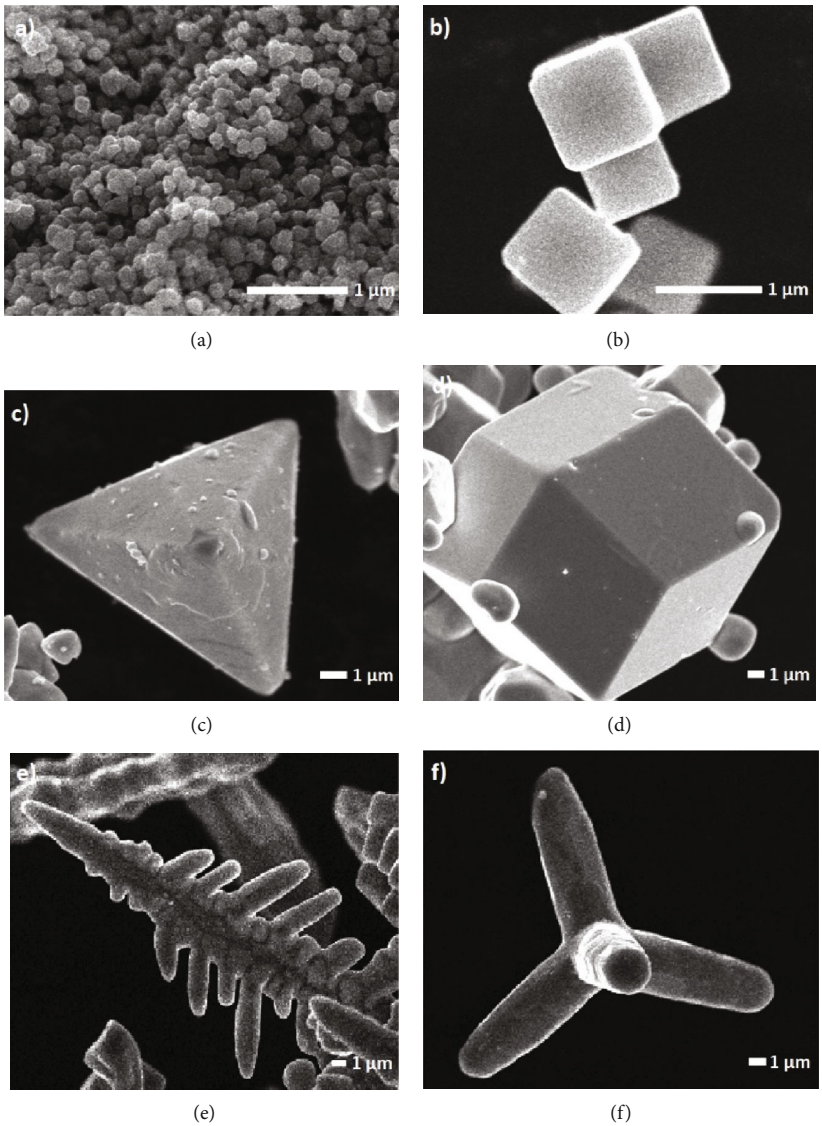

(a) (b) (c) (d) (e) (f)

FIGURE 1: SEM images of Ag_3PO_4 at different shapes: (a) s-SOMPs, (b) c-SOMPs, (c) th-SOMPs, (d) rd-SOMPs, (e) b-SOMPs, and (f) t-SOMPs particles.

[30]. Figure 1(d) shows the rd-SOMPs consisting of 12 walls, which are congruent rhombuses. The obtained structure has also a smooth surface with a diameter of 5-17 μm. Dong et al. also synthesized rhombic dodecahedral crystals with a diameter of 200-600 nm, while Bi et al. with a size between 4 and 7 μm [31, 32]. Typical b-SOMPs obtained under static conditions are presented in Figure 1(e). The resulting multiarmed dendrites with developed subbranches are characterized by a shoulder length of approximately 25 μm. Wang et al. explained that it is impossible to obtain Ag_3PO_4 without addition of HMT during the synthesis because silver orthophosphate is soluble at low pH values [33]. Dong et al. obtained branched structures using a reaction solvent during the synthesis consisting of H_2O and DMF. The length of the branches obtained was between 5 and 10 μm [18]. The SEM image in Figure 1(f) shows the morphology of the t-SOMPs. t-SOMPs obtained in the presence of urea have four arms in the form of cylindrical microrods with an average diameter of 2.5 μm and a length of 11-30 μm. Dong et al. received silver orthophosphate in the form of a dendritic long tetrapod with a shoulder length of about 20-30 μm. t-SOMPs with longer dendritic arms arose when glacial acetic acid was added to the system, acting as shape-controlling agents [29]. Based on the obtained morphology, it can be concluded that obtaining different shapes of Ag_3PO_4 depends on the adjustment of external experimental conditions (mixing, ultrasonic treatment), as well as through pH control or the addition of appropriate structure-controlling agents (PVP, ammonia, and HMT). The crystal structure of different Ag_3PO_4 shapes was

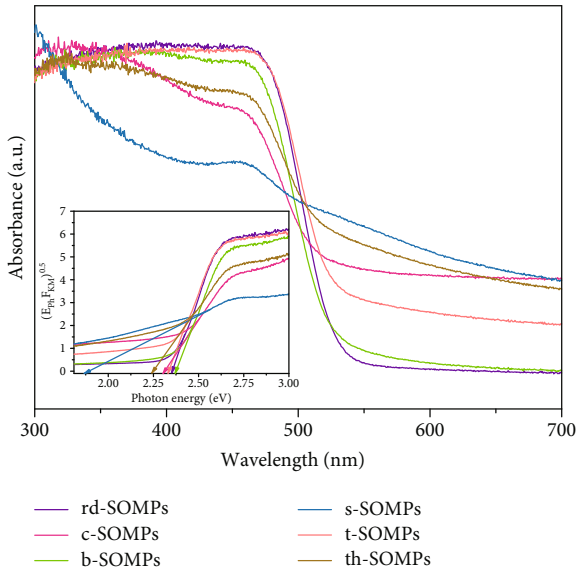

Figure 2: UV–Vis/DRS spectrum of Ag_3PO_4 photocatalysts in different shapes. Determination of the bandgap is shown in inset.

characterized by pXRD in a previous work prepared by Zwara et al. [16]. The obtained results indicated the success of the experiment and obtaining Ag_3PO_4 crystallites. Moreover, it confirms the high purity of the samples. Additionally, pXRD reflections are sharp which suggest high crystallinity of the material.

3.2. Absorption Properties. Figure 2 shows the UV–Vis/DRS absorption spectra and the Kubelka–Munk function transformation plot vs. photon energy for all as-prepared SOMPs. Analysis by UV–Vis/DRS spectroscopy has shown that SOMPs absorb irradiation in the range of around 510-590 nm. s-SOMPs and th-SOMPs absorb visible light at a wavelength less than 590 nm, while in the form of c-SOMPs at 575 nm. The spectra presented by Dong et al. show that Ag_3PO_4 with the structure of irregular spheres and tetrahedrons absorbs visible light with the same wavelength at 525 nm. In contrast, absorption for ankles was estimated by Bi et al. and had an edge at 520 nm [31]. t-SOMPs, rd-SOMPs, and b-SOMPs have an absorption edge at 550, 540, and 535 nm, respectively. Dong et al. also estimated the absorption edge for tetrapod and branched form at 525 nm, while absorption at wavelengths shorter than 550 nm was determined by Bi et al [31, 34]. Bandgaps of the obtained Ag_3PO_4 shapes are shown in Figure 2 (inset). The lowest value of the energy gap was observed for the spheres and the highest for the branched structure and was calculated to be 1.86 eV and 2.37 eV, respectively. Tetrahedrons, cubes, tetrapods, and rhombic dodecahedrals were characterized by energy bands of 2.24 eV, 2.31 eV, 2.33 eV, and 2.35 eV. The difference in the obtained values indicates the multifaceted morphology on nanoparticles. In addition, the different shapes of absorption bands, in particular Ag_3PO_4 spheres, may result from the content and distribution on the surface of reduced Ag metallic particles.

Table 1: Minimal inhibitory concentrations of SOMPs against reference strains of microorganism.

	MIC (μg/mL)			
	Staphylococcus aureus	*Staphylococcus aureus* (MRSA)	*Candida albicans*	*Aspergillus niger*
t-SOMPs	64	16	8	8
c-SOMPs	8	8	4	1
s-SOMPs	8	8	4	8
th-SOMPs	16	16	8	8
b-SOMPs	32	32	8	4
rd-SOMPs	64	64	16	8

Table 2: Minimal biofilm eradication concentrations of SOMPs against reference strains of microorganism.

	MBEC (μg/mL)			
	Staphylococcus aureus	*Staphylococcus aureus* (MRSA)	*Candida albicans*	*Aspergillus niger*
t-SOMPs	128	32	8	8
c-SOMPs	32	16	8	2
s-SOMPs	64	16	16	8
th-SOMPs	128	16	16	16
b-SOMPs	256	32	64	16
rd-SOMPs	512	64	63	32

3.3. Antimicrobial Activity. All of the examined SOMPs shapes exhibited antimicrobial activity against tested staphylococci and fungi (Tables 1 and 2). Among them, the most active were c-SOMPs with the lowest minimal inhibitory concentrations of 8 μg/mL against reference *S. aureus* ATCC 25923 and MRSA ATCC 33591 and 4 μg/mL and 1 μg/mL against *C. albicans* and *A. niger*, respectively. Interestingly, the antibiofilm activity of c-SOMPs was 1- to 2-fold dilution lower than in the case of MICs. Moreover, the same relation was found for other SOMPs with an exception of *S. aureus* ATCC 25923 strain for which MBECs of th-SOMPs, b-SOMPs, and r-SOMPs were 8 times higher than MICs. In Supplementary Table 1, we provide MIC values for clinically used antimicrobial agents as reference.

3.4. Cytotoxicity of SOMPs. Figure 3 illustrates changes in the viability of the cells measured by MTT assay after treatment with different shapes of SOMPs. In Table 3, we presented IC_{50} values for SOMPs. All tested shapes decreased the viability of the cells in a concentration-dependent manner. It is clear that shape is an important modulator of SOMPs cytotoxicity. c-SOMPs were the most cytotoxic shape. In the highest tested concentration (10 μg/mL), they decreased the viability of hFOB1.19 cells to around 40%, MC3T3-E1 cells to around 30%, Saos-2 and C2C12 cells to around 20%, and HDF cells to around 10%. t-SOMPs had the smallest effect on cells viability. In the highest tested concentration (10 μg/mL), they decreased the viability of hFOB1.19 cells

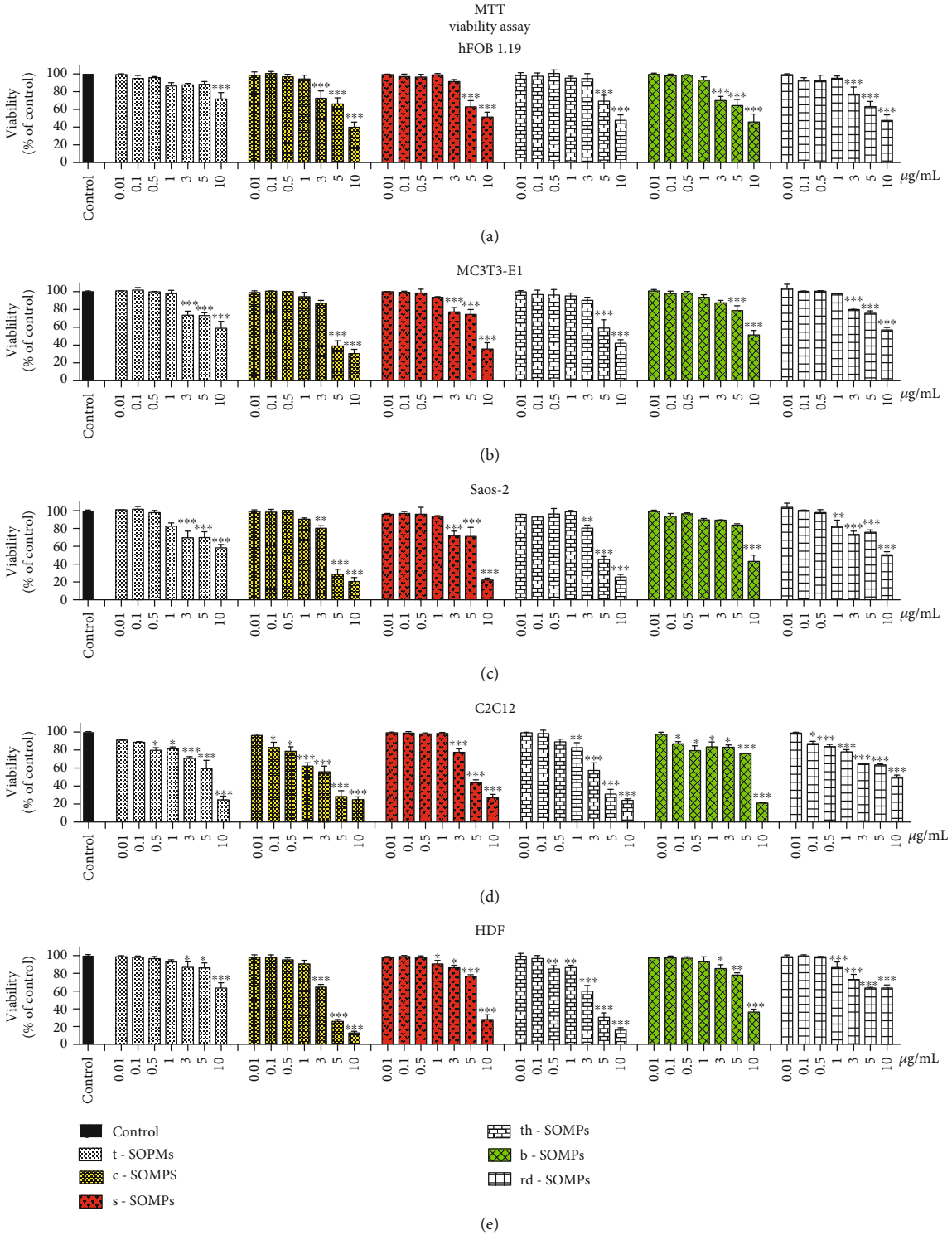

Figure 3: Impact of SOMPs on cell viability. Viability, measured by MTT assay of (a) hFOB1.19 cells, (b) MC3T3-E1, (c) Saos-2, (d) C2C12, and (e) HDF cells exposed to different shapes of SOMPs after 24 h. Color bars indicate shapes of SOMPs selected for further analysis. Data are presented as mean ± SD. $^{*}p < 0.05$, $^{**}p < 0.01$, $^{***}p < 0.001$.

to around 75%, MC3T3-E1, and HDF cells to around 60%, Saos-2 cells to around 55%, and C2C12 cells to around 25%. It can be deducted that hFOB1.19 cells were the most resistant and C2C12 cells were the most susceptible to tested SOMPs. Importantly, SOMPs can be selectively cytotoxic only to bacteria and fungi and not harmful to mammalian

Table 3: IC_{50} values for different shapes of SOMPs (MTT assay). The values are approximated to decimal parts.

	IC_{50} (μg/mL) (MTT assay)				
	hFOB1.19	MC3T3-E1	Saos-2	C2C12	HDF
t-SOMPs	>10	>10	>10	7.34	>10
c-SOMPs	5.97	4.94	4.79	3.73	4.93
s-SOMPs	>10	7.60	8.01	4.84	8.17
th-SOMPs	>10	6.62	5.19	4.50	5.00
b-SOMPs	>10	>10	8.34	9.08	8.36
rd-SOMPs	>10	>10	>10	>10	>10

cell lines. For example, c-SOMPs in MIC and MBEC concentration for *Aspergillus niger* are not cytotoxic to all cell lines apart from C2C12 cells. Moreover, there is no doubt that bacteria and fungi are more susceptible to SOMPs than mammalian cells.

3.5. Impact of SOMPs on Cell Proliferation. Figure 4 illustrates changes in the proliferation of the cells measured by BrdU assay after treatment with different shapes of SOMPs. In Table 4, we presented IC_{50} values for the test. All SOMPs influenced cell proliferation in a concentration-dependent manner. Similar to MTT assay, t-SOMPs had the smallest effect, whereas c-SOMPs, the highest on BrdU assay results. Also, hFOB1.19 were the most resistant cells and C2C12 the most susceptible ones. Generally, SOMPs statistically significantly decreased cell proliferation (BrdU assay) in lower concentration than needed to reduce cell viability (MTT assay).

Based on antimicrobial and cytotoxicity screening, we decided to further examine three shapes of SOMPs (c-SOMPs, s-SOMPs, and b-SOPMs). They are highlighted by color bars on plots throughout Figures 3 and 4.

3.6. Impact of SOMPs on ROS and Oxidative Stress-Related Proteins Levels. Increased ROS production was seen in C2C12 and absent in hFOB1.19 cells (Figures 5(a) and 6(a)). Only c-SOMPs and s-SOMPs, both in 5 μg/mL concentration, statistically significant increased level of ROS in C2C12 cells. We also examined levels of oxidative stress-related proteins. SOD1 levels in hFOB1.19 cells were not significantly changed (Figure 6(c)). SOD1 levels were only increased when C2C12 cells were treated with c-SOMPs (3 μg/mL). Interestingly, the same shape of silver orthophosphate in higher concentration (5 μg/mL) decreased levels of SOD1 (Figure 5(c)). Our SOMPs did not impact SOD2 levels (Figures 5(d) and 6(d)). All tested shapes (c-SOMPs, s-SOMPs, b-SOPMs) in all concentrations increased the levels of SOD3 in hFOB1.19 cells (Figure 6(e)). c-SOMPs (in 3 μg/mL concentration) and b-SOMPs (in 5 μg/mL concentration) increased levels of SOD3 in C2C12 cells (Figure 5(e)). In hFOB1.19 cells, GPX4 levels were increased after incubation with s-SOMPs (3 and 5 μg/mL), whereas in C2C12 cells after treatment with 3 and 5 μg/mL c-SOMPs (Figures 5(f) and 6(f)).

3.7. Impact of SOMPs on MMP1, MMP3, p16-ARC, and NF-κB Levels. Figure 7 presents the impact of SOMPs on MMP1, MMP3, p16-ARC, and NF-κB levels. Our microparticles increased levels of MMP1 and MMP3 proteins. MMP1 levels were elevated when hFOB1.19 cells were treated with 5 μg/mL of b-SOMPs and when C2C12 cells were incubated with 3 μg/mL of c-SOMPs or 5 μg/mL of b-SOMPs (Figures 7(b) and 7(g)). c-SOMPs (3 and 5 μg/mL) and s-SOMPs (3 and 5 μg/mL) increased levels of MMP3 in both cell lines (Figures 7(c) and 7(h)). Moreover, b-SOMPs (3 μg/mL) increased levels MMP3 on C2C12 cells. NF-κB levels were elevated in C2C12 cells were treated with 5 μg/mL of c-SOMPs or s-SOMPs (Figures 7(d) and 7(i)). p16ARC levels were decreased in C2C12 cells after incubation with c-SOMPs, s-SOMPs, or b-SOMPs in 5 μg/mL concentration (Figures 7(e) and 7(j)).

3.8. Analysis of Cell Cycle. c-SOMPs statistically significantly decreased percentage of hFOB 1.19 cells in G0/G1 phase, in 3 and 5 μg/mL concentrations (Figure 8). Moreover, c-SOMPs in a concentration of 5 μg/mL statistically significantly decreased percentage of C2C12 cells in G0/G1 phase (Figure 9). Other changes in cell cycle distribution were not observed (Figures 8 and 9). s-SOMPs and b-SOMPs have no impact on the cell cycle distribution of hFOB1.19 and C2C12 cells.

3.9. TEM Analysis. TEM analysis (Figure 10) has shown that c-SOMPs, s-SOMPs, and b-SOPMs in 3 μg/mL concentration are not internalized by the C2C12 cells. Furthermore, we did not observe any ultrastructure changes within the cells.

4. Discussion

In the study, we synthesized and assessed SOMPs as a potential biomaterial. Antimicrobial properties and safety of potential application were taken into concern. We have shown that cytotoxicity and antimicrobial properties were shape- and concentration-dependent. Furthermore, SOMPs can be harmful to bacteria and fungi in concentrations safe for mammalian cell lines. It is the first study in which SOMPs or SONPs were examined in mammalian cells an *in vitro* model. Also, data about the cytotoxicity of other MPs are very limited.

4.1. Antimicrobial Properties. Antibacterial agents can be separated into two groups: semiconductors and metal-based ones. SOMPs belong to both, which greatly expand their antibacterial potential [35]. Thus, we hypothesized that SOMPs synthesized by our group will exhibit antimicrobial activity,

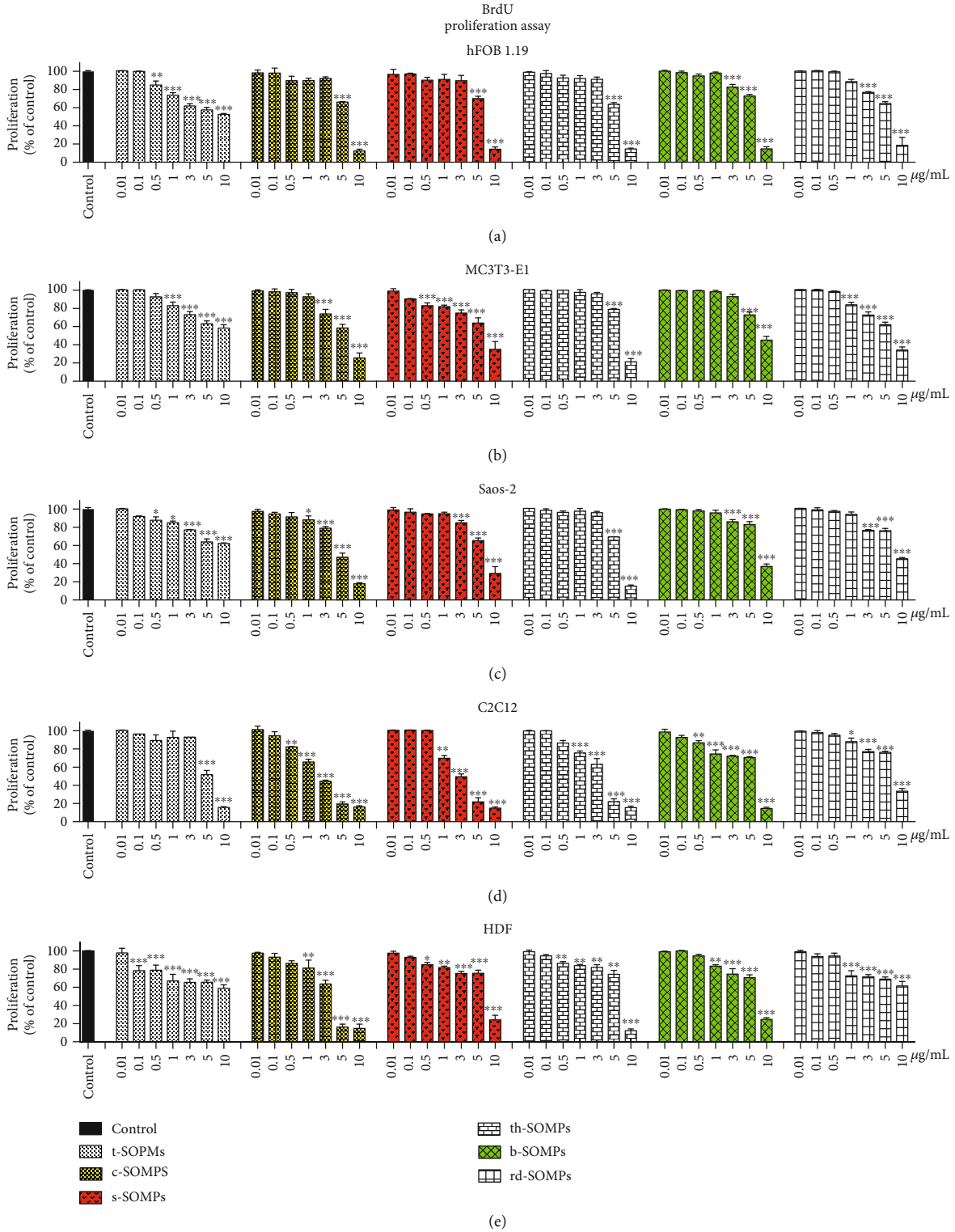

Figure 4: Impact of SOMPs on cell proliferation. Proliferation, measured by BrdU assay of (a) hFOB1.19 cells, (b) MC3T3-E1, (c) Saos-2, (d) C2C12, and (e) HDF cells exposed to different shapes of SOMPs after 24 h. Color bars indicate shapes of SOMPs selected for further analysis. Data are presented as mean ± SD. $^{*}p < 0.05$, $^{**}p < 0.01$, $^{***}p < 0.001$.

Table 4: IC_{50} values for different shapes of SOMPs (BrdU assay). The values are approximated to decimal parts.

	IC_{50} (μg/mL) (BrdU assay)				
	hFOB1.19	MC3T3-E1	Saos-2	C2C12	HDF
t-SOMPs	>10	>10	>10	7.12	>10
c-SOMPs	7.88	6.60	6.67	2.50	4.82
s-SOMPs	8.14	6.24	7.27	3.19	8.48
th-SOMPs	7.64	8.13	7.69	4.59	8.44
b-SOMPs	8.29	7.17	8.55	8.39	7.54
rd-SOMPs	>10	5.88	7.06	7.58	>10

which was confirmed experimentally. Moreover, shape-dependent antimicrobial properties of SOMPs were revealed. Among tested ones, c-SOMPs and s-SOPMPs were characterized by the highest activity. This should be emphasized that the tested SOMPs acted against both planktonic and biofilm forms of pathogens. Biofilm is a complex structure built from cells and extracellular matrix. It is known that pathogens in a biofilm are more resistant to treatment than planktonic forms [5]. Biofilm is poorly penetrated by antibiotics and immunological cells which makes its treatment a daunting challenge [2, 4, 5]. Furthermore, biofilm can easily be formed on foreign bodies that intruded into the human body, so it is clear that it is a major clinical problem [4]. Therefore, we decided to measure MBEC in addition to MIC. We focused on four pathogens: *S. aureus*, *MRSA*, *C. albicans*, and *A. niger*. Selected pathogens are well known as an etiological factor of bone- and/or implant-related infections [2, 3, 36, 37]. As a matter of fact, only a few studies have examined the antibacterial properties of SOMP, while antifungal and antibiofilm effects have not been previously reported.

Panthi et al. have shown that 200 nm SOMPs can be effective against *S. aureus*, *Escherichia coli*, *Klebsiella pneumoniae*, and *Pseudomonas aeruginosa* [38]. Also, Chudobova et al. have shown that 200-300 nm silver orthophosphate particles can be effective against *S. aureus* with the half-maximal inhibitory concentration equals 268.2 μM [39]. While Liu et al. have reported the effectiveness of SOMPs against *E. coli* (DH-5α) [40]. However, the tested SOMPs decreased the viability of *E. coli* only at a concentration range of 10-100 μg/mL, which means they are less effective than SOMPs described in this study. On the other hand, Yeo et al. have shown that c-SOMPs are more effective than rd-SOMPs against *E. coli* which is consistent with our data [41]. That phenomenon was explained by the fact that c-SOMPs are able to release more Ag^+ ions than rd-SOMPs [41]. Furthermore, they found that SOMPs exhibit better antibacterial activity compared to similar structures made from Ag_2O or CuO [41]. In fact, several mechanisms of the antimicrobial properties of SOMPs are described (Table 5). It should be highlighted that Ag_3PO_4 itself in a concentration of 5 μg/mL can inhibit the growth of *S. aureus* as well [42].

4.2. Cytotoxicity Screening. In the study, we decided to use three cell lines as a bone model. Apart from human fetal osteoblasts (hFOB1.19) and mouse preosteoblast (MC3T3-E1), osteosarcoma cells were also used (Saos-2). Although derived from cancer often, Saos-2 cells are used as a bone cell model [43, 44]. Skin and muscle cells (HDF and C2C12 cells) were also used in cytotoxicity screening, as models of tissues which can potentially come in contact with SOMP-coated implant. We decide to use as many as 5 different cell lines and two different assays (MTT and BrdU), as it is proven to increase the quality and reliability of cytotoxicity screening [45, 46]. MTT assays estimate cell viability by measuring mitochondrial metabolism, whereas BrdU assays assess cell proliferation and DNA synthesis by determining 5-bromo-2′-deoxyuridine incorporation [45, 47]. Both MTT and BrdU have shown similar results. Generally, in the same conditions, cytotoxicity assessed by BrdU was higher than that assessed by MTT assay, which is consistent with literature data comparing those assays [48].

We clearly have shown that the cytotoxicity of our SOMPs was shape-dependent. c-SOMPs were the most cytotoxic ones, whereas t-SOMPs had the smallest effect on cell viability. Also, the response of different cell lines varies. SOMPs had the highest effect on the viability of C2C12 cells and the smallest on hFOB1.19 (based on IC_{50} comparison). Motskin et al. have examined the impact of 2-3 μm hydroxyapatite MPs on human monocytes-macrophages (HMM), as they used MTT assay. They have shown concentration- and size-dependent cytotoxicity of MPs. The bigger the MPs were, the less cytotoxic they were [49]. He et al. have made a similar conclusion; however, they used spherical mesoporous silica MPs [50]. In our study, the biggest t-SOMPs were also the least cytotoxic. However, their nanoparticles have shown a significant decrease in cell viability in >250 μg/mL concentration [49].

4.3. Oxidative Stress Induction. SOMPs are known to release free electrons, therefore, inducing ROS productions and oxidative stress [40]. ROS are the byproduct of metabolism and also can be used by cells as signalling molecules. However, the increased level of ROS can be lethal [51]. Excess of ROS can disturb cellular homeostasis and that condition is commonly called oxidative stress [51]. Several protein levels can be changed when oxidative stress occurs. NF-κB (nuclear factor kappa-light-chance-enhancer of activated B cells) is a transcriptional factor involved in physiological regulations as well as in response to injury. Moreover, NF-κB can be activated by ROS [52]. SOD1, SOD2, SOD3, and GPX4 are part of an antioxidative

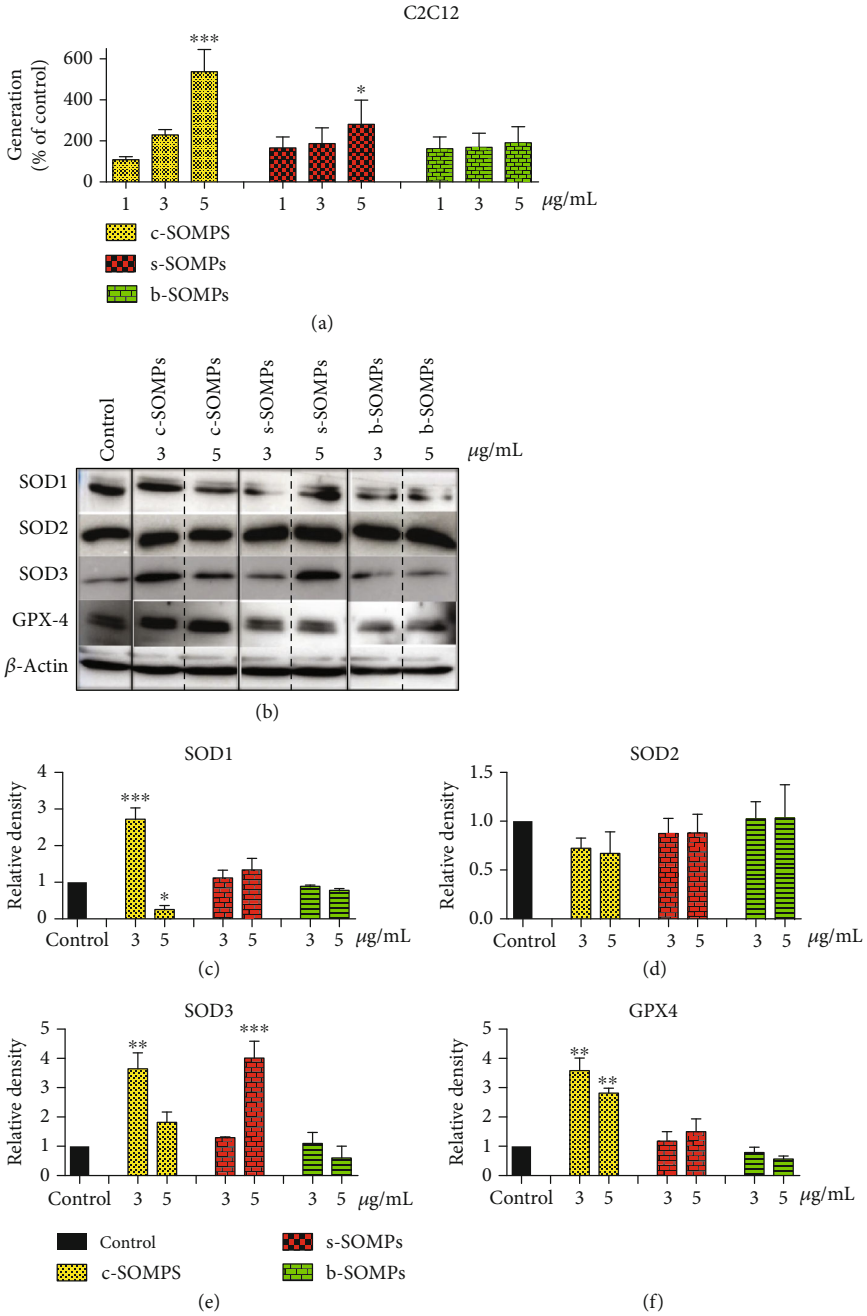

Figure 5: Impact of SOMPs on oxidative stress in C2C12 cells. (a) ROS levels, (b) representative Western blots, (c) quantification of SOD1 levels, (d) quantification of SOD2 levels, (e) quantification of SOD3 levels, and (f) quantification of GPX4 levels in C2C12 cells after incubation with c-SOMPs, s-SOMPs, or b-SOPMs for 24 h. Data are presented as mean ± SD. $^{*}p < 0.05$, $^{**}p < 0.01$, $^{***}p < 0.001$.

system of the cells [52]. Hence, we decided to examine the impact of selected SOMPs on ROS, levels, and expression on selected oxidative-stress response proteins: SOD1, SOD2, SOD3, GPX4, and NF-κB. Our SOMPs increased ROS production. Also, we observed changes in SOD1, SOD3, GPX4, and NF-κB. SOD2 levels were not affected. Mainly levels of mentioned proteins were elevated, with one exception. Interestingly, SOD1 levels in C2C12 could be either increased or decreased with regard to c-SOMPs concentration (more detailed description in sections 3.6 and 3.7 of the manuscript). We suggest that when oxidative stress is mild and not prolonged antioxidative protein levels will be increased (upregulation in order to fight danger). However, prolonged or intensive oxidative stress can impair the functioning of the cells, causing a decrease in protein levels. Our hypothesis is consistent with literature data [53]. Therefore, we suggest that SOMPs in some condition can trigger oxidative stress. A similar

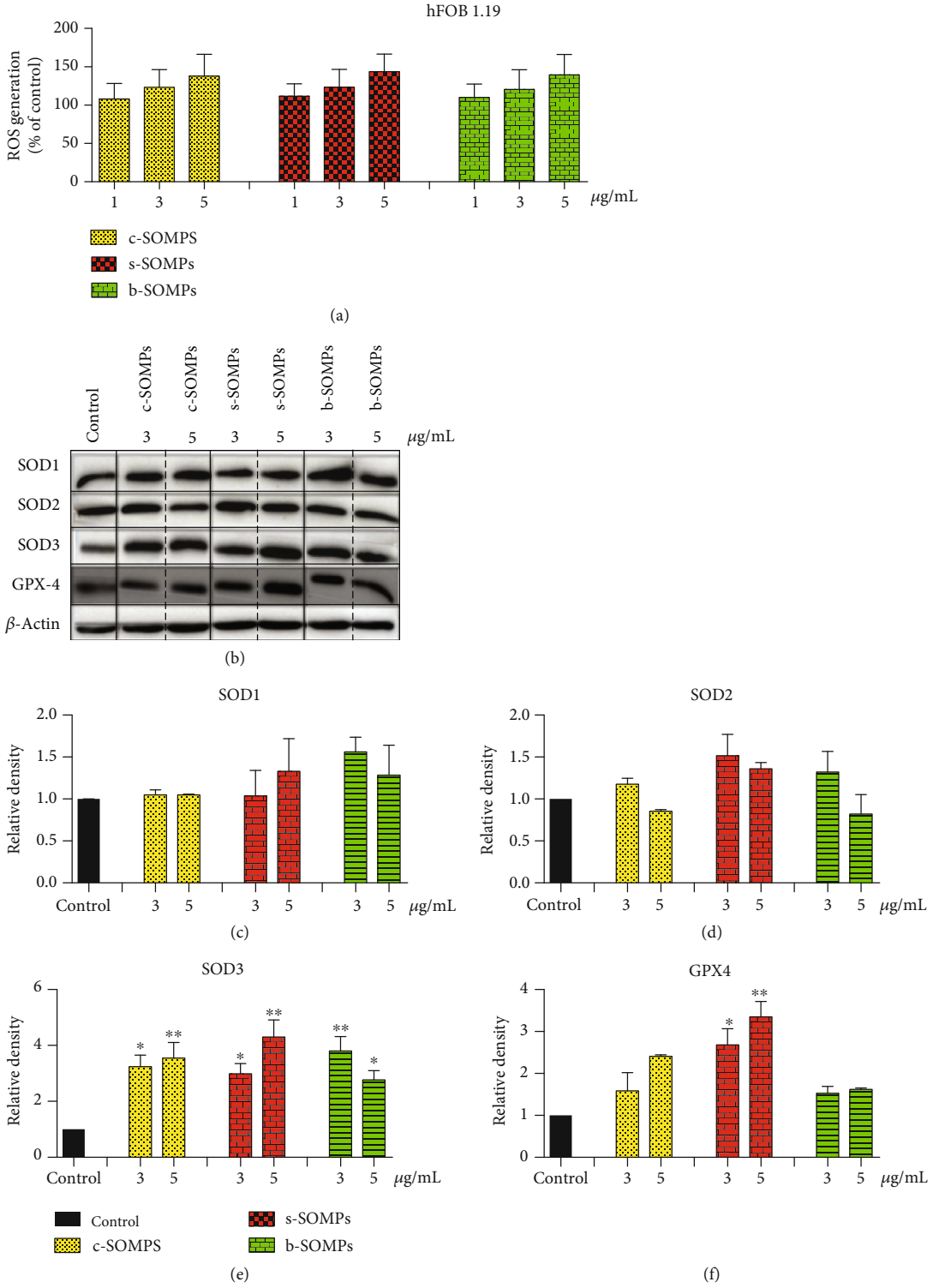

Figure 6: Impact of SOMPs on oxidative stress in hFOB1.19 cells. (a) ROS levels, (b) representative Western blots, (c) quantification of SOD1 levels, (d) quantification of SOD2 levels, (e) quantification of SOD3 levels, and (f) quantification of GPX4 levels in hFOB1.19 cells after incubation with c-SOMPs, s-SOMPs, or b-SOPMs for 24 h. Data are presented as mean ± SD. $^{*}p < 0.05$, $^{**}p < 0.01$, $^{***}p < 0.001$.

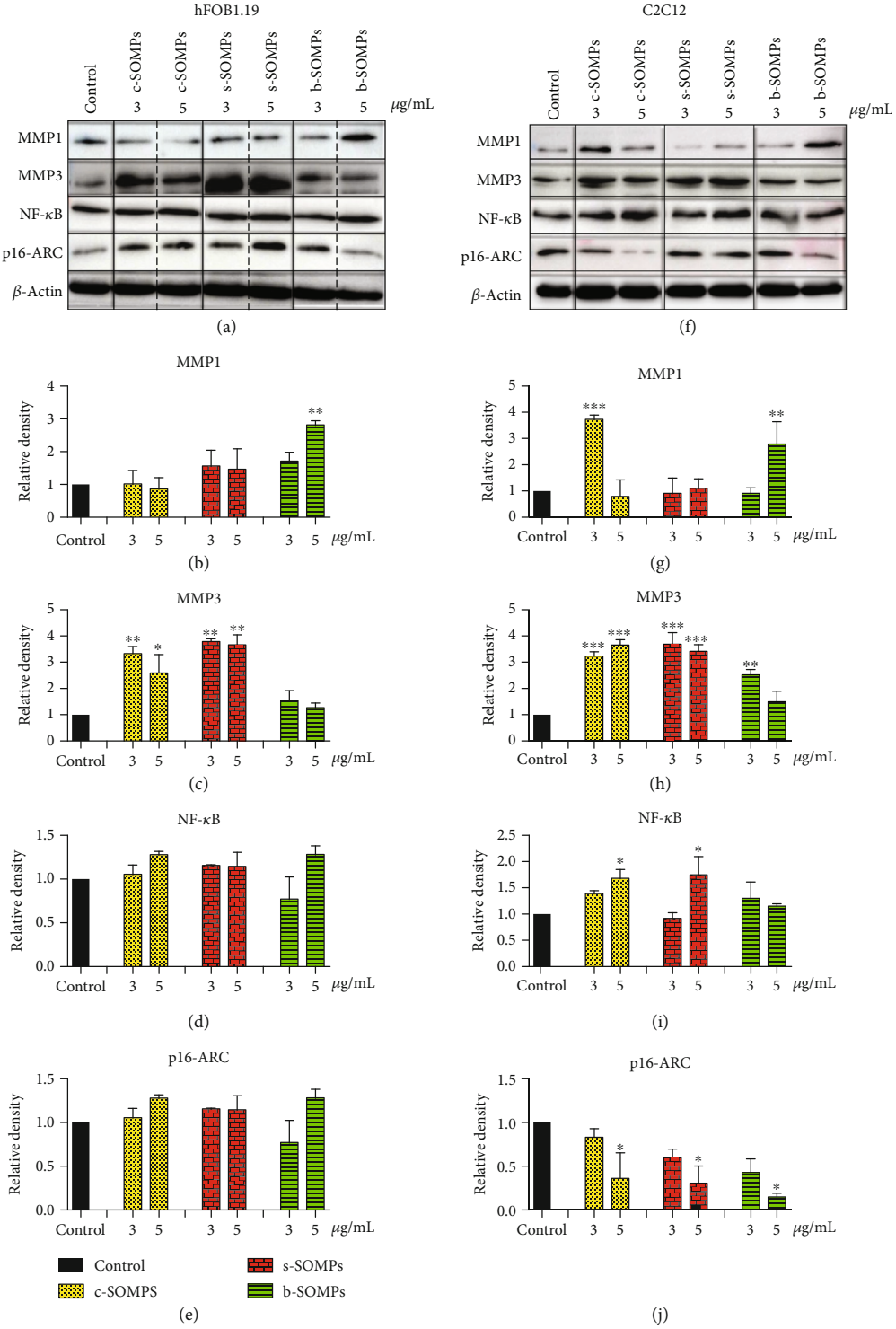

Figure 7: Impact of SOMPs on selected proteins levels. Representative Western blot analysis of (a) hFOB1.19 and (b) C2C12 cells after 24 h incubation with c-SOMPs, s-SOMPs, or b-SOPMs. Quantitative analysis of (b), (g) MMP1; (c), (h) MMP3; (d), (i) NF-κB, and (e); and (j) p16-ARC levels on hFOB1.19 and C2C12 cell lines, respectively. Data are presented as mean ± SD. $^{*}p < 0.05$, $^{**}p < 0.01$, $^{***}p < 0.001$.

observation had been made for other MPs. Santos et al. have shown that different sizes of porous silica microparticles in >1 mg/mL concentration can trigger ROS production in human colon carcinoma (Caco-2) cells [54]. Also, AgNPs could increase ROS production in a shape-dependent manner [55]. The highest amount of ROS

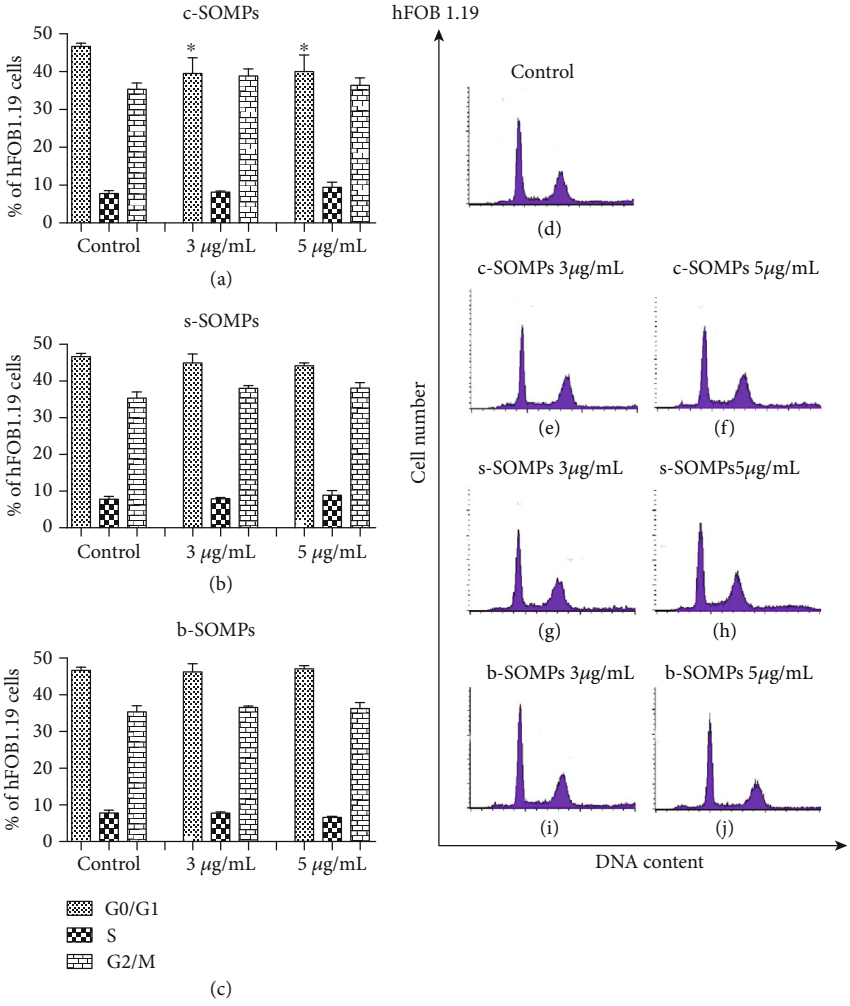

FIGURE 8: The cell cycle distribution for hFOB 1.19 cells. Percentage of cells in each cell cycle phase after treatment with (a) c-SOMPs, (b) s-SOMPs, and (c) b-SOMPs. Representative histograms (d) control, (e), (f) c-SOMPs; (g), (h) s-SOMPs; and (i), (j) b-SOMPs. Data are presented as mean ± SD. $^{*}p < 0.05$.

were produced by human fibroblast cells after treatment with 12.8 nm triangular AgNPs [55].

4.4. Impact at Proinflammatory Proteins. An implant as any foreign body may cause inflammation [56]. In order to examine if our SOMPs can trigger inflammation, we examined three proteins: NF-κB, MMP-1, and MMP-3. NF-κB was mentioned above as its levels can be changed in response to the excess of ROS [52]. However, this transcription factor has several roles and it is crucial for the inflammatory response [57]. MMP-1 and MMP-3 are collagen destruction enzymes which are elevated when inflammation occurs [58]. We have shown that some SOMPs increased levels of NF-κB, MMP-1, and MMP-3. It may suggest that they act as proinflammatory agents. Similar to our findings, literature data suggest that Ag_3PO_4 in 50 μg/mL concentration in human non-small-cell lung carcinoma cells (H1299) can increase levels of IL-8, which is a proinflammatory cytokine [42].

4.5. Impact on Cell Cycle. Cell division is crucial for proper wound healing, so possible antimicrobial agents to be used on implant should interfere with the cell cycle. In our study, only c-SOMPs decreased the percentage of cells in G0/G1 phase. Other MPs also can cause changes in the cell cycle. Chinde et al. have shown that tungsten oxide MPs can increase percentages of cells in G2/M phases in human lung carcinoma cells (A549) [59].

4.6. Internalization, Ultrastructure Changes, and Impact on the Cytoskeleton. We performed TEM analysis in order to assess whether SOMPs are internalized or caused any changes in cell ultrastructure. We saw deletion in p16-ARC levels; however, any visible changes in cells morphology were observed. p16-ARC is protein involved in actin polymerization, thus cytoskeleton formation. SOMPs were also not internalized by C2C12 cells. Motskin et al. have shown that HMM cells can internalize 2-3 μm hydroxyapatite MPs. However, their study was performed on macrophages, which biological functions are based on ability to

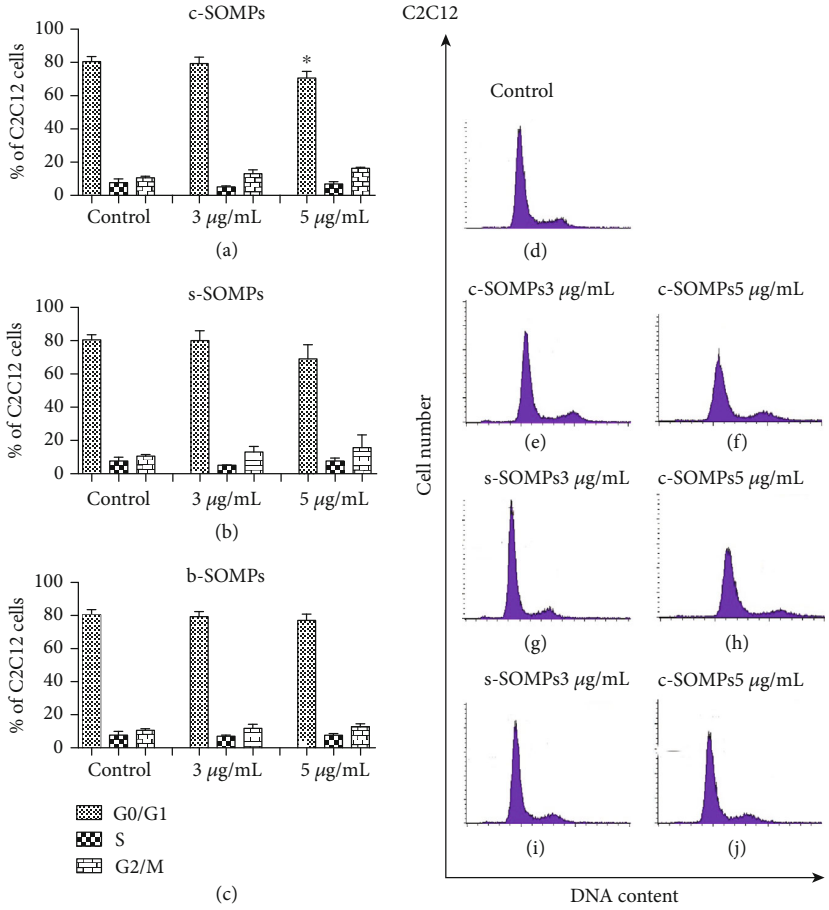

FIGURE 9: The cell cycle distribution for C2C12 cells. . Percentage of cells in each cell cycle phase after treatment with (a) c-SOMPs, (b) s-SOMPs, (c) b-SOMPs. Representative histograms (d) control, (e), (f) c-SOMPs; (g), (h) s-SOMPs; (i), (j) b-SOMPs. Data are presented as mean ± SD. $^{*}p < 0.05$.

phagocytosis; so, they are more likely to uptake large particles [49]. They also used much greater concentration (125 μg/mL) compared to our experiments. Similarly, He et al. have shown that mesoporous silica microparticles can be internalized into lysosomes. They conducted a study on mammary gland adenocarcinoma cells (MDA-MB-468). Again, they used a higher concentration than that used in our study [50].

4.7. Safety of Potential Applications. Our SOMPs have antimicrobial properties. Importantly, they can be selectively cytotoxic to bacteria and fungi and still be not harmful to mammalian cells. However, like any medication, they have also a side effect. In a higher concentration, they are cytotoxic to a mammalian cell. Also, they can induce inflammation and oxidative stress. Silver itself also can be noxious to mammalian cells. Unfortunately, there are no international standards regarding safe silver nano- or microparticle concentrations for humans. According to the U.S. Environmental Protection Agency, National Center for Environmental Assessments, an oral dose of 0.014 mg/kg/24 h of silver can be harmful and cause argyria [60]. However, due to much smaller doses and only local administration, it is highly unlikely that silver-coated implants can cause any adverse effect due to silver overdose. Moreover, nowadays, silver is commonly used in dressings with only one cause of argyria being reported (in an individual with 30% skin burnt) [61], which further support the safety of local application of silver. Commonly used antimicrobial agents also can decrease cell viability. For example, broad-spectrum antibiotic polymyxin B in 50 μg/mL concentration reduces the viability of human erythroleukemia cells (K562) by one-fifth [62]. Wang et al. have shown that amphotericin B, colistin-M, and amikacin can decrease viability, measured by MTT assay, of pig corneal epithelial cells [63]. Duewelhenke et al. have shown that other clinically used drugs (cefazolin, ciprofloxacin, tetracycline, rifampicin, clindamycin, azithromycin, chloramphenicol, linezolid) can be cytotoxic to primary human osteoblasts (PHO), MG63 osteosarcoma (MG-63) and cervical cancer (HeLa) cells [64]. They observed decreased viability (MTT assay) and cell proliferation (BrdU assay) [64]. Their results are especially relevant for us because in the study they used a similar methodology and *in vitro* model; moreover, they also examined antibiotics used in treating bone infections.

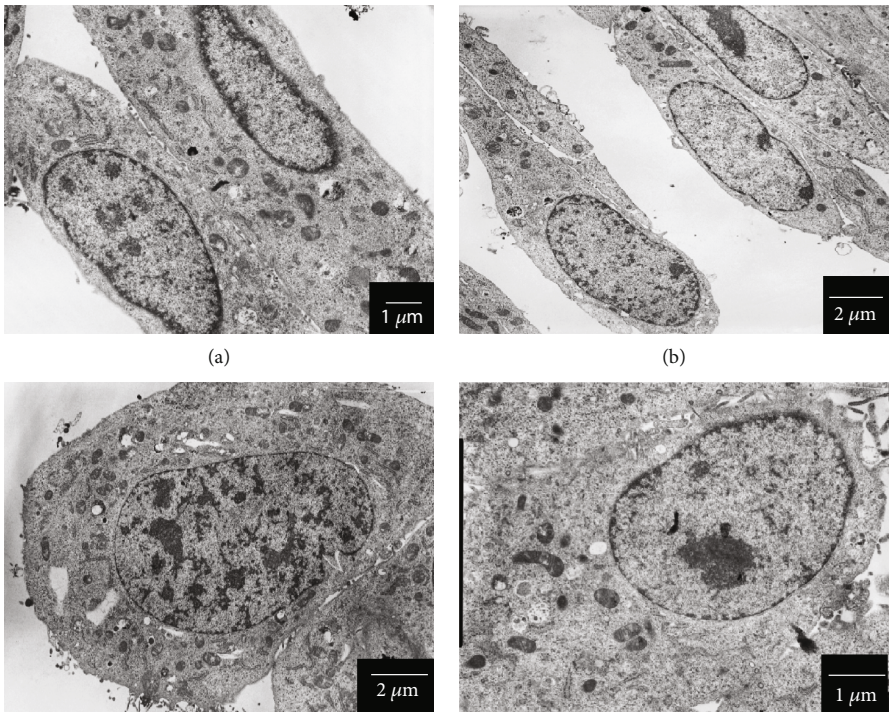

Figure 10: Morphology of C2C12 cells examined by TEM. (a) control cells, (b) cells treated with c-SOMPs (3 μg/mL), (c) cells treated with s-SOMPs (3 μg/mL), and (d) cells treated with b-SOMPs (3 μg/mL). Scale bar is present on the bottom right side of each picture.

Table 5: Possible mechanism underlying antibacterial properties of SOMPs.

Mechanism	Reference
Due to large surface and high surface energy, SOMPs can absorb bacteria	[38, 40]
SOMPs may release Ag^+ ions which themselves are antibacterial agents	[38, 40, 41]
SOPMs under visible light can generate free electrons, therefore generating ROS which can lead to DNA damage	[38, 40]
PO_4^{3-} ions can be released from SOMPs and interfere with ATP $\leftarrow \rightarrow$ ADP conversion, which will impair bacterial metabolism	[38, 40]

5. Conclusion

We synthesized and characterized six shapes of silver orthophosphate microparticles (tetrapod, cubes, spheres, tetrahedrons, branched, and rhombic dodecahedrons). SOPMs had antimicrobial properties (both on planktonic and biofilm forms of pathogens), they were more efficient against fungi than bacteria. c-SOMPs and s-SOMPs had the best antimicrobial properties. Cytotoxicity of SOMPs was shape- and concentration-dependent. hFOB1.19 cells were the most resistant and C2C12 cells were the most susceptible to tested SOMPs. c-SOMPs were the most cytotoxic and t-SOMPs the least. Some of SOMPs can induce oxidative stress and increased levels of proinflammatory markers in the cells. SOMPs did not cause ultrastructure changes in C2C12 cells.

Based on good antimicrobial properties, mild cytotoxicity, no impact on cell cycle, and ultrastructure of the cells, we gather that spheres are the best shape of the silver orthophosphate microparticles for potential biomedical usage.

Abbreviations

SOMPs: Silver orthophosphate microparticles
t-SOMPs: Tetrapod silver orthophosphate microparticles
c-SOMPs: Cubical silver orthophosphate microparticles
s-SOMPs: Spherical silver orthophosphate microparticles
th-SOMPs: Tetrahedral silver orthophosphate microparticles
b-SOMPs: Branched silver orthophosphate microparticles
rd-SOMPs: Rhombic dodecahedral silver orthophosphate microparticles.

Data Availability

The experimental data used to support the findings of this study are included within the article or are available from the corresponding author upon request.

Disclosure

The funders had no role in study design, data collection, and analysis, decision to publish, or preparation of the article.

Conflicts of Interest

The authors declare that there is no conflict of interest regarding the publication of this paper.

Acknowledgments

Authors would like to thank Dr. Anna Malankowska for her impact on the study. Authors would like to thank Dr. Hab. Edyta Brzóska-Wójtowicz for C2C12 cell line donation. KPS and IIS acknowledges funding form grant "Wpsieramy rozwoj" by CEDROB S.A SK and IIS acknowledges funding from Medical University of Gdansk (ST-02-0046/07/259).

Supplementary Materials

Supplementary Table 1: minimal inhibitory concentrations (μg/mL) of conventional drugs against reference strains of microorganism. *(Supplementary Materials)*

References

[1] H. van de Belt, D. Neut, W. Schenk, J. R. van Horn, H. C. van der Mei, and H. J. Busscher, "Infection of orthopedic implants and the use of antibiotic-loaded bone cements: A review," *Acta Orthopaedica Scandinavica*, vol. 72, no. 6, pp. 557–571, 2001.

[2] R. O. Darouiche, "Treatment of Infections Associated with Surgical Implants," *The New England Journal of Medicine*, vol. 350, no. 14, pp. 1422–1429, 2004.

[3] A. Trampuz and A. F. Widmer, *Current Opinion in Infectious Diseases*, vol. 19, no. 4, pp. 349–356, 2006.

[4] J. W. Costerton, P. S. Stewart, and E. P. Greenberg, "Bacterial Biofilms: A Common Cause of Persistent Infections," *Science*, vol. 284, no. 5418, article 1318, 1322 pages, 1999.

[5] R. Saginur, M. S. Denis, W. Ferris et al., "Multiple combination bactericidal testing of staphylococcal biofilms from implant-associated infections," *Antimicrobial Agents and Chemotherapy*, vol. 50, no. 1, pp. 55–61, 2006.

[6] M. Kazemzadeh-Narbat, J. Kindrachuk, K. Duan, H. Jenssen, R. E. W. Hancock, and R. Wang, "Antimicrobial peptides on calcium phosphate-coated titanium for the prevention of implant-associated infections," *Biomaterials*, vol. 31, no. 36, pp. 9519–9526, 2010.

[7] D. Zhang, W. Liu, X. D. Wu et al., "Efficacy of novel nano-hydroxyapatite/polyurethane composite scaffolds with silver phosphate particles in chronic osteomyelitis," *Journal of Materials Science: Materials in Medicine*, vol. 30, no. 6, p. 59, 2019.

[8] J. Jiang, L. Li, K. Li et al., "Antibacterial nanohydroxyapatite/-polyurethane composite scaffolds with silver phosphate particles for bone regeneration," *Journal of Biomaterials Science, Polymer Edition*, vol. 27, no. 16, pp. 1584–1598, 2016.

[9] J. S. Lee and W. L. Murphy, "Functionalizing calcium phosphate biomaterials with antibacterial silver particles," *Advanced Materials*, vol. 25, no. 8, pp. 1173–1179, 2013.

[10] L. C. Natale, Y. Alania, M. C. Rodrigues et al., "Synthesis and characterization of silver phosphate/calcium phosphate mixed particles capable of silver nanoparticle formation by photoreduction," *Materials Science and Engineering: C*, vol. 76, pp. 464–471, 2017.

[11] K. Niska, N. Knap, A. Kędzia, M. Jaskiewicz, W. Kamysz, and I. Inkielewicz-Stepniak, "Capping agent-dependent toxicity and antimicrobial activity of silver nanoparticles: an *in vitro study*. Concerns about potential application in dental practice," *International Journal of Medical Sciences*, vol. 13, no. 10, pp. 772–782, 2016.

[12] D. Krupa, J. Baszkiewicz, J. A. Kozubowski et al., "Effect of phosphorus-ion implantation on the corrosion resistance and biocompatibility of titanium," *Biomaterials*, vol. 23, no. 16, pp. 3329–3340, 2002.

[13] S. Monge, B. Canniccioni, A. Graillot, and J. J. Robin, *Biomacromolecules*, vol. 12, p. 1973, 2011.

[14] Z. Yi, J. Ye, N. Kikugawa et al., "An orthophosphate semiconductor with photooxidation properties under visible-light irradiation," *Nature Materials*, vol. 9, no. 7, pp. 559–564, 2010.

[15] X. Guo, C. Chen, S. Yin, L. Huang, and W. Qin, "Controlled synthesis and photocatalytic properties of Ag_3PO_4 microcrystals," *Journal of Alloys and Compounds*, vol. 619, pp. 293–297, 2015.

[16] J. Zwara, E. Grabowska, T. Klimczuk, W. Lisowski, and A. Zaleska-Medynska, "Shape-dependent enhanced photocatalytic effect under visible light of Ag_3PO_4 particles," *Journal of Photochemistry and Photobiology A: Chemistry*, vol. 367, pp. 240–252, 2018.

[17] Z. M. Yang, Y. Y. Liu, L. Xu, G. F. Huang, and W. Q. Huang, "Facile shape-controllable synthesis of Ag_3PO_4 photocatalysts," *Materials Letters*, vol. 133, pp. 139–142, 2014.

[18] P. Dong, Y. Wang, H. Li, H. Li, X. Ma, and L. Han, "Shape-controllable synthesis and morphology-dependent photocatalytic properties of Ag_3PO_4 crystals," *Journal of Materials Chemistry A*, vol. 1, no. 15, p. 4651, 2013.

[19] H. Lin, H. Ye, B. Xu, J. Cao, and S. Chen, "Ag_3PO_4 quantum dot sensitized $BiPO_4$: A novel *p–n* junction $Ag_3PO_4/BiPO_4$ with enhanced visible-light photocatalytic activity," *Catalysis Communications*, vol. 37, pp. 55–59, 2013.

[20] M. Li, M. Chen, J. Wang, and F. Teng, "Branching growth of novel silver phosphate dendrites and the greatly improved photocatalytic activity by the active {110} facets," *CrystEngComm*, vol. 16, no. 7, pp. 1237–1240, 2014.

[21] J. Wang, F. Teng, M. Chen, J. Xu, Y. Song, and X. Zhou, "Facile synthesis of novel Ag_3PO_4 tetrapods and the {110} facets-dominated photocatalytic activity," *CrystEngComm*, vol. 15, no. 1, pp. 39–42, 2013.

[22] Clinical and Laboratory Standards Institute (CLSI), *Methods for Dilution Antimicrobial Susceptibility Tests f or Bacteria That Grow Aerobically; Approved St Andard—Ninth Edition, CLSI Standard M07-A9*, Clinical and Laboratory Standard Institute, Wayne, PA, USA, 2012.

[23] Clinical and Laboratory Standards Institute (CLSI), *Reference Method for Broth Dilution Antifungal Susceptibility Testing of Yeasts. 3rd Edition, CLSI Standard M27*, Clinical and Laboratory Standard Institute, Wayne, PA, USA, 2008.

[24] D. Migoń, M. Jaśkiewicz, D. Neubauer et al., "Alanine Scanning Studies of the Antimicrobial Peptide Aurein 1.2," *Probiotics and Antimicrobial Proteins*, vol. 11, no. 3, pp. 1042–1054, 2019.

[25] M. Maciejewska, M. Bauer, D. Neubauer, W. Kamysz, and M. Dawgul, "Influence of amphibian antimicrobial peptides and short lipopeptides on bacterial biofilms formed on contact lenses," *Materials*, vol. 9, no. 11, p. 873, 2016.

[26] K. P. Steckiewicz, E. Barcinska, A. Malankowska et al., "Impact of gold nanoparticles shape on their cytotoxicity against

human osteoblast and osteosarcoma in in vitro model. Evaluation of the safety of use and anti-cancer potential," *Journal of Materials Science: Materials in Medicine*, vol. 30, no. 2, p. 22, 2019.

[27] M. M. Bradford, "A rapid and sensitive method for the quantitation of microgram quantities of protein utilizing the principle of protein-dye binding," *Analytical Biochemistry*, vol. 72, no. 1-2, pp. 248–254, 1976.

[28] X. Yan, Q. Gao, J. Qin, X. Yang, Y. Li, and H. Tang, "Morphology-controlled synthesis of Ag_3PO_4 microcubes with enhanced visible-light-driven photocatalytic activity," *Ceramics International*, vol. 39, no. 8, pp. 9715–9720, 2013.

[29] L. Dong, P. Wang, S. Wang, P. Lei, and Y. Wang, "A simple way for Ag_3PO_4 tetrahedron and tetrapod microcrystals with high visible-light-responsive activity," *Materials Letters*, vol. 134, pp. 158–161, 2014.

[30] J. Wan, E. Liu, J. Fan et al., "In-situ synthesis of plasmonic Ag/Ag_3PO_4 tetrahedron with exposed {111} facets for high visible-light photocatalytic activity and stability," *Ceramics International*, vol. 41, no. 5, pp. 6933–6940, 2015.

[31] Y. Bi, S. Ouyang, N. Umezawa, J. Cao, and J. Ye, "Facet Effect of Single-Crystalline Ag_3PO_4 Sub-microcrystals on Photocatalytic Properties," *Journal of the American Chemical Society*, vol. 133, no. 17, pp. 6490–6492, 2011.

[32] C. Dong, J. Wang, K. L. Wu et al., "Rhombic dodecahedral Ag_3PO_4 architectures: controllable synthesis, formation mechanism and photocatalytic activity," *CrystEngComm*, vol. 18, no. 9, pp. 1618–1624, 2016.

[33] J. Wang, S. Lou, P. Sun et al., "Surface control and photocatalytic activity of branched silver orthophosphate dendrites," *ChemCatChem*, vol. 6, no. 7, pp. 2021–2027, 2014.

[34] P. Dong, Y. Yin, N. Xu, R. Guan, G. Hou, and Y. Wang, "Facile synthesis of tetrahedral Ag_3PO_4 mesocrystals and its enhanced photocatalytic activity," *Materials Research Bulletin*, vol. 60, pp. 682–689, 2014.

[35] A. Wu, C. Tian, W. Chang et al., "Morphology-controlled synthesis of Ag_3PO_4 nano/microcrystals and their antibacterial properties," *Materials Research Bulletin*, vol. 48, no. 9, pp. 3043–3048, 2013.

[36] P. Koehler, D. Tacke, and O. A. Cornely, "Aspergillosis of bones and joints – a review from 2002 until today," *Mycoses*, vol. 57, pp. 323–335, 2014.

[37] M. N. Gamaletsou, J. Meletiadis, S. Chatziioannou et al., "Experimental *Candida albicans* osteomyelitis: Microbiologic, antigenic, histologic, and ^{18}FDG-PET-CT imaging characteristics in a newly established rabbit model," *Medical Mycology*, vol. 57, no. 8, pp. 1011–1017, 2019.

[38] G. Panthi, R. Ranjit, H. Y. Kim, and D. Das Mulmi, "Size dependent optical and antibacterial properties of Ag_3PO_4 synthesized by facile precipitation and colloidal approach in aqueous solution," *Optik*, vol. 156, pp. 60–68, 2018.

[39] D. Chudobova, K. Cihalova, S. Dostalova et al., "Comparison of the effects of silver phosphate and selenium nanoparticles on *Staphylococcus aureus* growth reveals potential for selenium particles to prevent infection," *FEMS Microbiology Letters*, vol. 351, no. 2, pp. 195–201, 2014.

[40] J. K. Liu, C. X. Luo, J. D. Wang, X. H. Yang, and X. H. Zhong, "Controlled synthesis of silver phosphate crystals with high photocatalytic activity and bacteriostatic activity," *CrystEngComm*, vol. 14, no. 24, p. 8714, 2012.

[41] B. E. Yeo, Y. Seo, H. Park, and Y. D. Huh, "Facet Effect of Ag_3PO_4 Crystals on Antibacterial Activities," *Bulletin of the Korean Chemical Society*, vol. 36, no. 7, pp. 1904–1907, 2015.

[42] M. K. Kim and D.-S. Kim, "Effect of the Ag_3PO_4 on Staphylococcus aureus Growth and Human Immunity," *Biomedical Science Letters*, vol. 24, no. 1, pp. 30–34, 2018.

[43] E. M. Czekanska, M. J. Stoddart, R. G. Richards, and J. S. Hayes, "In search of an osteoblast cell model for in vitro research," *European Cells and Materials*, vol. 24, pp. 1–17, 2012.

[44] M. Ahmad, M. B. McCarthy, and G. Gronowicz, "An in vitro model for mineralization of human osteoblast-like cells on implant materials," *Biomaterials*, vol. 20, no. 3, pp. 211–220, 1999.

[45] N. A. Monteiro-Riviere, A. O. Inman, and L. W. Zhang, "Limitations and relative utility of screening assays to assess engineered nanoparticle toxicity in a human cell line," *Toxicology and Applied Pharmacology*, vol. 234, no. 2, pp. 222–235, 2009.

[46] D. D. Allen, R. Caviedes, A. M. Cárdenas, T. Shimahara, J. Segura-Aguilar, and P. A. Caviedes, "Cell lines as in vitro models for drug screening and toxicity studies," *Drug Development and Industrial Pharmacy*, vol. 31, no. 8, pp. 757–768, 2005.

[47] K. Lappalainen, I. Jääskeläinen, K. Syrjänen, A. Urtti, and S. Syrjänen, "Comparison of cell proliferation and toxicity assays using two cationic liposomes," *Pharmaceutical Research*, vol. 11, no. 8, pp. 1127–1131, 1994.

[48] W. Bergler, G. Petroiami, and A. Schadel, "Feasibility of proliferation studies using the BrdU and MTT assays with a head and neck carcinoma cell line," *ORL*, vol. 55, no. 4, pp. 230–235, 1993.

[49] M. Motskin, D. M. Wright, K. Muller et al., "Hydroxyapatite nano and microparticles: Correlation of particle properties with cytotoxicity and biostability," *Biomaterials*, vol. 30, no. 19, pp. 3307–3317, 2009.

[50] Q. He, Z. Zhang, Y. Gao, J. Shi, and Y. Li, "Intracellular Localization and Cytotoxicity of Spherical Mesoporous Silica Nano- and Microparticles," *Small*, vol. 5, no. 23, pp. 2722–2729, 2009.

[51] A. Manke, L. Wang, and Y. Rojanasakul, "Mechanisms of Nanoparticle-Induced Oxidative Stress and Toxicity," *BioMed Research International*, vol. 2013, Article ID 942916, 15 pages, 2013.

[52] A. Bowie and L. A. J. O'Neill, "Oxidative stress and nuclear factor-κB activation∗: A reassessment of the evidence in the light of recent discoveries," *Biochemical Pharmacology*, vol. 59, no. 1, pp. 13–23, 2000.

[53] A. C. Childs, S. L. Phaneuf, A. J. Dirks, T. Phillips, and C. Leeuwenburgh, "Doxorubicin treatment in vivo causes cytochrome C release and cardiomyocyte apoptosis, as well as increased mitochondrial efficiency, superoxide dismutase activity, and Bcl-2: Bax ratio," *Cancer Research*, vol. 62, no. 16, pp. 4592–4598, 2002.

[54] H. A. Santos, J. Riikonen, J. Salonen et al., "In vitro cytotoxicity of porous silicon microparticles: Effect of the particle concentration, surface chemistry and size," *Acta Biomaterialia*, vol. 6, no. 7, pp. 2721–2731, 2010.

[55] T. Saliev, D. M. Baiskhanova, A. Akhmetova et al., "Impact of electromagnetic fields on *in vitro* toxicity of silver and graphene nanoparticles," *Electromagnetic Biology and Medicine*, vol. 38, no. 1, pp. 21–31, 2019.

[56] K. S. Jones, "Effects of biomaterial-induced inflammation on fibrosis and rejection," *Seminars in Immunology*, vol. 20, no. 2, pp. 130–136, 2008.

[57] P. P. Tak and G. S. Firestein, "NF-κB: a key role in inflammatory diseases," *The Journal of Clinical Investigation*, vol. 107, no. 1, pp. 7–11, 2001.

[58] K. A. Brogden, G. K. Johnson, S. D. Vincent, T. Abbasi, and S. Vali, "Oral inflammation, a role for antimicrobial peptide modulation of cytokine and chemokine responses," *Expert Review of Anti-infective Therapy*, vol. 11, no. 10, pp. 1097–1113, 2013.

[59] S. Chinde, Y. Poornachandra, A. Panyala et al., "Comparative study of cyto- and genotoxic potential with mechanistic insights of tungsten oxide nano- and microparticles in lung carcinoma cells," *Journal of Applied Toxicology*, vol. 38, no. 6, pp. 896–913, 2018.

[60] US Environmental Protection Agency, *Sliver (CASRN-7440-22-4), Integrated Risk Information System (IRIS), Environmental Criteria and Assessment Office, Office of Health and Environmental Assessment*, Cincinnati, OH, USA, 2019 https://cfpub.epa.gov/ncea/iris/iris_documents/documents/subst/0099_summary.pdf.

[61] T. Faunce and A. Watal, "Nanosilver and global public health: international regulatory issues," *Nanomedicine*, vol. 5, no. 4, pp. 617–632, 2010.

[62] A. K. Duwe, C. A. Rupar, G. B. Horsman, and S. I. Vas, "In vitro cytotoxicity and antibiotic activity of polymyxin B nonapeptide," *Antimicrobial Agents and Chemotherapy*, vol. 30, no. 2, pp. 340-341, 1986.

[63] H.-Z. Wang, C.-H. Chang, C.-P. Lin, and M.-C. Tsai, "Using MTT Viability Assay to Test the Cytotoxicity of Antibiotics and Steroid to Cultured Porcine Corneal Endothelial Cells," *Journal of Ocular Pharmacology and Therapeutics*, vol. 12, p. 35, 2009.

[64] N. Duewelhenke, O. Krut, and P. Eysel, "Influence on mitochondria and cytotoxicity of different antibiotics administered in high concentrations on primary human osteoblasts and cell lines," *Antimicrobial Agents and Chemotherapy*, vol. 51, no. 1, pp. 54–63, 2007.

Gdańsk, dnia 24.09.2020

Karol Paweł Steckiewicz
.....
(tytuł zawodowy, imię i nazwisko)

OŚWIADCZENIE

Jako współautor pracy pt. Modified nanoparticles as potential agents in bone diseases: cancer and implant-related complications (Nanomaterials. 2020; 10:658), oświadczam, iż mój własny wkład merytoryczny w przygotowanie, przeprowadzenie i opracowanie badań oraz przedstawienie pracy w formie publikacji to:

udział w opracowaniu koncepcji pracy,

zebranie danych i przygotowanie manuskryptu.

Jednocześnie wyrażam zgodę na przedłożenie w/w pracy przez Karola Pawła Steckiewicza jako część rozprawy doktorskiej w formie spójnego tematycznie zbioru artykułów opublikowanych w czasopismach naukowych.

Oświadczam, iż samodzielna i możliwa do wyodrębnienia część ww. pracy wykazuje indywidualny wkład Karola Pawła Steckiewicz przy opracowywaniu koncepcji, zebraniu danych, opracowaniu i interpretacji wyników tej pracy.

Karol P. Steckiewicz
.....
(podpis współautora)

Gdańsk, dnia 24.09.2020 r.

Prof. dr hab. Iwona Inkielewicz – Stępniak
.....
(tytuł zawodowy, imię i nazwisko)

OŚWIADCZENIE

Jako współautorka pracy pt. Modified nanoparticles as potential agents in bone diseases: cancer and implant-related complications (Nanomaterials. 2020; 10:658), oświadczam, iż mój własny wkład merytoryczny w przygotowanie, przeprowadzenie i opracowanie badań oraz przedstawienie pracy w formie publikacji to:

nadzór merytoryczny nad przygotowaniem publikacji.

Jednocześnie wyrażam zgodę na przedłożenie w/w pracy przez Karola Pawła Steckiewicza jako część rozprawy doktorskiej w formie spójnego tematycznie zbioru artykułów opublikowanych w czasopismach naukowych.

Oświadczam, iż samodzielna i możliwa do wyodrębnienia część ww. pracy wykazuje indywidualny wkład Karola Pawła Steckiewicz przy opracowywaniu koncepcji, zebraniu danych, opracowaniu i interpretacji wyników tej pracy.

.....
(podpis współautorki)

Gdańsk, dnia 24.09.2020

Karol Paweł Steckiewicz

.....

(tytuł zawodowy, imię i nazwisko)

OŚWIADCZENIE

Jako współautor pracy pt. Impact of gold nanoparticles shape on their cytotoxicity against human osteoblast and osteosarcoma in in vitro model: evaluation of the safety of use and anti-cancer potential (J Mater Sci Mater Med. 2019; 30(2):22), oświadczam, iż mój własny wkład merytoryczny w przygotowanie, przeprowadzenie i opracowanie badań oraz przedstawienie pracy w formie publikacji to:

udział w opracowywaniu koncepcji pracy, wykonanie badań eksperymentalnych, opracowanie i interpretacja wyników. przygotowanie manuskryptu.

Jednocześnie wyrażam zgodę na przedłożenie w/w pracy przez Karola Pawła Steckiewicza jako część rozprawy doktorskiej w formie spójnego tematycznie zbioru artykułów opublikowanych w czasopismach naukowych.

Oświadczam, iż samodzielna i możliwa do wyodrębnienia część ww. pracy wykazuje indywidualny wkład Karola Pawła Steckiewicz przy opracowywaniu koncepcji, wykonywaniu części eksperymentalnej, opracowaniu i interpretacji wyników tej pracy. Udział procentowy Karola Pawła Steckiewicza w powstanie w/w pracy oceniam na 50 %.

Karol P. Steckiewicz

.....

(podpis współautora)

Gdańsk, dnia 21.09.2020

Dr Ewelina Barcińska

.....

(tytuł zawodowy, imię i nazwisko)

OŚWIADCZENIE

Jako współautorka pracy pt. Impact of gold nanoparticles shape on their cytotoxicity against human osteoblast and osteosarcoma in in vitro model: evaluation of the safety of use and anti-cancer potential (J Mater Sci Mater Med. 2019; 30(2):22), oświadczam, iż mój własny wkład merytoryczny w przygotowanie, przeprowadzenie i opracowanie badań oraz przedstawienie pracy w formie publikacji to:

pomoc w tworzeniu manuskryptu.

Jednocześnie wyrażam zgodę na przedłożenie w/w pracy przez Karola Pawła Steckiewicza jako część rozprawy doktorskiej w formie spójnego tematycznie zbioru artykułów opublikowanych w czasopismach naukowych.

Oświadczam, iż samodzielna i możliwa do wyodrębnienia część ww. pracy wykazuje indywidualny wkład Karola Pawła Steckiewicz przy opracowywaniu koncepcji, wykonywaniu części eksperymentalnej, opracowaniu i interpretacji wyników tej pracy. Udział procentowy Karola Pawła Steckiewicza w powstanie w/w pracy oceniam na 50 %.

Ewelina Barcińska

.....

(podpis współautorki)

Gdańsk, dnia 10.09.2020

Dr inż. Anna Malankowska

.....

(tytuł zawodowy, imię i nazwisko)

OŚWIADCZENIE

Jako współautorka pracy pt. Impact of gold nanoparticles shape on their cytotoxicity against human osteoblast and osteosarcoma in in vitro model: evaluation of the safety of use and anti-cancer potential (J Mater Sci Mater Med. 2019; 30(2):22), oświadczam, iż mój własny wkład merytoryczny w przygotowanie, przeprowadzenie i opracowanie badań oraz przedstawienie pracy w formie publikacji to:

synteza oraz charakterystyka nanocząstek złota w różnych kształtach.

Jednocześnie wyrażam zgodę na przedłożenie w/w pracy przez Karola Pawła Steckiewicza jako część rozprawy doktorskiej w formie spójnego tematycznie zbioru artykułów opublikowanych w czasopismach naukowych.

Oświadczam, iż samodzielna i możliwa do wyodrębnienia część ww. pracy wykazuje indywidualny wkład Karola Pawła Steckiewicz przy opracowywaniu koncepcji, wykonywaniu części eksperymentalnej, opracowaniu i interpretacji wyników tej pracy. Udział procentowy Karola Pawła Steckiewicza w powstanie w/w pracy oceniam na 50 %.

.....

(podpis współautorki)

Gdańsk, dnia 21-09-2020

Dr n. med. Agata Zauszkiewicz – Pawlak

.....

(tytuł zawodowy, imię i nazwisko)

OŚWIADCZENIE

Jako współautorka pracy pt. *Impact of gold nanoparticles shape on their cytotoxicity against human osteoblast and osteosarcoma in in vitro model: evaluation of the safety of use and anti-cancer potential* (J Mater Sci Mater Med. 2019; 30(2):22), oświadczam, iż mój własny wkład merytoryczny w przygotowanie, przeprowadzenie i opracowanie badań oraz przedstawienie pracy w formie publikacji to:

wykonanie zdjęć przy użyciu Transmisyjnego Mikroskopu Elektronowego dla próbek biologicznych i ich opis do manuskryptu.

Jednocześnie wyrażam zgodę na przedłożenie w/w pracy przez Karola Pawła Steckiewicza jako część rozprawy doktorskiej w formie spójnego tematycznie zbioru artykułów opublikowanych w czasopismach naukowych.

Oświadczam, iż samodzielna i możliwa do wyodrębnienia część ww. pracy wykazuje indywidualny wkład Karola Pawła Steckiewicz przy opracowywaniu koncepcji, wykonywaniu części eksperymentalnej, opracowaniu i interpretacji wyników tej pracy. Udział procentowy Karola Pawła Steckiewicza w powstanie w/w pracy oceniam na 50%.

2020 -09- 21

Agata Zauszkiewicz-Pawlak

.....

(podpis współautorki)

Poznań, dnia 10.09.2020

Dr Grzegorz Nowaczyk
.....
(tytuł zawodowy, imię i nazwisko)

OŚWIADCZENIE

Jako współautor pracy pt. Impact of gold nanoparticles shape on their cytotoxicity against human osteoblast and osteosarcoma in in vitro model: evaluation of the safety of use and anti-cancer potential (J Mater Sci Mater Med. 2019; 30(2):22), oświadczam, iż mój własny wkład merytoryczny w przygotowanie, przeprowadzenie i opracowanie badań oraz przedstawienie pracy w formie publikacji to:

wykonanie analiz przy użyciu Transmisyjnego Mikroskopu Elektronowego i Skaningowego Mikroskopu Elektronowego dla nanocząstek.

Jednocześnie wyrażam zgodę na przedłożenie w/w pracy przez Karola Pawła Steckiewicza jako część rozprawy doktorskiej w formie spójnego tematycznie zbioru artykułów opublikowanych w czasopismach naukowych.

Oświadczam, iż samodzielna i możliwa do wyodrębnienia część ww. pracy wykazuje indywidualny wkład Karola Pawła Steckiewicz przy opracowywaniu koncepcji, wykonywaniu części eksperymentalnej, opracowaniu i interpretacji wyników tej pracy. Udział procentowy Karola Pawła Steckiewicza w powstanie w/w pracy oceniam na 50 %.

Grzegorz Nowaczyk
.....
(podpis współautora)

Gdańsk, dnia 11.05.2020

Prof. dr hab. inż. Adriana Zaleska – Medynska
.....
(tytuł zawodowy, imię i nazwisko)

OŚWIADCZENIE

Jako współautorka pracy pt. Impact of gold nanoparticles shape on their cytotoxicity against human osteoblast and osteosarcoma in in vitro model: evaluation of the safety of use and anti-cancer potential (J Mater Sci Mater Med. 2019; 30(2):22), oświadczam, iż mój własny wkład merytoryczny w przygotowanie, przeprowadzenie i opracowanie badań oraz przedstawienie pracy w formie publikacji to:

nadzór merytoryczny nad syntezą i charakteryzacją nanocząstek złota w różnych kształtach.

Jednocześnie wyrażam zgodę na przedłożenie w/w pracy przez Karola Pawła Steckiewicza jako część rozprawy doktorskiej w formie spójnego tematycznie zbioru artykułów opublikowanych w czasopismach naukowych.

Oświadczam, iż samodzielna i możliwa do wyodrębnienia część ww. pracy wykazuje indywidualny wkład Karola Pawła Steckiewicz przy opracowywaniu koncepcji, wykonywaniu części eksperymentalnej, opracowaniu i interpretacji wyników tej pracy. Udział procentowy Karola Pawła Steckiewicza w powstanie w/w pracy oceniam na 50 %.

KIEROWNIK
Katedra Technologii Środowiska
prof. dr hab. inż. Adriana Zaleska-Medynska

.....
(podpis współautorki)

Gdańsk, dnia 24.09.2020 r.

Prof. dr hab. Iwona Inkielewicz – Stępniak
.....
(tytuł zawodowy, imię i nazwisko)

OŚWIADCZENIE

Jako współautorka pracy pt. Impact of gold nanoparticles shape on their cytotoxicity against human osteoblast and osteosarcoma in in vitro model: evaluation of the safety of use and anti-cancer potential (J Mater Sci Mater Med. 2019; 30(2):22), oświadczam, iż mój własny wkład merytoryczny w przygotowanie, przeprowadzenie i opracowanie badań oraz przedstawienie pracy w formie publikacji to:

nadzór merytoryczny nad badaniami biologicznymi i przygotowaniem publikacji.

Jednocześnie wyrażam zgodę na przedłożenie w/w pracy przez Karola Pawła Steckiewicza jako część rozprawy doktorskiej w formie spójnego tematycznie zbioru artykułów opublikowanych w czasopismach naukowych.

Oświadczam, iż samodzielna i możliwa do wyodrębnienia część ww. pracy wykazuje indywidualny wkład Karola Pawła Steckiewicz przy opracowywaniu koncepcji, wykonywaniu części eksperymentalnej, opracowaniu i interpretacji wyników tej pracy. Udział procentowy Karola Pawła Steckiewicza w powstanie w/w pracy oceniam na 50 %.

.....
(podpis współautorki)

Gdańsk, dnia 24.09.2020

Karol Paweł Steckiewicz

.....

(tytuł zawodowy, imię i nazwisko)

OŚWIADCZENIE

Jako współautor pracy pt. Assessment of anti-tumor potential and safety of application of glutathione stabilized gold nanoparticles conjugated with chemotherapeutics (Int J Med Sci. 2020;17(6)), oświadczam, iż mój własny wkład merytoryczny w przygotowanie, przeprowadzenie i opracowanie badań oraz przedstawienie pracy w formie publikacji to:

udział w opracowywaniu koncepcji pracy, wykonanie badań eksperymentalnych, opracowanie i interpretacja wyników. przygotowanie manuskryptu.

Jednocześnie wyrażam zgodę na przedłożenie w/w pracy przez Karola Pawła Steckiewicza jako część rozprawy doktorskiej w formie spójnego tematycznie zbioru artykułów opublikowanych w czasopismach naukowych.

Oświadczam, iż samodzielna i możliwa do wyodrębnienia część ww. pracy wykazuje indywidualny wkład Karola Pawła Steckiewicz przy opracowywaniu koncepcji, wykonywaniu części eksperymentalnej, opracowaniu i interpretacji wyników tej pracy. Udział procentowy Karola Pawła Steckiewicza w powstanie w/w pracy oceniam na 55 %.

Karol P. Steckiewicz

.....

(podpis współautora)

Gdańsk . dnia 21.09.2020

Dr Ewelina Barcińska

.....

(tytuł zawodowy, imię i nazwisko)

OŚWIADCZENIE

Jako współautorka pracy pt. Assessment of anti-tumor potential and safety of application of glutathione stabilized gold nanoparticles conjugated with chemotherapeutics (Int J Med Sci. 2020;17(6)), oświadczam, iż mój własny wkład merytoryczny w przygotowanie, przeprowadzenie i opracowanie badań oraz przedstawienie pracy w formie publikacji to:

udział w opracowywaniu koncepcji pracy, udział w części eksperymentalnej.

Jednocześnie wyrażam zgodę na przedłożenie w/w pracy przez Karola Pawła Steckiewicza jako część rozprawy doktorskiej w formie spójnego tematycznie zbioru artykułów opublikowanych w czasopismach naukowych.

Oświadczam, iż samodzielna i możliwa do wyodrębnienia część ww. pracy wykazuje indywidualny wkład Karola Pawła Steckiewicz przy opracowywaniu koncepcji, wykonywaniu części eksperymentalnej, opracowaniu i interpretacji wyników tej pracy. Udział procentowy Karola Pawła Steckiewicza w powstanie w/w pracy oceniam na 55 %.

Ewelina Barcińska

.....

(podpis współautorki)

Warszawa, dnia 14.09.2020

Mgr Ewelina Tomczyk

.....

(tytuł zawodowy, imię i nazwisko)

OŚWIADCZENIE

Jako współautorka pracy pt. Assessment of anti-tumor potential and safety of application of glutathione stabilized gold nanoparticles conjugated with chemotherapeutics (Int J Med Sci. 2020;17(6)), oświadczam, iż mój własny wkład merytoryczny w przygotowanie, przeprowadzenie i opracowanie badań oraz przedstawienie pracy w formie publikacji to:

synteza oraz charakterystyka nanocząstek złota.

Jednocześnie wyrażam zgodę na przedłożenie w/w pracy przez Karola Pawła Steckiewicza jako część rozprawy doktorskiej w formie spójnego tematycznie zbioru artykułów opublikowanych w czasopismach naukowych.

Oświadczam, iż samodzielna i możliwa do wyodrębnienia część ww. pracy wykazuje indywidualny wkład Karola Pawła Steckiewicz przy opracowywaniu koncepcji, wykonywaniu części eksperymentalnej, opracowaniu i interpretacji wyników tej pracy. Udział procentowy Karola Pawła Steckiewicza w powstanie w/w pracy oceniam na 55 %.

E. Tomczyk

.....

(podpis współautorki)

Warszawa, dnia 11.09.2020

Dr Michał Wójcik
mwojcik@chem.uw.edu.pl
Wydział Chemii, Uniwersytet Warszawski
ul. Pasteura 1, Warszawa

.....
(tytuł zawodowy, imię i nazwisko)

OŚWIADCZENIE

Jako współautor pracy pt. Assessment of anti-tumor potential and safety of application of glutathione stabilized gold nanoparticles conjugated with chemotherapeutics (Int J Med Sci. 2020;17(6)), oświadczam, iż mój własny wkład merytoryczny w przygotowanie, przeprowadzenie i opracowanie badań oraz przedstawienie pracy w formie publikacji to:

nadzór merytoryczny nad syntezą i charakterystyką nanocząstek złota.

Jednocześnie wyrażam zgodę na przedłożenie w/w pracy przez Karola Pawła Steckiewicza jako część rozprawy doktorskiej w formie spójnego tematycznie zbioru artykułów opublikowanych w czasopismach naukowych.

Oświadczam, iż samodzielna i możliwa do wyodrębnienia część ww. pracy wykazuje indywidualny wkład Karola Pawła Steckiewicz przy opracowywaniu koncepcji, wykonywaniu części eksperymentalnej, opracowaniu i interpretacji wyników tej pracy. Udział procentowy Karola Pawła Steckiewicza w powstanie w/w pracy oceniam na 55 %.

Michał Wójcik

.....
(podpis współautora)

Gdańsk, dnia 24.09.2020r.

Prof. dr hab. Iwona Inkielewicz – Stępniak
.....
(tytuł zawodowy, imię i nazwisko)

OŚWIADCZENIE

Jako współautorka pracy pt. Assessment of anti-tumor potential and safety of application of glutathione stabilized gold nanoparticles conjugated with chemotherapeutics (Int J Med Sci. 2020;17(6)), oświadczam, iż mój własny wkład merytoryczny w przygotowanie, przeprowadzenie i opracowanie badań oraz przedstawienie pracy w formie publikacji to:

nadzór merytoryczny nad badaniami biologicznymi i przygotowaniem publikacji.

Jednocześnie wyrażam zgodę na przedłożenie w/w pracy przez Karola Pawła Steckiewicza jako część rozprawy doktorskiej w formie spójnego tematycznie zbioru artykułów opublikowanych w czasopismach naukowych.

Oświadczam, iż samodzielna i możliwa do wyodrębnienia część ww. pracy wykazuje indywidualny wkład Karola Pawła Steckiewicz przy opracowywaniu koncepcji, wykonywaniu części eksperymentalnej, opracowaniu i interpretacji wyników tej pracy. Udział procentowy Karola Pawła Steckiewicza w powstanie w/w pracy oceniam na 55 %.

.....
(podpis współautorki)

Gdańsk . dnia 24.09.2020

Karol Paweł Steckiewicz
.....
(tytuł zawodowy, imię i nazwisko)

OŚWIADCZENIE

Jako współautor pracy pt. Shape-depended biological properties of Ag_3PO_4 microparticles: evaluation of antimicrobial properties and cytotoxicity in *in vitro* model - safety assessment of potential clinical usage (Oxid Med Cell Longev. 2019; 2019:6740325), oświadczam, iż mój własny wkład merytoryczny w przygotowanie, przeprowadzenie i opracowanie badań oraz przedstawienie pracy w formie publikacji to:

udział w opracowywaniu koncepcji pracy, wykonanie badań eksperymentalnych, opracowanie i interpretacja wyników, przygotowanie manuskryptu.

Jednocześnie wyrażam zgodę na przedłożenie w/w pracy przez Karola Pawła Steckiewicza jako część rozprawy doktorskiej w formie spójnego tematycznie zbioru artykułów opublikowanych w czasopismach naukowych.

Oświadczam, iż samodzielna i możliwa do wyodrębnienia część ww. pracy wykazuje indywidualny wkład Karola Pawła Steckiewicz przy opracowywaniu koncepcji, wykonywaniu części eksperymentalnej, opracowaniu i interpretacji wyników tej pracy. Udział procentowy Karola Pawła Steckiewicza w powstanie w/w pracy oceniam na 55 %.

Karol P. Steckiewicz
.....
(podpis współautora)

Gdańsk, dnia...11.09.2020

mgr Julia Zwara
.....
(tytuł zawodowy, imię i nazwisko)

OŚWIADCZENIE

Jako współautorka pracy pt. Shape-depended biological properties of Ag_3PO_4 microparticles: evaluation of antimicrobial properties and cytotoxicity in *in vitro* model - safety assessment of potential clinical usage (Oxid Med Cell Longev. 2019; 2019:6740325), oświadczam, iż mój własny wkład merytoryczny w przygotowanie, przeprowadzenie i opracowanie badań oraz przedstawienie pracy w formie publikacji to:

synteza i charakterystyka mikrocząstek fosforanu (V) srebra w różnych kształtach.

Jednocześnie wyrażam zgodę na przedłożenie w/w pracy przez Karola Pawła Steckiewicza jako część rozprawy doktorskiej w formie spójnego tematycznie zbioru artykułów opublikowanych w czasopismach naukowych.

Oświadczam, iż samodzielna i możliwa do wyodrębnienia część ww. pracy wykazuje indywidualny wkład Karola Pawła Steckiewicz przy opracowywaniu koncepcji, wykonywaniu części eksperymentalnej, opracowaniu i interpretacji wyników tej pracy. Udział procentowy Karola Pawła Steckiewicza w powstanie w/w pracy oceniam na 55 %.

.....Zwara Julia.....
(podpis współautorki)

Gdańsk, dnia 28.09.2020

dr Maciej Jaśkiewicz
.....
(tytuł zawodowy, imię i nazwisko)

OŚWIADCZENIE

Jako współautor pracy pt. Shape-depended biological properties of Ag_3PO_4 microparticles: evaluation of antimicrobial properties and cytotoxicity in *in vitro* model - safety assessment of potential clinical usage (Oxid Med Cell Longev. 2019; 2019:6740325), oświadczam, iż mój własny wkład merytoryczny w przygotowanie, przeprowadzenie i opracowanie badań oraz przedstawienie pracy w formie publikacji to:

wykonanie analiz mikrobiologicznych.

Jednocześnie wyrażam zgodę na przedłożenie w/w pracy przez Karola Pawła Steckiewicza jako część rozprawy doktorskiej w formie spójnego tematycznie zbioru artykułów opublikowanych w czasopismach naukowych.

Oświadczam, iż samodzielna i możliwa do wyodrębnienia część ww. pracy wykazuje indywidualny wkład Karola Pawła Steckiewicz przy opracowywaniu koncepcji, wykonywaniu części eksperymentalnej, opracowaniu i interpretacji wyników tej pracy. Udział procentowy Karola Pawła Steckiewicza w powstanie w/w pracy oceniam na 55 %.

Jaśkiewicz Maciej

.....
(podpis współautora)

Gdańsk, dnia 22.09.20

mgr inż. Szymon Kowalski
.....
(tytuł zawodowy, imię i nazwisko)

OŚWIADCZENIE

Jako współautor pracy pt. Shape-depended biological properties of Ag_3PO_4 microparticles: evaluation of antimicrobial properties and cytotoxicity in *in vitro* model - safety assessment of potential clinical usage (Oxid Med Cell Longev. 2019; 2019:6740325), oświadczam, iż mój własny wkład merytoryczny w przygotowanie, przeprowadzenie i opracowanie badań oraz przedstawienie pracy w formie publikacji to:

nadzór nad analizami cytometrycznymi.

Jednocześnie wyrażam zgodę na przedłożenie w/w pracy przez Karola Pawła Steckiewicza jako część rozprawy doktorskiej w formie spójnego tematycznie zbioru artykułów opublikowanych w czasopismach naukowych.

Oświadczam, iż samodzielna i możliwa do wyodrębnienia część ww. pracy wykazuje indywidualny wkład Karola Pawła Steckiewicz przy opracowywaniu koncepcji, wykonywaniu części eksperymentalnej, opracowaniu i interpretacji wyników tej pracy. Udział procentowy Karola Pawła Steckiewicza w powstanie w/w pracy oceniam na 55 %.

Szymon Kowalski
.....
(podpis współautora)

Gdańsk, dnia 24.08.2020

Prof. dr hab. Wojciech Kamysz
.....
(tytuł zawodowy, imię i nazwisko)

OŚWIADCZENIE

Jako współautor pracy pt. Shape-depended biological properties of Ag_3PO_4 microparticles: evaluation of antimicrobial properties and cytotoxicity in *in vitro* model - safety assessment of potential clinical usage (Oxid Med Cell Longev. 2019; 2019:6740325), oświadczam, iż mój własny wkład merytoryczny w przygotowanie, przeprowadzenie i opracowanie badań oraz przedstawienie pracy w formie publikacji to:

nadzór merytoryczny nad badaniami mikrobiologicznymi.

Jednocześnie wyrażam zgodę na przedłożenie w/w pracy przez Karola Pawła Steckiewicza jako część rozprawy doktorskiej w formie spójnego tematycznie zbioru artykułów opublikowanych w czasopismach naukowych.

Oświadczam, iż samodzielna i możliwa do wyodrębnienia część ww. pracy wykazuje indywidualny wkład Karola Pawła Steckiewicz przy opracowywaniu koncepcji, wykonywaniu części eksperymentalnej, opracowaniu i interpretacji wyników tej pracy. Udział procentowy Karola Pawła Steckiewicza w powstanie w/w pracy oceniam na 55 %.

Kamysz
.....
(podpis współautora)

Gdańsk, dnia 11.09.2020

Prof. dr hab. inż. Adriana Zaleska Medynska
.....
(tytuł zawodowy, imię i nazwisko)

OŚWIADCZENIE

Jako współautorka pracy pt. Shape-depended biological properties of Ag_3PO_4 microparticles: evaluation of antimicrobial properties and cytotoxicity in *in vitro* model - safety assessment of potential clinical usage (Oxid Med Cell Longev. 2019; 2019:6740325), oświadczam, iż mój własny wkład merytoryczny w przygotowanie, przeprowadzenie i opracowanie badań oraz przedstawienie pracy w formie publikacji to:

nadzór merytoryczny nad syntezą i charakteryzacją
mikrocząstek fosforanu (V) srebra w różnych kształtach.

Jednocześnie wyrażam zgodę na przedłożenie w/w pracy przez Karola Pawła Steckiewicza jako część rozprawy doktorskiej w formie spójnego tematycznie zbioru artykułów opublikowanych w czasopismach naukowych.

Oświadczam, iż samodzielna i możliwa do wyodrębnienia część ww. pracy wykazuje indywidualny wkład Karola Pawła Steckiewicz przy opracowywaniu koncepcji, wykonywaniu części eksperymentalnej, opracowaniu i interpretacji wyników tej pracy. Udział procentowy Karola Pawła Steckiewicza w powstanie w/w pracy oceniam na 55 %.

KIEROWNIK
Katedra Technologii Środowiska
prof. dr hab. inż. Adriana Zaleska-Medynska

.....
(podpis współautorki)

Gdańsk, dnia 24.09.2020r.

Prof. dr hab. Iwona Inkielewicz - Stępniak
.....
(tytuł zawodowy, imię i nazwisko)

OŚWIADCZENIE

Jako współautorka pracy pt. Shape-depended biological properties of Ag_3PO_4 microparticles: evaluation of antimicrobial properties and cytotoxicity in *in vitro* model - safety assessment of potential clinical usage (Oxid Med Cell Longev. 2019; 2019:6740325), oświadczam, iż mój własny wkład merytoryczny w przygotowanie, przeprowadzenie i opracowanie badań oraz przedstawienie pracy w formie publikacji to:

nadzór merytoryczny nad badaniami biologicznymi i przygotowaniem publikacji.

Jednocześnie wyrażam zgodę na przedłożenie w/w pracy przez Karola Pawła Steckiewicza jako część rozprawy doktorskiej w formie spójnego tematycznie zbioru artykułów opublikowanych w czasopismach naukowych.

Oświadczam, iż samodzielna i możliwa do wyodrębnienia część ww. pracy wykazuje indywidualny wkład Karola Pawła Steckiewicz przy opracowywaniu koncepcji, wykonywaniu części eksperymentalnej, opracowaniu i interpretacji wyników tej pracy. Udział procentowy Karola Pawła Steckiewicza w powstanie w/w pracy oceniam na 55 %.

.....
(podpis współautorki)